

**QUANTIFICATION OF RHODIUM IN SERIES OF  
INORGANIC AND ORGANOMETALLIC  
COMPOUNDS**

**T.T. CHIWESHE**

# QUANTIFICATION OF RHODIUM IN SERIES OF INORGANIC AND ORGANOMETALLIC COMPOUNDS

*A thesis submitted to meet the requirements for the degree of*  
**Magister Scientiae**

in the

FACULTY OF NATURAL AND AGRICULTURAL SCIENCES  
DEPARTMENT OF CHEMISTRY

at the

UNIVERSITY OF THE FREE STATE  
BLOEMFONTEIN

by

**TREVOR TRYMORE CHIWESHE**

*Promoter*

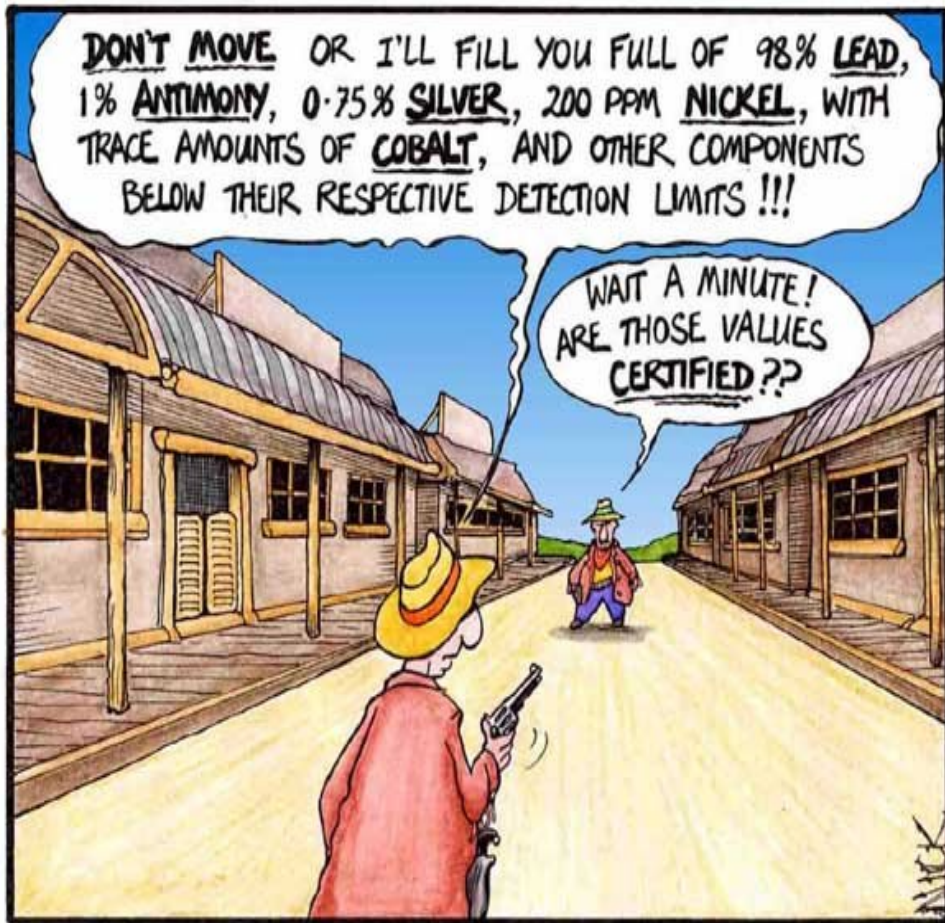
Prof. W. Purcell

*Co-promoters*

Dr. J. A. Venter and Dr. T. Mtshali

November 2009

STRANGE MATTER  
by nick d. kim  
strange-matter.com



ANALYTICAL CHEMISTS IN THE WILD WEST

# Declaration by candidate

---

“I hereby assert that the dissertation submitted for the degree Magister in Chemistry, at the University of the Free State is my own original work and has not been previously submitted to any other institution of higher education. I further declare that all sources cited or quoted are indicated and acknowledged by means of a comprehensive list of references.”

**Signature**.....

*Chiweshe Trevor Trymore*

**Date** .....

# Acknowledgements

---

I would like to express my sincere gratitude and appreciation to the following people for their contributions towards this study:

- My *supervisor*, **Prof. W. Purcell** for his positive attitude and guidance through the research project. He was really helpful and I learnt considerably from him;
- My *co-supervisors*, **Dr J. Venter** and **Dr T. Mtshali** for their guidance encouragement and constant reassurance during the time of my study;
- I wish extend my sincere gratitude to my group colleagues for the help and laughter we shared and above all for providing such a friendly environment conducive for this study;
- Special thanks to *Mrs K. Brown* and family for the support and love throughout my studies together with my mother *Mrs S. R. Chiweshe* and my grandfather *Mr T. J. Sibindi* for the constant encouragement. May the good Lord bless you all.

*Trevor Teymore Chiweshe*

# Table of contents

---

<b>LIST OF FIGURES.....</b>	<b>vii</b>
<b>LIST OF TABLES.....</b>	<b>xi</b>
<b>LIST OF SCHEMES.....</b>	<b>xiv</b>
<b>LIST OF ABBREVIATIONS.....</b>	<b>xv</b>
<b>KEYWORDS.....</b>	<b>xviii</b>
<b>SUMMARY.....</b>	<b>xix</b>
<b>OPSOMMING.....</b>	<b>xxi</b>
<b>CHAPTER 1 .....</b>	<b>1</b>
1 Literature survey.....	1
1.1 Discovery of rhodium.....	1
1.2 Occurrence and distribution.....	2
1.3 Sources of rhodium.....	6
1.3.1 Extraction of rhodium from the ore.....	6
1.3.2 Alternative source of rhodium from spent nuclear fuel.....	11
1.4 Economic value.....	14
1.5 Applications and uses of rhodium.....	16
1.6 Physical and Chemical properties.....	20
1.6.1 Crystallographic structure of rhodium.....	21
1.7 Rhodium chemistry.....	22
1.7.1 Inorganic complexes.....	23
1.7.1.1 Rhodium halides.....	25
1.7.1.2 Rhodium oxides.....	26
1.7.2 Organometallic complexes.....	26
1.8 Motivation of this study.....	28
1.9 Aim of this study.....	30
<b>CHAPTER 2 .....</b>	<b>32</b>
2 Analytical techniques for rhodium determination - literature survey.....	32
2.1 Introduction.....	32
2.2 Analytical methods used for rhodium analysis.....	35

---

## Table of contents

---

2.2.1	Spectrophotometric methods.....	35
2.2.1.1	Ultraviolet – visible absorption spectrometry (UV-Vis).....	35
2.2.2	Chromatographic techniques (separation and isolation).....	40
2.2.3	Gravimetric and titrimetric techniques.....	42
2.2.4	Spectrometric techniques.....	45
2.2.5	Atomic absorption spectrometry (AAS and GF-AAS).....	47
2.3	Digestion techniques.....	48
2.3.1	Sample decomposition by acids and fluxes.....	48
2.3.2	Microwave digestion.....	50
2.3.3	Conclusion.....	51
<b>CHAPTER 3</b>	.....	<b>52</b>
3	Selection of analytical techniques.....	52
3.1	Introduction.....	53
3.2	Spectroscopic measurements.....	53
3.2.1	Introduction.....	53
3.2.2	Principles of spectral origin and measurements.....	53
3.2.3	Selection of analytical lines.....	57
3.2.4	Methods in spectroscopic analysis.....	58
3.2.4.1	Direct calibration method.....	59
3.2.4.2	Standard addition method.....	61
3.2.4.3	Internal standard addition.....	62
3.3	Validation of analytical methods.....	63
3.3.1	The validation parameters.....	64
3.3.2	Validation procedure.....	65
3.3.3	Detection limits.....	70
3.4	ICP-OES.....	72
3.4.1	Outline of the ICP-OES procedure.....	72
3.4.2	Sample introduction system.....	74
3.4.3	The plasma torch.....	74
3.4.3.1	Nebulizer and chamber.....	76
3.4.3.2	Levelers.....	77
3.4.3.3	RF coil.....	77
3.4.4	Spectrometer.....	78
3.5	Microwave digestion.....	79

---

## Table of contents

---

3.5.1.1	Equipment.....	80
3.5.1.2	Sample digestion.....	82
3.6	Thermal gravimetric analysis (TGA) and the Differential scanning calorimetry (DSC).....	83
3.6.1.1	Introduction.....	83
3.6.1.2	Thermal Gravimetric Analysis (TGA).....	83
3.6.1.3	Differential scanning calorimetry (DSC).....	86
3.7	Conclusion.....	88
<b>CHAPTER 4</b>		
4	Quantitative determination of rhodium.....	90
4.1	Introduction.....	90
4.2	General experimental conditions and procedures.....	91
4.2.1	Preparation of distilled water.....	91
4.2.2	Weighing.....	91
4.2.3	Microwave digestion.....	91
4.2.4	ICP-OES.....	92
4.2.5	Microscope scanning.....	93
4.2.6	Thermal gravimetric analysis (TGA).....	93
4.2.7	Differential scanning calorimetry (DSC).....	94
4.3	Reagents and glassware.....	94
4.4	CRM preparation and qualitative analysis.....	95
4.4.1	Description of the CRM.....	95
4.4.2	Preparation of the CRM samples.....	96
4.4.2.1	<i>Calculations of the theoretical concentration of rhodium in the CRM (0.500 g) sample.....</i>	<i>96</i>
4.4.3	Qualitative analysis of the CRM and the selection of the rhodium wavelength.....	97
4.5	Detection limits and quantitative analysis of rhodium in CRM.....	99
4.5.1	Preparation of linear calibration curves.....	99
4.5.2	Detection limits of rhodium.....	100
4.5.3	Quantitative determination of rhodium using the direct calibration method for the CRM samples digested in an open beaker.....	101
4.5.3.1	Preparation of the CRM samples.....	101



---

## Table of contents

---

4.5.3.2	Preparation of the standard solutions and the quantitative determination of rhodium.....	101
4.5.4	Quantitative determination of rhodium using the direct calibration method from the CRM samples digested in a microwave.....	104
4.5.4.1	Preparation of the CRM samples.....	104
4.5.4.2	Preparation of the standard solutions and the quantitative determination of rhodium.....	104
4.5.4.3	Determining the precision of the results after microwave digestion of the CRM samples.....	106
4.5.5	Quantitative determination of rhodium from CRM using the standard addition method.....	107
4.5.5.1	Preparation of the CRM analyte samples.....	107
4.5.5.2	Preparation of the standard solutions and the quantitative determination of rhodium.....	108
4.5.6	Quantitative determination of rhodium from the CRM using the internal standard addition method.....	110
4.5.6.1	Selection of the internal standard.....	110
4.5.6.2	Determination of rhodium using yttrium and cobalt internal standards.....	113
4.5.6.2.1	Preparation of the CRM samples.....	113
4.5.6.2.2	Preparation of the the rhodium and yttrium standards.....	113
4.5.6.2.3	Quantitative determination of the percentage recovery of rhodium	
4.5.6.3	Determination of rhodium using cobalt internal standard.....	114
4.5.6.3.1	Preparation of the CRM samples.....	114
4.5.6.3.2	Preparation of the rhodium standards and quantitative determination of rhodium.....	115
4.6	Qualitative and quantitative determination of rhodium in rhodium metal powder (99.99 % purity).....	117
4.6.1	Determination of rhodium using direct calibration method.....	117
4.6.1.1	Preparation of the rhodium metal powder samples.....	117
4.6.1.2	Preparation of the rhodium standard solutions and the quantitative determination of rhodium.....	118
4.6.2	Determination of rhodium using the cobalt internal standard.....	119
4.6.2.1	Preparation of the rhodium metal powder analyte samples.....	119

---

## Table of contents

---

4.6.2.2	Preparation of the standard solution and quantitative determination of rhodium.....	119
4.7	Quantitative determination of a rhodium in $\text{RhCl}_3 \cdot x\text{H}_2\text{O}$ .....	121
4.7.1	Analysis of $\text{RhCl}_3 \cdot x\text{H}_2\text{O}$ using IR spectroscopy and visual inspection using a Microscope.....	122
4.7.2	DSC and TGA analysis of $\text{RhCl}_3 \cdot x\text{H}_2\text{O}$ .....	124
4.7.2.1	Differential scanning calorimetry (DSC).....	124
4.7.2.2	Thermal gravimetric analysis (TGA).....	125
4.7.3	Quantitative analysis of $\text{RhCl}_3 \cdot x\text{H}_2\text{O}$ in $\text{HNO}_3$ (65.0 %) using the cobalt internal standard method.....	127
4.7.3.1	Preparation of the $\text{RhCl}_3 \cdot x\text{H}_2\text{O}$ analyte samples.....	127
4.7.3.2	Preparation of the rhodium standard solutions and the quantitative determination of rhodium.....	127
4.7.4	Quantitative analysis of $\text{RhCl}_3 \cdot x\text{H}_2\text{O}$ in $\text{HCl}$ (32.0 %) using the cobalt internal standard method.....	129
4.7.4.1	Preparation of the $\text{RhCl}_3 \cdot x\text{H}_2\text{O}$ analyte samples.....	129
4.7.4.2	Preparation of the rhodium standards and the quantitative determination of rhodium.....	129
4.7.5	The effect of unmatched acid matrix ( $\text{HCl}$ , $\text{HBr}$ and $\text{HNO}_3$ ) towards rhodium recovery (ruggedness and /or robustness).....	130
4.7.5.1	Preparation of the $\text{RhCl}_3 \cdot x\text{H}_2\text{O}$ analyte samples.....	131
4.7.5.2	Preparation of the rhodium standards and the quantitative determination of rhodium.....	131
4.7.6	Determining the effect of chloride ions ( $\text{Cl}^-$ ) towards rhodium recovery using the direct calibration method.....	133
4.7.6.1	Preparation of the $\text{RhCl}_3 \cdot 3\text{H}_2\text{O}$ analyte samples.....	133
4.7.6.2	Preparation of the standard solutions and the quantitative determination of rhodium.....	134
4.7.7	Quantitative determination of rhodium in different concentrations of halide salts ( $\text{NaCl}$ , $\text{KCl}$ and $\text{RbCl}$ ) using the direct calibration method.....	135
4.7.7.1	Preparation of the $\text{RhCl}_3 \cdot 3\text{H}_2\text{O}$ and the halide salts solutions.....	135
4.7.7.2	Preparation of the rhodium standard solutions and the quantitative determination of rhodium.....	136
4.8	Synthesis and analysis of organometallic complexes.....	139

---

## Table of contents

---

4.8.1	Synthesis of different rhodium complexes.....	140
4.8.1.1	Synthesis of [Rh(acac)(CO) <sub>2</sub> ].....	140
4.8.1.2	Synthesis of [Rh(acac)(PPh <sub>3</sub> )(CO)] .....	141
4.8.1.3	Synthesis of [Rh(acac)(PPh <sub>3</sub> )(CO)(Me)(I)].....	142
4.8.1.4	Synthesis of [Rh(cupf)(CO) <sub>2</sub> ] .....	143
4.8.1.5	Synthesis of [Rh(cupf)(PPh <sub>3</sub> )(CO)].....	144
4.8.1.6	Synthesis of [Rh(cupf)(PPh <sub>3</sub> )(CO)(Me)(I)].....	145
4.8.2	Quantitative determination of rhodium from the newly synthesized organometallic complexes.....	146
4.8.2.1	Preparation of the organometallic complexes for rhodium determination.....	146
4.8.2.2	Preparation of the standard solutions and the quantitative determination of rhodium.....	147
4.9	Conclusion.....	151
<b>CHAPTER 5</b>		
5	Validation of results.....	153
5.1	Introduction.....	153
5.2	Validation of the ICP-OES instrumentation.....	154
5.2.1	Method description.....	154
5.3	Validation of the CRM results.....	155
5.4	Validation of the rhodium metal results.....	158
5.5	Validation of the RhCl <sub>3</sub> ·3H <sub>2</sub> O results.....	161
5.6	Validation of the organometallic complexes results.....	162
5.7	Conclusion.....	168
<b>Chapter 6</b>		
6	Evaluation of this study and future research.....	170
6.1	Degree of success with regard to the set objectives.....	170
6.2	Future research.....	171
<b>Appendix 7.....</b>		<b>CD</b>

# List of figures

---

<b>Figure 1.1:</b> William Hyde Wollaston (1766 – 1828) .....	1
<b>Figure 1.2:</b> A fragment of Wollaston notebook .....	2
<b>Figure 1.3:</b> Percentage distribution of PGM across the world .....	3
<b>Figure 1.4:</b> Sperrylite and Laurite hollingworthite .....	4
<b>Figure 1.5:</b> Percentage of the world supply of PGM in 2006 .....	6
<b>Figure 1.6:</b> Cross section through the Bushveld Igneous Complex (BIC) .....	7
<b>Figure 1.7:</b> The Bushveld Igneous Complex showing the Merensky reef mines .....	8
<b>Figure 1.8:</b> Comparison of PGM output between the Merensky and the UG2 reefs...	8
<b>Figure 1.9:</b> Open pit PGM mine near Rustenburg .....	9
<b>Figure 1.10:</b> Powdered rhodium metal .....	10
<b>Figure 1.11:</b> Products of uranium nuclear fission .....	11
<b>Figure 1.12:</b> Comparison of rhodium and platinum price for the past 5 years .....	15
<b>Figure 1.3:</b> Cumulative growth of PGM purchases (1974 to 2003) .....	16
<b>Figure 1.14:</b> Rhodium plated jewellery .....	18
<b>Figure 1.15:</b> Use of rhodium in the Monsanto process .....	19
<b>Figure 1.16:</b> Face centered cubic lattice of rhodium metal .....	21
<b>Figure 1.17:</b> Molecular model of the lattice structure of the face centered cubic structure of rhodium .....	22
<b>Figure 2.1:</b> Complexation of rhodium(III) with 5-Br-PAPS .....	36
<b>Figure 2.2:</b> Structure of N- $\alpha$ -(5-bromopyridyl)-N'-benzoyl thiourea (BrPBT).....	37
<b>Figure 2.3:</b> Spectral curves of rhodium hypochlorite solutions at different pH values obtained from varying hypochlorite solution to $[\text{Rh}^{3+}] = 1 \times 10^{-3} \text{ M}$ .....	39

---

## List of figures

---

<b>Figure 2.4:</b> Spectral curves for rhodium (III) solutions colour-developed with tin(II) chloride .....	40
<b>Figure 2.5:</b> Structure of $[\text{Cr}(\text{NCS})_4(\text{amine})_2]^-$ .....	44
<b>Figure 3.1:</b> Schematic of an ICP-OES.....	54
<b>Figure 3.2:</b> Excitation and emission of the electromagnetic radiation.....	55
<b>Figure 3.3:</b> The electromagnetic spectrum.....	56
<b>Figure 3.4:</b> Emission of radiation upon relaxation from an excited state.....	57
<b>Figure 3.5:</b> Determination of the analyte signal.....	58
<b>Figure 3.6:</b> Direct calibration method.....	59
<b>Figure 3.7:</b> Comparison of the analyte signal to the standard signal.....	60
<b>Figure 3.8:</b> Standard addition calibration curve.....	61
<b>Figure 3.9:</b> The normal distribution at 95 % confidence interval .....	67
<b>Figure 3.10:</b> Linear relationship between the x and y values.....	68
<b>Figure 3.11:</b> A calibration curve plot showing limit of detection (LOD), limit of quantification (LOQ), dynamic range and limit of linearity (LOL).....	71
<b>Figure 3.12:</b> The relationship between the limit of detection (LOD) (red) and the limit of quantification (LOQ) (blue).....	72
<b>Figure 3.13:</b> Sample preparation and determination by ICP-OES.....	73
<b>Figure 3.14:</b> Major components and layout of a typical ICP-OES instrument.....	74
<b>Figure 3.15:</b> Plasma touch.....	75
<b>Figure 3.16:</b> Plasma torch assay.....	77
<b>Figure 3.17:</b> A polychromator for simultaneous analysis of radiation.....	78
<b>Figure 3.18:</b> Microwave digestion technique.....	80
<b>Figure 3.19:</b> Section through a microwave magnetron.....	81
<b>Figure 3.20:</b> Cross section of a magnetron.....	81
<b>Figure 3.21:</b> Rectangular structure of a waveguide.....	82
<b>Figure 3.22:</b> Sample heating by microwave energy.....	83

---

## List of figures

---

<b>Figure 3.23:</b> Structural appearance of TGA.....	84
<b>Figure 3.24:</b> TGA graph.....	85
<b>Figure 3.25:</b> Phase changes in TGA analysis.....	86
<b>Figure 3.26:</b> Schematic diagram of a heat flux DSC.....	86
<b>Figure 3.27:</b> DSC sample pans.....	87
<b>Figure 3.28:</b> DSC graph.....	88
<b>Figure 4.1:</b> ICP-OES “profile” function showing the combination of the matrices and the analyte signal in the CRM close to the rhodium most sensitive line, 343.489 nm.....	98
<b>Figure 4.2:</b> Rhodium atomic line indicating possible interfering species.....	99
<b>Figure 4.3:</b> Calibration curve of rhodium at a wavelength of 343.489 nm.....	100
<b>Figure 4.4:</b> Comparison of the undigested residue of the CRM in different acids...	103
<b>Figure 4.5:</b> IR spectrum for the solid remained after CRM digested in microwave conditions in HCl.....	106
<b>Figure 4.6:</b> Quantitative determination of Rh in CRM using the standard addition method.....	109
<b>Figure 4.7:</b> Comparison of IR scan for dried and hydrated $\text{RhCl}_3 \cdot x\text{H}_2\text{O}$ .....	122
<b>Figure 4.8:</b> Changes in $\text{RhCl}_3 \cdot x\text{H}_2\text{O}$ appearance at 35, 159, 241 and 400 °C respectively.....	123
<b>Figure 4.9:</b> DSC scan of $\text{RhCl}_3 \cdot x\text{H}_2\text{O}$ .....	124
<b>Figure 4.10:</b> Changes in weight (mass) of $\text{RhCl}_3 \cdot x\text{H}_2\text{O}$ .....	126
<b>Figure 4.11:</b> Effects of the acid matrix towards rhodium recovery.....	133
<b>Figure 4.12:</b> Decrease in rhodium recovery with increase conc. of both $\text{Na}^+$ and $\text{Cl}^-$ ions.....	135
<b>Figure 4.13:</b> Effects of halide salts in rhodium recovery.....	136
<b>Figure 4.14:</b> Matrix correction with cobalt internal standard.....	138
<b>Figure 4.15:</b> Synthesis of the different organometallic complexes.....	139
<b>Figure 4.16:</b> Infra-red spectrum of $[\text{Rh}(\text{acac})(\text{CO})_2]$ .....	141

---

## List of figures

---

<b>Figure 4.17:</b> Infra-red spectrum of $[\text{Rh}(\text{acac})(\text{PPh}_3)(\text{CO})]$ .....	142
<b>Figure 4.18:</b> Infra-red spectrum of $[\text{Rh}(\text{acac})(\text{CO})\text{PPh}_3(\text{Me})(\text{I})]$ .....	143
<b>Figure 4.19:</b> Infrared spectrum of $[\text{Rh}(\text{cupf})(\text{CO})_2]$ .....	144
<b>Figure 4.20:</b> Infra-red spectrum of $[\text{Rh}(\text{cupf})(\text{PPh}_3)(\text{CO})]$ .....	145
<b>Figure 4.21:</b> Infra red spectrum of $[\text{Rh}(\text{cupf})(\text{PPh}_3)(\text{CO})(\text{CH}_3)(\text{I})]$ .....	146

# List of tables

---

<b>Table 1.1:</b> Predicted world reserves of PGM in 2006 .....	5
<b>Table 1.2:</b> Different rhodium isotopes generated during nuclear fission .....	14
<b>Table 1.3:</b> Rhodium supply and demand figures for the period 2004 – 2006 .....	17
<b>Table 1.4:</b> Physical and chemical properties of rhodium metal .....	21
<b>Table 1.5:</b> Examples of compounds with rhodium in different oxidation states .....	23
<b>Table 1.6:</b> Rhodium recovery from different organometallic complexes .....	28
<b>Table 2.1:</b> A summary of different analytical techniques .....	34
<b>Table 2.2:</b> Platinum group metals recoveries from perchloric acid solution .....	42
<b>Table 2.3:</b> Levels of measurement of different techniques .....	46
<b>Table 3.1:</b> Summary of the ICP-OES methods of analysis.....	63
<b>Table 3.2:</b> Validation criteria.....	66
<b>Table 4.1:</b> Microwave digestion conditions for the PGM (PGM XF100-8).....	92
<b>Table 4.2:</b> ICP-OES operating conditions for the rhodium analysis.....	93
<b>Table 4.3:</b> TGA measurement conditions.....	94
<b>Table 4.4:</b> Certified concentration values of platinum, palladium and rhodium in 5.0 g mass of the reference material at 95 % confidence interval.....	95
<b>Table 4.5:</b> Determination of the detection limit of rhodium.....	100
<b>Table 4.6:</b> Quantitative results from open beaker digestion of the CRM's.....	102
<b>Table 4.7:</b> Quantitative results of rhodium recovery after microwave digestion.....	105
<b>Table 4.8:</b> Determination of precision in % Rh recovery after microwave digestion in HCl.....	107
<b>Table 4.9:</b> Results of rhodium recovery using the standard addition method.....	109
<b>Table 4.10:</b> Comparison of the 1 <sup>st</sup> , 2 <sup>nd</sup> and 3 <sup>rd</sup> ionization energies of yttrium, rhodium and cobalt.....	111



---

## List of tables

---

<b>Table 4.11:</b> Comparison of the electromagnetic wavelengths, detection limits and interferences for Rh analysis between Y and Co in the ICP-OES analysis.....	112
<b>Table 4.12:</b> Experimental results of rhodium determination using yttrium internal standard in HNO <sub>3</sub> .....	114
<b>Table 4.13:</b> Quantitative results of rhodium recovery in the CRM using cobalt internal standard.....	116
<b>Table 4.14:</b> Determination of rhodium recovery from the direct calibration curve...	118
<b>Table 4.15:</b> Quantitative determination of rhodium from rhodium powder using cobalt as internal standard.....	120
<b>Table 4.16:</b> Percentage recovery of rhodium from RhCl <sub>3</sub> ·xH <sub>2</sub> O.....	128
<b>Table 4.17:</b> Results of the determination of Rh from RhCl <sub>3</sub> ·xH <sub>2</sub> O in HCl.....	130
<b>Table 4.18:</b> Quantitative analysis of rhodium in RhCl <sub>3</sub> ·3H <sub>2</sub> O using unmatched acid matrix.....	131
<b>Table 4.19:</b> The effects of chloride ions in rhodium determination.....	134
<b>Table 4.20:</b> Rhodium percentage recovery from RhCl <sub>3</sub> ·3H <sub>2</sub> O in different chloride salt solutions using direct calibration.....	137
<b>Table 4.21:</b> Percentage of rhodium recovery from RhCl <sub>3</sub> ·3H <sub>2</sub> O in different chloride salts using cobalt internal standard.....	138
<b>Table 4.22:</b> Quantitative determination of rhodium from in [Rh(acac)(CO) <sub>2</sub> ].....	147
<b>Table 4.23:</b> Quantitative determination of rhodium in [Rh(acac)(PPh <sub>3</sub> )(CO)].....	148
<b>Table 4.24:</b> Quantitative determination of rhodium in [Rh(acac)(PPh <sub>3</sub> )(CO)(CH <sub>3</sub> )(I)] .....	148
<b>Table 4.25:</b> Quantitative determination of rhodium in [Rh(cupf)(CO) <sub>2</sub> ].....	149
<b>Table 4.26:</b> Quantitative determination of rhodium [Rh(cupf)(PPh <sub>3</sub> )(CO)].....	149
<b>Table 4.27:</b> Quantitative determination of rhodium in [Rh(cupf)(PPh <sub>3</sub> )(CO)(CH <sub>3</sub> )(I)] .....	150

---

## List of tables

---

<b>Table 4.28:</b> A summary of the rhodium percentage recovery of the rhodium metal, inorganic and organometallic complexes using the cobalt internal standard addition method.....	151
<b>Table 5.1:</b> Validation results of the ICP-OES of the method.....	154
<b>Table 5.2:</b> Validation of the CRM results for the cobalt internal standard method...	157
<b>Table 5.3:</b> Validation of the CRM results for the yttrium internal standard method..	158
<b>Table 5.4:</b> Validation of rhodium in rhodium metal at 95 % confidence interval using cobalt internal standard method.....	160
<b>Table 5.5:</b> Validation of rhodium in $\text{RhCl}_3 \cdot 3\text{H}_2\text{O}$ at 95 % confidence interval using cobalt internal standard method.....	161
<b>Table 5.6:</b> Validation of rhodium in $[\text{Rh}(\text{acac})(\text{CO})_2]$ at 95 % confidence interval using cobalt internal standard method.....	162
<b>Table 5.7:</b> Validation of rhodium in $[\text{Rh}(\text{acac})(\text{CO})(\text{PPh}_3)]$ at 95 % confidence interval using cobalt internal standard method.....	163
<b>Table 5.8:</b> Validation of rhodium in $[\text{Rh}(\text{acac})(\text{PPh}_3)(\text{CO})(\text{Me})(\text{I})]$ at 95 % confidence interval using cobalt internal standard method.....	164
<b>Table 5.9:</b> Validation of rhodium in $[\text{Rh}(\text{cupf})(\text{CO})_2]$ at 95 % confidence interval using cobalt internal standard method.....	165
<b>Table 5.10:</b> Validation of rhodium in $[\text{Rh}(\text{cupf})(\text{PPh}_3)(\text{CO})]$ at 95 % confidence interval using cobalt internal standard method.....	166
<b>Table 5.11:</b> Validation of rhodium in $[\text{Rh}(\text{cupf})(\text{PPh}_3)(\text{CO})(\text{Me})(\text{I})]$ at 95 % confidence interval using cobalt internal standard method.....	167
<b>Table 5.12:</b> A summary of the results accepted or rejected.....	168
<b>Table 5.13:</b> A summary of the validated parameters.....	169
<b>Table 6.1:</b> Comparison of the first ionization energies of cobalt, rhodium and iridium.....	171

# List of schemes

---

<b>Scheme 1.1:</b> Rhodium extraction from the PGM ore .....	10
<b>Scheme 1.2:</b> Fission of uranium and the subsequent fission of rhodium .....	13
<b>Scheme 1.3:</b> Substitution reactions in rhodium aqua-complexes .....	24
<b>Scheme 1.4:</b> Substitution reactions in rhodium chlorido-complexes .....	24
<b>Scheme 2.1:</b> Reaction scheme for the separation of rhodium using BrPBT .....	38

# List of abbreviations

---

PGM	Platinum Group metals
CRM	Certified Reference Material
ERM <sup>®</sup> -504	European Reference Material
BIC	Bushveld Igneous Complex
UG2	Upper Group 2 reef
ISO	Organization for Standardization

## Analytical equipment

AAS	Atomic absorption spectroscopy
XRF	X-ray fluorescence
UV-Vis	Ultraviolet–visible absorption spectrometry
ICP-OES	Inductive coupled plasma-optical emission spectroscopy
ICP-MS	Inductive coupled plasma-mass spectrometry
GF-AAS	Graphite furnace-atomic absorption spectrometry
WDXRF	Wavelength-dispersive X-ray fluorescence
FA	Fire assay
TGA	Thermal gravimetric analysis
DSC	Differential scanning calorimetry
CID	Charge injection devise
PMT	Photomultiplier tube

## Ligands

acac	Acetylacetone
cupf	Cupferron (ammonium salt of N-nitrosophenyl hydroxylamine)
PPh <sub>3</sub>	Triphenylphosphine
Me	Methyl
5-Br-PAPS	2-(5-Bromo-2-pyridylazo)-5-(N-propyl-N-sulphopropylamino) phenol

---

## List of abbreviations

---

PAR	4-(2-pyridylazo) resorcinol
EDTA	Ethylenediaminetetraacetic acid

### Units

Bq	Becquerel
Ci	Curie
oz	Ounce
%	Percentage
Kg	Kilogram
°C	Degrees Celsius
ppm	Parts per million
ppb	Parts per billion

### Statistical terms

LOD	Limit of detection
LOQ	Limit of quantitation
$r^2$	Linear regression line
S	Standard deviation
RSD	Relative standard deviation
LOL	Limit of linearity
$H_a$	Alternative hypothesis
$H_0$	Null hypothesis

### Chemistry terms

Conc.	Concentration
Syn	Synthetic radioisotope
DP	Decay product
$\epsilon$	Electron capture sometimes called Inverse Beta decay
$\gamma$	Gamma rays
IT	Internal conversion
DE	Decay energy

---

## List of abbreviations

---

$\beta+$	Positron emission sometimes called beta plus
NA	Natural abundance
$\beta-$	Beta minus
DM	Decay mode
PTFE	Polytetrafluoroethylene
EIE	Easily ionized elements

# Keywords

---

Rhodium

Quantitative analysis

Qualitative analysis

Dissolution

Unmatched matrix

Matrices

Analysis

Determination

Organometallic complexes

Inorganic complexes

Robust

Ruggedness

Precision

Accuracy

Linearity

Detection limits

Crystallize

Wavelength

# Opsomming

---

Die hoofdoel van die navorsing was om 'n analitiese metode daar te stel om die persentasie herwinning van rodium te kwantifiseer en te optimiseer deur van induktief-gekoppelde plasma optiese-emissie spektrometrie (IGP-OES) gebruik te maak. Eerstens is 'n GVM (gesertifiseerde verwysingsmateriaal) gebruik om die effektiwiteit van die metode te bepaal. Daarna is rodiummetaal gebruik asook 'n anorganiese rodium monster en laastens verskeie organometaalverbindings om deeglike herwinnings te verseker in verskillende matrikse.

Kwantitatiewe analise van rodium, deur van 'n kobalt interne standaard gebruik te maak, het uitstekende resultate vir die GVM, die metaal asook  $\text{RhCl}_3 \cdot x\text{H}_2\text{O}$  met ongeveer 99.0 % + opbrengs gelewer. Deur 'n yttrium interne standaard te gebruik, is resultate van ongeveer 140.0 % vir dieselfde monsters verkry. Die drastiese verskille in herwinningspersentasies word onder andere toegeskryf aan die verskille in eerste ionisasie energie tussen kobalt ( $760.41 \text{ kJ mol}^{-1}$ ) en yttrium ( $599.86 \text{ kJ mol}^{-1}$ ) in vergelyking met rodium ( $719.68 \text{ kJ mol}^{-1}$ ). Die groot verskil tussen die eerste ionisasie energie van rodium en yttrium maak yttrium minder geskik as interne standaard vir rodium analises.

Resultate het ook getoon dat rodiumherwinning in die geval van  $\text{RhCl}_3 \cdot x\text{H}_2\text{O}$  deur die gebruik van die kobalt interne standaard beïnvloed word deur die teenwoordigheid van maklik ioniseerbare elemente (MIE), soos alkali metale, asook ongelyke suurkonsentrasie van die standaardoplossings en die analietoplossing. Rodiumherwinnings in die verskillende matrikse het 'n duidelike afname van tussen 2 en 14 % getoon, afhangende van die hoeveelheid alkali-metaal of addisionele suur wat in die monsters teenwoordig was en het duidelik die robuustheid van die metode geaffekteer.

Die eksperimentele resultate vir die rodium analise is verder geverifieer deur verskeie valideringsparameters, wat akkuraatheid, presisie, spesifiekheid, ens. insluit, te



bereken om te bepaal of die nuwe analitiese metode geskik is vir rodium analises met voldoening aan internasionale standaarde. Die akkuraatheid van die metode in terme van rodiumherwinning vanuit die GVM, rodiummetaal en  $\text{RhCl}_3 \cdot x\text{H}_2\text{O}$  is vanaf die herwinningspersentasies van die monsters respektiewelik as 100.01, 99.69 en 99.79 % bereken. Die persentasie rodiumherwinning vir die organometaalverbindings was afhanklik van die suiwerheid van die komplekse en het tussen 81.43 en 99.97 % gewissel, met 'n relatiewe standaardafwyking tussen 0.26 en 1.87 vir al die monsters. Die selektiwiteit en spesifiekheid van rodium in die monsters is bepaal deur die standaardafwyking van die helling ( $s_a$ ) en die standaardafwyking van die afsnit ( $s_b$ ) wat respektiewelik as 0.00029 – 0.00936 en 0.00102 – 0.03338 bereken is. Die onsekerheidwaarde van die kalibrasiekurve (c) het tussen 0.0093 en 0.0795 gewissel. Die metode blyk sensitief te wees vir suurmatrikse en MIE soos bepaal deur die gradiënt (m) van die van die kalibrasiekromme wat tussen 0.2174 en 0.2933 gevarieer het tydens die analise van  $\text{RhCl}_3 \cdot x\text{H}_2\text{O}$ . Die limiet van deteksie (LVD) en limiet van kwantifisering (LVK) vir rodium is respektiewelik as 0.0040865 dpm en 0.040856 dpm bereken en is geskik vir die kwantifisering van rodium in spoorelement konsentrasies. Die reglynigheid van die kalibrasiekromme is vanaf die berekende regressiekoëffisiënt ( $r^2$  en  $r$ ) bepaal en het tussen 0.997 tot 1.00 gevarieer.

Die aanvaarbaarheid van die eksperimentele resultate is met behulp van die  $t$ -statistiese toets, met 'n 95 % betroubaarheidsinterval, bepaal soos wat dit deur die ISO 17025-standaard aanbeveel word. Die berekende statistiese waardes ( $t_{krities}$ ) vir die GVM, rodium metaal,  $\text{RhCl}_3 \cdot x\text{H}_2\text{O}$ ,  $[\text{Rh}(\text{cupf})(\text{CO})_2]$  en  $[\text{Rh}(\text{cupf})(\text{PPh}_3)(\text{Me})(\text{I})]$ , is respektiewelik as -1.12, -0.50, 0.00, 0.00 en -1.60, bereken, wat aanvaarbaar volgens die 95 % betroubaarheidsinterval is. Die resultate wat behulp van hierdie analitiese metode verkry is, het dan ook getoon dat die meerderheid van die eksperimentele metings herhaalbaar is, behalwe waar die matriks-effekte uiters kompleks is en ook wanneer die suiwerheid van die monsters onder verdenking is wanneer.

# Summary

---

The main objective of this research was to establish an analytical method using inductively coupled plasma optical emission spectrometry (ICP-OES) to accurately quantify and optimize the percentage recovery of rhodium. Firstly a CRM was used to establish the effectiveness of the method and then rhodium metal, an inorganic sample and finally different organometallic compounds were analyzed to ensure proper recovery in different matrices.

Quantitative determination of rhodium using cobalt as an internal standard yielded excellent results for the CRM, rhodium metal and  $\text{RhCl}_3 \cdot x\text{H}_2\text{O}$  of 99.0 % + compared to the yttrium internal standard which yielded values in the region of 140.0 %. This difference in percentage recovery was attributed to the differences in the first ionisation energy of cobalt ( $760.41 \text{ kJ mol}^{-1}$ ) and yttrium ( $599.86 \text{ kJ mol}^{-1}$ ) to that of rhodium ( $719.68 \text{ kJ mol}^{-1}$ ). The large ionization energy difference between rhodium and yttrium made yttrium less suitable as an internal standard of rhodium analysis.

Results also indicated that the rhodium recovery in  $\text{RhCl}_3 \cdot x\text{H}_2\text{O}$ , using the cobalt internal standard method, were shown to be influenced by the presence of easily ionized elements (EIE) such as the alkaline metals as well as unmatched acid(s) derived from sample preparation. These matrices were shown to decrease the percentage recovery of rhodium by between 2 to 14 % depending on the amount of acid or alkali metals that were added, which affected the robustness of the rhodium recovery.

The experimental results for the rhodium analysis were validated for a large number of validation parameters, which included accuracy, precision, specificity, *etc.* to confirm whether the newly developed analytical procedure was suitable for the rhodium determination in terms of internationally required standards. The accuracy of the method in the rhodium determination of the CRM, rhodium metal and

---

## Summary

---

$\text{RhCl}_3 \cdot x\text{H}_2\text{O}$ , were determined from the percentage recoveries of rhodium from these samples and calculated as 100.01, 99.69 and 99.79 % respectively. The percentage recovery of rhodium from the organometallic complexes was dependent on the purity of the complexes and the results were shown to vary from 81.43 to 99.97 %, with relative standard deviation (RSD) of between 0.26 and 1.87 for all the samples. The selectivity and specificity for rhodium in these samples were determined by the standard deviation of the slope ( $s_a$ ) and standard deviation of the intercept ( $s_b$ ) and was between 0.00029 – 0.00936 and 0.00102 – 0.03338 respectively. The uncertainties of the calibration curve ( $c$ ) were between 0.0093 and 0.0795. The method was found to be sensitive to the acid matrices and EIE as was determined from the gradient ( $m$ ) of the calibration curve which ranged from 0.2174 to 0.2933 in the determination of rhodium in  $\text{RhCl}_3 \cdot x\text{H}_2\text{O}$ . The rhodium limit of detection (LOD) and limit of quantitation (LOQ) were determined to be 0.0040865 and 0.040865 ppm respectively, which was feasible for measuring trace amounts of rhodium. The linearity of the calibration curve was determined from the regression coefficient ( $r^2$  and  $r$ ) and ranged from 0.997 to 1.00.

Statistical tests of the experimental results were calculated using the hypothesis test of the  $t$ -statistic at 95 % confidence interval to determine whether the results were acceptable as recommended by ISO 17025. The results determined from the CRM, rhodium metal,  $\text{RhCl}_3 \cdot x\text{H}_2\text{O}$ ,  $[\text{Rh}(\text{cupf})(\text{CO})_2]$  and  $[\text{Rh}(\text{cupf})(\text{PPh}_3)(\text{Me})(\text{I})]$  with  $t$  values of -1.12, -0.50, 0.00, 0.00 and -1.60 respectively, were accepted at 95 % confidence interval using the  $t$ -statistic test. The results obtained using this method was shown to be reproducible for all the experimental measurements except in the cases where the matrix effects were very complex and/or the purity of the sample under suspicion.

# 1 Literature survey

---

## 1.1 Discovery of rhodium

Rhodium<sup>1</sup> was discovered in 1803 by an English chemist, William Hyde Wollaston (**Figure 1.1**) from a crude platinum ore he obtained from South America. This took place shortly after his discovery of palladium, while he was busy developing and improving the technology of platinum refining.



**Figure 1.1:** William Hyde Wollaston (1766-1828)

Wollaston called his metal “N-nov<sup>m</sup>”, a Greek word meaning “rose”<sup>2</sup> due to the distinctive red colour of the rhodium salts<sup>3</sup> that he obtained after the separation of platinum and palladium from the ore (**Figure 1.2**). The term “N-nov<sup>m</sup>” is usually found with the motto “Dat Rosa Mel Apibus” a Greek phrase meaning “the rose gives the

---

<sup>1</sup> N. Greenwood and A. Earnshaw, *Chemistry of the elements*, Pergamon Press, Oxford, (1984)

<sup>2</sup> <http://nautilus.fis.uc.pt/st2.5/scenes-e/elem/e04510.html> (cited on 05/07/09)

<sup>3</sup> <http://www.vanderkrogt.net/elements/elem/rh.html> (cited on 05/07/09)

bees honey". The motto was commonly used by 17<sup>th</sup> century Rosicrucian's to represent the rose cross<sup>4</sup> which was the reference for the rhodium colour.

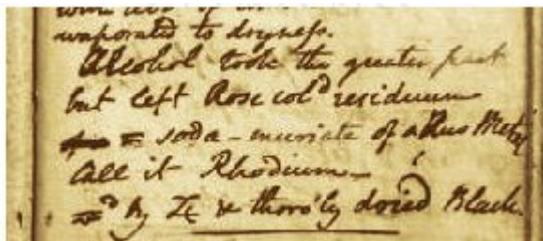


**Figure 1.2:** Fragment of Wollaston's notebook

Figure 1.2 shows a fragment of Wollaston's notebook when he named rhodium<sup>5</sup> in 1804. Translated, it reads as follows:

**My inquiries having terminated more successfully than I had expected, I design in the present Memoir to improve the existence, and to examine the properties, of another metal, hitherto unknown, which may not improperly be distinguished by the name of *Rhodium*, from the rose-colour of a dilution of the salts containing it.**

## 1.2 Occurrence and distribution

Rhodium is a member of the platinum family (group) or commonly called the platinum group metals (PGM)<sup>6</sup> which includes iridium, platinum, osmium and ruthenium. These elements are sometimes divided according to their densities into a heavier triad, comprising platinum, iridium and osmium, and a lighter triad, consisting of palladium, rhodium and ruthenium. This group of metals are occasionally referred to as precious metals due to their high economic value<sup>7,8</sup> and scarcity with respect to worldwide deposits and abundances in the earth's crust (0.001 g/ton).

---

<sup>4</sup> M. Heindel, *Christian Rosenkreuz and the Order of Rosicrucians*, (1908 - 1919)

<sup>5</sup> W. H. Wollaston, *Philos. Trans. R. Soc. London*, (1804), 94, p. 419

<sup>6</sup> F. R. Hartley, *Chemistry of the Platinum group metals*, Elsevier Oxford, (1991), p. 25

<sup>7</sup> W. P. Griffith, *The Chemistry of the Rare Platinum Metals (Os, Ru, Ir and Rh)*, Interscience, London (1967)

The major PGM deposits worldwide are located in South Africa (Gauteng and North West Province), Russia (north of Siberia) and in Canada (Ontario)<sup>9</sup> as shown on the map in **Figure 1.3**.

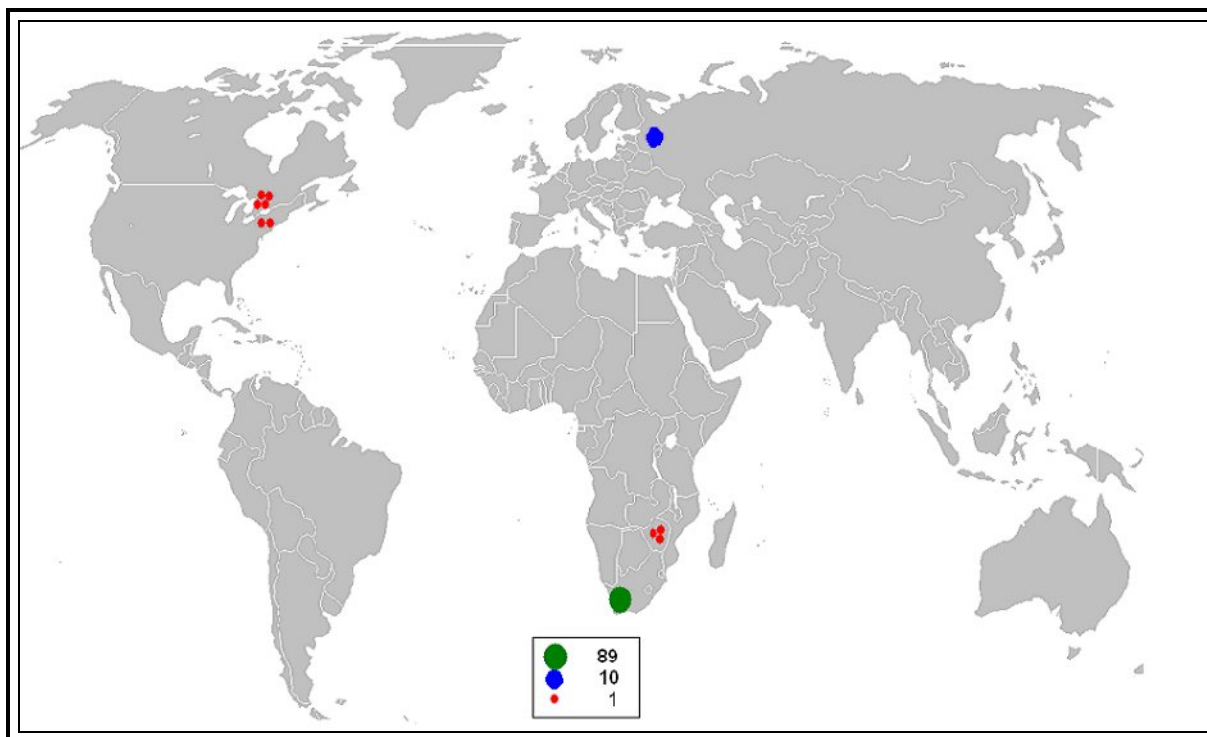


**Figure1.3:** Percentage distribution of PGM across the world<sup>9</sup>

Sperrylite<sup>10</sup> is a platinum arsenide mineral with a general formula  $(Pt, Ir)As_2$  and contains approximately 2 - 4 % Ni, 1.5 - 2.1 % Cu, 5 - 9 % S and differing proportions of mixed PGM. These minerals occurs in a wide array and includes hollingworthite  $(Rh, Pt)AsS$ <sup>11</sup>, Rh-S-rich sperrylite<sup>12</sup>, platarsite  $(Pt, Rh, Ir)AsS$ <sup>13</sup>, isoferroplatinum

---

<sup>8</sup> R. V. Parish, *The metallic elements*, Longman, London, (1977)

<sup>9</sup> [http://en.wikipedia.org/wiki/Platinum\\_group](http://en.wikipedia.org/wiki/Platinum_group) (cited on 05/07/09)

<sup>10</sup> T. L. Grokhovskaya, V. V. Distler, A. A. Zakharov and S. F. Klyunin, I. P. Laputina, *Associations of Platinum-group minerals in the Lakkulaisvaara layered intrusion, northern Karelia. Dokl Akad Nauk.*, (1989), 306, pp. 430 - 434

<sup>11</sup> A. E. Boudreau, E. A. Mathez and I. S. McCallum, *Halogen geochemistry of the Stillwater and Bushveld Complexes: evidence for transport of the platinum-group elements by Cl-rich fluids. J. Petrol.*, (1986), 27, pp. 967 - 986

<sup>12</sup> I. S. McCallum, *Investigations of the Stillwater Complex, part V. Apatites as indicators of evolving fluid composition. Contrib Mineral Petrol.*, (1989), 102, pp. 138 - 153

(Pt,Rh)<sub>3</sub>Fe<sup>14</sup>, cooperite [(Pt,Pd,Ni)S], laurite [RuS<sub>2</sub>], kotulskite [Pd(Te,Bi)], merenskyite [(Pd,Pt)(Te,Bi)<sub>2</sub>], sudburyite [(Pd,Ni)Sb], omeiite [(Os,Ru)As<sub>2</sub>], testibiopalladite [PdTe(Sb,Te)] and niggliite [PtSn]. Sperrylite is normally found in the nickel ore deposit of Canada (Sudbury Basin in Ontario), and in and the Oktyabr'skoye copper-nickel deposit of Russia (Eastern-Siberian region). Both sperrylite and hollingworthite (**Figure 1.4**) occurs in the layered igneous complex of the Bushveld region of South Africa.

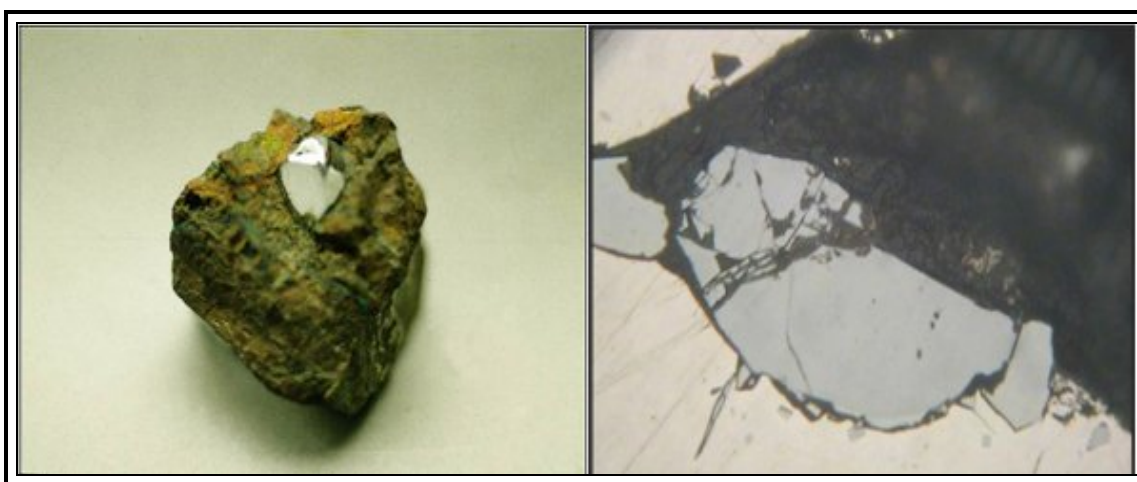


**Figure 1.4:** Sperrylite and Laurite hollingworthite <sup>15</sup>

During the past decade, more than 20 new minerals containing the PGM have been identified from deposits that were obtained in Russia, South Africa and Canada. These discoveries have been of more than general mineralogical interest and they have provided valuable new information on the geological processes involved in the formation of rhodium deposits. These minerals normally occur as small grains (maximum diameter of about 40 micron) which are closely inter-grown with hollingworthite and rhodium rich-sperrylite. Both hollingworthite and sperrylite contains arsenic, sulphur and other PGM in different proportions. Rhodium in

---

<sup>13</sup> V. S. Dokuchaeva, A. A. Zhangurov and Z. A. Fedotov, *Imandrovsky lopolitha - a new large layered intrusion in the Kola Peninsula. Dokl Akad Nauk.*, (1982), 265, pp. 1231 - 1234

<sup>14</sup> R. T. Flynn and C. W. Burnham, *An experimental determination of rare earth partition coefficients between a chloride containing vapor phase and silicate melts. Geochim Cosmochim Acta.*, (1978), 42, pp. 685 - 701

<sup>15</sup> <http://www.mii.org/Minerals/photoplat.html> (cited on 15/07/09)

hollingworthite varies between 20 - 30 % whilst in Rh-rich sperrylite it ranges from 10 - 15 %.<sup>16</sup>

South Africa contains the world's largest known PGM deposits and is the principal exporter of these precious metals, exporting close to 60 % of the world's supply.<sup>17</sup> The annual world production of rhodium is estimated between 22 000<sup>18</sup> and 25 000 kg, according to the Principal Metals Online website.<sup>19</sup>

In 2006, South Africa's known reserve base of PGM represented 87.7 % of the world total reserves (**Table 1.1**). The pie chart (**Figure 1.5**) shows the global distribution of PGM output in 2006 as a percentage of the top producer.<sup>20</sup>

**Table 1.1:** Predicted world reserves of PGM in 2006

Country	Reserve base		
	Kilograms (x1000)	%	Rank
South Africa	70 000	87.7	1
Russia	6 600	8.3	2
USA	2 000	2.5	3
Canada	390	0.5	4
Other	850	1.1	-
<b>TOTAL</b>	<b>79 840</b>	<b>100.0</b>	

---

<sup>16</sup> S. H. U. Bowie and K. Taylor, *A system of ore mineral identification*, *Mining Mag.*, (1996), pp. 337 - 345

<sup>17</sup> J. Matthey, *Platinum 2004*; *Matthey Public Limited Company*, (2004)

<sup>18</sup> <http://seekingalpha.com/article/158115-rhodium-the-most-precious-precious-metal> (cited on 17/09/09)

<sup>19</sup> [www.kitco.com](http://www.kitco.com) (cited on 16/08/09)

<sup>20</sup> <http://www.mineweb.com/mineweb/view/mineweb/en/page35?oid=81154&sn=Detail> (cited on 22/07/09)



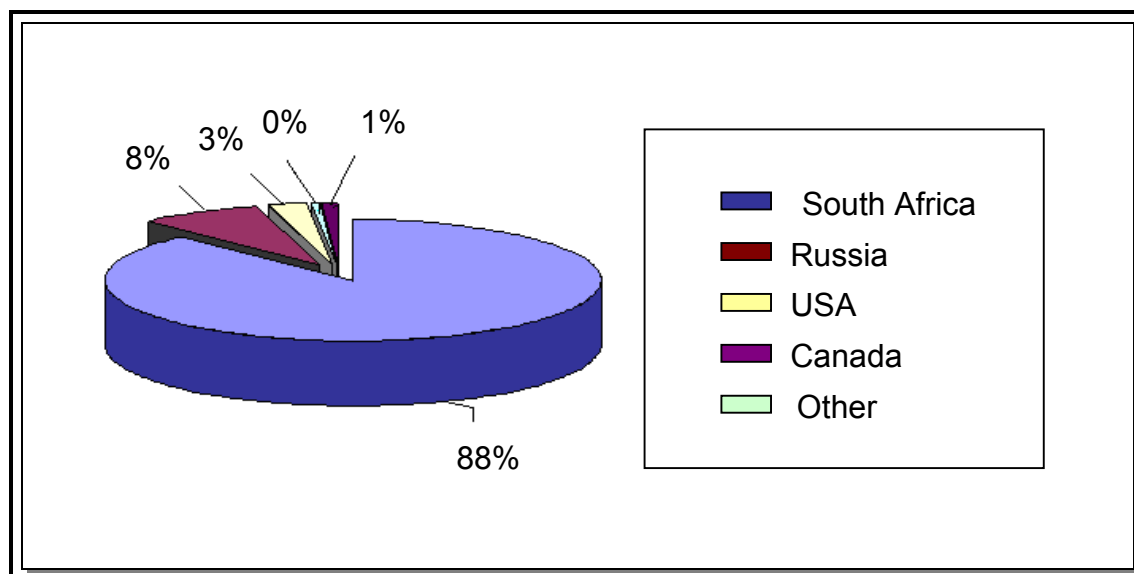


**Figure 1.5:** Percentage of the world supply of PGM in 2006

## 1.3 Sources of rhodium

### 1.3.1 Extraction of rhodium from the ore

In South Africa, rhodium ore deposits are found mainly in the three layered suits of the Bushveld Igneous Complex (BIC). The Bushveld complex is the world's largest mafic-ultramafic layered intrusion and encompasses the Limpopo and part of the North West Province. BIC is an igneous (volcanic) intrusion in the earth's crust that was formed when the molten rock solidified in layers before reaching the earth's surface. The first layer consists of the volcanic rocks, followed by both the basaltic magma and the intrusive basalt that solidified before reaching the earth's surface. These intrusions were brought near or on the earth's surface through erosion to form what appears as the edge of a great geological basin.<sup>21</sup> These three layered suites are the Merensky reef (0.3 to 0.9 m in thickness), the Upper Group 2 reef, UG2 (18 m to 36 m) and the Plat reef (275 m) as shown in (**Figure 1.6**).

---

<sup>21</sup> <http://geosphere.geoscienceworld.org/cgi/content/extract/2/7/352> (cited on 17/09/09)

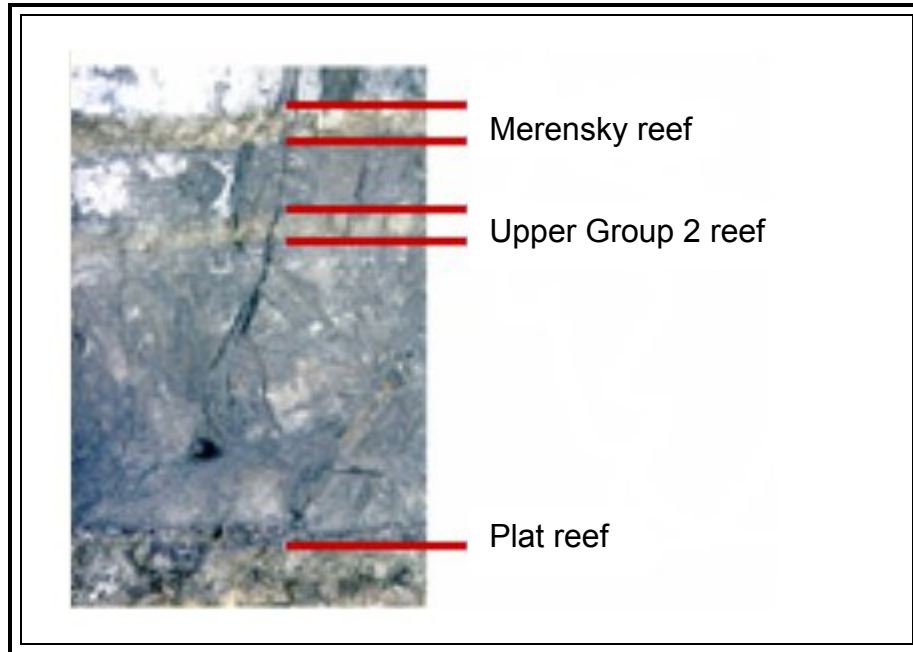


**Figure 1.6:** Cross section through the Bushveld Igneous Complex (BIC).

The Merensky and the UG2 reefs contain approximately (90 %) of the world's PGM reserves. Intensive mining activities (**Figure 1.9**) are taking place in this area as illustrated by **Figure 1.7**, which shows the distribution of the PGM mines in the Merensky reef. A comparison of the PGM output between the Merensky and the UG2 reefs is shown in **Figure 1.8**.

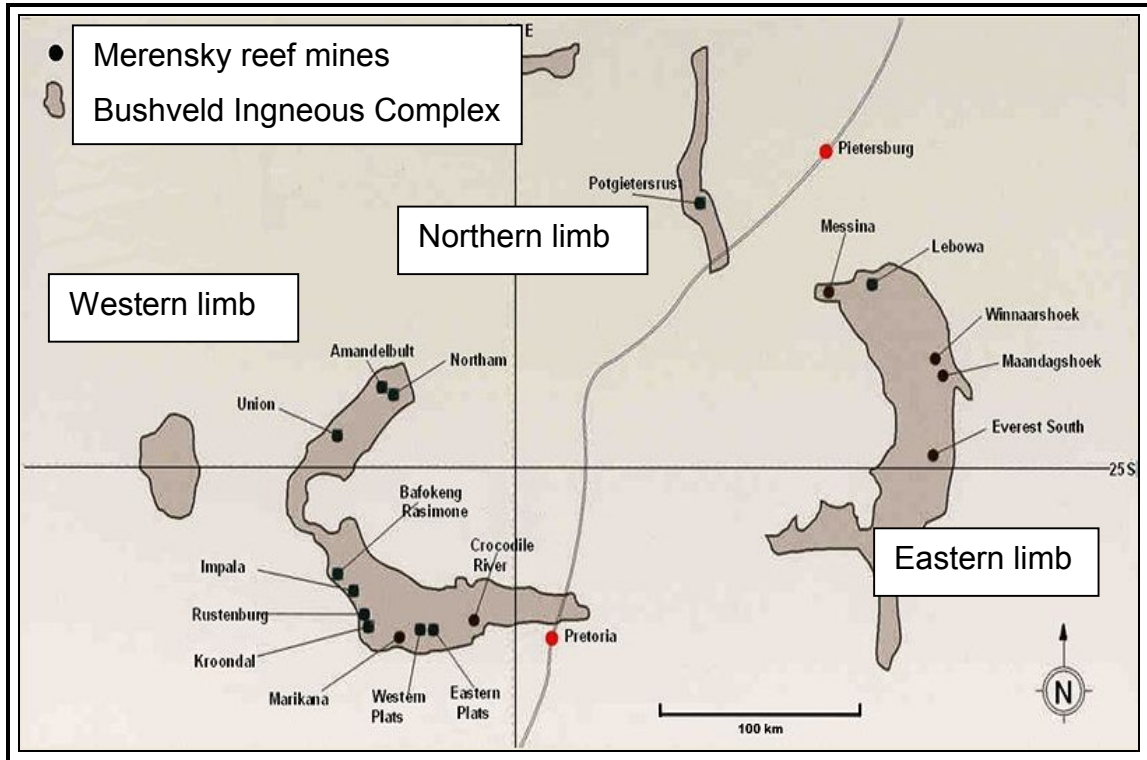


**Figure 1.7:** The Bushveld Igneous Complex showing the Merensky reef mines.<sup>22</sup>

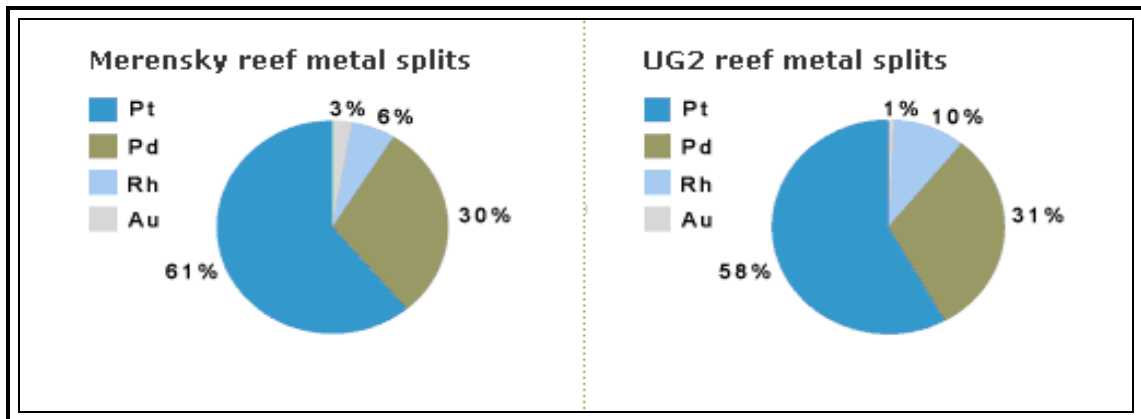


**Figure 1.8:** Comparison of PGM output between the Merensky and the UG2 reefs.<sup>23</sup>

<sup>22</sup> [http://en.wikipedia.org/wiki/Bushveld\\_Igneous\\_Complex](http://en.wikipedia.org/wiki/Bushveld_Igneous_Complex) (cited on 27/08/09)

<sup>23</sup> [http://www.northam.co.za/business/merensky\\_ug2\\_reef.htm](http://www.northam.co.za/business/merensky_ug2_reef.htm) (cited on 27/08/09)



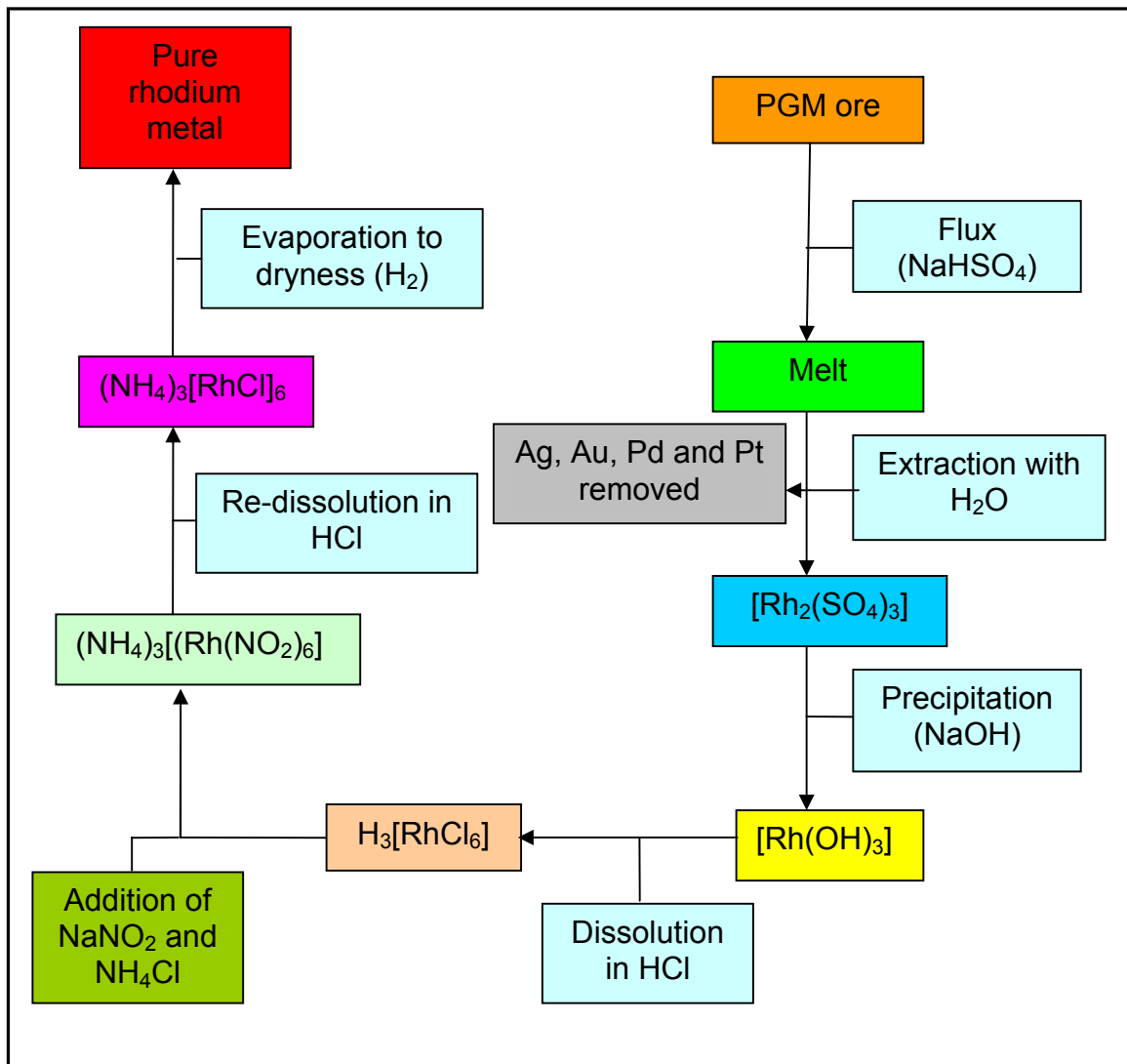
**Figure 1.9:** Open pit PGM mine near Rustenburg<sup>24</sup>

The separation and purification of rhodium from other platinum group metals represent the most difficult aspects in platinum metals purification. The poor extractability of rhodium is mainly ascribed to the very inert nature of chloridocomplexes of rhodium towards ligand substitution reactions with extracting agents, as well as their labile character towards aquation.<sup>25</sup> Due to the difficulties of rhodium extraction, it is usually the last metal recovered (**Figure 1.10**) and refined in most precious metals separation schemes, as shown in **Scheme 1.1**.

---

<sup>24</sup> <http://www.nuwireinvestor.com/articles/rhodium-investment-the-rarest-of-precious-metals-51515.aspx> (cited on 29/08/09)

<sup>25</sup> E. Benguerel, G. P. Demopoulos and G. B. Harris, *Hydrometallurgy*, (1996), 40, pp. 135 - 152



Scheme 1.1: Rhodium extraction from the PGM ore<sup>26</sup>

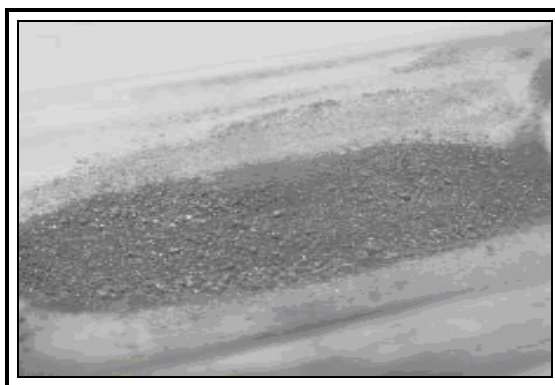
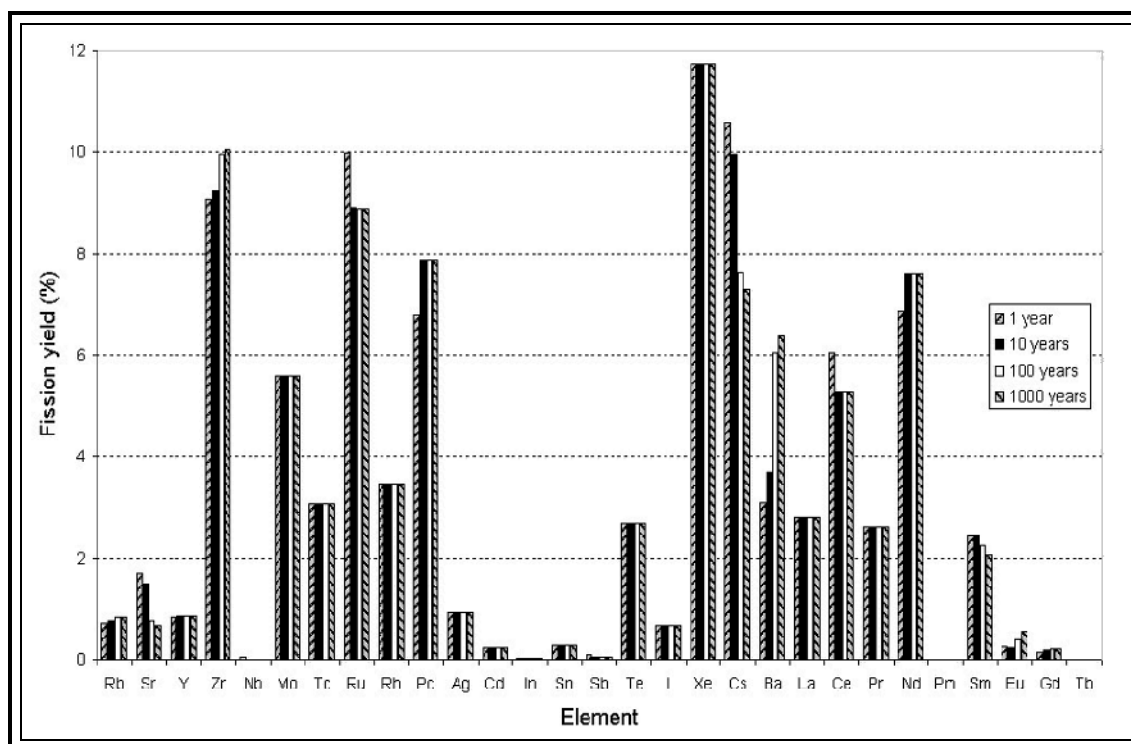


Figure 1.10: Powdered rhodium metal

<sup>26</sup> <http://www.hcrosscompany.com/precious/rhodium.htm> (cited on 29/08/09)

### 1.3.2 Alternative source of rhodium from spent nuclear fuel

Rhodium can also be extracted from used nuclear fuel which is no longer useful in sustaining of a nuclear reactor.<sup>27</sup> During the fission reaction the unstable uranium nuclei is fragmented into a large number of new elements which are given in **Figure 1.11**. These elements include the formation of the PGM (including their different isotopes) with up to 0.133 kg of rhodium from 1 kg of spent nuclear fuel.



**Figure 1.11:** Products of uranium nuclear fission

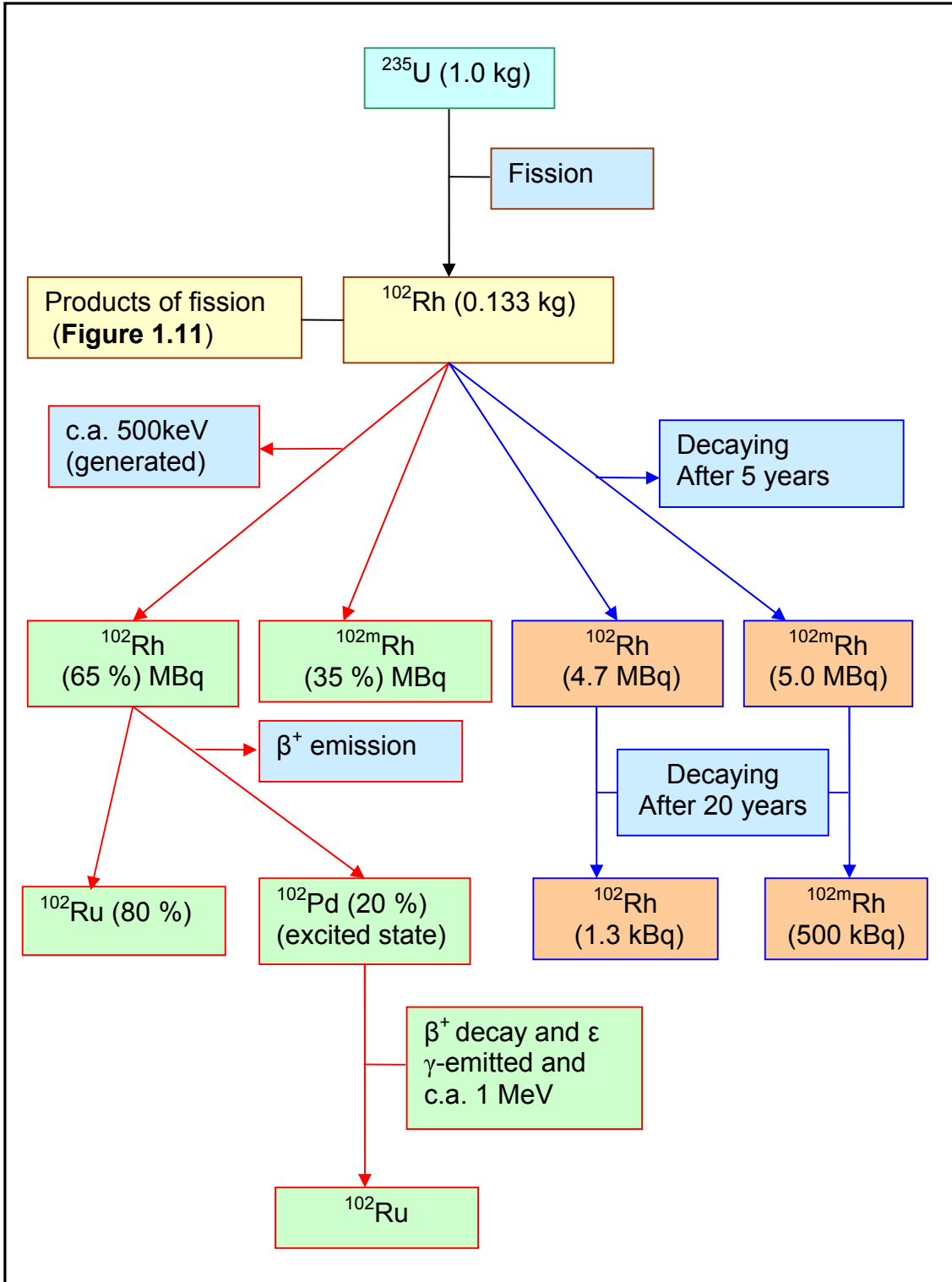
The rhodium which is formed in this reaction is represented by at least seven different isotopes as indicated in **Table 1.2**. The longest lived radioisotope of rhodium is  $^{102m}\text{Rh}$  and has a half life of 2.9 years, while that in the ground state ( $^{102}\text{Rh}$ ) has a half life of 207 days. If nuclear fuel is allowed to stand for more than five years,<sup>28</sup> much of the rhodium will decay leaving 4.7 megabecquerel (MBq) of  $^{102}\text{Rh}$  and 5.0 MBq of  $^{102m}\text{Rh}$ . If the rhodium metal was left for 20 years after fission (approximately 7 half lives), then the 13.3 g of rhodium metal would contain 1.3 kBq

<sup>27</sup> <http://www.chemurope.com/lexikon/e/Rhodium/> (cited on 01/09/09)

of  $^{102}\text{Rh}$  and 0.5 MBq of  $^{102\text{m}}\text{Rh}$  as shown in **Scheme 1.2**. This is approximately  $1.35 \times 10^{-3}$  Ci which means that the radioactive rhodium has decayed to the levels which are extremely low and almost at levels which are acceptable to be used for industrial processes. The big drawback of this process is the possible excessive exposure to high nuclear radiation during the separation of the rhodium from other radioactive metals, which render this alternative rhodium source as impractical with the current technology.

---

<sup>28</sup> [http://en.wikipedia.org/wiki/Synthesis\\_of\\_precious\\_metals](http://en.wikipedia.org/wiki/Synthesis_of_precious_metals) (cited on 17/09/09)



**Scheme 1.2:** Fission of uranium and the subsequent fission of rhodium<sup>29</sup>

<sup>29</sup> <https://www.kitcomm.com/showthread.php?t=9476> (cited on 27/09/09)



**Table 1.2:** Different rhodium isotopes generated during nuclear fission.

<b>*Selected isotopes of rhodium</b>					
<b>Isotope</b>	<b>NA</b>	<b>Half-life</b>	<b>DM</b>	<b>DE-(MeV)</b>	<b>DP</b>
<sup>99</sup> Rh	syn	16.1 days	ε	-	<sup>99</sup> Ru
			γ	0.089; 0.353; 0.528	-
<sup>101m</sup> Rh	syn	4.34 days	ε	-	<sup>101</sup> Ru
			IT	0.157	<sup>101</sup> Rh
			γ	0.306; 0.545	-
<sup>101</sup> Rh	syn	3.3 years	ε	-	<sup>101</sup> Ru
			γ	0.127; 0.198; 0.325	-
<sup>102m</sup> Rh	syn	2.9 years	ε	-	<sup>102</sup> Ru
			γ	0.475 ; 0.631; 0.697; 1.046	-
<sup>102</sup> Rh	syn	207 days	ε	-	<sup>102</sup> Ru
			β+	0.826; 1.301	<sup>102</sup> Ru
			β-	1.151	<sup>102</sup> Pd
			γ	0.475; 0.628	-
<sup>103</sup> Rh	100%	Rhodium is stable with 58 neutrons			
<sup>105</sup> Rh	syn	35.36 hours	β-	0.247; 0.260; 0.566	<sup>105</sup> Pd
			γ	0.306; 0.318	-

\*See list of abbreviations

## 1.4 Economic value

Rhodium is extremely expensive due to the demand and supply constraint in the world's market and its price has been steadily increasing since 2003 according to the metal dealer Kitco Precious Metals (KPM)<sup>19</sup> (see **Figure 1.12** and **Table 1.3**). In a five-year span beginning from 2003, rhodium had an average price of

\$3,224.51/oz (ounce), climbing higher than \$9,000/oz between January and April of last year (2008). Expectations are that rhodium will keep outpacing other precious metals e.g. platinum (**Figure 1.12**) in price as its use in diesel and non-diesel catalytic converters is expected to continue in the near future. Johnson Matthey<sup>30</sup> predicts that South Africa will benefit much more from the ever skyrocketing prices of rhodium than from gold as a result of the supply shortages and the increase in demand of this commodity (see **Table 1.3**).

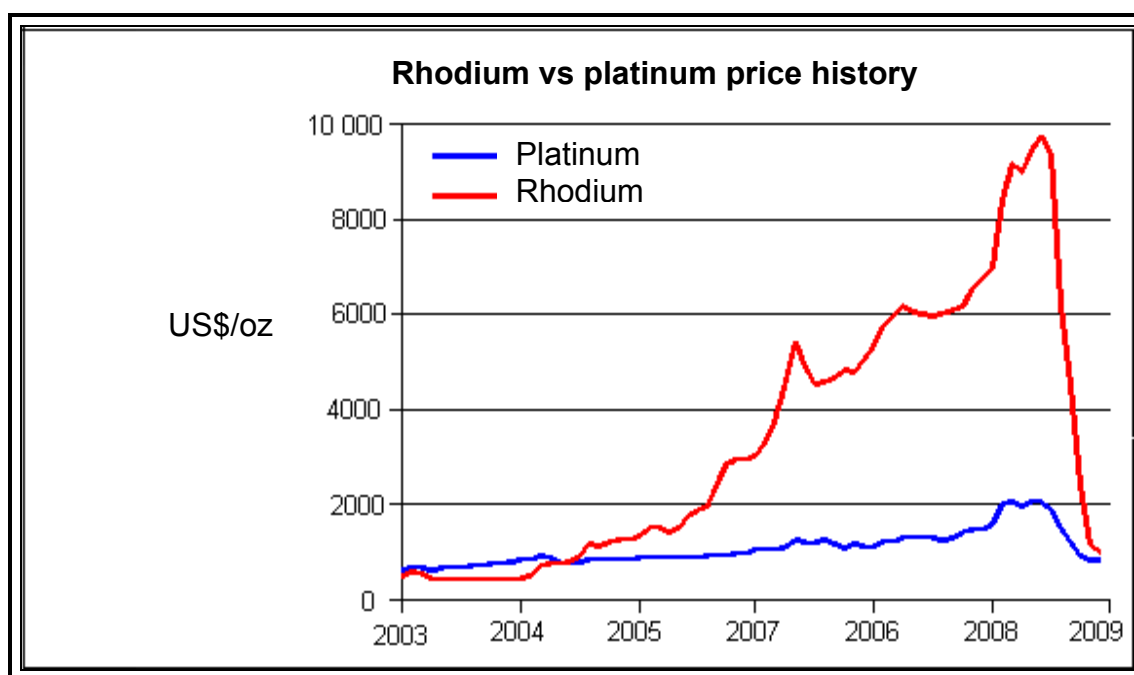


**Figure 1.12:** Comparison of rhodium and platinum price for the past 5 years<sup>31</sup>

One of the main drives in the rhodium price is the demand and consumption of rhodium by the U.S. automobile industry. The total global supply of rhodium together with the 3.5 tonnes of rhodium obtained from recycling (2003 value)<sup>31</sup> is not sufficient to satisfy the current annually demand of the market. Rhodium demand by China and other European countries is also expected to increase due to the high usage of the metal in the automobile and jewellery industry. The overall demand of the PGM over the past three decades is shown in **Figure 1.13**.

---

<sup>30</sup> <http://www.matthey.com/> (cited on 30/08/09)

<sup>31</sup> Platinum 2004, Johnson Matthey Public Limited Company (2004)

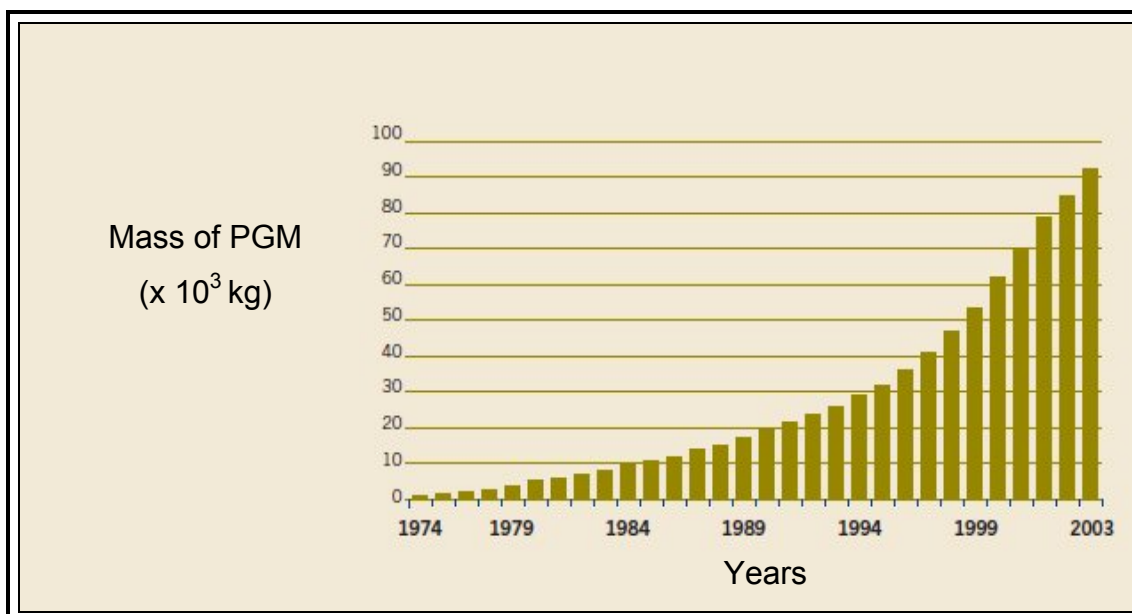


**Figure 1.13:** Cumulative growth of PGM purchases (1974 to 2003).<sup>32</sup>

The trend in PGM demand has been consistent for more than a decade and these significant changes in rhodium demand have led to the skyrocketing of the rhodium price. Rhodium demand has been outpacing the growth in supply by 1.2 % in 2006, to a record level of approximately  $24 \times 10^3$  kg, as seen in **Table 1.3**, boosted by increasing uptake of the metal for use in automotive and manufacturing industries.

## 1.5 Applications and uses of rhodium

Rhodium has a number of interesting applications in industry, ranging from the making of expensive jewellery to the use as an effective catalyst in a number of important industrial processes for the large scale synthesis of organic compounds. Rhodium is also used as an alloying agent for hardening and improving the corrosion resistance<sup>33</sup> of platinum and palladium. These alloys are used in furnace windings, bushings for glass fibre production, electrodes for aircraft spark plugs, laboratory

<sup>32</sup> [http://www.platinum.matthey.com/uploaded\\_files/Pt2004/30%20Years%20of%20Autocats.pdf](http://www.platinum.matthey.com/uploaded_files/Pt2004/30%20Years%20of%20Autocats.pdf) (cited on 17/09/09)

<sup>33</sup> S. S. Cramer and J. C. Bernard, *Materials Park*, ASM International., (1990), pp. 393 - 396

crucibles<sup>34</sup> and thermocouple elements. A wire alloyed with 10 % rhodium and 90 % platinum forms an excellent thermocouple for measuring high temperatures in an oxidizing atmosphere.<sup>35</sup>

**Table 1.3:** Rhodium supply and demand figures for the period 2004 – 2006<sup>36</sup>

<b>Rhodium supply</b>			
<b>Countries</b>	<b>2004</b> (x1000) kg	<b>2005</b> (x1000) kg	<b>2006</b> (x1000) kg
South Africa	16.641	17.775	19.561
Russia	2.835	2.551	2.693
North America	0.482	0.567	0.567
Others	0.454	0.482	0.539
<b>Total supply</b>	<b>20.411</b>	<b>21.376</b>	<b>23.360</b>
<b>Rhodium demand</b>			
Auto-industry	17.520	23.502	24.607
Chemical	1.219	1.361	1.361
Electrical	0.227	0.283	0.255
Glass	1.304	1.616	1.701
Other	0.397	0.567	0.624
<b>Total Demand</b>	<b>20.667</b>	<b>23.445</b>	<b>23.729</b>
Supply versus Demand	Supply deficit of 0.255	Supply deficit of 2.070	Supply deficit of 0.369

Rhodium also provides a shiny hard surface when applied as a coating to other metals and is used in jewellery and other decorative applications as a finisher as

---

<sup>34</sup> R. D. Lide, *Reference book of chemical and physical data*. Boca Raton, CRC Press., (2004), pp. 4 - 26

<sup>35</sup> <http://www.britannica.com/EBchecked/topic/501671/rhodium> (cited on 17/09/09)

<sup>36</sup> [http://www.platinum.matthey.com/uploaded\\_files/2007/07\\_other.pdf](http://www.platinum.matthey.com/uploaded_files/2007/07_other.pdf) (cited on 30/09/09)

shown in **Figure 1.14**. Plated rhodium is very hard and has a high reflectance, which makes it also useful for optical instruments and provides resistance to tarnish for the protection of reactive metals such as sterling silver,<sup>37</sup> Fe and Al. It is also used in high quality pen surfaces due to its high chemical and mechanical resistance. These pens include Graf von Faber-Castell<sup>38</sup> and Caran D'ache.<sup>39</sup>



**Figure 1.14:** Rhodium plated jewellery

In 1979 the Guinness Book of World Records gave Paul McCartney a rhodium-plated coin like disc for being history's all-time best-selling songwriter and recording artist. Guinness has also noted items such as the world's "Most Expensive Pen" or "Most Expensive Board Game" as containing rhodium.<sup>40</sup>

Rhodium plays a major role in the car manufacturing industry where it is used as a catalytic converter to effectively converts  $\text{NO}_x$  (mainly NO and  $\text{NO}_2$ ) to harmless nitrogen with little or no ammonia formation.<sup>41</sup> It also plays a major role in industrial chemical production processes where it is used as catalysts e.g. in the Monsanto

---

<sup>37</sup> [http://sterling\\_silver.totallyexplained.com/](http://sterling_silver.totallyexplained.com/) (cited on 17/09/09)

<sup>38</sup> <http://faber-castell.totallyexplained.com/> (cited on 17/09/09)

<sup>39</sup> [http://caran\\_d\\_ache\\_company.totallyexplained.com/](http://caran_d_ache_company.totallyexplained.com/) (cited on 17/09/09)

<sup>40</sup> <http://www.reference.com/browse/wiki/Rhodium> (cited on 30/08/09)

<sup>41</sup> K. C. Tailor, *Catal. Rev. Sci. Eng.* (1993), 35, p. 457

process (**Figure 1.15**) for the catalytic carbonylation of methanol to produce acetic acid.

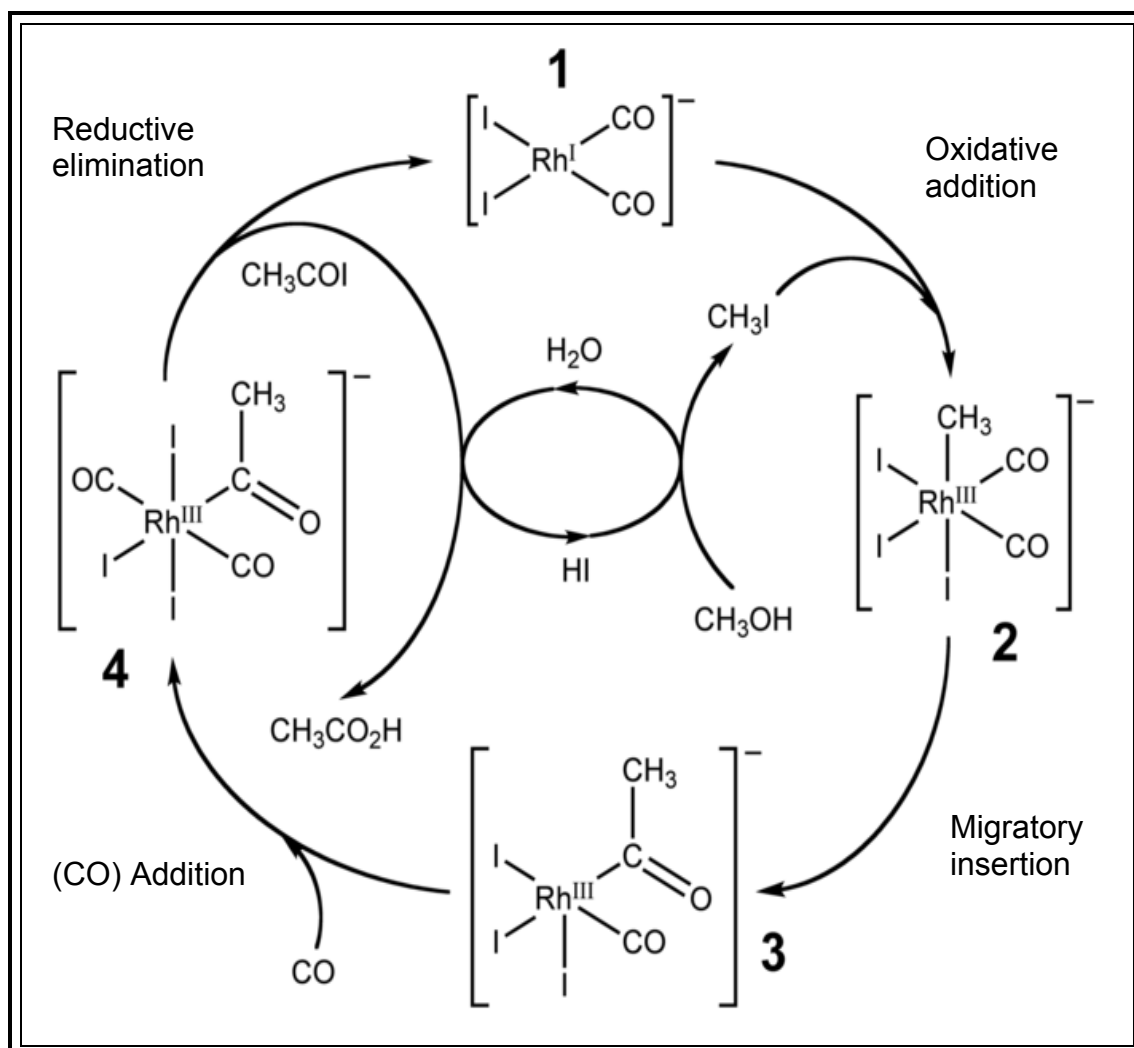


**Figure 1.15:** Use of rhodium in the Monsanto process<sup>42</sup>

In the Monsanto process, methanol is converted to acetic acid *via* a four step pathway catalysed by the active rhodium anion,  $\text{cis}-[\text{Rh}(\text{CO})_2\text{I}_2]^-$ . The first step is the oxidative addition of methyl iodide to  $\text{cis}-[\text{Rh}(\text{CO})_2\text{I}_2]^-$  to form the hexacoordinate Rh(III) species  $[(\text{CH}_3)\text{Rh}(\text{CO})_2\text{I}_3]^-$ . This anion rapidly transforms, *via* the migration of a methyl group to the carbonyl ligand, affording the pentacoordinate acetyl Rh(III) complex  $[(\text{CH}_3\text{CO})\text{Rh}(\text{CO})\text{I}_3]^-$ . The five-coordinate complex then reacts with carbon monoxide to form a six coordinate dicarbonyl complex which decomposes by reductive elimination to form the acetic acid iodine compound ( $\text{CH}_3\text{COI}$ ) and

regenerate the active form of the Rh(I) catalyst. Acetyl iodide is then hydrolyzed to acetic acid in the last phase of the process.

Rhodium catalysts also exhibit the scope and versatility that probably are unmatched by many other elements.<sup>43</sup> Among the rhodium-catalysed reactions that have received significant attention are the hydrogenation of olefins,<sup>44</sup> including the first commercial asymmetric catalytic process (synthesis of L-3,4-dihydroxyphenylalanine, for the treatment of Parkinson's disease<sup>45,46</sup>), hydrogenation of arenes,<sup>47</sup> hydroformylation of olefins and olefin diene codimerisation.<sup>48</sup> The best known example of a rhodium catalyst is the Wilkinson's catalyst chloridotris(triphenylphosphine)rhodium(I), [RhCl(PPh)<sub>3</sub>], which is used in the hydrogenation of alkenes.<sup>49</sup> Another well known catalyst is the Rh(diphosphine) complex commonly known as the Knowles' catalyst, [Rh(PPh)<sub>2</sub>(CO)<sub>2</sub>], which is used in the hydrogenation of enamides.<sup>50</sup>

## 1.6 Physical and Chemical properties

Rhodium is highly reflective, hard and durable, among its numerous other physical characteristics. It is unaffected by oxygen up to 600 °C, but at higher temperatures close to its melting point (1966 °C) it absorbs oxygen from the atmosphere and solidify to form the sesquioxide, Rh<sub>2</sub>O<sub>3</sub>. Rhodium is completely insoluble in nitric acid and dissolves slightly in aqua regia at room temperature, but dissolves completely in boiling concentrated hydrochloric acid and is also attacked by molten alkalis. Some of the major physical and chemical properties are presented in **Table 1.4**.

---

<sup>42</sup> <http://wapedia.mobi/en/File:Monsanto-process-catalytic-cycle.png> (cited on 17/09/09)

<sup>43</sup> J. Halpern, *Chem. Eng. News.*, (2003), 8, p. 114

<sup>44</sup> J. F. Young, J. A. Osborn, F. H. Jardine and G. Wilkinson, *J. Chem. Comm.*, (1965), 7, p. 131

<sup>45</sup> W. S. Knowles and M. J. Sabacky, *J. Chem. Comm.*, (1968), p. 1445

<sup>46</sup> W. S. Knowles, *J. Chem. Ed.*, (1986), 63, p. 222

<sup>47</sup> H. Y. H. Gao and J. Robert, *Angew. Chem., Int. Ed.*, (2000), 39 (4), pp. 622 – 629

<sup>48</sup> R. Cramer, *J. Am. Chem. Soc.*, (1967) 7, pp. 1633 – 1639

<sup>49</sup> J. A. Osborn, F. H. Jardine, J. F. Young and G. Wilkinson, *J. Chem. Soc. A.*, (1966), 526, pp. 175 - 183

<sup>50</sup> X. Y. Huang, R. X. Li, H. Chen and X. J. Li, *Chinese Chemical Letters.*, (2003), 14, pp. 623 – 626

**Table 1.4:** Physical and chemical properties of rhodium metal

Physical properties	
Density ( $\text{g}\cdot\text{cm}^{-3}$ ):	12.41
Melting Point (K):	1966 °C
Boiling Point (K):	3727 °C
Appearance:	silvery-white, hard metal
Atomic Radius (pm):	134
Atomic Volume ( $\text{cc}/\text{mol}$ ):	8.3
Covalent Radius (pm):	125
Ionic Radius:	68 (+3e)
Chemical properties	
Specific Heat (@20 °C $\text{J}/\text{g mol}$ ):	0.244
Fusion Heat ( $\text{kJ}\cdot\text{mol}^{-1}$ ):	21.8
Evaporation Heat ( $\text{kJ}\cdot\text{mol}^{-1}$ ):	494
Electronegativity:	2.28 (Pauling); 1.45 (Allred Rochow)
First Ionizing Energy ( $\text{kJ}\cdot\text{mol}^{-1}$ ):	719.5
Electron affinity (M-M-)/ $\text{kJ}\cdot\text{mol}^{-1}$ :	-162
Incompatibilities:	Chlorine trifluoride, oxygen difluoride
Valence Electron Potential (-eV):	64

### 1.6.1 Crystallographic structure of rhodium

Lattice: Lattice Constant ( $\text{\AA}$ ): 3.800

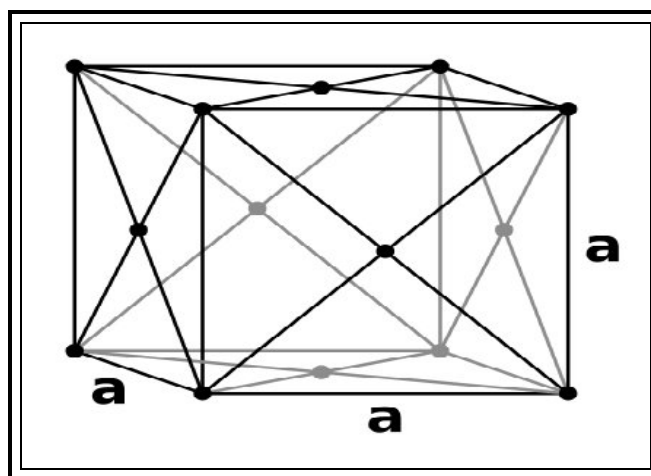


**Figure 1.16:** Face-centered cubic lattice of rhodium metal



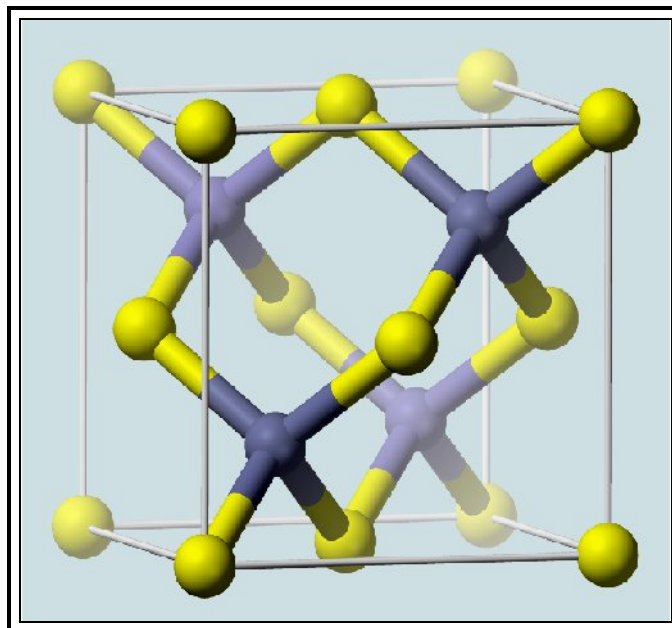


**Figure 1.17:** Molecular model of the lattice structure of the face centered cubic structure of rhodium.<sup>51</sup>

## 1.7 Rhodium chemistry

Rhodium, as a member of the fourth transition metal series has a formal electronic configuration of  $[\text{Ar}]4d^85s^1$ . The most common or stable oxidation states of rhodium is the +1 oxidation state ( $[\text{Ar}]4d^85s^0$ ) with the loss of the 5s electron and the +3 oxidation state ( $[\text{Ar}]4d^65s^0$ ) with the loss of the 5s and two 4d electrons. Another interesting aspect of rhodium chemistry is that octahedral complexes of Rh(III) are all diamagnetic due to the tendency of the  $d^6$  configuration to adopt the low-spin  $t_{2g}^6$  arrangement. Research has shown that rhodium form different inorganic and organometallic complexes with oxidation states ranging from -1 to +5 as shown in **Table 1.5**.

---

<sup>51</sup> <http://en.wikipedia.org/wiki/File:Sphalerite-unit-cell-depth-fade-3D-balls.png> (cited on 30/08/09)

**Table: 1.5:** Examples of compounds with rhodium in different oxidation states.

Oxidation State	Compound
Rh <sup>-I</sup>	[Rh(CO) <sub>4</sub> ] <sup>-</sup>
Rh <sup>0</sup>	[Rh <sub>4</sub> (CO) <sub>12</sub> ]
Rh <sup>I</sup>	[RhCl(PPh <sub>3</sub> ) <sub>3</sub> ]
Rh <sup>II</sup>	[Rh <sub>2</sub> (O <sub>2</sub> CCH <sub>3</sub> )]
Rh <sup>III</sup>	[Rh <sub>2</sub> O <sub>3</sub> ] , [RhF <sub>3</sub> ] , [RhCl <sub>3</sub> ]
Rh <sup>IV</sup>	[RhO <sub>2</sub> ] , [RhF <sub>4</sub> ] , [RhCl <sub>6</sub> ] <sup>2-</sup>
Rh <sup>V</sup>	[RhF <sub>5</sub> ] <sub>4</sub> , [RhF <sub>6</sub> ] <sup>-</sup>

### 1.7.1 Inorganic complexes

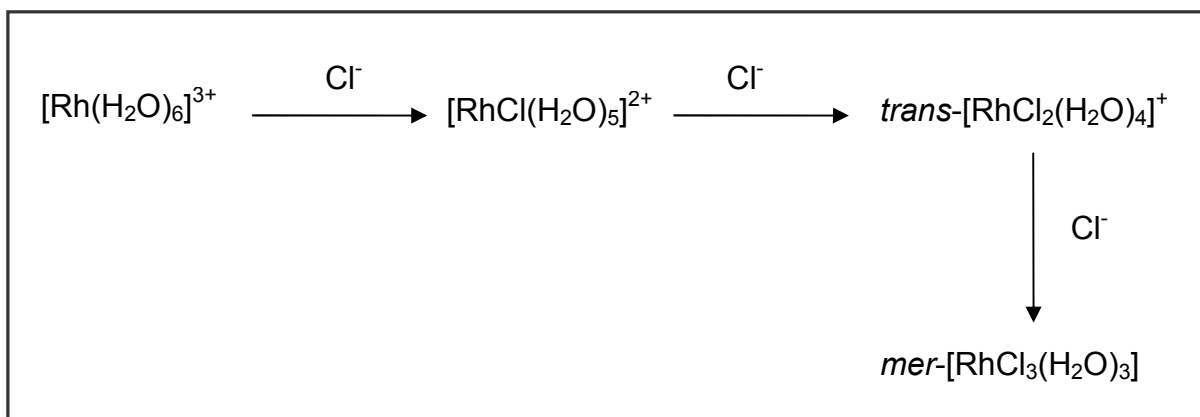
Inorganic complexes in the medium and higher oxidation states, as is the case for the rest of the transition metals, are stabilized by strong electron donating ligands (low end of the electrochemical series) such as oxo, halide and to a lesser extent nitrogen containing ligands. Amongst the vast number of rhodium complexes, a few examples such as [RhCl(PPh<sub>3</sub>)<sub>3</sub>], [Rh(NH<sub>3</sub>)<sub>6</sub>]Cl<sub>3</sub>, [RhH(NH<sub>3</sub>)<sub>5</sub>]SO<sub>4</sub> and [RhH(Cl)<sub>2</sub>(PPh<sub>3</sub>)<sub>3</sub>] (all water insoluble) can be mentioned. Rhodium is said to be the only element in the second or third transition series that possesses a definite, well-characterized aqua ion, which is the stable yellow rhodium hexaqua ion [Rh(H<sub>2</sub>O)<sub>6</sub>]<sup>3+</sup>. The rhodium ion is obtained by dissolution of Rh<sub>2</sub>O<sub>3</sub> (aq) in cold mineral acids, or as the perchlorate by repeated evaporation of HClO<sub>4</sub> solutions of RhCl<sub>3</sub> (aq).<sup>52</sup>

When [Rh(H<sub>2</sub>O)<sub>6</sub>]<sup>3+</sup> is heated with dilute hydrochloric acid, it forms different cationic species such as the yellow [RhCl(H<sub>2</sub>O)<sub>5</sub>]<sup>2+</sup> and [RhCl<sub>2</sub>(H<sub>2</sub>O)<sub>4</sub>]<sup>+</sup> complexes.<sup>53</sup> Further addition of the mineral acid (increase in Cl<sup>-</sup> concentration) results in the formation of the red *cis* and *trans*-[RhCl<sub>3</sub>(H<sub>2</sub>O)<sub>3</sub>] isomers, the two red anions of [RhCl<sub>4</sub>(H<sub>2</sub>O)<sub>2</sub>]<sup>-</sup> and [RhCl<sub>5</sub>(H<sub>2</sub>O)]<sup>2-</sup> and finally the rose-pink anionic complex, [RhCl<sub>6</sub>]<sup>3-</sup>. These

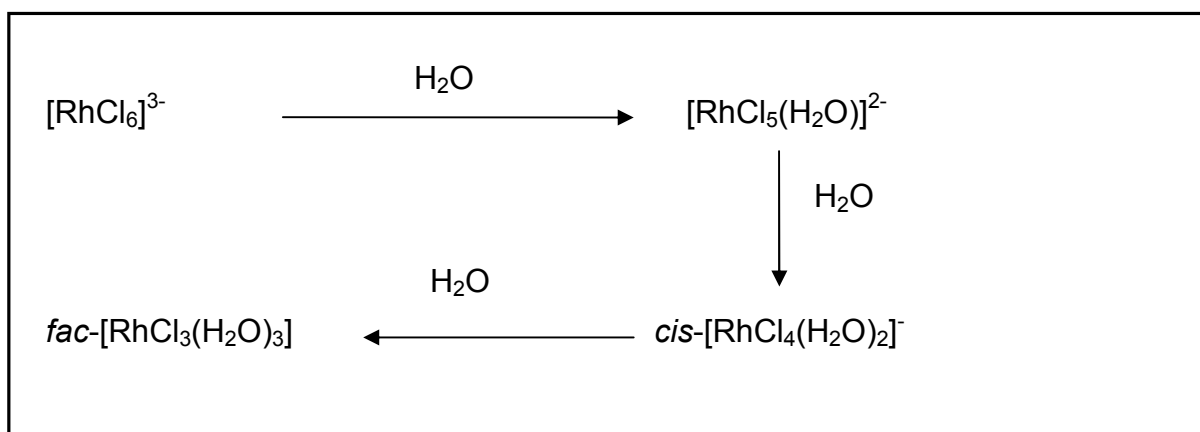
<sup>52</sup> H. Taube, *Rates and Mechanisms of Substitution in Inorganic Complexes in Solution*, *Chem. Rev.*, (1952), 50, pp. 69 – 126

<sup>53</sup> W. C. Wolsey, C. A Reynolds and J. Kleinberg, *Inorg. Chem.*, (1963), 2, p. 463

substitutions are of the form  $[\text{Rh}(\text{H}_2\text{O})_{6-x}\text{Cl}_x]^{(3-x)+}$  and are all believed to follow a dissociative ( $\text{S}_{\text{N}}1$ ) mechanism<sup>54</sup> as indicated in **Scheme 1.3** and *vice versa* (**Scheme 1.4**).



**Scheme 1.3:** Substitution reactions in rhodium aqua-complexes



**Scheme 1.4:** Substitution reactions in rhodium chlorido-complexes

The extent to which each complex exists depends primarily on the chloride concentration, but also, to a lesser degree, on the temperature and the pH of the solution.

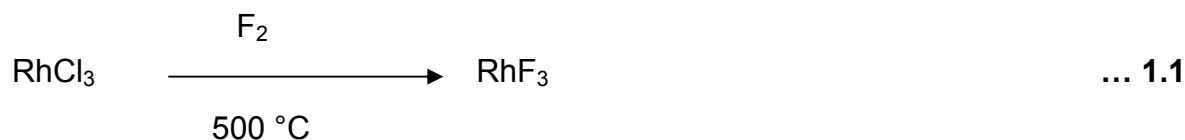
---

<sup>54</sup> S. I. Ginzberg, *Analytical Chemistry of the Platinum Metals*. Wiley, New York., (1975), pp. 102 - 106 and pp. 434 - 458

## 1.7.1.1 Rhodium halides

Rhodium (III) has extensive halide chemistry. The dark red  $\text{RhCl}_3 \cdot x\text{H}_2\text{O}$  is mostly used in the preparation of other rhodium complexes due to its solubility in water and alcohols and is produced by the action of hydrochloric acid on resquioxide ( $\text{Rh}_2\text{O}_3$ ) to form the water-soluble salt. The precise composition of the hydrated specie is most of the time uncertain and varies between 3 and 6 of which 3 or 4 is the most common.<sup>55</sup>  $\text{RhCl}_3 \cdot x\text{H}_2\text{O}$  gives red-brown solutions when dissolved in water or alcohol.

Alternatively, insoluble rhodium trihalides can be hydrolysed by the action of cold mineral acids (e.g. hydrochloric and hydrobromic acid) to form water soluble compounds such as  $\text{RhCl}_3 \cdot x\text{H}_2\text{O}$  and  $\text{RhBr}_3 \cdot x\text{H}_2\text{O}$  respectively, which are both dark red and mildly hygroscopic.  $\text{RhI}_3$  exists as a black powder and is very hygroscopic.<sup>56</sup>  $\text{RhF}_3$  can conveniently be made by the fluorination of rhodium trichloride (**Equation 1.1**).



$\text{RhF}_3$  has a hexagonal close-packed crystal structure (hcp) with both fluorine and rhodium occupying 1/3 of the octahedral holes. Various  $\text{RhF}_3$  hydrates have been reported and include the one shown in **Equation 1.2**.<sup>57,58</sup>



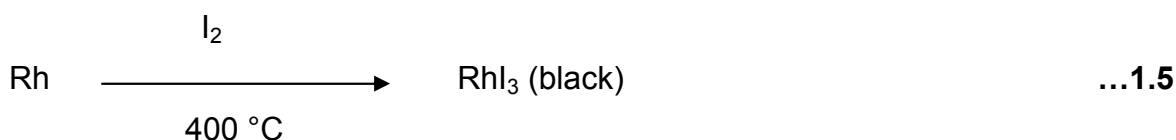
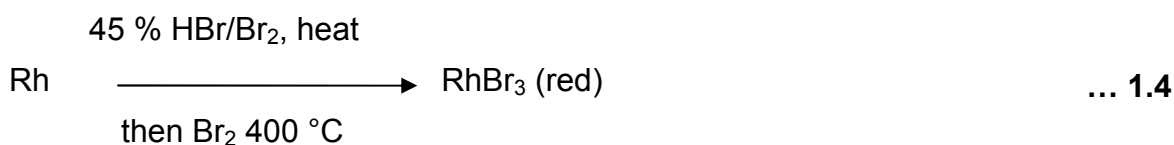
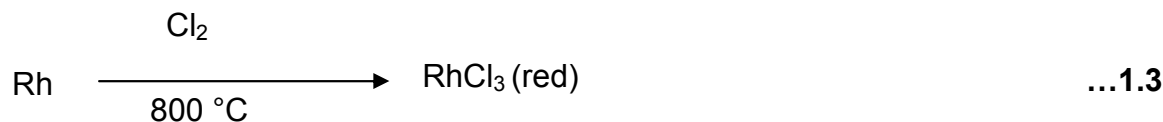
<sup>55</sup> E. Blasius and Z. W. Preetz, *Anorgan and Allegem. Chem.*, (1965), 1, p. 335

<sup>56</sup> <http://www.riyngroup.com/?en-p-d-887.html> (cited on 17/09/09)

<sup>57</sup> <http://www.scribd.com/doc/6792553/638473> (cited on 30/09/09)

<sup>58</sup> <http://www.freepatentsonline.com/5420317.pdf> (cited on 29/09/09)

The formation of other rhodium halide compounds is illustrated in **Equation 1.3 to 1.5**.



The  $\text{RhX}_3$  (where X represents the halide atom) products have the  $\text{AlCl}_3$  cubic close packed layered structure (unconfirmed for  $\text{RhI}_3$ ) with estimated bond lengths of 1.961 Å (Rh-F), 2.337 Å (Rh-Cl) and 2.48 Å (Rh-Br).<sup>59</sup>

### 1.7.1.2 Rhodium oxides

The next important type of rhodium complex is those containing oxygen (oxo) as ligand which stabilises the metal in the high oxidation state and unlike ruthenium and osmium which also belongs to the PGM, Rh forms no volatile oxygen compounds. The known stable oxides include  $\text{Rh}_2\text{O}_3$ ,  $\text{RhO}_2$ ,  $\text{RhO}_2 \cdot x\text{H}_2\text{O}$ ,  $\text{Na}_2\text{RhO}_3$ ,  $\text{Sr}_3\text{LiRhO}_6$  and  $\text{Sr}_3\text{NaRhO}_6$ .

### 1.7.2 Organometallic complexes

An interesting aspect of the organometallic (compounds containing a direct bond between the metal ion and a carbon atom) chemistry of rhodium is the large number of these complexes that exist in the +3 oxidation state which is regarded as a

---

<sup>59</sup> J. Reed and P. Eisenberger, *Structural Crystallography and Crystal Chemistry Acta.*, (1978), 34, pp. 344 - 346

medium oxidation state, while organometallic complexes normally exist with the metal in the low oxidation state. Not surprising is the fact that most of these complexes are stabilized by  $\pi$ -acid ligands (containing electron withdrawing properties) such as CO,  $\text{PR}_3$  and alkenes, which are at the high end of the spectrochemical series, to form complexes such as  $[\text{Rh}(\text{CO})_2(\text{PPh})_2]$ ,  $[\text{Rh}(\text{CO})_4]^-$ ,  $[\text{Rh}(\text{CH}_3)(\text{I})(\text{PPh}_3)_2(\text{CO})_2]$  and  $[\text{Rh}(\text{CH}_3)(\text{CO})_2(\text{I})]$ .

Organometallic complexes of rhodium are normally encountered in the +1 or +3 oxidation state with the lowest known oxidation state of -1.<sup>60</sup> The +3 oxidation state ( $d^6$ ) is probably the preferred state, due to the stability of the low spin  $t_{g2}$  orbital configuration and it generally forms octahedrally coordinated rhodium(III) complexes.<sup>61</sup> Those with the metal in the +1 oxidation state normally has a  $d^8$  electron configuration and their complexes are either four square-planar or five-coordinate trigonal bipyramidal structures e.g.  $[\text{Rh}(\text{acac})(\text{CO})_2]$  and  $[\text{Rh}(\text{CO})_2(\text{PPh}_3)_2\text{I}]$  respectively.<sup>62</sup> The formation of Rh(III) from Rh(I) in a 2 electron oxidation step with the simultaneous addition of methyl iodide is a key step in the catalytic synthesis of acetic acid in Monsanto process. From the same process, researchers have shown that these reactions can be reversible<sup>63</sup> and that the reversibility of such reactions connecting the Rh(I) and Rh(III) oxidation states are responsible for many of the catalytic transformations which are encountered in organorhodium chemistry.<sup>40</sup>

Organometallic complexes of Rh(II) such as  $[\text{Rh}(\eta^5\text{-C}_5\text{Me}_5)_2]$  and  $[\text{Rh}(\eta^3\text{-TMPP})_2][\text{BF}_4]_2$  (TMPP = tris(2,4,6-trimethoxyphenyl)phosphine)<sup>64</sup> with the metal in the high +4 and +5 states are rare due to their instability and mainly appears as intermediates in catalytic reactions.

---

<sup>60</sup> <http://en.wikipedia.org/wiki/Rhodium> (cited on 17/09/09)

<sup>61</sup> F. A. Cotton and G. Wilkinson, *Advanced Inorganic Chemistry, A Comprehensive Text*. Wiley, New York, 4<sup>th</sup> ed. (1980), p. 943

<sup>62</sup> O. Koshevoy, V. Sizova, P. Tunik, A. Lough and A. J. Poë, *Eur. J. of Inorg Chem.*, (2005), 22, pp. 4516 - 4520

<sup>63</sup> R. P. Hughes, *Comprehensive coordination chemistry*, Edited by G. Wilkinson, Pergamon Press, Oxford, (1987), 5, p. 278

<sup>64</sup> K. R. Dunbar and S. C. Haefner, *Amer. Chem Soc.*, (1992), 11, pp. 1431 - 1433

## 1.8 Motivation of this study

For many years, quantitative determination of rhodium in inorganic and organometallic complexes<sup>61-65</sup> has received little attention due to the complexity of the methods involved. One of the main problems associated with rhodium analysis has been the low recovery of the metal from well identified rhodium compounds and this issue has been in the spotlight for over a decade as revealed by many research articles.<sup>65-70</sup> Rhodium recoveries obtained for different organometallic complexes are shown in **Table 1.6**.

**Table 1.6:** Rhodium recovery from different organometallic complexes

Compound	Percentage recovered of other elements				Percentage rhodium recovered
	P	C	H	O	
$\text{RhC}_{25}\text{H}_{25}\text{O}_3\text{PI}^{66}$	102.30	-	-	102.43	98.71
$\text{Rh}_3\text{C}_{29}\text{H}_{33}\text{O}_2\text{Cl}_2\text{N}_6^{67}$	-	103.06	105.57	-	96.85
$\text{RhC}_{50}\text{H}_{43}\text{O}_8\text{P}_2\text{NI}^{68}$	-	99.64	101.99	99.33	99.47
$\text{RhPF}_3\text{IC}_{24}\text{H}_{19}\text{O}_3^{69}$	100.22	104.10	81.89	-	92.33
$\text{RhC}_{28}\text{H}_{28}\text{O}_2\text{NSI}\cdot\text{CH}_3\text{I}^{70}$	101.52	102.69	100.00	-	81.34

-Not quantified

From these results it is clear that the recovery of the non-metals are mostly all well within expectable levels, while those for the rhodium are all well below 100 %. The

<sup>65</sup> C. B. Ojeba and F. S. Rojas, *Talanta*, (2005), 67, pp. 1 - 19

<sup>66</sup> S. S. Basson, J. G. Leipoldt, A. Roodt, J. A. Venter and T. J. Van der Walt, *Inorg. Chim Acta.*, (1986), 119, pp. 35 - 38

<sup>67</sup> J. A. Bailey, S. L. Grundry and S. R. Stobart, *Inorg. Chim Acta.*, (1996), 243, pp. 47 - 56

<sup>68</sup> G. J. Lamprecht, G. J. van Zyl and J. G. Leipoldt, *Inorg. Chim Acta.*, (1989), 164, pp. 69 - 72

<sup>69</sup> S. S. Basson, J. G. Leipoldt and J. T. Nel, *Inorg. Chim Acta.*, (1984), 84, pp. 167 - 172

<sup>70</sup> S. S. Basson, *Mikroanalytisches Labor Pascher HPT 1 and HPT 2*, (1986)

relatively low recovery of the metal in most of these cases raised a two-fold question, namely, (i) is the low recovery due to impure organometallic complexes or (ii) due to poor selectivity, sensitivity and robustness of the analytical methods used to determine the rhodium quantity. In another example it was found that crystals suitable for structure determinations such as the *trans*-Methyliodo-N-benzoyl-N-phenylhydroxyaminobis-(triphenylphosphite)rhodium(III)  $[\text{Rh}(\text{BPHA})(\text{P}(\text{OPh})_3)_2(\text{CH}_3)(\text{I})]$ <sup>64,71</sup> were also analysed and a recovery of less than 97 % was obtained.

Although the introduction of classical spectrometric techniques such as the ICP-OES, ICP-MS, AAS and XRF in the determination of rhodium have been reported, it was found that the accuracy of these techniques are hampered mainly by acid matrix effects, chemical interference<sup>72,73,74</sup> and low detection limits. Research has shown that acid matrix variation are one of the main factors contributing to low rhodium recovery in spectrometric techniques due to the changes in analyte behaviour, while inferior sensitivity and poor selectivity<sup>75</sup> of these techniques at trace levels have resulted in unsatisfactory recoveries (67 to 87 %).<sup>76</sup>

The problem associated with the quantification of rhodium is also demonstrated in the next example. Rhodium used in catalysts such as rhodium hydridocarbonyl tris(triphenylphosphine),  $[\text{HRh}(\text{CO})(\text{PPh}_3)_3]$ , for the hydroformylation of olefins must be reactivated periodically and/or recovered from the by-products for re-use (U.S. Patent 4,390,473). Different techniques of rhodium determination in organometallic and inorganic catalysts, such as the precipitation and the adsorption through ion exchange materials e.g. magnesium silicate, alloying of the rhodium carbonyl catalysts with materials such as mercury and decomposition of the unmodified rhodium carbonyl complexes by heating with aqueous formic acid which dissolves

---

<sup>71</sup> S. S. Basson, J. G. Leipoldt, A. Roodt and J. A. Venter, *Inorg. Chim Acta.*, (1986), 118, pp. 45 - 47

<sup>72</sup> S. Calmotti, C. Dossi, S. Rechia and G. M. Zanderighi, *Spectrosc.Eur.*, (1996), 8, p. 18

<sup>73</sup> R. R. Barefoot, *Anal. Chim. Acta.*, (2004), 509, p. 119

<sup>74</sup> M. Balcerzak, *Anal. Sci.*, (2002), 18, p. 737

<sup>75</sup> F. E. Beamish, *The Analytical Chemistry of the Noble Metals*, Pergamon, Oxford, (1966)

<sup>76</sup> A. Marucco, *Nucl. Instr. Meth. Phys. Res.* (2004), 213, p. 486



the rhodium into the aqueous phase as rhodium formate, have been reported in various articles including the U.S. Patent 4,388,217 and European Patent 255,389. The reported rhodium percentage recoveries were in the range 73 - 95 %.<sup>77, 78</sup>

From these examples it should be clear that the determination of rhodium in inorganic and organometallic complexes has been a difficult task due to the unexpected complexity of the chemistry involved in the analytical methods, as well as the equipment required.<sup>79</sup> Most of the techniques employed in the past involved tedious separation and pre-concentration processes prior to analysis.<sup>80</sup> Determination of rhodium using these techniques was always carried out after chemical separation, which is complicated and time-consuming. Although most of the techniques demonstrated superior sensitivity and detection levels with pure compounds, they were hampered by inaccurate results due to different and mostly unexpected interferences.

The main aim of this study therefore was centered on developing an in-house analytical technique for the quantitative determination of rhodium at trace levels in different inorganic and organometallic compounds.

### 1.9 Aim of this study

The main objective of this research was to:

- Develop an analytical procedure that can accurately determine and quantify rhodium in the metallic state as well as in organometallic and inorganic complexes;
- Establish measurement traceability in analysing a rhodium CRM;

---

<sup>77</sup> <http://www.freepatentsonline.com/4390473.html> (cited on 23/09/09)

<sup>78</sup> <http://www.wipo.int/pctdb/en/wo.jsp?wo=1991008050&IA=US1990006787&DISPLAY=DESC> (cited on 22/09/09)

<sup>79</sup> F. E. Beamish, *Talanta*, (1960), 5, p. 1

<sup>80</sup> W. Gerner and H. Foster, *J. Radioanal. Chem*, (1972), 12, pp. 497 - 504

- Statistically validate these methods;
- Determine the influence of different acids as well as alkali metal ions on the rhodium recovery;
- Optimize ICP-OES operating conditions for the determination of rhodium at trace levels.

# 2 Analytical techniques for rhodium determination - literature survey

---

## 2.1 Introduction

Methods to separate rhodium from other elements in rhodium containing minerals, as well as its quantification, started immediately after its discovery in 1803. Most of the techniques developed at that time were centered on the red colour of the rhodium salts,<sup>81</sup> which were highly distinguished amongst many elements and offered a clear indication of the presence of rhodium.

During the early 1920's rhodium ornaments were used as a symbol of wealth<sup>82</sup> and for trading, due to the novelty of their chrome-like brightness to prospective customers.<sup>83</sup> It was quickly realised that disparity existed between the real and the perceived economic value of these ornaments, which prompted the search for methods to extract, separate and accurately quantify the rhodium content in different samples. Numerous analytical techniques for the determination of rhodium were developed since the late 1950's and most of these were based on spectrophotometric, chromatographic, gravimetric and titrimetric techniques. These techniques were very helpful, but due to the limited knowledge on rhodium chemistry at that stage, researchers were unable to completely separate rhodium from its ores and to establish a reliable method that could accurately quantify rhodium.

---

<sup>81</sup> <http://www.vanderkrogt.net/elements/elem/rh.html> (cited on 05/07/09)

<sup>82</sup> <http://www.christianet.com/bullion/rhodiumbullion.htm> (cited on 27/09/09)

<sup>83</sup> <http://www.artisanplating.com/faqs/rhodiumfaqs.html> (cited on 10/10/09)

The traditional techniques have since been replaced by the development of more modern techniques such as the inductive coupled plasma, including both optical emission (ICP-OES)<sup>84,85</sup> and mass spectrometry (ICP-MS)<sup>86</sup>, atomic absorption spectrometry (AAS)<sup>87,88</sup> and X-ray fluorescence (XRF),<sup>89</sup> which produce very reliable results with detection limits in the parts per million range. A summary of these techniques with respect to their advantages and disadvantages are given in **Table 2.1**.

---

<sup>84</sup> R. A. Conte, J. M. Mermet, J. D. A. Rodrigues and J. L. Martino, *J. Anal. Atomic Spectrometry*, (1997), 12, pp. 1215 - 1220

<sup>85</sup> O. N. Grebneva, I. V. Kubrakova, T. F. Kudinova and N. M. Kuz'min, *Spectrochimica Acta Part B.*, (1997), 52, pp. 1151 - 1159

<sup>86</sup> C. Qing, T. Shibata, K. Shinotsuka, M. Yoshikawa and Y. Tatsumi, *Frontier research on earth evolution*, (2003), 1, pp. 357 - 362

<sup>87</sup> J. M. Scarborough, *Anal. Chem.*, (1969), 41, p. 250

<sup>88</sup> R. C. Mallett, D. C. G. Pearton, E. J. King and T. W. Steele, *J. S. Afr. Anal. Chem.*, (1976), 48, pp. 142 - 174

<sup>89</sup> V. John, I. C. Gilfrich, T. C. Noyan, D. K. Huang, K. Smith, *Advances in X-Ray Analysis*. (1995), 39, p. 137

**Table 2.1:** A summary of different analytical techniques <sup>90</sup>

Technique	Advantages	Disadvantages
<b>ICP-OES/MS</b>	Extremely fast, low level of interference, extensive linear dynamic range, multi element detection, accurate and precise	Solid samples have to be converted into aqueous solutions. Spectral interferences due to molecular species in MS. Spectral interferences due to other elements in OES
<b>AAS</b>	Fast, accurate, well documented	Must have element specific lamps, short linear dynamic range, aqueous solution required
<b>GF-AAS</b>	Fast, extremely accurate, well documented, extremely low detection limits	Must have element specific lamps, very short linear dynamic range, aqueous solution required
<b>XRF</b>	Relatively simple sample preparation, few interferences	Very slow
<b>UV-Vis</b>	Simple to use	Poor in selectivity and sensitivity

The uses of these techniques for rhodium analysis have been reported in various articles<sup>84-89</sup> and some of them have been shown to be suitable for rhodium analysis in the trace and ultra-trace (ppm to ppb) levels.

In order to develop new methods for the accurate determination of rhodium, it is crucial that sufficient information of the old and current techniques be studied to understand the limitations and advantages of these techniques and to be able to recognize possible opportunities for improvement. In this chapter, a general overview of the research that has been done to date in the quantification and determination of rhodium in different samples will be discussed. The selection of an analytical technique(s) for both quantification and dissolution of rhodium will also be discussed in more detail.

---

<sup>90</sup>S. J. Lotter, *Identification and Quantification of Impurities in Zircon, PDZ and other Relevant Zirconium Products*, M.Sc study, University of the Free State (2008), p. 39

## **2.2 Analytical methods used for rhodium analysis**

### **2.2.1 Spectrophotometric methods**

#### **2.2.1.1 Ultraviolet–visible absorption spectrometry (UV-Vis)**

UV-Vis spectrophotometry was historically the first instrumental technique used for the quantification of small amounts of rhodium in various geological materials such as PGM ores (see **Chapter 1, Section 1.2**). The high degree of chemical similarity of PGM, resulting in the formation of complexes of similar composition and properties, was found to limit the direct application of UV-Vis spectrophotometry in the analysis of multi-component samples.<sup>91</sup> Literature showed that in spite of these limitations to this analytical method, various ligands with greater selectivity for rhodium such as *p*-nitrosodimethylaniline,<sup>92</sup> 1-(2-pyridylazo)-2-naphthol,<sup>93</sup> 5-(2-pyridylazo)-*p*-cresol,<sup>94</sup> rhodamine 6G<sup>95</sup> and diphenylcarbazide<sup>96</sup> were employed in the quantification of the metal. In 1982 a very promising bidentate ligand, 2-(5-Bromo-2-pyridylazo)-5-(N-propyl-N-sulphopropylamino) phenol (5-Br-PAPS)<sup>97</sup> was first synthesized by Makino *et al.*<sup>98</sup> It was found that 5-Br-PAPS forms a reddish-violet chelate with rhodium according to the reaction shown in **Figure 2.1**.

---

<sup>91</sup> J. C. Sternberg, H. S. Stillo and R. H. Schwendeman. *Anal. Chem.*, (1960), 32, p. 84

<sup>92</sup> R. B. Wilson and W. D. Jacobs, *Anal. Chem.*, (1961), 33, p. 1654

<sup>93</sup> A. I. Busev, V. M. Ivanov, N. N. Gorbunova and V. G. Cresl, *Tr. Kom. Anal. Khim., Akad. Nauk. SSSR*, (1969), 17, p. 360

<sup>94</sup> G. G. Goroshko, Y. M. Dedkov and A. N. Ernakov, *Zh. Anal. Khim.*, (1978), 33, p. 1114

<sup>95</sup> K. Kalinowski and Z. Marczenko, *Mikrochim. Acta.*, (1985), 1, p.167

<sup>96</sup> K. Sarmah and H. K. Das, *J. Indian Chem. Soc.*, (1985), 62, p. 631

<sup>97</sup> Y. Shijo, K. Nakaji and T. Shimizu, *Analyst*, (1988), 113, pp. 519 - 521

<sup>98</sup> T. Makino, M. Saito, D. Horiguchi and K. Kina, *Clin. Chim. Acta.*, (1982), 120, p.127

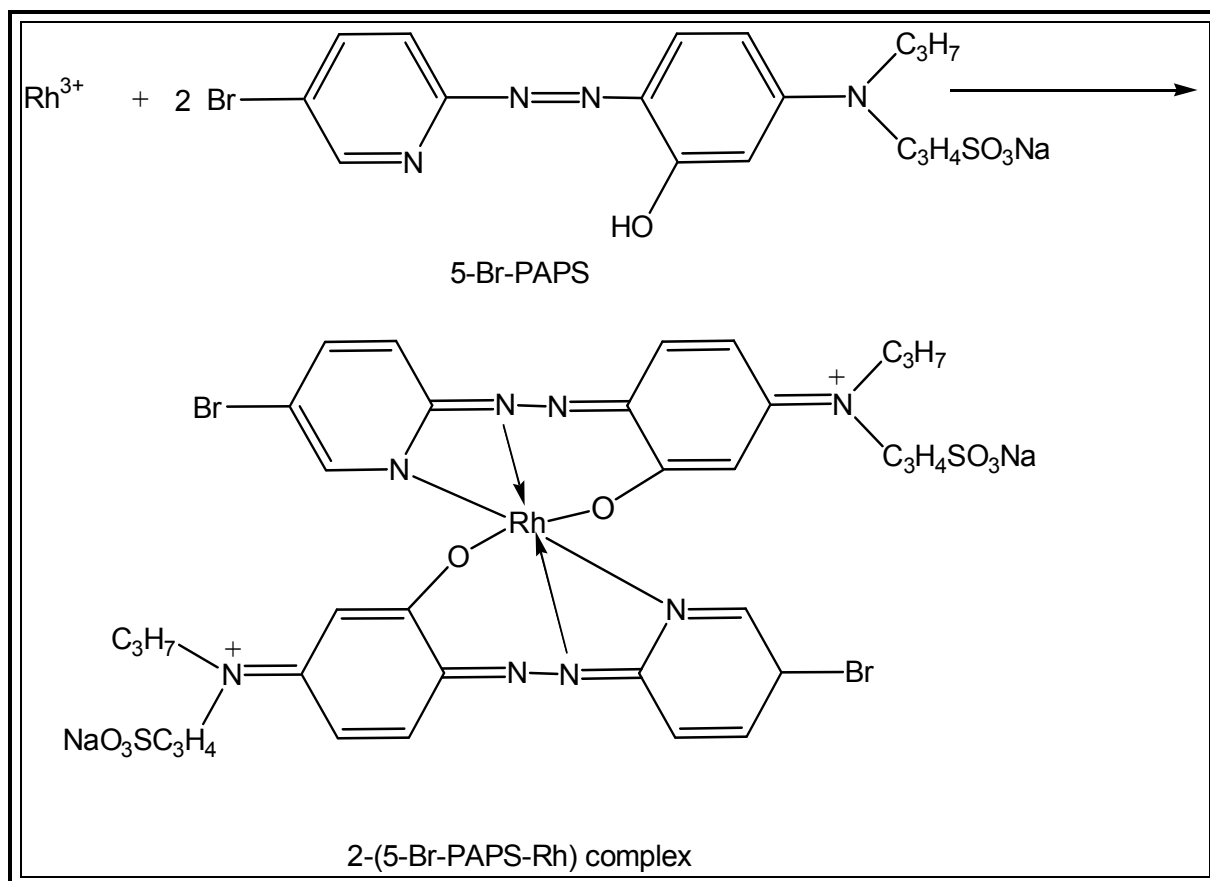


**Figure 2.1:** Complexation of rhodium (III) with 5-Br-PAPS

Organic ligands possessing an extensively delocalized  $\pi$ -electron system, such as BrPBT and EDTA,<sup>99</sup> have been shown to improve the sensitivity and selectivity of the spectrophotometric techniques. The major drawback of these methods is the long time (ca.1 h) required for the full colour development.

Makino *et al* demonstrated that 5-Br-PAPS reacts with rhodium(III) in the ratio 1:2 (metal:ligand) at 95 °C to form a water-soluble complex which has a molar absorptivity of  $1.09 \times 10^5 \text{ mol}^{-1} \text{ cm}^{-1}$  at 600 nm. 5-Br-PAPS was found to have comparable chelating properties to 4-(2-pyridylazo)resorcnol (PAR), but was more sensitive than (PAR), which has a molar absorptivity of  $1 \times 10^4 \text{ mol}^{-1} \text{ cm}^{-1}$  at 600 nm.<sup>100</sup> In 1983, 5-Br-PAPS was used for the first time in the spectrophotometric

<sup>99</sup> Y. Shijo, K. Nakaji and T. Shimizu, *Analyst*, (1988), 13, pp. 519 - 521

<sup>100</sup> K. S. Krishna, V. A. Badri, and K. D. Arun, *Microchim Acta.*, (1969), 4, pp. 694 - 697

determination of cobalt(II),<sup>101</sup> nickel(II) and ruthenium(III),<sup>102</sup> which later turned out to be a more sensitive reagent for the spectrophotometric determination of rhodium(III). It was also found that the rhodium(III)-5-Br-PAPS complex is extremely stable and that the addition of EDTA does not replace the bidentate ligand, as was the case for metals such as Co, Ni, Ru, V and Zn. In fact, it was found that the colour intensity of the Rh(III) complex increases with the addition of EDTA.<sup>99</sup>

Research has also revealed that selectivity in the spectrophotometric determinations of rhodium can be achieved/enhanced by the use of other masking agents such as N- $\alpha$ -(5-bromopyridyl)-N'-benzoyl thiourea (BrPBT)<sup>103</sup> and EDTA.<sup>104</sup> In a study performed by Das *et al.*<sup>103</sup> it was found that N- $\alpha$ -(5-bromopyridyl)-N'-benzoyl thiourea (BrPBT) (**Figure 2.2**) reacts strongly as chelating ligand, which allows for the spectrophotometric determination of rhodium(III). It was also found that the addition of BrPBT rhodium(III) in a hot acetate solution can be quantitatively extracted from ethanol-chloroform mixture (1:10) as shown in reaction **Scheme 2.1**.

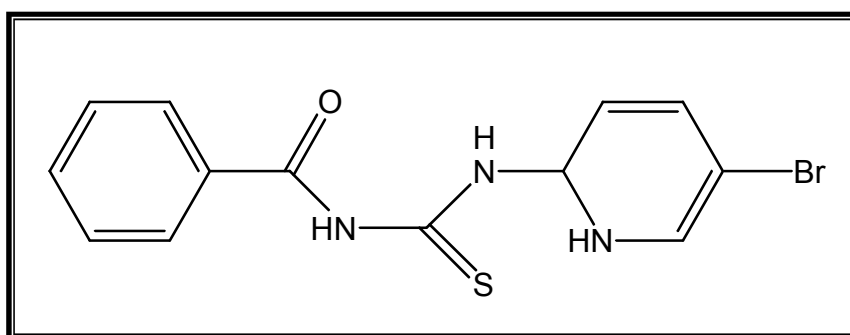


**Figure 2.2:** Structure of N- $\alpha$ -(5-bromopyridyl)-N'-benzoyl thiourea (BrPBT)

---

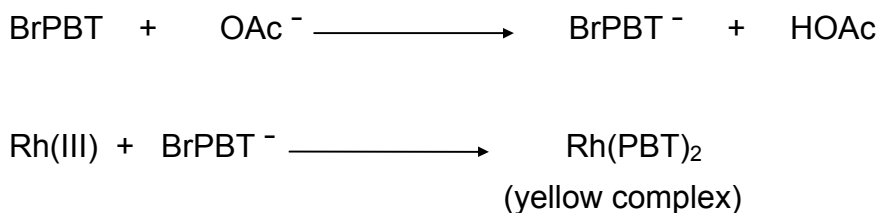
<sup>101</sup> K. Oshita, H. Wada and G. Nakagawa, *Anal. Chim. Acta.*, (1983), 149, p. 269

<sup>102</sup> Y. Shijo, K. Nakaji and T. Shimizu, *Nippon Kagaku Kaishi*, (1987), p. 31

<sup>103</sup> D. K. Das, M. Majumdar, S. C. Shome and Z. Fresenius, *Anal. Chem.*, (1977) 286, pp. 249 - 250

<sup>104</sup> <http://www.csass.org/v51n2p92.pdf> (cited on 25/09/09)





**Scheme 2.1:** Reaction scheme for the separation of rhodium using BrPBT

The most favourable pH range for complete extraction of the metal with BrPBT was found to be 6.2 to 7.1.<sup>116</sup> The metal complex showed a maximum absorption at 350 nm and obeys Beer's law at the same wavelength for the metal ion concentration ranging between 0.44 and 4.4 ppm. Results from this study indicated little or no interferences from the PGM's and the base metals, with the exception of Pt(IV), with the rhodium analysis.

The literature study also revealed a number of analytical techniques for rhodium that employed non-chelating techniques for quantification. One of these techniques were employed by Ayres and Young,<sup>105</sup> whose technique was based on the formation of a blue coloured complex (maximum absorbance at 520 nm) of rhodium(III) solutions which was reacted with hypochlorite in a 1:1 ratio.<sup>106</sup>

In their research Ayres and Young demonstrated that rhodium can be determined using different colour codes depending on the pH of the solution. Ayres<sup>107</sup> obtained an intense blue colour after he added a large excess of hypochlorite to a rhodium analyte solution (10 ppm) in the pH range of 5 to 7. He also found that at higher concentrations of rhodium (exceeding  $1 \times 10^{-3}$  M) and varying the hypochlorite concentrations, different colours were formed depending upon the final pH of the

<sup>105</sup> G. H. Ayres and H. F. Young, *Anal. Chim.*, (1950), 22, p. 1403

<sup>106</sup> G. H. Ayres, B. L. Tuffly and J. S. Forrester, *Anal. Chem.*, (1955), 27, pp. 1742 - 1744

<sup>107</sup> G. H. Ayres, *J. Anal. Chem.*, (1953), 25, pp.1622 - 1627

solution. The rhodium-perchlorate combination gave a yellow-orange at pH 11 to 12, green at pH 8, blue at pH 6 and purple at pH of about 2<sup>108</sup> as shown in **Figure 2.3**.

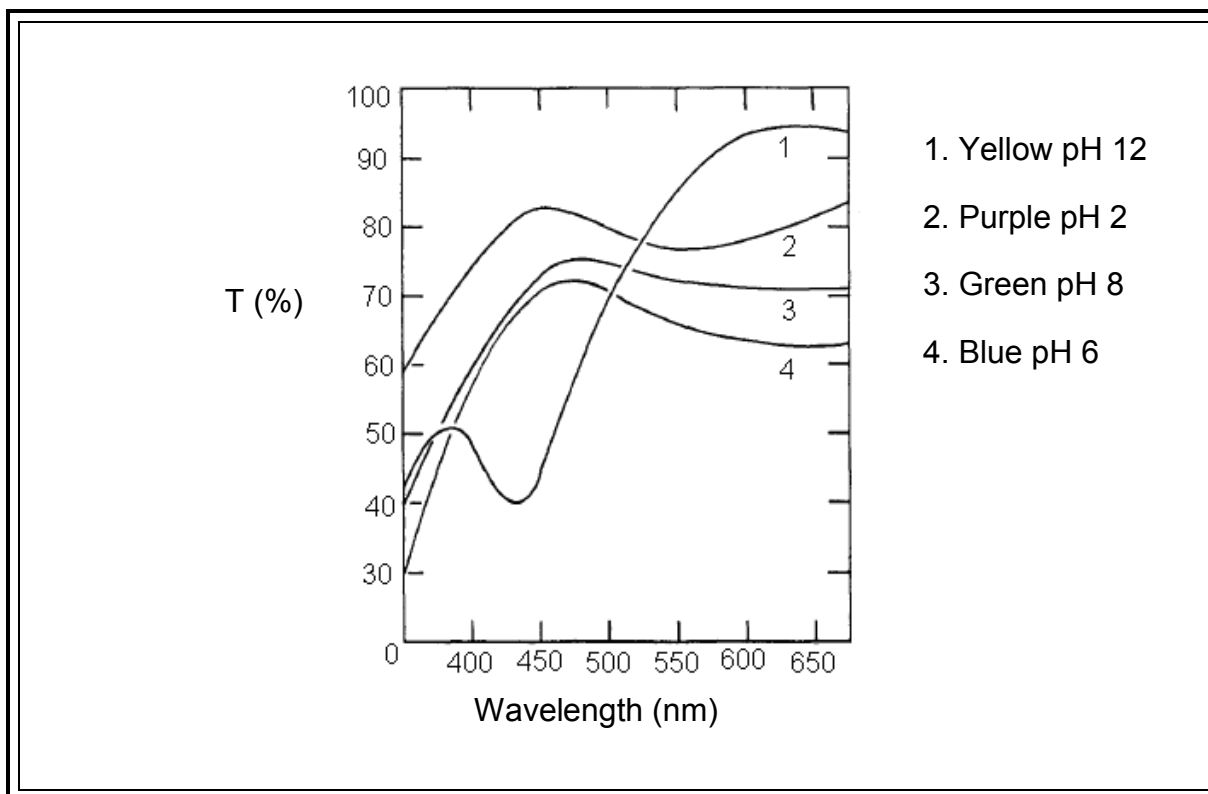


**Figure 2.3:** Spectral curves of rhodium hypochlorite solutions at different pH values obtained from varying hypochlorite solution to  $[\text{Rh}^{3+}] = 1 \times 10^{-3} \text{ M}$ .

The use of coloured complexes in rhodium determination was further used by Ivanov<sup>109</sup> who demonstrated that rhodium(III) salts in hydrochloric acid solution slowly develops a red colour when treated with tin(II) chloride, regardless of the initial colour of the analyte solution.<sup>110</sup> This method was first noted in 1913,<sup>111</sup> later re-examined by several researchers,<sup>112,113</sup> and finally used as a qualitative test for

<sup>108</sup> H. F. Young, *Ph.D. dissertation, University of Texas, (1953)*

<sup>109</sup> V. N. Ivanov, *J. Russ. Phys. Chem. Soc.*, (1913), 50, p. 460

<sup>110</sup> B. L. Tuffly, *Ph.D. dissertation, University of Texas, (1952)*

<sup>111</sup> V. N. Ivanov, *J. Russ. Phys. Chem. Soc.*, (1954), 50, p. 460

<sup>112</sup> A. D. Maynes and W. A. E. McBryde, *Analyst.*, (1954), 79, p. 23

<sup>113</sup> G. H. Ayres and F. Young, *Anal. Chem.*, (1955), 27, p. 1742

rhodium.<sup>114,115,116,117</sup> The maximum absorption dependence on the concentration of a rhodium solution is illustrated by **Figure 2.4** which shows the development of the red colour of the rhodium(III) solution with tin(II) chloride. The identity of this red coloured rhodium species was never properly established.

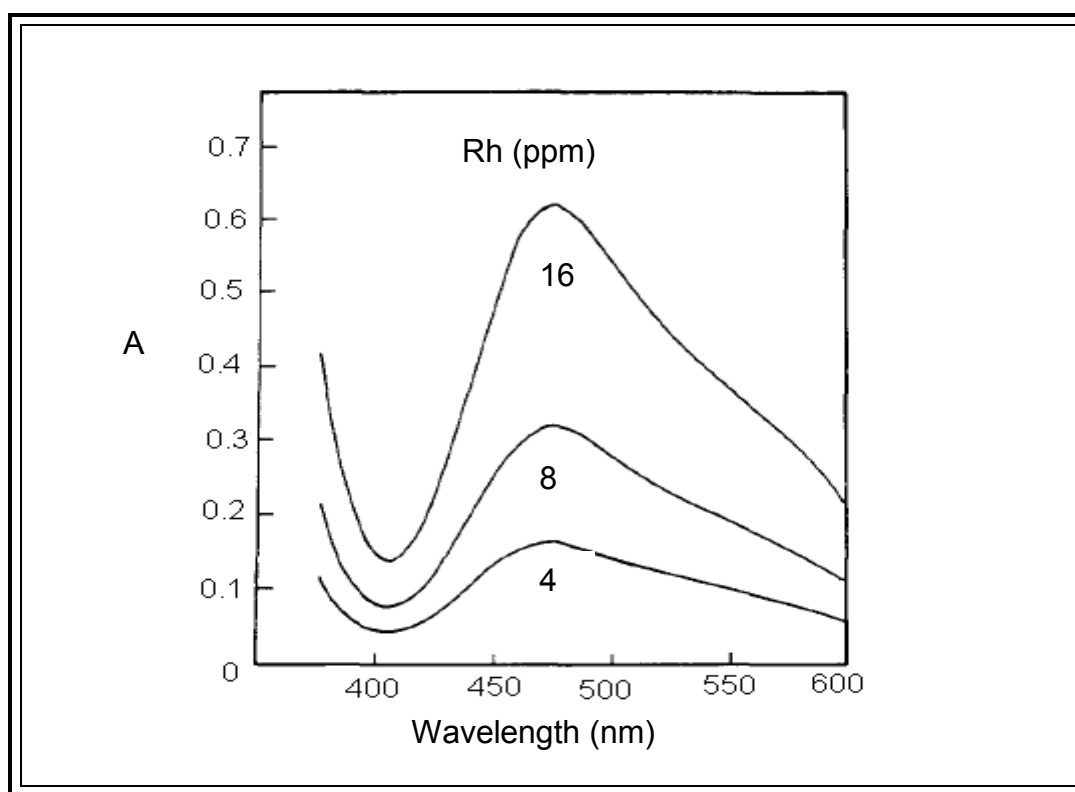


**Figure 2.4:** Spectral curves for rhodium(III) solutions colour-developed with tin(II) chloride using 2 ppm.

### 2.2.2 Chromatographic techniques (separation and isolation)

A number of researchers followed a different approach to rhodium quantification. Their approach was to try to eliminate all possible interference by separating rhodium from other metal ions and then to quantify the isolated metal. One of the first methods employed for the determination of rhodium was the use of perchloric acid.

<sup>114</sup> S. O. Thompson, F. E. Beamish. and M. Scott, *Chem. Anal.*, (1955), 9, p. 420

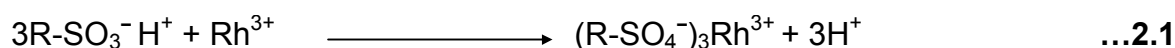
<sup>115</sup> H. Wolbling, *Ber.*, (1934), 67, p. 773

<sup>116</sup> P. Bouvet, *Ann. pharm. franc.*, (1947), 5, p. 293

<sup>117</sup> A. S. Jnr Ileyer and G. H Ayres, *J. Ani. Chern. Soc.*, (1977), 1, p. 267

This method has been reported for its effectiveness in the selective removal of rhodium from PGM.<sup>118</sup> The first attempt to separate rhodium from the PGM was made in the early 1960's by Faye.<sup>119,120</sup> His procedure involved the pretreatment of the PGM (platinum, palladium, rhodium and iridium) with perchloric acid, then aqua regia and finally with concentrated hydrochloric acid to form soluble chloro-complexes, which were easy to separate and then he finally succeeded in the elution of rhodium solution using a cation exchange resin (Dowex 50 x 8). His results were initially not acknowledged due to lack of chemical sufficient evidence and the explosiveness of perchloric acid when heating to almost dryness.

The second attempt to convert perchloric acid solutions of rhodium to chlorides were made by Van Loon and Page<sup>121</sup> around the same time. Their methods were based on evaporating the perchloride acid with the subsequent addition of 1 M sodium hydroxide, as well as sodium chloride and heating the yellow solution to a pink colour at a pH of 2.5. The final phase of their analysis involved the separation of the PGM using ion exchange chromatography. This method proved to have been successful and a lot of chemical information was presented, which then stimulated other researchers to expand on these results. Different PGM were eluted using different acid concentrations. **Equation 2.1** illustrates the substitution reaction occurring during the adsorption of rhodium.



In an earlier study, Stevenson *et al.*<sup>122</sup> found that rhodium can be successfully eluted with hydrochloric acid in cation exchange resins after a complete conversion of the perchloric acid solution to chlorides. Karttunen and Evans<sup>123,124</sup> also applied the

---

<sup>118</sup> M. H. Kurbatov and C. W. Townley, *J. Inorg and Nuclear Chemistry*, (1961), 18 pp.19 - 23

<sup>119</sup> G. H. Faye, *Mines Branch Research Report. R. 154, Mineral Sciences Division*, (1965)

<sup>120</sup> G.H. Faye and W. B. Inman, *Analyt. Chemistry*, (1963), 35, p. 985

<sup>121</sup> G. Van Loon and J. Page, *Talanta*, (1965), 12, p. 227

<sup>122</sup> P. C. Stevenson, A. A. Franke, R. Borg, and W. Nervik, *J. Amer. Chem. Soc.*, (1953), 75, p. 4876

<sup>123</sup> J. O. Karttunen and H. B. Evans, *Analyt. Chem.*, (1960), 82, p. 917

<sup>124</sup> H. B. Evans, C. A. A. Bloomquist and J. P. Hughes, *Analyt. Chem.*, (1962), 34, p. 1692

same concept for the cation exchanger to elute rhodium from the uranium fission products using hydrochloric acid. Sen Gupta and Beamish<sup>125,126</sup> confirmed the conversion of the perchlorate to chlorides when they recovered rhodium from the cation exchange resin of platinum group metals by first converting the perchlorate solution of rhodium to chlorides using the same technique.

Experimental results by Sandell<sup>127</sup> (tabulated in **Table 2.2**) using the above mentioned techniques showed that the recovery of rhodium, platinum, palladium and iridium eluted with hydrochloric acid were generally satisfactory with an average recovery of 94 %.

**Table 2.2** Platinum group metals recoveries from perchloric acid solution

No.	Added ( $\mu\text{g}$ )				Recovered ( $\mu\text{g}$ )			
	Pt	Pd	Rh	Ir	Pt	Pd	Rh	Ir
1	150	50	103	52	144	50	97	21
2	150	50	103	52	150	47	92	30
3	150	50	103	52	134	48	102	29
4		50				50		
5	100				100			

### 2.2.3 Gravimetric and titrimetric techniques

The gravimetric and titrimetric methods have an advantage of having a higher precision but with the drawback of being time consuming, labor intense and the involvement of a large number of stages in the method. The gravimetric and

---

<sup>125</sup> J. C. Sen Gupta and F. E. Beamish, *Analyt. Chemistry*, (1962), 84, p.1761

<sup>126</sup> J. C. Sen Gupta and F. E. Beamish, *The American Mineralogist*, (1963), 48, p. 379

<sup>127</sup> E. B. Sandell, *Colorimetric Determination of Metals*, 3rd Ed. New York: Interscience Publishers, (1959), p. 721

titrimetric methods are usually used in cases when quicker methods do not afford the desired precision.<sup>128, 129, 130</sup>

Gravimetric and volumetric methods have been mostly applied for the determination of rhodium at higher-content values,<sup>131</sup> using the fire assay method. Faye and Inman<sup>132</sup> described the fire assay procedure for rhodium separation from its ore using molten tin as flux. Complete precipitation of rhodium was however obtained using lead and nickel sulphide fluxes. Their research indicated that the recovery of the rhodium metal was highly dependent on the separation of the flux composition and the choice of experimental conditions e.g. the temperature, which controlled the retention of the metal by the slag. Success in the quantitative recovery of the rhodium was also found to be dependent on the experience and skill of the analyst, who has to optimize the flux composition and fusion conditions.

An example of a modern gravimetric technique is the oxidimetric spectrophotometric method developed by Ganescu *et al.*<sup>133</sup> Rhodium was determined from the precipitation of the dark-red  $[\text{Rh}(\text{Rod})_2\text{Cl}_2][\text{Cr}(\text{NCS})_4(\text{amine})_2]$  complex (where Rod =  $\text{Et}_3\text{N}$ ,  $\text{CH}_2\text{Cl}_2$  reagent) which was extracted using organic solvents. The structure of  $[\text{Cr}(\text{NCS})_4(\text{amine})_2]^-$  which is sometimes referred to as Reinecke's salt is shown in **Figure 2.5** and the associated reaction it undergoes with rhodium in **Equations 2.2** and **2.3**.

---

<sup>128</sup> Y. A. Zolotov, G. M. Varshal and V. M. Ivanov, *Analytical Chemistry of Platinum Group Metals*, Moscow: URSS, (2003)

<sup>129</sup> S. I. Ginzburg, N. A. Ezerskaya and I. V. Prokof'eva, *Analytical Chemistry of Platinum Metals*, Moscow: Nauka, (1972)

<sup>130</sup> F. F. Beamish, *The Analytical Chemistry of Noble Metals*, Oxford: Pergamon, (1966)

<sup>131</sup> Alloys-Gravimetric Determination with Dimethyl glyoxime. *Doc. ISO 11490*

<sup>132</sup> G. H. Faye and W. R. Inman, *Anal. Chem.*, (1968), 34, p. 972

<sup>133</sup> I. Ganescu, I. Papa, D. C. Preda, A. Ganescu, L. Chirigiu and A. Barbu, *Chimie*, (2001), 9, p. 49

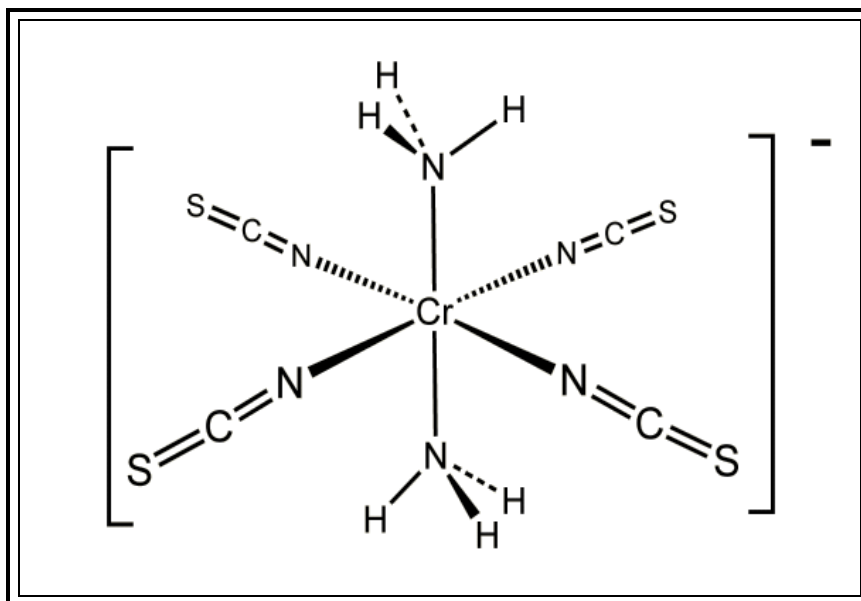
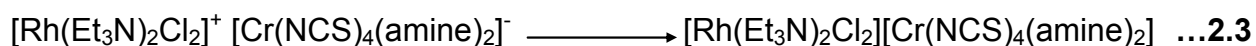


Figure 2.5: Structure of  $[\text{Cr}(\text{NCS})_4(\text{amine})_2]^-$ <sup>134</sup>

### Reactions



The quantitative determination of rhodium was done using statistical analysis methods. The association complex involved in this method was reported to have a well-determined composition, very good thermal stability and very soluble in organic solvents, which all contribute to the success of this method in the analysis of rhodium. The method is mostly applied in the determination of rhodium in geological ores, alloys and catalysts.

Yoshino *et al.*<sup>135</sup> proposed a back-titration method for rhodium(III) complexes with EDTA solution. The method was based on the rapid chelation of rhodium(III) ions

<sup>134</sup> [http://en.wikipedia.org/wiki/Reinecke's\\_salt](http://en.wikipedia.org/wiki/Reinecke's_salt) (cited on 12/10/09)

with EDTA in water-ethanol solutions. The optimum amount of rhodium for the analysis was found to be in the range 0.5 to 10 mg and the standard deviation of the recovered rhodium was approximately 0.76 %.<sup>136</sup> He also found that the addition of ethanol resulted in the remarkable enhancement of the rate of chelation of EDTA with rhodium(III). It was this remarkable observation that he applied to determine rhodium using the back-titration of rhodium(III) complexes. The major drawback of this technique was the interference of other metal ions which reacted with EDTA as well and required separation prior to titration.

### 2.2.4 Spectrometric techniques

The rapid development of the electronic industry in the last 30 years led to the development of a number of sophisticated analytical equipment which allow for the determination of elements in the parts per billion range. These include atomic absorption spectrometry, both flame (AAS) and the graphite furnace (GF-AAS), X-ray fluorescence (XRF), X-ray diffraction (XRD), inductively coupled plasma-optical emission<sup>137</sup> (ICP-OES) and mass spectrometry<sup>138</sup> (ICP-MS). The minimum level of measurement of rhodium for these and other techniques have been compared and summarized in **Table 2.3**.

---

<sup>135</sup> Y. Yoshino, S. Hatazawa, M. Saito and A. Ouchi, *Chemical Society of Japan.*, (1980), pp. 1085 - 1088

<sup>136</sup> F. E. Beamish and J. C. van Loon, *Analysis of Noble metals*, Academic Press, New York, (1977), p. 115

<sup>137</sup> R. K. Winge, V. A. Fassel, V. J. Peterson and M. A. Floyd, *Inductively Coupled Plasma Atomic Emission Spectroscopy. An Atlas of Spectral Information*, Elsevier, Amsterdam, (1993)

<sup>138</sup> L. Bencs, K. Ravindra and R. Van Grieken, *Spectrochim. Acta.*, (2003), 58B, p. 1723



**Table 2.3:** Levels of measurement of different techniques

Technique	Concentration range				
	Sub-ppb	ppb	ppm	0.1 %	Above 0.1 %
ICP-OES			yes	yes	
ICP-MS	yes	yes	yes		
AAS			yes	yes	yes
GF-AAS	yes	yes	yes	yes	yes
NAA	yes	yes	yes		
Electrochemical techniques		yes	yes	yes	
Spectrophotometry			yes	yes	yes
Gravimetric and titrimetric methods				yes	yes
Chromatography		yes		yes	yes

An example of the use of ICP for rhodium analysis is the research done by Mokgalaka *et al.*<sup>139</sup> on the presence of the metal in converter matte. They developed an internal standard method for ICP-OES determination of rhodium after having successfully separated and dissolved the rhodium metal in converter matte. Although the method was effective for the determination of rhodium, the choice of the internal standard (Sn) was very critical in obtaining recoveries close to 100 %. Marjanovic<sup>140</sup> went on to test for the usefulness of the simplified generalized standard additions method (GSAM) for slurry nebulization-ICP-OES determination of rhodium in converter matte. The results obtained were highly dependent on the level of the ion matrix and on the completeness of sample dissolution. The use of an internal standard has been approved by the International Organization for Standardization (ISO), e.g. yttrium (Y), which has been recommended to correct for the matrix effects in ICP-OES as an internal standard for platinum group metals.<sup>141,142, 143</sup>

<sup>139</sup> N. S. Mokgalaka, R. I. McCrindle, B. M. Botha and L. Marjanovic, *S Afr. J. Chem.*, (2002), 55, p. 72

<sup>140</sup> X. Dai, C. Koeberl and H. Froschl, *Anal. Chim. Acta.*, (2001), 436, p. 79

<sup>141</sup> International Organization for Standardization: Atomic Absorption. Doc. ISO/WD 11492

### 2.2.5 Atomic absorption spectrometry (AAS and GF-AAS)

Instrumental techniques such as the conventional atomic absorption spectrometry (AAS)<sup>144</sup> and X-ray fluorescence<sup>145</sup> have also been applied for the determination of rhodium. Rhodium content has on at least one occasion, been determined in alumina supported catalyst material by AAS.<sup>146</sup>

In 1978, N. M. Potter<sup>147</sup> and his co-workers reported the determination of low levels of rhodium in platinum-rhodium loaded, automotive catalyst material. Their analysis was based on the heated GF-AAS. The GF-AAS,<sup>148</sup> technique had been shown to be more sensitive than the flame technique (AAS).<sup>149</sup> In GF-AAS dissolved materials can be analyzed directly by the selection of the most appropriate furnace conditions which do not need chemical separation prior to analysis. The drawback encountered by Potter with this technique was that it was not able to accurately determine rhodium from samples containing silica, organic binders, or insoluble  $\alpha$ -alumina as they were difficult to dissolve.

The wavelength-dispersive X-ray fluorescence (WDXRF) technique has been used in the determination of rhodium and has the advantage of having simple sample preparation and a rapid method of measurement.<sup>150</sup> O. V. Borisov *et al.*<sup>151</sup> employed

---

<sup>142</sup> International Organization for Standardization: Determination of Platinum in Platinum Jewellery Alloys-Method Using Inductively Coupled Plasma Emission Spectrometry on a Solution with Yttrium as Internal Standard. Doc. ISO/DIS 11494.2, (2007)

<sup>143</sup> R. Kovacevica, M. Todorovicb, D. Manojlovicb and J. Muticb, *J. Iran. Chem. Soc.*, (2008), 5, pp. 336 - 341

<sup>144</sup> J. G. Sen Gupta, *Miner. Sci. Eng.*, (1973), 5, p. 207

<sup>145</sup> P. N. Gerrard and N. Westwood, *J. S. Afr. Chem. Inst.*, (1972), 25, p 285

<sup>146</sup> G. R. List, J. P. Friedrich, W. F. Kwolek and C. D. Evans, *J. Am. Oil Chem. Soc.*, (1972), 50, p 210

<sup>147</sup> N. M. Potter, *Anal. Chem.*, (1978), 50, pp. 769 - 772

<sup>148</sup> P. Roy, V. Balaram, A. Bhattacharaya, P. Nasipuri, and M. Satyanarayanan, *Research Communications. Current science*, (2007), 93, pp. 1122 - 1125

<sup>149</sup> D. Guerin and J. S. Ah. *Chem. Inst.*, (1972), 25, p 230

<sup>150</sup> S. Kallmann and P. Blumberg, *Talanta*, (1980), 27, p. 827

this technique in the determination of rhodium from automotive catalytic converters. He found that the technique was not permissible to trace and ultra-trace analysis as the limits of detection of this technique were poor (5 - 15 ppm). He also found that rhodium lines for analysis were interfered by palladium. Samples containing palladium had to be separated prior to analysis.

Comparisons made between results obtained from WDXRF with those from ICP-MS revealed that the results obtained from the WDXRF technique were in good agreement with those from ICP-MS.<sup>151</sup> It was therefore concluded that the technique was capable of providing accurate and reliable results on condition that all possible interferences were eliminated.

## **2.3 Digestion techniques**

The success of the wet chemical analysis of any element depends critically upon the complete dissolution of the whole sample. The majority of the classical analytical techniques mentioned in the previous paragraphs require that the samples are introduced into the instrument in aqueous form. The determination of rhodium by spectrometric methods therefore requires its quantitative transformation into water soluble species which then form the basis of the detection. The high resistance of rhodium and other PGM such as ruthenium, osmium and iridium to acid attack, including *aqua regia*, limits the use of direct wet digestion procedures to their quantitative transformation into soluble species. Separation, pre-concentration and dissolution of samples are sometimes vital steps in rhodium analysis, owing to the very low concentration of rhodium in many samples and the complexity of the matrix.

### **2.3.1 Sample decomposition by acids and fluxes**

Rhodium metal is quite resistant to chemical attack by acids, even *aqua regia* and is attacked only slowly by boiling sulphuric acid. Alkaline fusion is the most commonly

---

<sup>151</sup> O. V. Borisov, D. M. Coleman, K. A. Oudsema and R. O. Carter, *J. Anal. Atomic Spec.*, (1997), 12, pp. (239 – 246)

used technique for oxidizing the metal. Potassium pyrosulphate fusion has been reported as a method that can completely convert rhodium to the water soluble  $\text{Rh}_2(\text{SO}_4)_3$ . Alternatively, if the fusion is accomplished with  $\text{NaHCO}_3$  and  $\text{KNO}_3$  or with  $\text{BaO}_2$ , insoluble rhodium oxides are formed. Fused metaphosphoric acid dissolves rhodium to some extent, while a mixture of  $\text{O}_2$  and  $\text{HCl}$  gas completely dissolves rhodium metal above  $150\text{ }^\circ\text{C}$ .

A number of reducing agents such as ammonium formate,  $\text{TiCl}_3$  and  $\text{Mg}$  have been used to reduce rhodium(III) to a black finely divided form of rhodium metal. Rhodium in this form is readily soluble in aqua regia or hot concentrated sulphuric acid. Research also indicates that complete dissolution of rhodium may be achieved either in concentrated hydrochloric acid or in the presence of sodium chlorate in a sealed tube at temperatures of  $125 - 150\text{ }^\circ\text{C}$ .<sup>152</sup>

The oxidation state of rhodium is an important factor when considering dissolution and reactivity. Strong alkaline oxidizing agents can dissolve rhodium, even molten bases such as sodium, phosphorus, silicon, arsenic, antimony and lead.

The more classical fusion method involves fusing the rhodium sample with a flux mixture at high temperatures (*ca.*  $1000\text{ }^\circ\text{C}$ ) to form soluble salts of the sample material. The traditional fire assay (FA)<sup>153</sup> technique for rhodium ores was known since the time of its discovery and this method is still used as an important step, especially in the separation. The choice of an appropriate flux depends on the sample matrix. Sodium carbonate, sodium tetraborate and sodium bisulphate<sup>154</sup> had been widely used as flux in rhodium dissolution from its metal ore.

Research indicated that rhodium and other PGM are partitioned into a glassy slag incorporated into nickel sulphide during fusion. The nickel sulphide separates from the slag as a clean shiny button where the slag (melt) is cooled. The nickel sulphide

---

<sup>152</sup> <http://www.statemaster.com/encyclopedia/Inorganic-compound> (cited on 12/10/09)

<sup>153</sup> W. M. Johnson and J. A. Maxwell, *Rock and Mineral Analysis, 2nd Ed.* Wiley, New York, (1981)

button is usually dissolved in acid to remove the nickel and sulphur, leaving a black precipitate of rhodium-sulphide. This can be analyzed directly using NAA,<sup>155</sup> or more commonly, the precipitate is taken into solution by dissolving it in water for analysis by AAS or ICP techniques. This method has been applied to a wide variety of rocks, and ores.

### 2.3.2 Microwave digestion

The use of microwave energy as a heat source in wet ashing procedures for rhodium containing samples was first demonstrated in 1975.<sup>156</sup> Several studies<sup>157,158,159</sup> compared the technique with different digestion procedures, and examples have been given of this technique's successful application to geological samples when analyzed by atomic absorption and emission spectroscopy. This technique has received novel attributes as a best dissolution technique due to its ability to completely decompose analytical materials using the high microwave energy (300 to 300 000 MHz) (see **Chapter 3, Section 3.5**). The sample preparation method for rhodium in this research was typically based on microwave digestion with concentrated hydrochloric acid.<sup>160,161</sup> Microwave dissolution proved to be faster, more controlled, more elegant, and more amenable to automation than the conventional open digestion techniques. The percentage of the rhodium content recovered was in line with the estimated values, indicating a complete dissolution of the analyte sample.

---

<sup>154</sup> J. C. Van Loon and R. R. Barefoot, *Determination of the Precious Metals. Selected Instrumental Methods*, John Wiley, New York, (1991)

<sup>155</sup> S. J. Parry, Simultaneous determination of the noble-metals in geological material by radiochemical neutron-activation analysis, *Analyst.*, (1980), 105, pp. 1157 - 1162

<sup>156</sup> A. Abu-Samra, J. S. Morris, S. R. Koirtyohann, *Anal. Chem.*, (1975), 47, pp. 1475 - 1477

<sup>157</sup> R. T. White, G. E. Douthit, *J. Assoc. Off. Anal. Chem.*, (1985), 68, pp. 766 - 769

<sup>158</sup> R. A. Nadkarni, *Anal. Chem.*, (1984), 56, pp. 2233 - 2237

<sup>159</sup> J. L. M. De Boer, F. J. M. Maessen, *J. Spectrochim. Acta, Part B*, (1983), 38, pp. 379 - 746

<sup>160</sup> O. V. Borisov, D. M. Coleman, K. A. Oudsema, R. O. Carter, *J. Anal. Atom. Spectrom.*, (1997), 12, p. 239

### 2.3.3 Conclusion

The discussions in the above paragraphs revealed that a considerable amount of work has been done to establish accurate methods for rhodium determination. These methods were mostly restricted to tedious sample preparation and the need to convert the rhodium to a certain ionic state (e.g.  $\text{Rh}^{3+}$ ). The percentage recoveries of these techniques were mostly dependent on the efficiency of the sample preparation method. Low rhodium recoveries as a result of incomplete digestion techniques stimulated the need to investigate new or alternative methods for sample digestion.

The introduction of microwave digestion in closed vessels in 1985 has improved the digestion procedures of most of the PGM, inorganic and organometallic compounds. This technique has enabled the reproducibility of procedures, accuracy and reduced digestion time. Among the different methods used, ICP-OES methods such as the standard addition method, the direct calibration method and the internal standard addition have been popular in its application, although some of them reported low percentage recovery. Internal standard addition has been shown to produce accurate results due to the ability to correct for different matrix effects. The choice of the internal standard needs to be critically analysed as it form the basis of good results (see **Chapter 3, Section 3.2.4.3**).

---

<sup>161</sup> E. Steiness, A. Rühling, H. Lippo, A. Mäkinen, *Accred. Qual. Assur.*, (1997), 2, pp. 243

# 3 Selection of analytical techniques

---

## 3.1 Introduction

A comprehensive literature study on the possible analytical techniques for rhodium analysis in inorganic and organometallic complexes was carried out to determine the appropriate technique(s) and method for the accurate determination of rhodium. The advantages and disadvantages of the analytical techniques were weighed against each other before the selection of the final method for this study. Factors like the availability of equipment, accuracy, as well as running and maintenance cost were also considered prior to the analysis. Inductive coupled plasma optical emission spectroscopy (ICP-OES) was found to be a convenient method due to a number of reasons that include high accuracy, low detection limits, its capability to determine many elements simultaneously and low cost of running and maintenance.

Efficient digestion techniques also had to be established for the successful and accurate determination of rhodium. Microwave digestion was found to be efficient (see **Chapter 2, Section 2.3.2**) and was chosen as method of sample digestion. During the quantification of the rhodium content in water soluble  $\text{RhCl}_3 \cdot x\text{H}_2\text{O}$  ( $x$  = unspecified number of crystal water molecules), techniques such as thermal gravimetric analysis (TGA) and differential scanning calorimetry (DSC) was used to quantify the water molecules to ensure a proper recovery calculation of the rhodium. The main objective of this chapter is to discuss the theory of ICP-OES, microwave digestion and the method validation applicable to this study.

## **3.2 Spectroscopic measurements**

### **3.2.1 Introduction**

The simultaneous and multi-element determination capabilities of inductively coupled plasma optical emission spectrometry (ICP-OES) draw the attention of the analytical community in the 70's.<sup>162</sup> The first commercial equipment was launched in 1974 and the technique is until today largely employed for routine analysis. ICP-OES has become the dominant source for rapid spectroscopic multi-element analysis as a result of a set of “legendary” attributes, including low detection limits, a wide linear dynamic range and high precision (see **Chapter 2, Table 2.1**). ICP-OES is sometimes referred to as inductive coupled plasma atomic emission spectrometry (ICP-AES). Unfortunately, the later designation is sometimes confused with Auger Electron Spectrometry (AES).<sup>163</sup> In the interest of clarity, the term inductively coupled plasma optical emission spectrometry (ICP-OES) has been rigidly adopted.

### **3.2.2 Principles of spectral origin and measurements**

Most of the spectrometric techniques, such as the ones listed in **Chapter 2, Section 2.2.4**, consist mainly of four modules of sample determination, which are the sample introduction system, a burner or torch assembly, spectrometer and a multi-element detector as shown for an ICP-OES spectrometer in **Figure 3.1**.

---

<sup>162</sup> R. A. Conte, J. M. Mermet, J. D. A. Rodrigues and J. L. Martino, *J. Anal. Atomic Spectrometry.*, (1997), 12, pp. 1215 - 1220

<sup>163</sup> [http://en.wikipedia.org/wiki/Inductively\\_coupled\\_plasma\\_atomic\\_emission\\_spectroscopy](http://en.wikipedia.org/wiki/Inductively_coupled_plasma_atomic_emission_spectroscopy) (cited on 15/09/09)



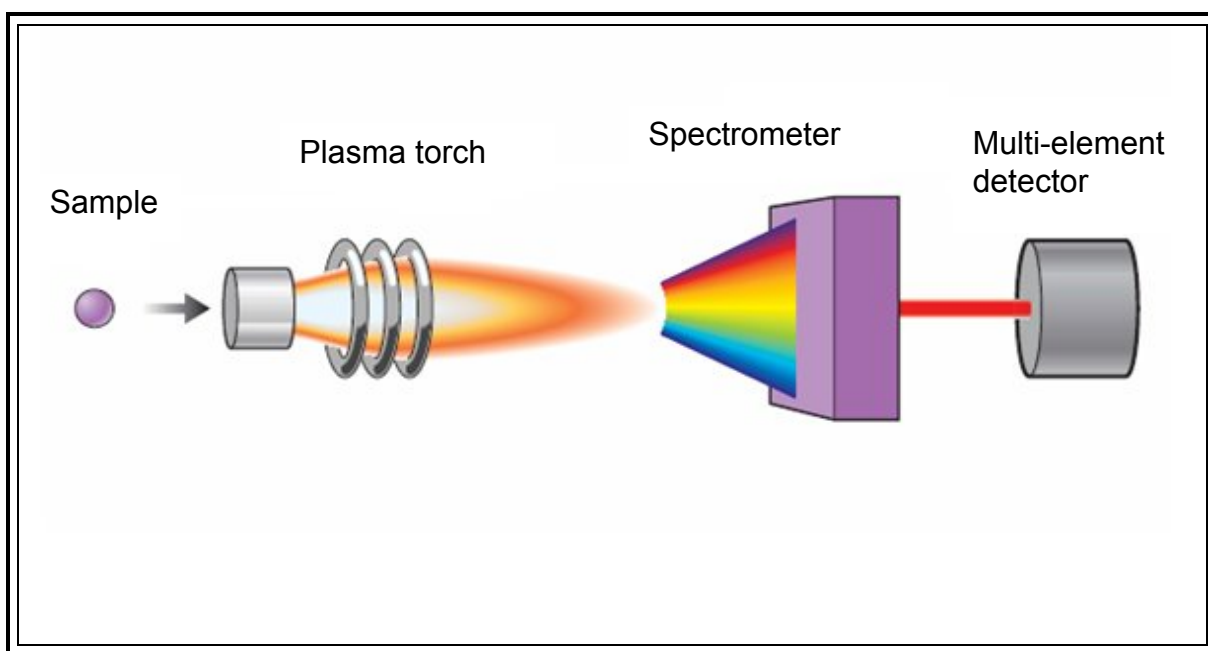


**Figure 3.1:** Schematic representation of an ICP-OES<sup>164</sup>

The spectral measurement of these techniques normally begins with the volatilization of the analyte sample into a fine mist/aerosol, which is then heated at high temperatures of approximately 10 000 °C and higher. The atom absorbs the energy and excites most of its electrons to orbitals of higher energy. An atom is less stable in the excited state and will decay back to the ground state by losing energy through collision with another particle or by emission of a particle of electromagnetic radiation, known as a photon. As a result of this energy loss, the electron returns to an orbital closer to the nucleus. An emission line is formed when an electron makes a transition from a particular discrete energy level of an atom ( $E_n$ ), to a lower energy state ( $E_{n-1}$ ), emitting a wavelength of a particular energy as shown in **Figure 3.2**.

<sup>164</sup> [http://cheminfo.chemi.muni.cz/chem\\_sekce/predmety/C7300/AES/Strana\\_38.pdf](http://cheminfo.chemi.muni.cz/chem_sekce/predmety/C7300/AES/Strana_38.pdf) (cited on 17/09/09)

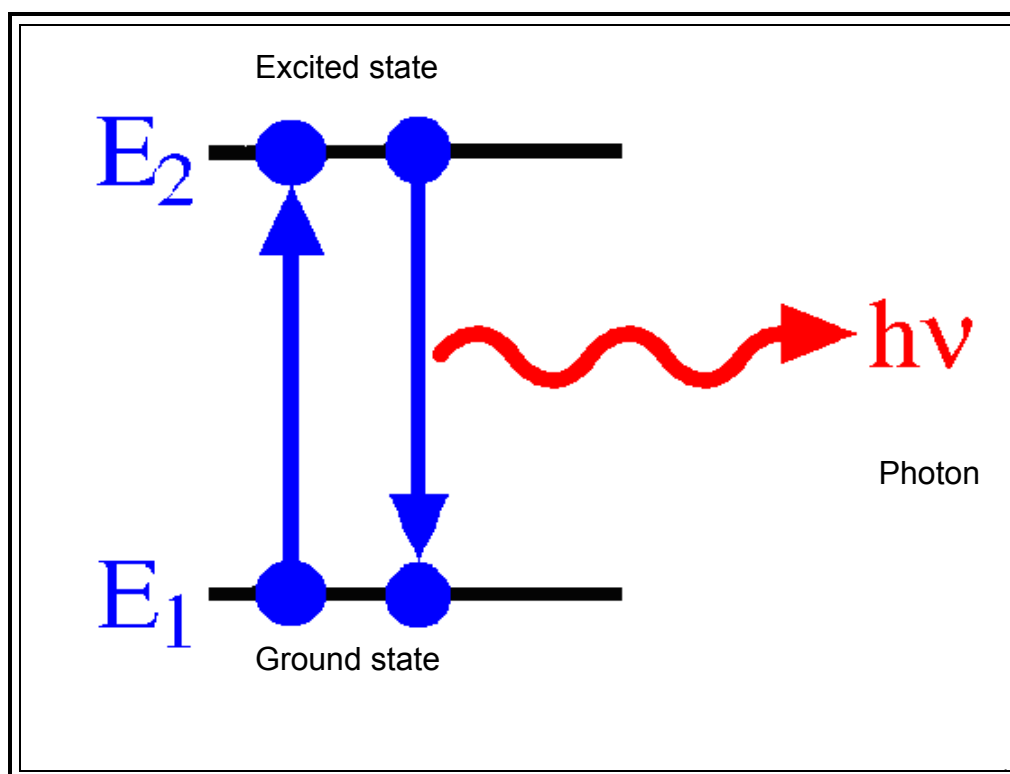


**Figure 3.2:** Excitation and emission of electromagnetic radiation<sup>165</sup>

An absorption line is formed when an electron makes a transition from a lower to a higher discrete energy state, with a photon being absorbed in the process. These absorbed photons generally come from the background continuum radiation and a spectrum will show a drop in the continuum radiation at the wavelength associated with the absorbed photons.

The emitted radiation can be easily detected when it is in the vacuum ultraviolet (VUV, 120–185 nm), ultraviolet (UV, 185–400 nm), visible (Vis, 400–700 nm) and near infrared regions (NIR, 700–850 nm). Although atoms emit electromagnetic radiation in the infrared, microwave and radiowave regions as well, the detection systems are less sensitive in these regions, therefore the VUV, UV, Vis and NIR regions are preferred. The ICP-OES measures the intensity of the emitted waves in the visible and ultraviolet region as shown on the electromagnetic spectrum as depicted in **Figure 3.3**.

<sup>165</sup> <http://en.wikipedia.org/wiki/Photon> cited on (19/10/09)

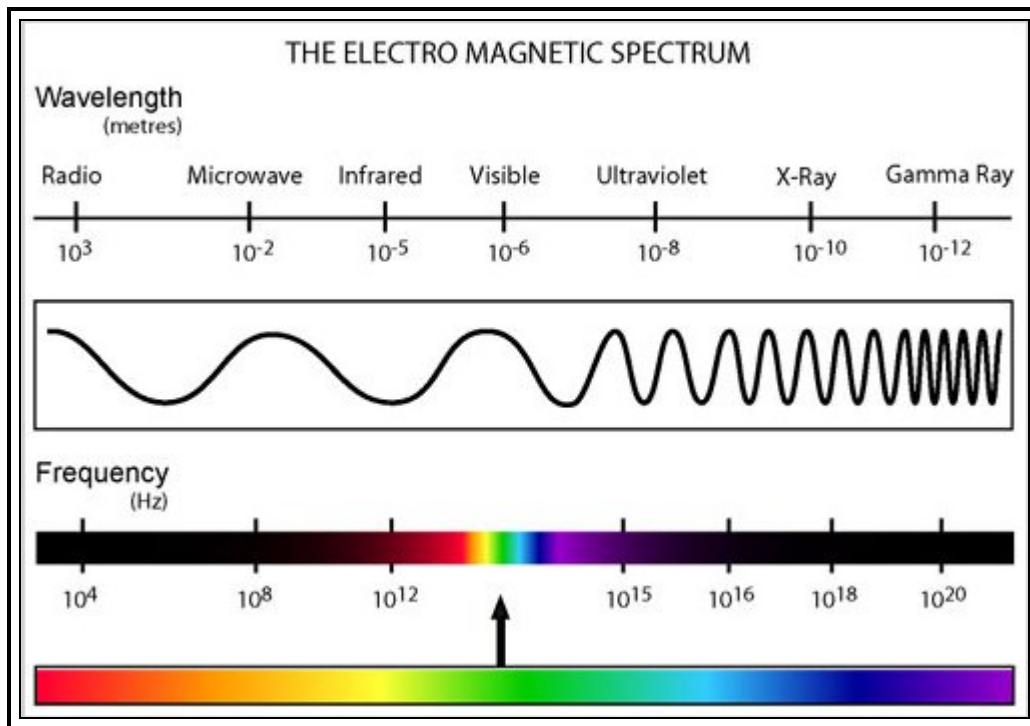


**Figure 3.3:** The electromagnetic spectrum<sup>166</sup>

Each element emits energy at a multiple of characteristic wavelengths and only the most common wavelength(s) is selected for measurement. The intensity of the energy emitted is equal to the intensity absorbed by an atom or ion as shown by the corresponding emission and absorption lines in **Figure 3.4**. A spectrum of many such photons will show an emission spike at the wavelength associated with these photons. The optical Echelle type grating system splits the emitted light from the plasma into a two-dimensional grid, which is collected by a CID (Charge Injection Device).

---

<sup>166</sup> [www.colourtherapyhealing.com/colour/electroma...](http://www.colourtherapyhealing.com/colour/electroma...) (cited on 15/09/09)

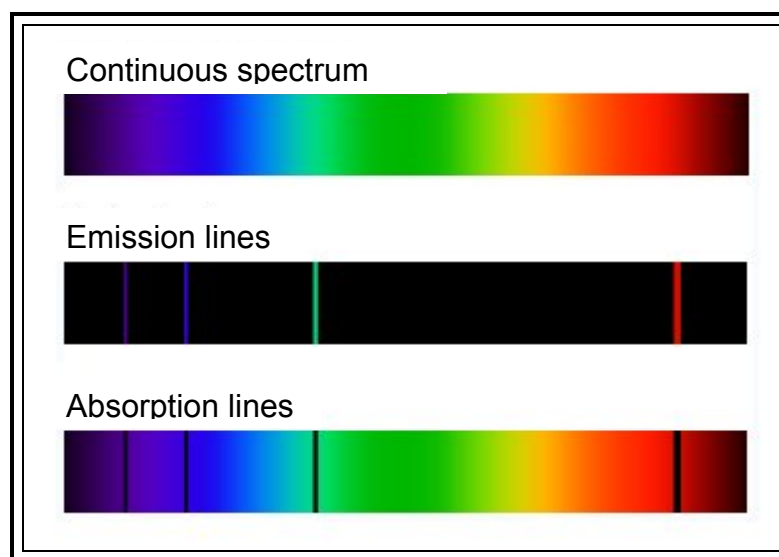


**Figure 3.4:** Emission of radiation upon relaxation from an excited state<sup>167</sup>

The emitted light is collected by the spectrometer and passes through a spectrum of its constituent wavelength. Within the spectrometer, this diffracted light is then measured by wavelength and amplified to yield an intensity measurement that can be converted to an elemental concentration by comparison with calibration standards. Quantitative information (concentration) is related to the amount of electromagnetic radiation that is emitted, whilst qualitative information (which elements are present) is related to the wavelength at which the radiation is absorbed or emitted.

### 3.2.3 Selection of analytical lines

The emitted light possesses different wavelengths depending on the decaying transition of the electron from the excited to the ground state. Elements can emit atomic, ionic or molecular wavelengths (lines), depending on their electronic state. An atomic line is produced when an excited electron decays back to the ground state, whilst an ionic line is produced from an ionic to ground state transition of an electron. Molecular lines are formed from the emission of electromagnetic radiation by excited molecules to their ground state.

---

<sup>167</sup> [Astro.unl.edu/naap/hr/hr\\_background1.html](http://Astro.unl.edu/naap/hr/hr_background1.html) (cited on 16/09/09)

If a specific line (P) is chosen for analysis, the net analyte signal ( $r_A$ ) is determined as the difference of a total signal ( $r_{A+B}$ ) and a background signal ( $r_B$ ) as illustrated by **Equation 3.1** and **Figure 3.5**.

$$r_A = (r_{A+B}) - r_B$$

... 3.1

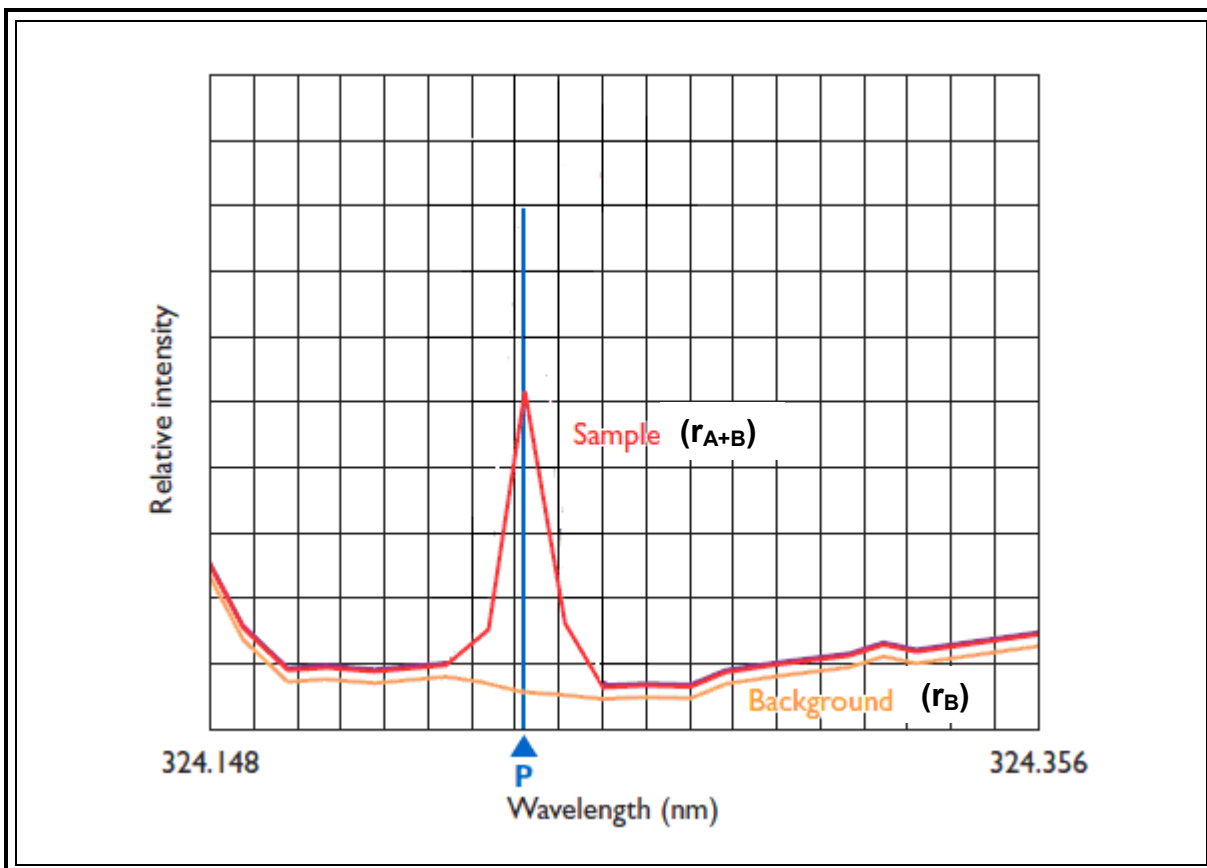


**Figure 3.5:** Determination of the analyte signal<sup>168</sup>

### 3.2.4 Methods in spectroscopic analysis

Matrix effects such as spectral interferences, as well as acid and chemical matrix effects are the most common problems in spectroscopic analysis. Slight differences in the matrix can cause a considerable systematic error, which can lead to bias in

<sup>168</sup> T. J. Manning and W. R. Grow, *Inductively Coupled Plasma-Atomic Emission Spectrometry*, (1997), 2, pp. 1 - 19

measurement of results. Different methods that can reduce this error and add to the accurate determination of rhodium have been employed, such as the direct calibration curve, standard addition and the internal standard addition method.

#### 3.2.4.1 Direct calibration method

The first of these methods involve the direct measurement of the intensity as a function of the concentration of the analyte species. A high-quality calibration curve has a linear regression coefficient ( $r^2$ , dimensionless) close to unity (1). The calibration curve forms the reference from which all analytical measurements are taken. The analyte concentration is therefore determined through extrapolation of the corresponding emission intensity (Y) and compared against the calibration curve as illustrated in **Figure 3.6**.

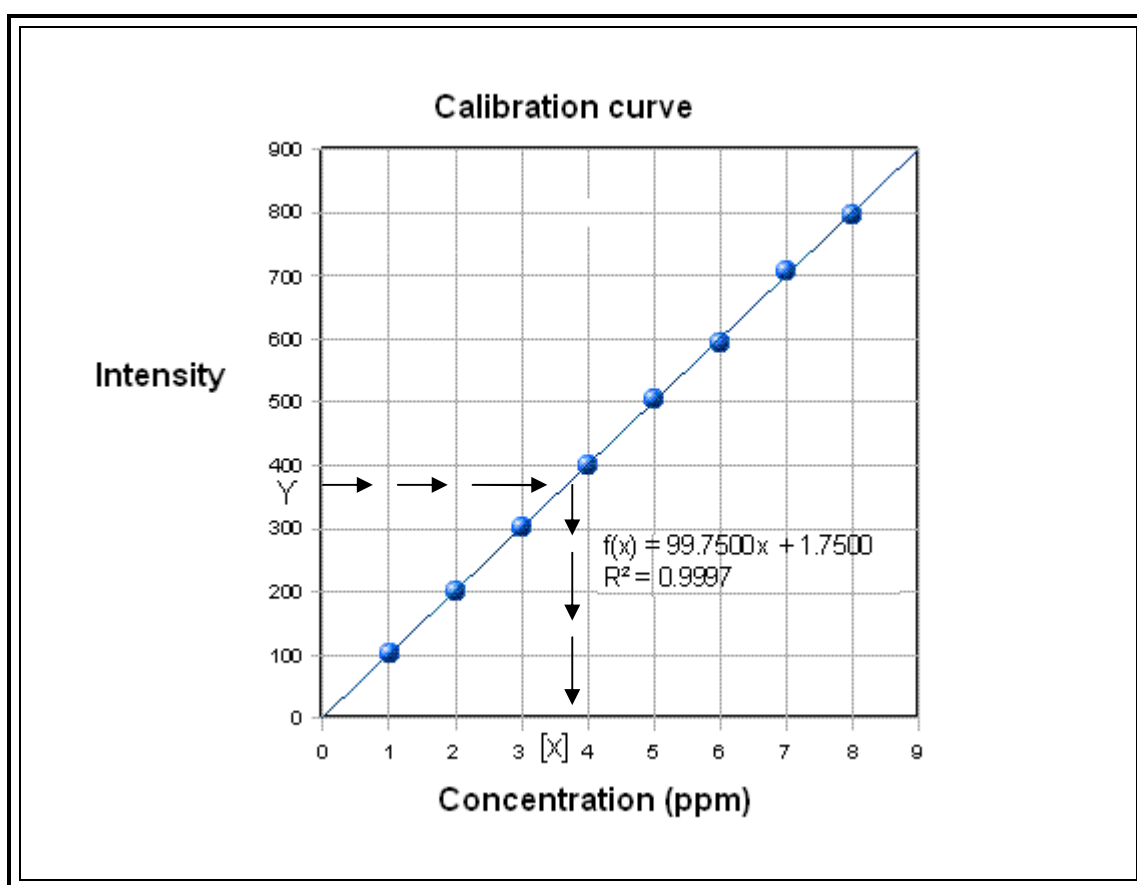


**Figure 3.6:** Direct calibration method

The concentrations of the analyte and the instrument response for each standard can be made to fit into a straight line using linear regression analysis. This yields a model described by the equation  $y = mx + y_0$ , where ( $y$ ) is the instrument response, ( $m$ ) is the sensitivity and ( $y_0$ ) is a constant that describes the background. The analyte concentration ( $x$ ) of unknown samples may also be calculated from this equation instead of being extrapolated.

The dynamic range of the calibration curve enables analyte solutions to be measured within a specified region. This is demonstrated by the maximum intensity of the standard solution compared to the intensity of the analyte specie(s) as shown in **Figure 3.7**. The direct calibration method has an advantage of being easy to construct, but is easily affected by spectral interference, acid matrix, changes of temperature in the nebulizer and chemical interferences. This method requires standards of high purity and the concentration of the standards needs to be accurately known.

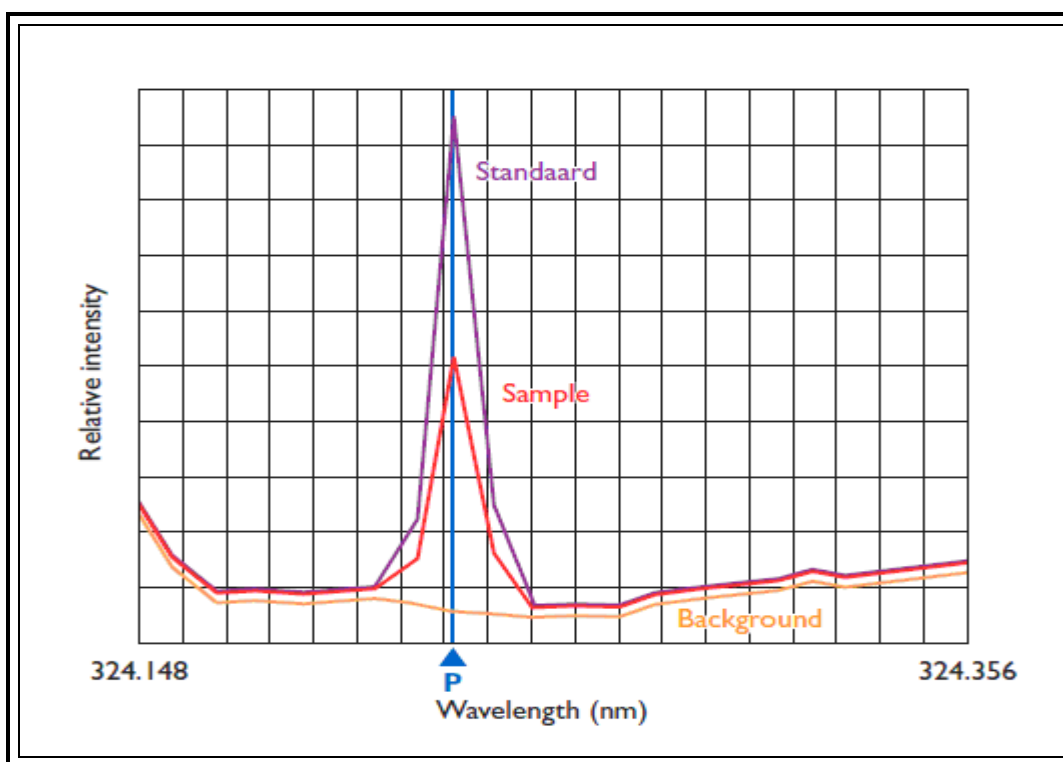


**Figure 3.7:** Comparison of the analyte signal to the standard signal<sup>169</sup>

<sup>169</sup> T. J. Manning and W. R. Grow, *Inductively Coupled Plasma-Atomic Emission Spectrometry*, (1997), 2, pp. 1 - 19

### 3.2.4.2 Standard addition method

The second method that can be employed is called the standard addition method. This method is used when the sample matrix cannot be matched with the standards and the samples. This is especially important when the matrix present in the analyte solution interact with the analyte to change the instrumental response, which will result in an incorrect determination with the use of the direct calibration method. In the standard addition method, small increments of standard solutions (spikes) of the factor 2x or 3x, (where x is the standard concentration) are added to the analyte samples. The impurities in the sample are therefore accounted for in the calibration curve as shown in **Figure 3.8**.

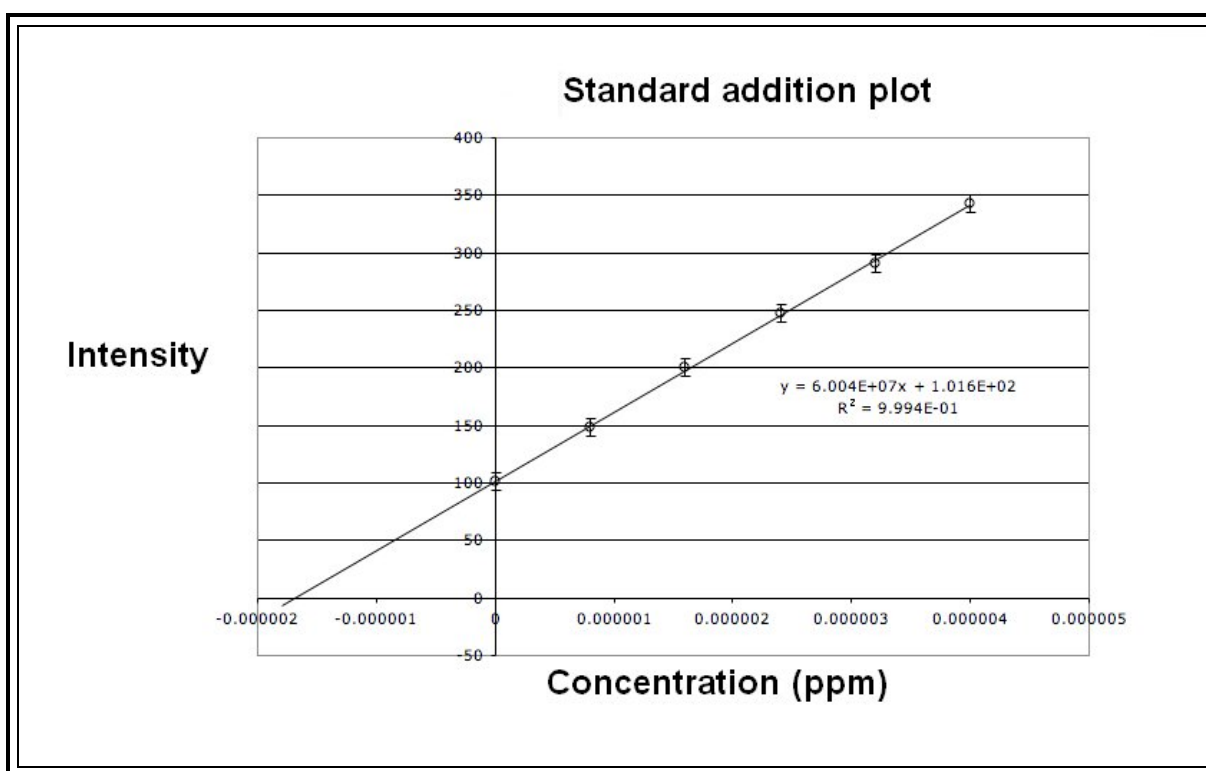


**Figure 3.8:** Standard addition calibration curve<sup>170</sup>

The concentration of the analyte solution is determined either by extrapolation of the calibration curve or from the equation of the curve. This method has an advantage of

<sup>170</sup> [http://en.wikipedia.org/wiki/Standard\\_addition](http://en.wikipedia.org/wiki/Standard_addition) (cited on 18/10/09)



counteracting spectral interferences caused by other elements in the analyte sample by enhancing the analyte signal. The drawback of this method is that it requires relatively large volumes of analyte sample (at least 100 ml, preferably 250 ml) for analysis and is easily affected by changes in temperature in the nebulizer.

#### **3.2.4.3 Internal standard addition**

Internal standardization is the last of the analytical method variations and has been the most commonly used approach towards correcting acid matrix<sup>171</sup> problems and interferences by easily ionized elements (EIE's) like Li, Na, K, Ca and Mg. The effect of acid matrix upon nebulization efficiency is such that a change in acid content from 5 to 10 % v/v will cause a decrease in efficiency of 10 to 35 % depending on the acid used, nebulizer design and liquid and gas flow rates. To compensate for the instrument response changes and the above mentioned matrixes, a known amount of the internal standard, different from the analyte, is added to the analyte solution. The success of this method depends entirely on the selection of a suitable internal standard that typically matches the properties of the analyte specie(s) such as ionization potentials. The signal from the analyte is compared (ratio) with the signal from the internal standard to determine analyte concentration. The concentration is determined from **Equation 3.2**.

$$\frac{A_x}{[X]} = F \left( \frac{A_s}{[S]} \right) \quad \dots 3.2$$

where F is the response factor of the instrument, [X] is the concentration of the analyte solution and the [S] is the concentration of the standard solution. The value of F close to unity gives the best linear slope, which can also be determined using the linear regression analysis method (see **Appendix 7**).

---

<sup>171</sup> A. S. Al-Ammara and R. M. Barnes, *J. Atomic Spec.*, (1998),19, pp. 18 - 22

The advantage of this method is that it is possible to compensate for the changes in analyte behaviour by comparing the analyte signal to that of the internal standard and to correct for the acid matrix effects. The drawback of this method is that it is very sensitive and any fluctuations in the plasma temperature results in the internal standard material adopting the same pattern of intensity of the analyte which will therefore affect the results.

A summary of the three methods used in ICP-OES analysis is given in **Table 3.1**.

**Table 3.1:** Summary of the ICP-OES methods of analysis

<b>Method</b>	<b>Advantages</b>	<b>Disadvantages</b>
Direct calibration	Easy to perform and no difficult calculations involved for determining the analyte concentration.	Easily affected by different matrix such as spectral and acid matrix.
Standard addition	No need to know the interfering species. Spectral interferences from interfering species are counteracted by enhancing the analyte signal.	Requires a lot of analyte solution for analysis (c.a. 100 ml and 250 ml)
Internal standard addition	It is capable of eliminating the interferences caused by the fluctuations of the physical and chemical properties of the analyte solution.	Material for the internal standard must have the same physical and chemical properties which make it difficult to find.

### **3.3 Validation of analytical methods**

Analytical method validation is one of the measures required by international regulations for compliance of analytical results in almost all areas of analysis to

ensure accurate and reliable results.<sup>172</sup> It also demonstrates the accuracy and reliability of the method for a particular analysis. In order to obtain credible and reliable results, validation parameters have to be analyzed and assessed.

### **3.3.1 The validation parameters<sup>173</sup>**

**Reagent blanks:** Reagents used during the analytical process (including solvents used for extraction or dissolution) are analyzed in isolation in order to see whether they contribute to the measurement signal. The measurement signal arising from the analyte can then be corrected accordingly.

**Samples / test materials:** Test materials taken from real samples are useful because of the information they yield on interferences. If the true analyte content of the test sample is accurately known, it can be used as a way of assessing the accuracy of the method. However, the true analyte content is usually difficult to determine unless there is the possibility of using other methods which are known to show negligible bias.

**Standards (Measurement):** These are traditionally thought of as solutions of single substance, but in practice can be anything in which a particular parameter or property has been characterized to a sufficient extent. It can be used for reference or calibration purposes.

**Reference materials:** Can be virtually any material used as a basis for reference and could include laboratory reagents of known purity, industrial chemicals, or other artifacts. The reference material needs only to be stable and homogenous and does not need to have a high degree of characterization, traceability and certification.

**Certified reference materials (CRM):** The characterization of the parameter of interest in a certified reference material is generally more strictly controlled than for a

---

<sup>172</sup> M. Thompson, S. L. R. Ellison and R. Wood, *Pure Appl. Chem.*, (2002), 74, pp. 835 - 855

<sup>173</sup> <http://www.reagecon.com/TechPapers/guidemethodvalidation.pdf> (cited on 25/10/09)

reference material, and in addition the characterized value is certified with a stated uncertainty by a recognized institution such as the National Institute of Standards and Technology (NIST) and International Organization for Standardization (ISO).<sup>174</sup> Characterization is normally done using several different methods, so that any bias in the characterization is reduced or even eliminated.

The basic purpose of CRM is to improve the comparability of measurements and to increase the credibility of the results. CRM can also be used at two different stages of the measurement process, for calibration i.e. as a tool to transfer traceability and for quality control, i.e. as a tool to verify the accuracy and the performance of a method.<sup>175</sup>

### **3.3.2 Validation procedure**

During the validation process, the method of analysis is assessed for accuracy, precision, specificity, limit of detection, limit of quantification, dynamic range, ruggedness and robustness.<sup>176</sup> A method is considered accurate if it has a high degree of recovery, precision and sensitivity as determined by the regression coefficient ( $r^2$ ) of at least 0.997. It is also supposed to be free from interferences (specificity), to have a detection limit in the parts per billion (ppb) range, wide linear dynamic range (ICP-OES,  $10^5$ - $10^6$  orders of magnitude), ruggedness (the degree of reproducibility) and robustness as accounted by low relative standard deviation (RSD). The summary of the validation criteria is given in **Table 3.2**.

---

<sup>174</sup> ISO, International vocabulary of basic and general terms in metrology, Geneva, (1993)

<sup>175</sup> Guide for the Production and Certification of BCR Reference Materials, EC, DG XII, Doc. BCR/48/93, December 15, (1994)

<sup>176</sup> Eurachem Guide, The Fitness for Purpose of Analytical Methods A Laboratory Guide to Method Validation and Related Topics, (1998)

**Table 3.2:** Validation criteria<sup>177</sup>

Method validation procedure	Parameter to be determined
Confirmation of identity and selectivity/specificity	Linear regression line ( $r^2$ )
Limit of detection (LOD)	3 x S of the blank
Limit of quantitation (LOQ)	10 x S of the blank
Working and linear ranges	The difference between LOQ and LOL
Accuracy	Selectivity and specificity ( $r^2$ )
Trueness	Method or reference comparison
Repeatability	Precision
Reproducibility	Robustness
Measurement uncertainty	Accuracy
Sensitivity	The gradient of the calibration
Ruggedness	Competency of analyst instrument

LOL = limit of linearity

$r^2$  = regression coefficient

S = standard deviation

The purpose of method validation is to demonstrate that the established method is fit for the intended purpose. Much of the method validation and development are performed in an iterative manner, with adjustments or improvements on the method parameters such as temperature (laboratory and spray chamber), concentration of reagents and equipment parameters such as RF power, nebulizer, spray chamber, as well as torch design and torch height.

Selectivity and specificity are measures of the reliability of measurements in the presence of interferences. The selectivity of a method is usually investigated by studying the method's ability to measure the analyte of interest in the presence of the possible interfering species of the analyte sample and the acid matrix. Sensitivity

<sup>177</sup> S. Seno, S. Ohtake and H. Kohno, *Analytical validation in practice at a quality control laboratory in the Japanese pharmaceutical industry, Accred. Qual. Assur.* (1997), 2, pp. 140 – 145

can be determined from the gradient of the calibration curve (see **Section 3.3.3; Figure 3.11**) and can also be determined using the least-squares method of the best straight line. Not all the data points of the calibration curve will fall exactly on the straight line (calibration curve) and deviations (residuals) from linearity usually occur. Regression analysis is normally applied to measure the uncertainties associated with the data points of the calibration curve. This uncertainty can be evaluated by specifying the percentage confidence interval (mostly 95 %) under stipulated degrees of freedom to which the outcome can be accepted or rejected using the hypothesis test.<sup>178</sup> In the hypothesis test there are two contradictory outcomes that influence the decision on whether to accept or reject the outcome. The first outcome can be regarded as a null hypothesis  $H_0$ , which states that the outcome  $\mu$  is equal to the known value  $\mu_0$  (i.e.  $\mu = \mu_0$ ). The second test is called the alternative hypothesis  $H_a$  which can be stated in several ways. The  $H_0$  can be rejected in favour of the  $H_a$  if  $\mu$  is different from  $\mu_0$  (i.e.  $\mu \neq \mu_0$ ). For tests with a larger number of experimental replicates (>20) such that the standard deviation (S) of the outcome values is a good estimate of the population standard deviation ( $\delta$ ), a z-statistic is used, and in the case where (S) is not known or is not a good estimate of  $\delta$ , a t-statistic is used. The rejection region for the z-statistic at 95 % percentage confidence level is shown in **Figure 3.9**.

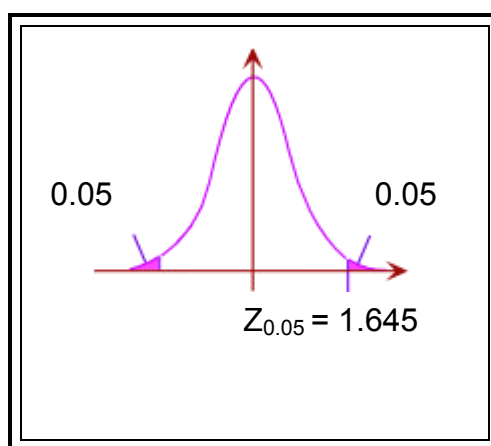


**Figure 3.9:** The normal distribution for the z-statistic at 95 % confidence interval

---

<sup>178</sup> D. A. Skoog, F. J. Holler and T. A. Nieman, *Principles of Instrumental Analysis*, Saunders College Publishing, USA, 5th ed., (1998), pp. 149 - 153.

The alternative hypothesis ( $H_a$ ) for  $\mu > \mu_0$  is rejected when  $z$  is greater than 1.64 ( $z_{crit}$ ) and for  $H_a: \mu < \mu_0$ ,  $z$  values less than -1.64 ( $z_{crit}$ ) are rejected. The  $z$  values are calculated as shown in **Equation 3.3** where  $\bar{x}$  is the mean of the outcomes and  $N$  is the sample size.

$$z = \frac{\bar{x} - u_0}{\left(\frac{s}{\sqrt{N}}\right)} \quad \dots 3.3$$

From the regression coefficient ( $r^2$ ) of the calibration curve, sensitivity is therefore determined as the measure of the correlation between the  $x$  and  $y$  values of the data points. A value closer to unity for  $r^2$  explains the best correlation between the  $x$  and  $y$  values and the better linear graph, as illustrated in **Figure 3.10**.

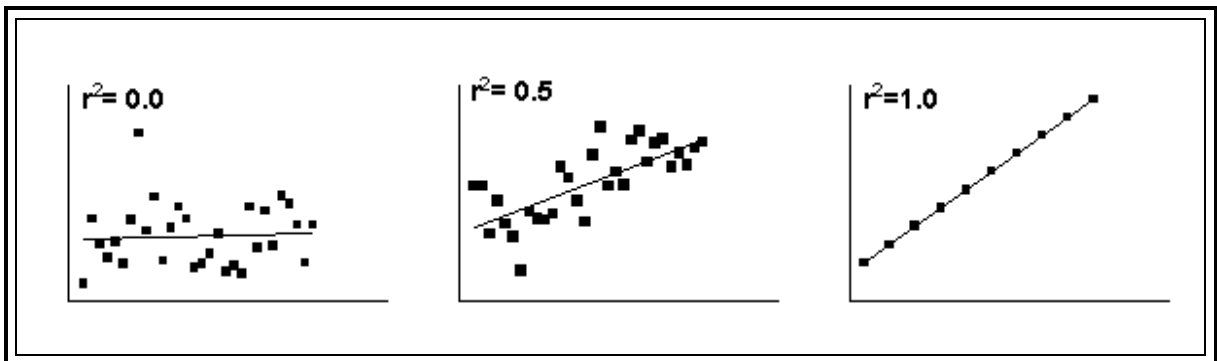


**Figure 3.10:** Linear relationship between the  $x$  and  $y$  values.<sup>179</sup>

The value of  $r^2$  is obtained from **Equation 3.4**

$$r^2 = \frac{(n \sum(xy) - \sum x \sum y)^2}{n \sum(x^2) - (\sum x)^2 \left[ n \sum(y^2) - (\sum y)^2 \right]} \quad \dots 3.4$$

where  $n$  is the number of data points along the calibration curve.

<sup>179</sup> [http://www.curvefit.com/linear\\_regression.htm](http://www.curvefit.com/linear_regression.htm) (cited on the 24/10/09)

Alternatively,  $r^2$  can also be obtained from **Equation 3.5**

$$r^2 = 1 - \frac{SS_{\text{resid}}}{SS_{\text{tot}}} \quad \dots 3.5$$

where  $SS_{\text{resid}}$  is the sum of the residuals and  $SS_{\text{tot}}$  is the sum of  $SS_{\text{resid}}$  squared. The difference between  $SS_{\text{tot}}$  and  $SS_{\text{resid}}$ ,  $SS_{\text{regr}}$ , indicates the variation of the y values from the curve. Dividing the sum of the squares ( $SS_{\text{tot}}$ ) by the appropriate number of degrees of freedom gives the mean square values for regression of the residuals (error) and also the F value which is used to test for the null hypothesis. The F value is calculated as shown in **Equation 3.6**,

$$F = \frac{\left( \frac{SS_{\text{regr}}}{X} \right)}{\left( \frac{SS_{\text{resid}}}{Y} \right)} \quad \dots 3.6$$

where X is the degrees of freedom corresponding to the difference between  $SS_{\text{tot}}$  and  $SS_{\text{resid}}$  and Y is the degree of freedom corresponding to the sum of the squares of the residuals.

The F value gives an indication of the significance of the regression. A value of F smaller than the F-values from the data tables<sup>180</sup> at a specified confidence level indicate that the null hypothesis should be accepted and the regression becomes less significant and *vice versa*.<sup>181</sup>

Precision or repeatability is the degree to which repeated measurements under unchanged conditions show the same results and is usually stated in terms of the

---

<sup>180</sup> <http://www.statsoft.com/textbook/sttable.html> cited on (29/10/09)

<sup>181</sup> D. A. Skoog, D. M. West, F. J. Holler and S. R. Crouch, *Fundamentals of Analytical Chemistry*, 8<sup>th</sup> Ed, (2004), pp. 195 - 201



relative standard deviation (**Equation 3.8**).<sup>182</sup> The relative standard deviation is preferred over the standard deviation (**Equation 3.7**) because it gives the percentage estimate of the deviation of the data points as opposed to the absolute standard deviation. Precision differs from accuracy in the sense that accuracy focuses on the degree of trueness while precision on the degree of reproducibility.

$$\text{Standard deviation (S)} = \left( \frac{\sum (x_i - \bar{x})^2}{N-1} \right)^{\frac{1}{2}} \quad \dots 3.7$$

$$\text{Relative standard deviation (RSD)} = \frac{S}{\bar{x}} 100 \% \quad \dots 3.8$$

where  $\sum x_i^2$  is the sum of the data points squared,  $\bar{x}$  is the mean of the data set and  $\sum \bar{x}_i^2$  is the sum of the mean of the data points.

Ruggedness is almost the same as precision, but differs in the sense that ruggedness is the degree of reproducibility of test results obtained by the analysis of the same samples under a variety of normal test conditions such as different laboratories, different analysts, different instruments and different analysis days.

Robustness can be described as the ability to reproduce the (analytical) method in different laboratories or under different circumstances without the occurrence of unexpected differences in the obtained result(s). A robustness test can be performed under different experimental conditions to evaluate the robustness of a method.

### 3.3.3 Detection limits

In quantitative analysis, it is important to know the lowest concentration (limit of detection (LOD)) of the analyte that can be detected by the method. Frequently the detection of the analyte does not simply cease at a threshold level, but tends to “fade” from a predictable signal/concentration ratio gradually to an indiscernible

---

<sup>182</sup> J. R. Taylor. *An Introduction to Error Analysis: The Study of Uncertainties in Physical Measurements*, (1999), pp. 128 - 129

response. For qualitative measurements, there is likely to be a concentration threshold below which specificity becomes unreliable (limit of linearity (LOL)). The threshold may vary if the experiment is repeated at another time with different reagents, fortification, spiking materials, etc. The “limit of quantitation” (LOQ) is the smallest concentration of analyte that can be determined with an acceptable level of repeatability, precision and trueness as illustrated in **Figure 3.11**.

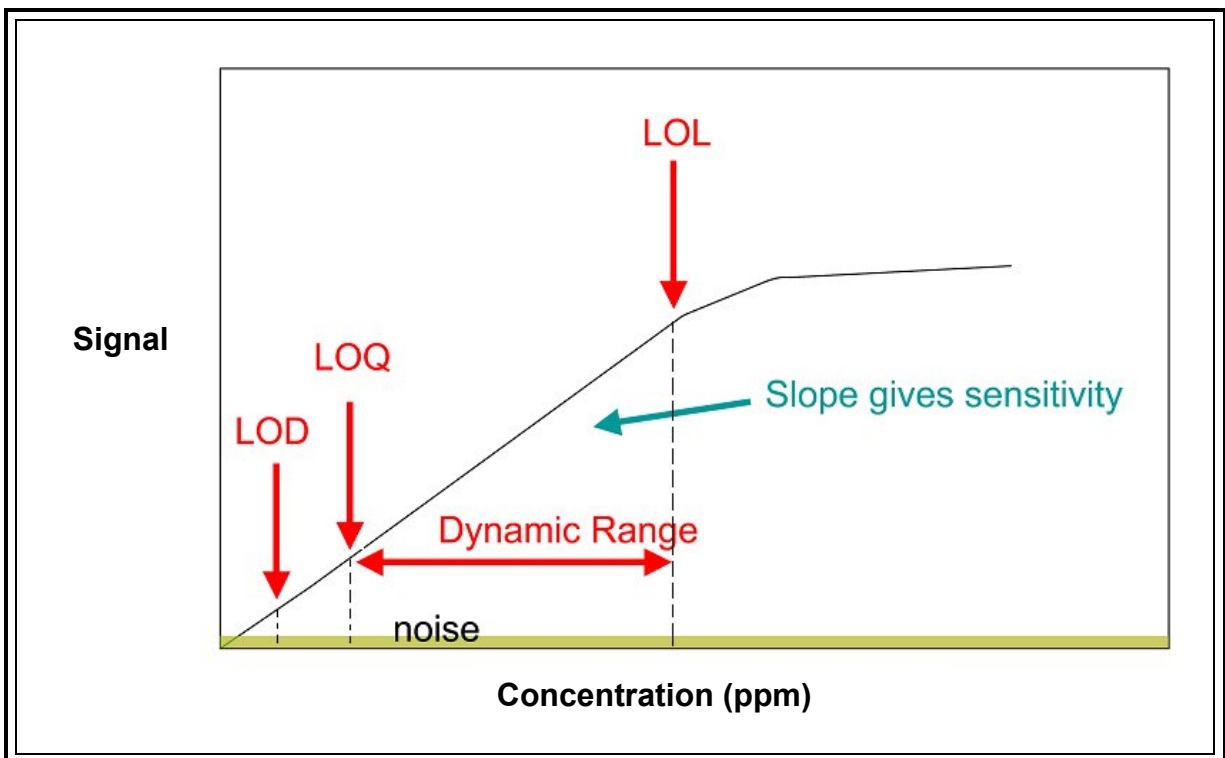


**Figure 3.11:** A calibration curve plot showing limit of detection (LOD), limit of quantitation (LOQ), dynamic range and limit of linearity (LOL).<sup>183</sup>

From the equation of the slope,  $y = mx + y_0$ , the limit of detection (LOD) and the limit of quantitation (LOQ) (**Figure 3.12**) is given by **Equation 3.9 and 3.10** respectively.

$$\text{Limit of detection (LOD)} = 3s / y_0 \quad \text{and} \quad \dots\mathbf{3.9}$$

$$\text{Limit of quantitation (LOQ) is } \text{LOQ} = 10s / y_0 \quad \dots\mathbf{3.10}$$

<sup>183</sup> [http://en.wikipedia.org/wiki/Calibration\\_curve](http://en.wikipedia.org/wiki/Calibration_curve) (cited 17/10/09)

where  $s$  is the standard deviation (see **Equation 3.7**) calculated from measuring 10 times the intensity of the blank solution.

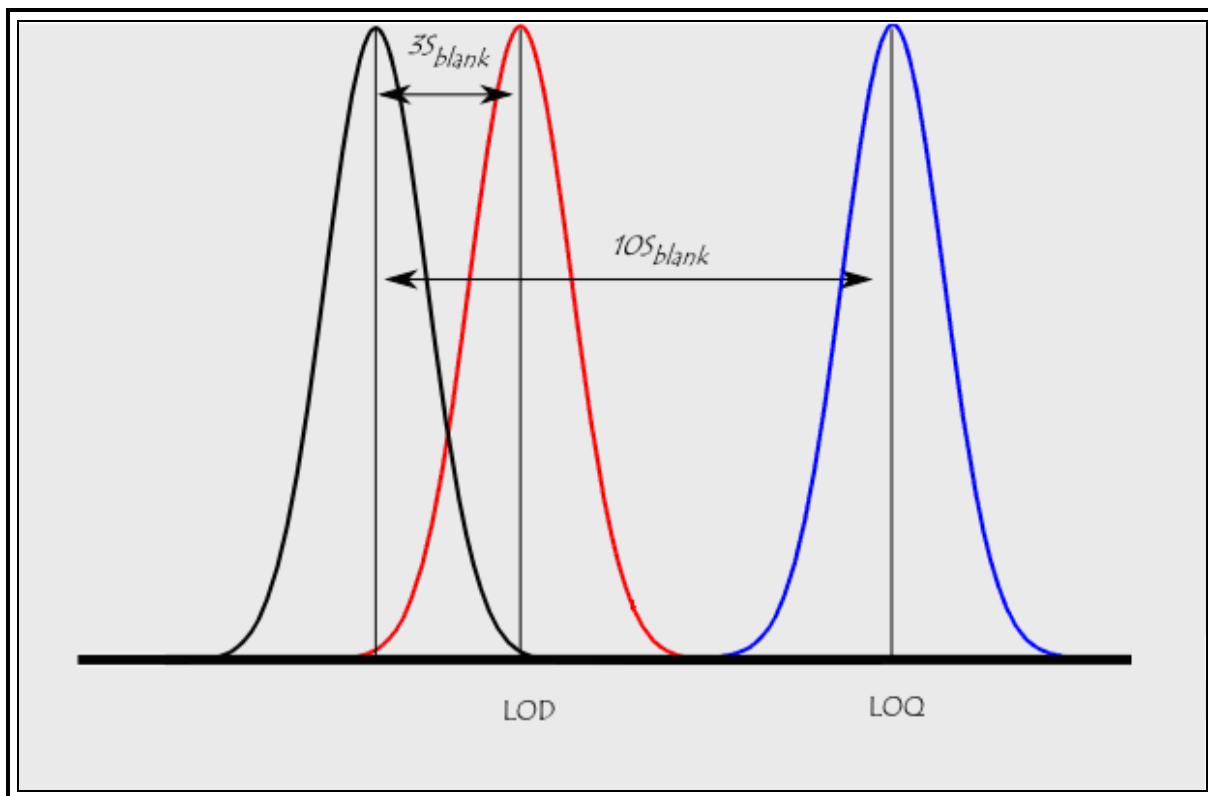


**Figure 3.12:** The relationship between the limit of detection (LOD) (red) and the limit of quantitation (LOQ) (blue).<sup>184</sup>

## 3.4 ICP-OES

### 3.4.1 Outline of the ICP-OES procedure

A graphical presentation of the sample preparation and analysis by ICP-OES are shown in **Figure 3.13**.

---

<sup>184</sup> [http://en.wikipedia.org/wiki/Detection\\_limit](http://en.wikipedia.org/wiki/Detection_limit) (cited 26/09/09)

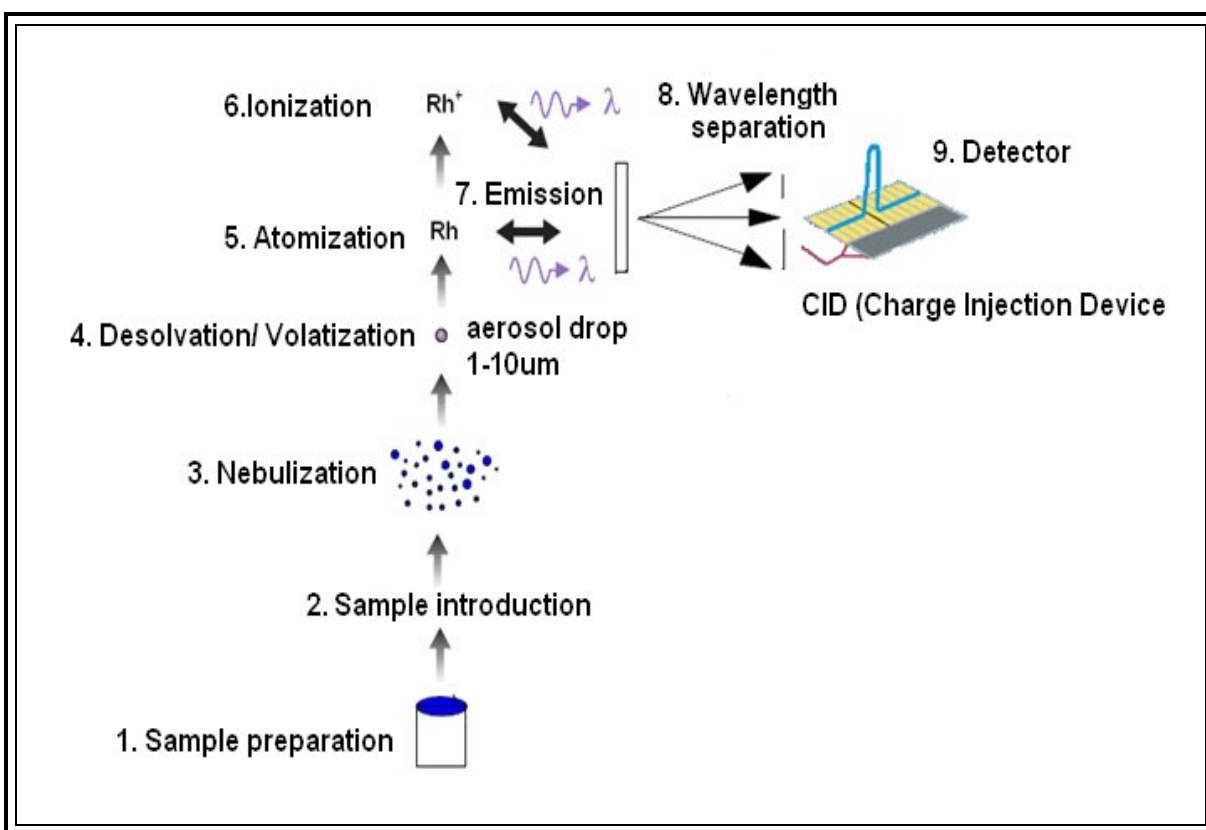


**Figure 3.13:** Sample preparation and determination by ICP-OES

Determination of a sample (in this case rhodium) begins with the sample preparation where the analyte sample is converted into a water soluble solution. The analyte solution is then introduced into the ICP-OES torch by the nebulizer to yield fine aerosol drops in the 1–10 μm range. The nebulized aerosol is heated at elevated temperatures (ca. 6 000 to 10 000 °C) in the argon plasma. Atoms (atomization) and ions (ionization) are formed by absorbing the heat energy. The electron transition that occurs when the electron of an excited atom or ion decays back to the ground state level release a photon of energy which is characteristic to a particular element. The emitted energy is characterized by the different wavelengths which are detected and quantified by the charge injection devise (CID).

The ICP-OES spectrometer consists of three main basic features which are the sample introduction system, the plasma torch and spectrometer as shown in **Figure 3.14**.

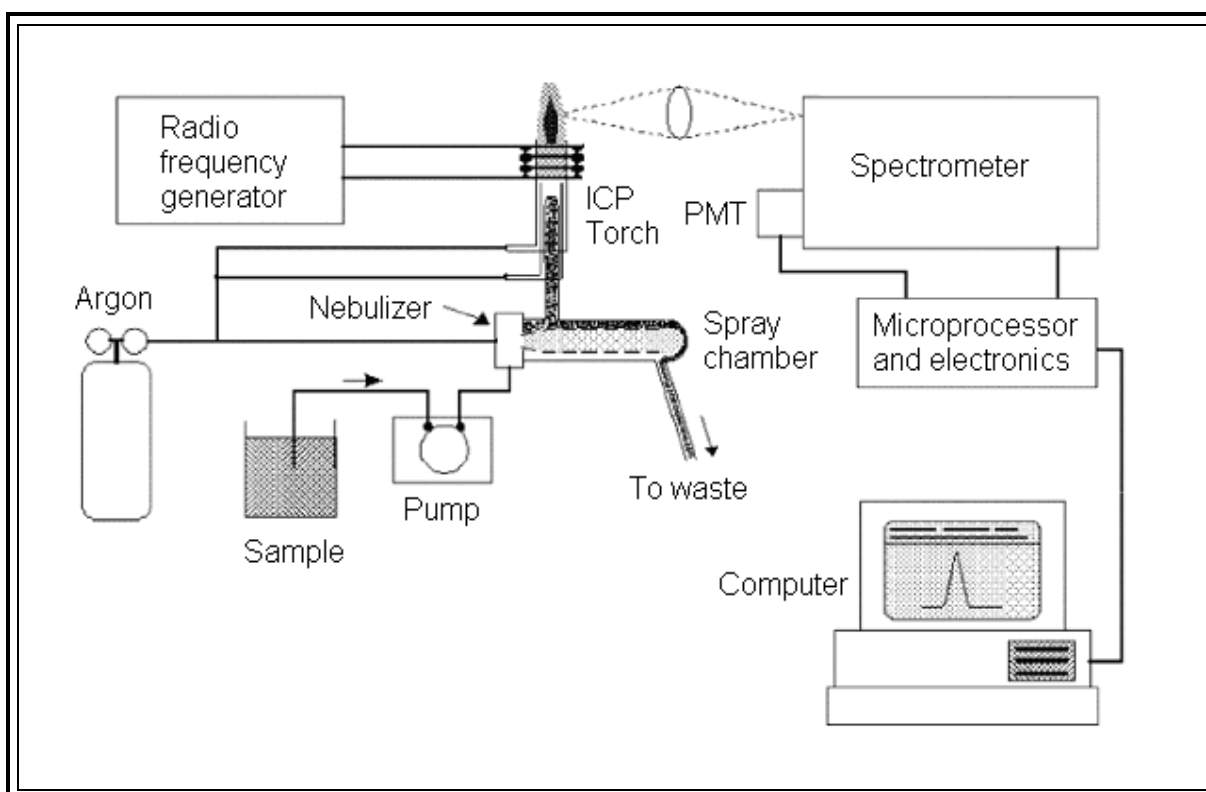


**Figure 3.14:** Major components and layout of a typical ICP-OES instrument<sup>185</sup>

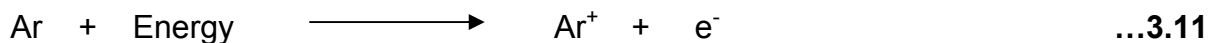
### 3.4.2 Sample introduction system

The sample introduction system on the ICP-OES consists of a peristaltic pump, PTFE Teflon tubing, a nebulizer and a spray chamber. The fluid sample is pumped into the nebulizer *via* the peristaltic pump, which then generates an aerosol mist and injects humidified argon gas into the chamber along with the sample.

### 3.4.3 The plasma torch

A plasma can be defined as a “luminous volume of partially ionized gas” containing an abundant concentration of cations and electrons. The plasma is generated from radio frequency (RF) magnetic fields induced by a copper coil wound around the top of a glass torch. The plasma used in atomic emission is formed by ionizing a flowing stream of argon gas, producing in this process argon ions and electrons as shown in **Equation 3.11**.

<sup>185</sup> M. Xiaoguo and L. Yibing, *Anal Chim. Acta.*, (2006), 579, pp. 47 - 52



The aerosol mist that accumulates in the spray chamber will have the largest mist particles and will settle out as waste while the finest particles are subsequently swept into the torch assembly. Approximately 1 % of the total solution eventually enters the torch as a mist, whereas the remainder is pumped away as waste.

The inductive coupled plasma torch has a triple-structure made of quartz, which consist of three concentric tubes, the outer tube (plasma gas), the middle tube (auxiliary gas), and the inner tube acting as the sample injector (carrier gas) as shown in **Figure 3.15**.

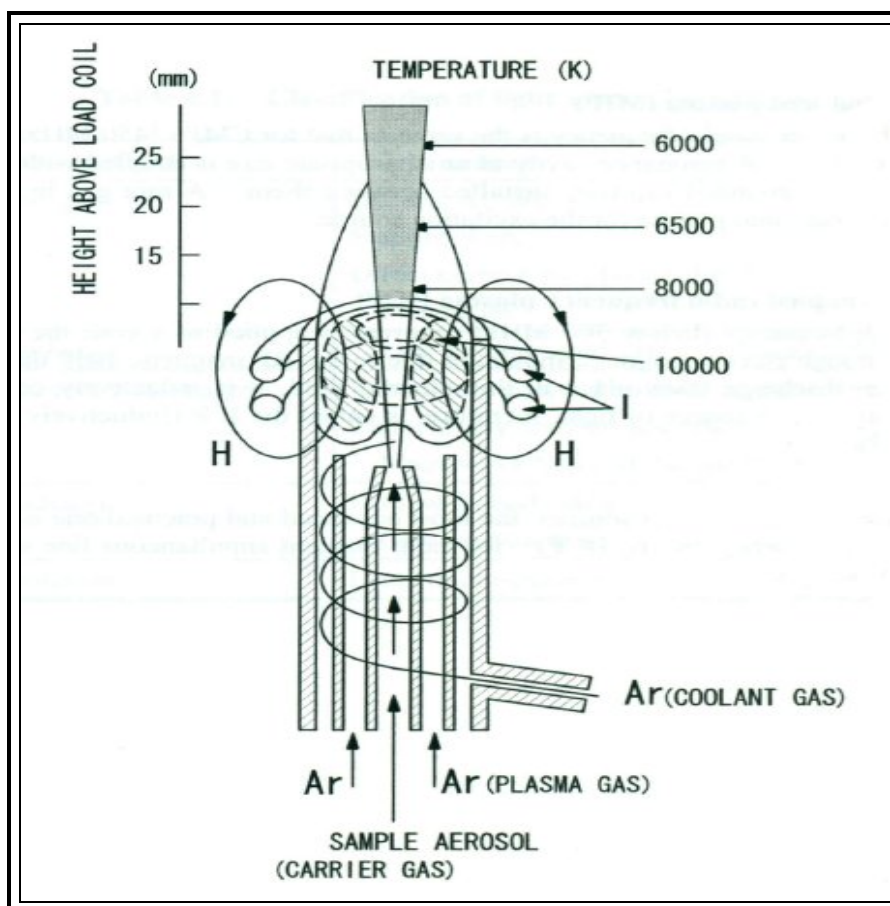


**Figure 3.15:** Gas flow through the plasma torch<sup>186</sup>

<sup>186</sup> C. B. Boss and K. J. Fredeen, *Concepts of Instrumentation and Techniques in Inductively Coupled Plasma Optical Emission Spectrometry*, (2004)

Argon gas is usually introduced as the coolant gas at the rate of 10 to 20 Lmin<sup>-1</sup>. The plasma gas usually flows at the rate of 0.4 to 1.4 L/min. The carrier gas also introduces the atomized sample solution droplets to the center of the plasma. It usually flows at the rate of 0.7 L/min. The flow rate of this carrier gas directly influences the amount of sample introduced. An excessive flow rate of the sample into the plasma will shorten the time spent at these high temperatures which will lead to poor atomization and sensitivity of samples.

A sample solution is introduced into the core of inductively coupled argon plasma (ICP), which generates a temperature of approximately 8 000 °C. At this temperature all elements become thermally excited and emit light at their characteristic wavelengths (see **Section 3.2.2**).

### **3.4.3.1 Nebulizer and chamber**

The nebulizer acts as an atomizer for the introduction of the sample to the plasma. The chamber selectively leads the atomized sample particles to the plasma by draining away the larger particles and sending the smaller ones to the torch as shown in **Figure 3.16**.

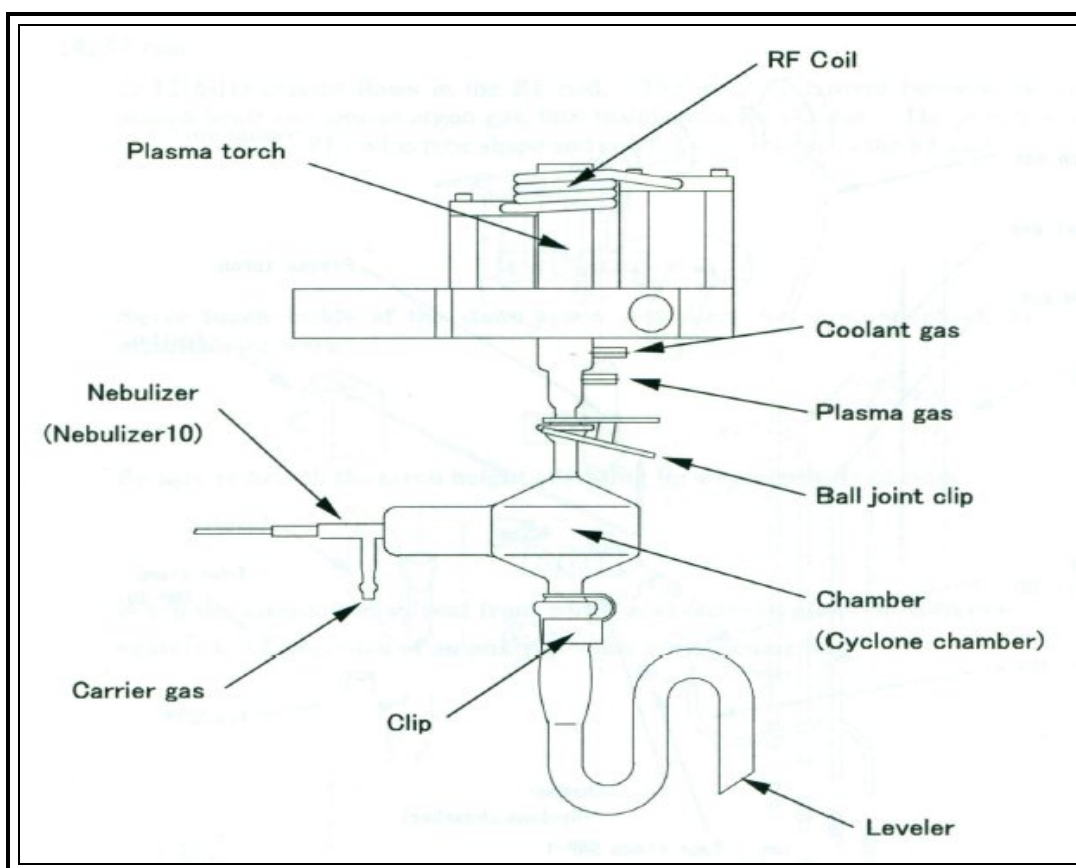


Figure 3.16: Plasma torch assembly<sup>187</sup>

#### 3.4.3.2 Levelers

This device provides two functions; one to maintain the chamber volume constant and the other to act as a valve which prevents pressure from entering the drain.

#### 3.4.3.3 RF coil

The radio frequency (RF) generates power for the sustainment of the plasma discharge. The power ranges between 700 and 1 500 watts and flows through the RF coil to the plasma. The inducted current between the coil and plasma then heats up and ionizes the argon gas, thus maintaining the plasma.

<sup>187</sup> <http://www.chemistry.adelaide.edu.au/external/soc-rel/content/icp.htm> (cited on 15/09/09)



### 3.4.4 Spectrometer

Light emitted from the plasma is focused onto the entrance slit of a monochromator or polychromator (**Figure 3.17**) to monitor emission from different elements either sequentially or simultaneously. Spectral lines caused by the transfer of an electron from one energy level to another produces intense lines whilst weak lines are formed where transition occurs with difficulty. The detected signals depend on both the number of analyte ions (or atoms) in the plasma and the fraction of those ions (or atoms) that are excited.

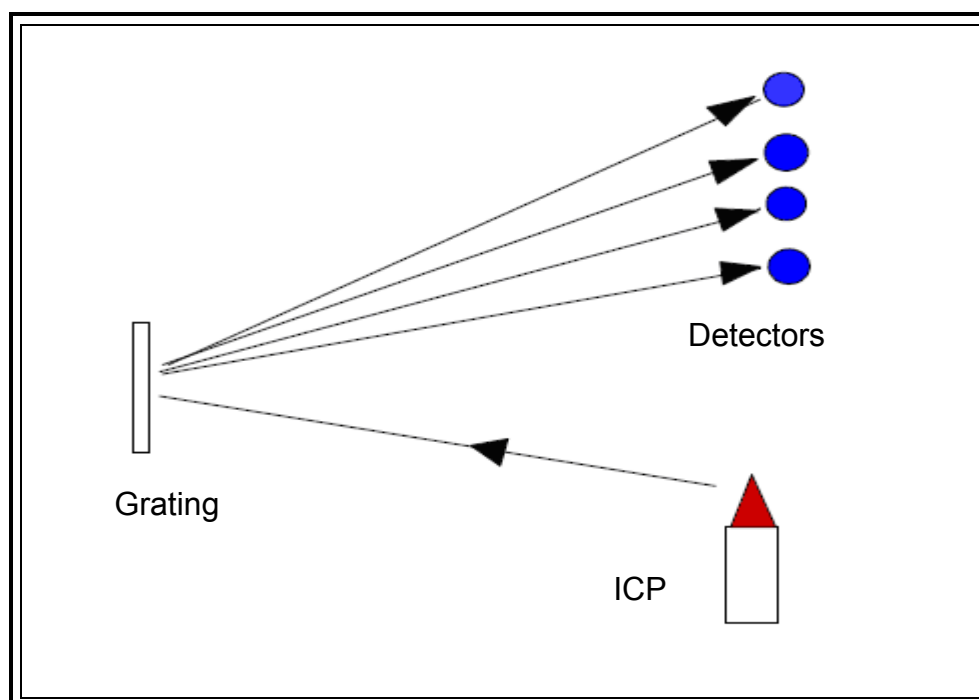


**Figure 3.17:** A polychromator for simultaneous analysis of light emission<sup>188</sup>

The ability of a polychromator to measure more than one analytical line at a time is a distinct advantage over a monochromator, but however, it suffers from a lack of flexibility. Thus, once the dispersion and detection systems are set in such a system, only certain analytical lines and elements may be measured.

The ICP-OES with the plasma oriented vertically is known as the “radial viewing” whilst the one with the plasma oriented horizontally is known as the “axial viewing”.

<sup>188</sup> [http://www.thespectroscopynet.com/Index.html?/Spectrometers\\_2.html](http://www.thespectroscopynet.com/Index.html?/Spectrometers_2.html) (cited on 15/09/09)

The former has the advantage of providing immediate venting of exhaust gases and waste heat to an overhead extraction system whilst the latter has the best sensitivity particularly in the environmental analyses of water and wastes.<sup>189</sup>

### **3.5 Microwave digestion<sup>190</sup>**

Analytical techniques such as ICP-OES, AAS and other atomic and molecular spectrometry techniques (see **Chapter 2, Section 2.2.4**) require quantitative transformation of the insoluble analyte samples into a soluble homogenous state prior to analysis. Typical methods of sample preparation include extraction, dissolution, or acidification and should result in a solution free of particulates for spectrometric analysis. The microwave digestion technique has been shown to depend on the direct coupling of electromagnetic radiation with the mineral acids solvents.<sup>191</sup> This technique makes use of the electromagnetic radiation with frequency in the 300 MHz to 300 GHz range and a wavelength ranging from 0.1 cm to 100 cm.

Microwave digesters make use of high temperatures and pressures to decompose analytical samples. Digestion under these conditions takes considerably less time to reach completion compared to decompositions limited by the boiling points of the same acids. Inorganic and organometallic substances that cannot be decomposed by mineral acids at their normal boiling points are normally decomposed successfully at elevated temperatures and pressures.<sup>192,193</sup>

---

<sup>189</sup> M. B. Knowles, T. T. Nham and S. J. Carter, *The latest advances in axially viewed simultaneous ICP-OES for elemental analysis*, (1998), 8, pp. 25 - 32

<sup>190</sup> A. Abu-Samra, J. S Morris and S. R Koirtyohann, *Anal. Chem.*, (1975), 47, pp 1475 - 1477

<sup>191</sup> A. Abu-Samra, J. S Morris and S. R. Koirtyohann, *Trace Subst. Environ. Health* (1975), 9, pp. 297 - 301

<sup>192</sup> E. Jackwerth and S. Gomscek, *Pure Appl. Chem.* (1984), 4, p. 56

<sup>193</sup> R. Bock. *A Handbook of Decomposition Methods in Analytical Chemistry*, (1979)

### 3.5.1 Equipment

A Perkin–Elmer multiwave 3 000 microwave (**Figure 3.18**) digester system was used in this study. An on-board computer is used for controlling heating and pressure variations needed for the digestion of the samples. The three major components are the magnetron (microwave generator), the microwave cavity and the wave guide.

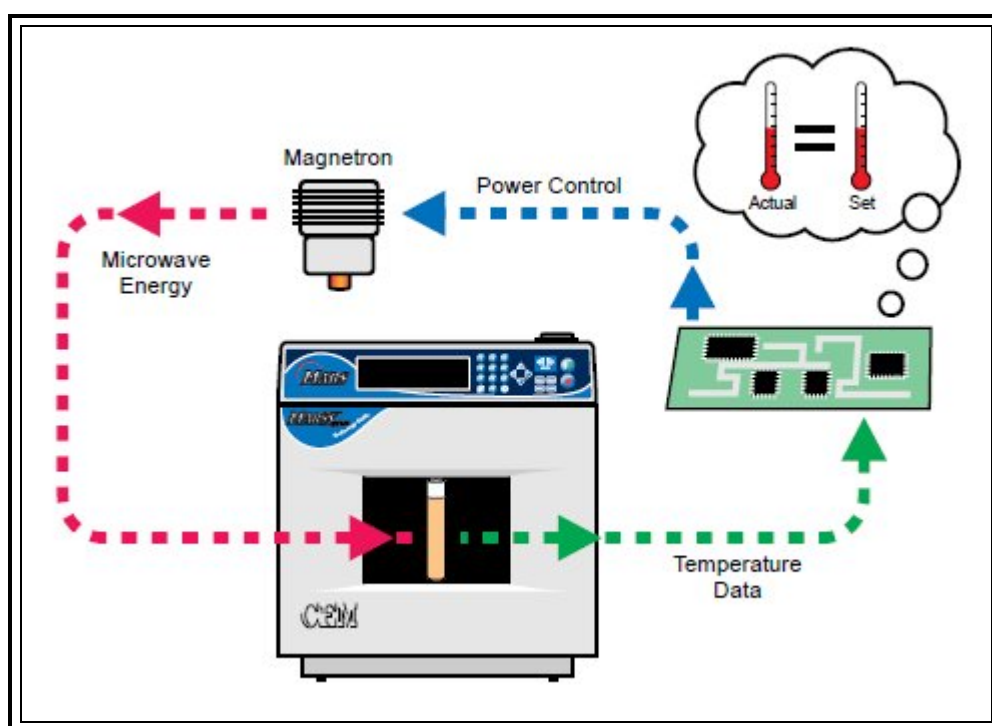


**Figure 3.18:** Microwave digestion technique<sup>194</sup>

The magnetron consists of an anode, which is fabricated from a cylindrical solid copper block, and a cathode, which is constructed of a high-emission material such as the centre of lobed, circular chamber as shown in **Figure 3.19** and **Figure 3.20**.

<sup>194</sup> [http://www.cem.de/documents/pdf/produkte/englisch/MARSXpress\\_rev2.pdf](http://www.cem.de/documents/pdf/produkte/englisch/MARSXpress_rev2.pdf) (cited on 10/09/09)

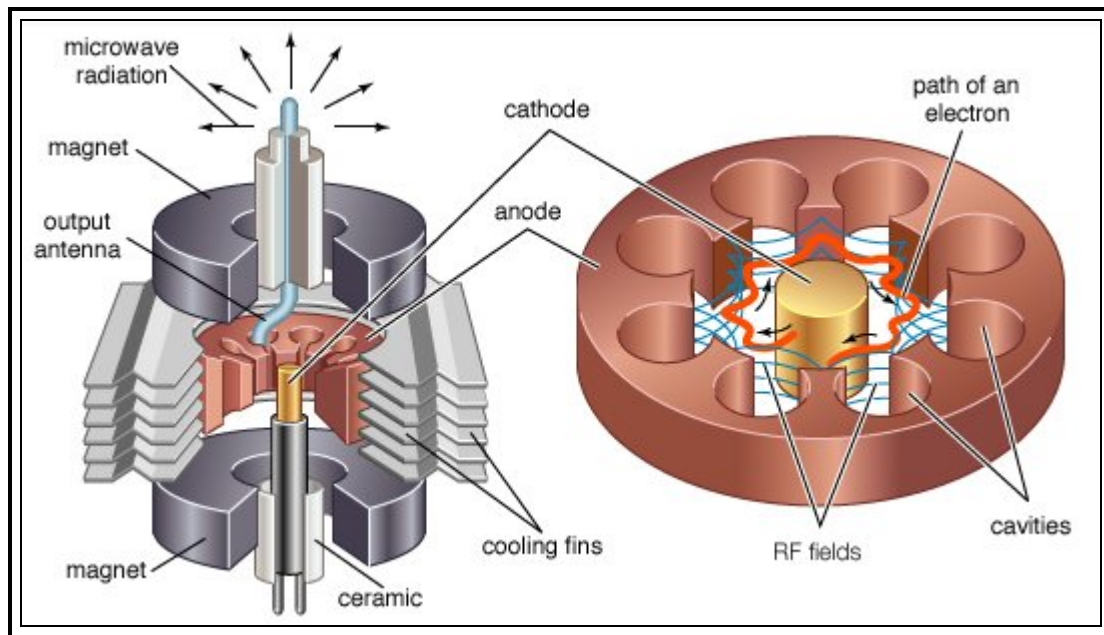


Figure 3.19: Section through a microwave magnetron<sup>195</sup>

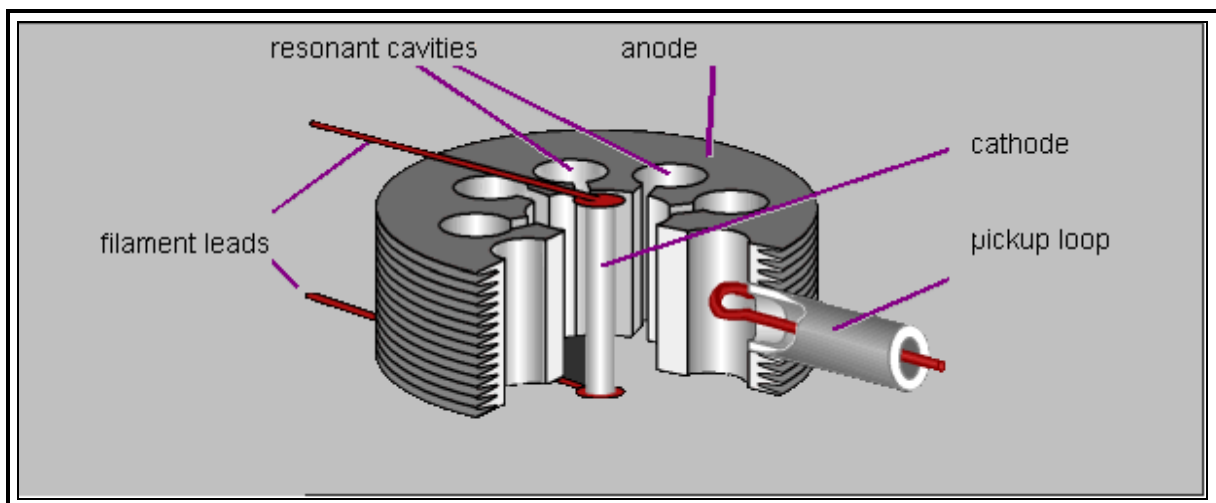


Figure 3.20: Cross section of a magnetron<sup>196</sup>

The 8, up to 20 cylindrical holes around the anode's circumference are the resonant cavities which are open along their length to allow the movement of electrons. A magnetic field parallel to the filament is imposed by a permanent magnet seated adjacent to it. This magnetic field causes the electrons, which are attracted to the positively charged outer part of the chamber, to spiral outward in a circular path

<sup>195</sup> [mainland.cctt.org/istf2008/generators.asp](http://mainland.cctt.org/istf2008/generators.asp) (cited on 10/09/09)

<sup>196</sup> <http://www.radartutorial.eu/08.transmitters/tx08.en.html> (cited 28/10/09)

rather than moving directly to this anode.<sup>197</sup> These electrons generate a high resonant frequency, which in turn causes them to bunch together into a group giving out microwave radiation. The microwave field is then conveyed by the waveguide (a metal tube usually of rectangular cross section as shown in **Figure 3.21**) to the digestion vessel.

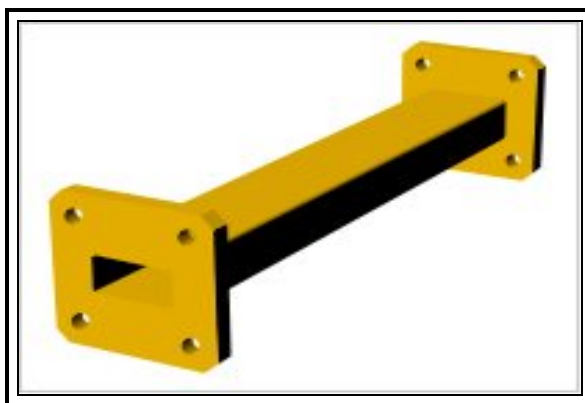


**Figure 3.21:** Rectangular structure of a waveguide<sup>198</sup>

Polytetrafluoroethylene (Teflon) based digestion vessels allow the microwave energy to penetrate through the walls of the vessel without being directly heated. Noeltner *et al.*<sup>199</sup> have demonstrated and recommended the use of these vessels to meet the analytical requirements and to achieve low blank background values necessary for accurate trace element determination.

### 3.5.2 Sample digestion

The generated microwaves results in an increased oscillation of the sample molecules. In conventional heating, the material's surface (e.g. Teflon) heats first and then the heat is transferred inward as shown in **Figure 3.22**.

---

<sup>197</sup> H. M. Kingston, L. B. Jassie, *Introduction to Microwave Sample Preparation Theory and Practice*, (1988)

<sup>198</sup> [http://en.wikipedia.org/wiki/Waveguide\\_\(electromagnetism\)](http://en.wikipedia.org/wiki/Waveguide_(electromagnetism)) (cited on 10/09/09)

<sup>199</sup> T. Noeltner, P. Maisenbacher and H. Puchelt, *Spectroscopy* (1990), 5, pp. 49 - 53

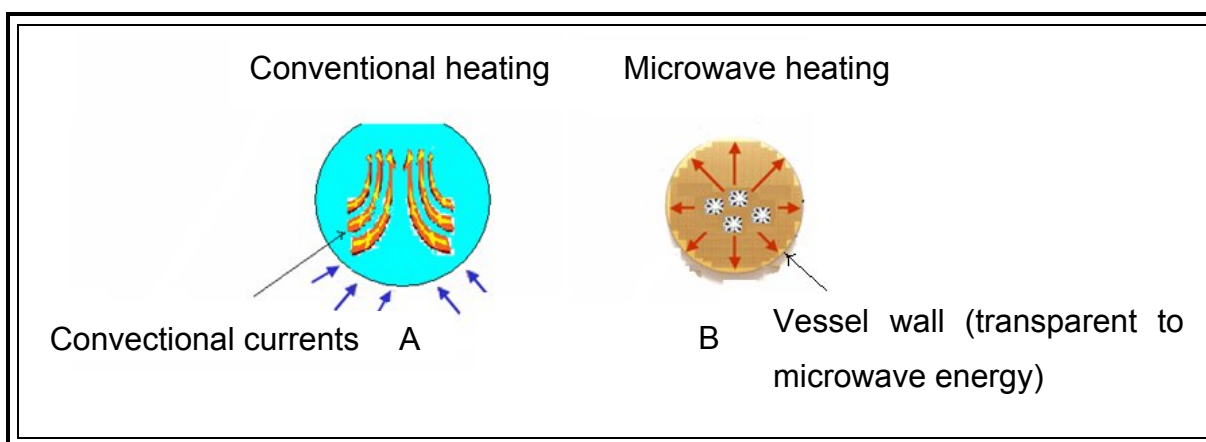


**Figure 3.22:** Sample heating by microwave energy<sup>200</sup>

In contrast to conventional heating, microwave heating generates heat within the material and heats the entire volume at about the same rate, resulting in shorter and more effective digestion.

## 3.6 Thermal Gravimetric Analysis (TGA) and Differential Scanning Calorimetry (DSC)

### 3.6.1 Introduction

In this study, TGA and DSC were used to determine the percentage of water of crystallization in  $\text{RhCl}_3 \cdot x\text{H}_2\text{O}$  so as to evaluate the success of the rhodium analysis. TGA and DSC are part of a group of techniques called “thermal analysis” and are based upon the detection of changes in the heat content (enthalpy) and the loss or gain in weight of the sample during the heating process.

### 3.6.2 Thermal Gravimetric Analysis (TGA)

Thermal gravimetric analysis (**Figure 3.23**) measures changes in the mass of a sample as a function of temperature and/or time.<sup>201</sup> The measurement is normally

<sup>200</sup> [www.dsgtek.com/technology.htm](http://www.dsgtek.com/technology.htm) (cited on 10/09/09)

<sup>201</sup> P. J. Haines, *The Royal Society of Chemistry, Cambridge, (2002)*

carried out in an inert atmosphere, such as helium or argon to prevent chemical interference.



**Figure 3.23:** View of a TGA apparatus<sup>202</sup>

In TGA a sample of the test material is placed into an alumina cup that is supported on, or suspended from an analytical balance located outside the furnace chamber. The balance is zeroed, and the sample cup is heated according to a predetermined thermal cycle. The balance sends the mass signal to the computer for storage, along with the sample temperature and the elapsed time. The TGA plots a curve of the TGA signal, converted to a percentage change of the mass on the Y-axis (green colour) against the reference material temperature on the X-axis (blue colour), as shown in **Figure 3.24**.

---

<sup>202</sup> [www.ibnusina.utm.my/about/index.php?option=co...](http://www.ibnusina.utm.my/about/index.php?option=co...) (cited on 15/09/09)

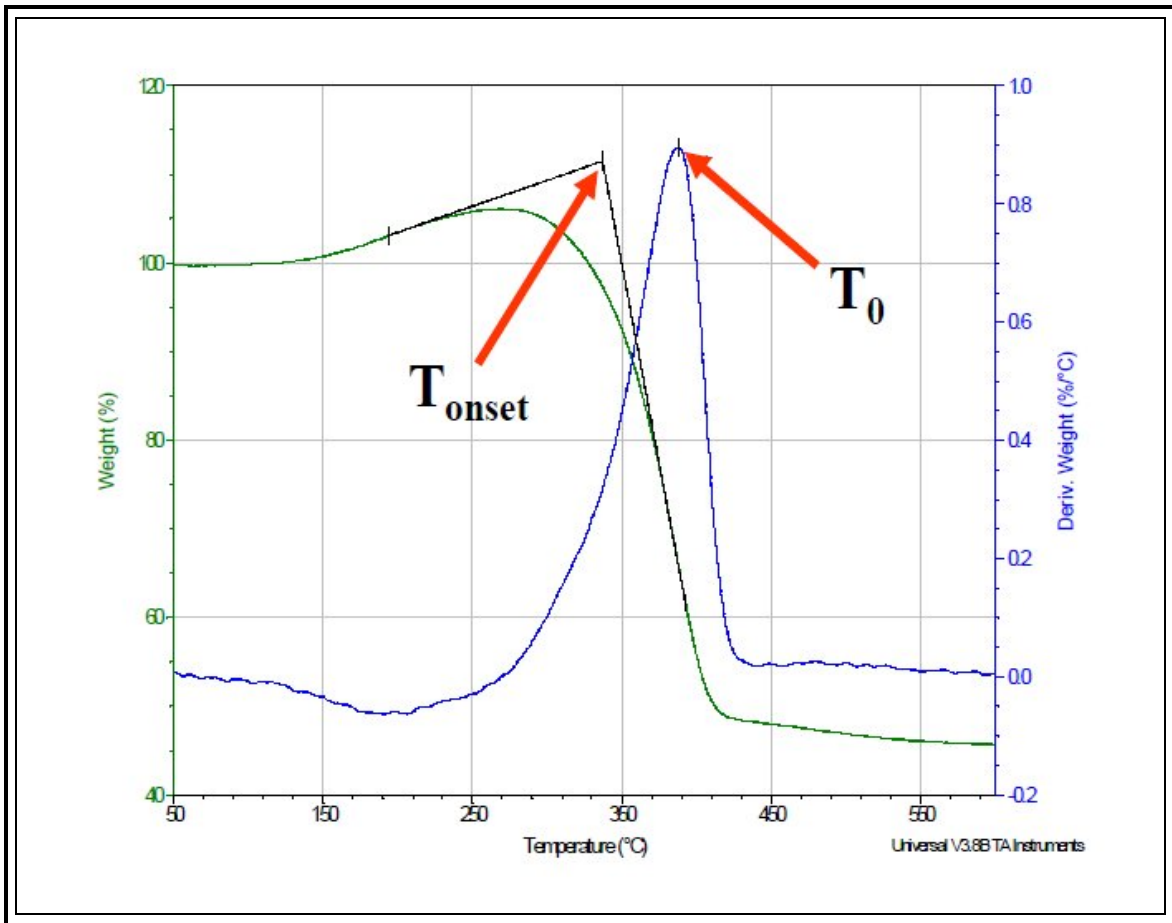


Figure 3.24: TGA graph<sup>203</sup>

The onset temperature ( $T_{\text{onset}}$ ) also indicates the temperature when oxidation begins, while the oxidation temperature ( $T_0$ ) refer to the temperature of the maximum rate of oxidation. The major phases in the TGA analysis can be summarized graphically as shown in **Figure 3.25**.

<sup>203</sup> <http://www.si-mex.com.mx/PDFS/orthon/Thermal%20Gravimetric%20Analysis%20brochure.pdf>  
(cited on 12/10/09)



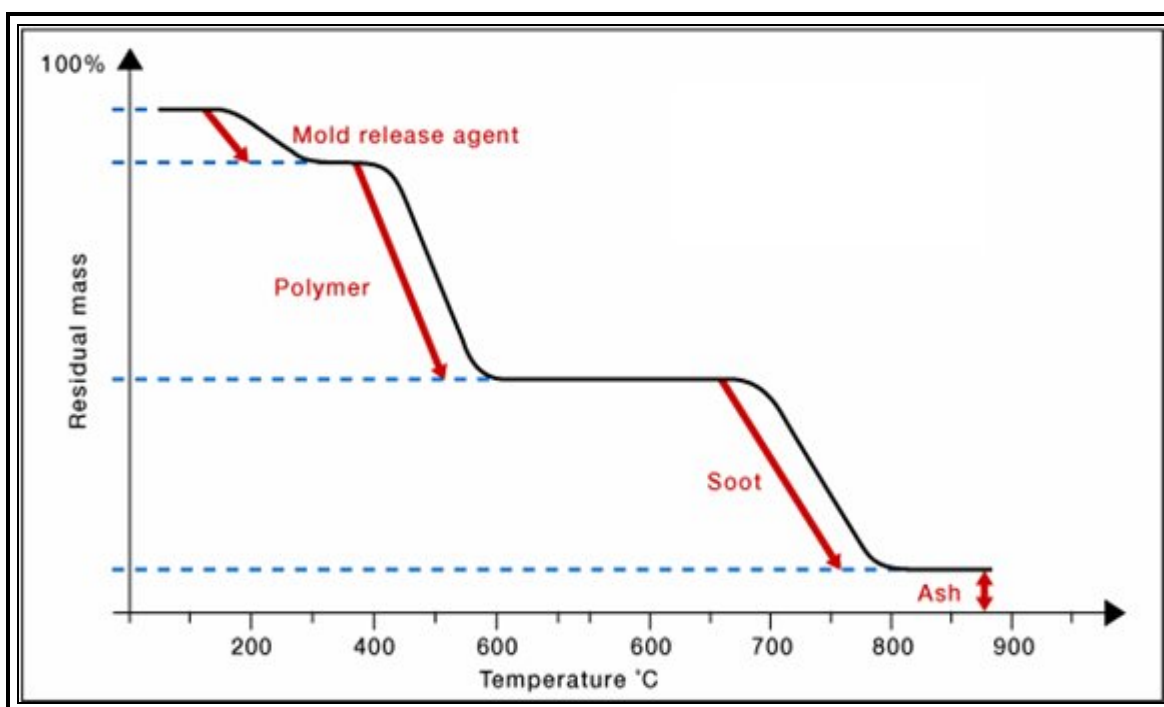


Figure 3.25: Phase changes in TGA analysis<sup>204</sup>

### 3.6.3 Differential scanning calorimetry (DSC)

The DSC provides information about thermal changes that do not involve a change in sample mass. The heat-flux DSC (Figure 3.26) is used for analysis due to its legendary attributes like high sensitivity and its ability to handle large sample volumes.

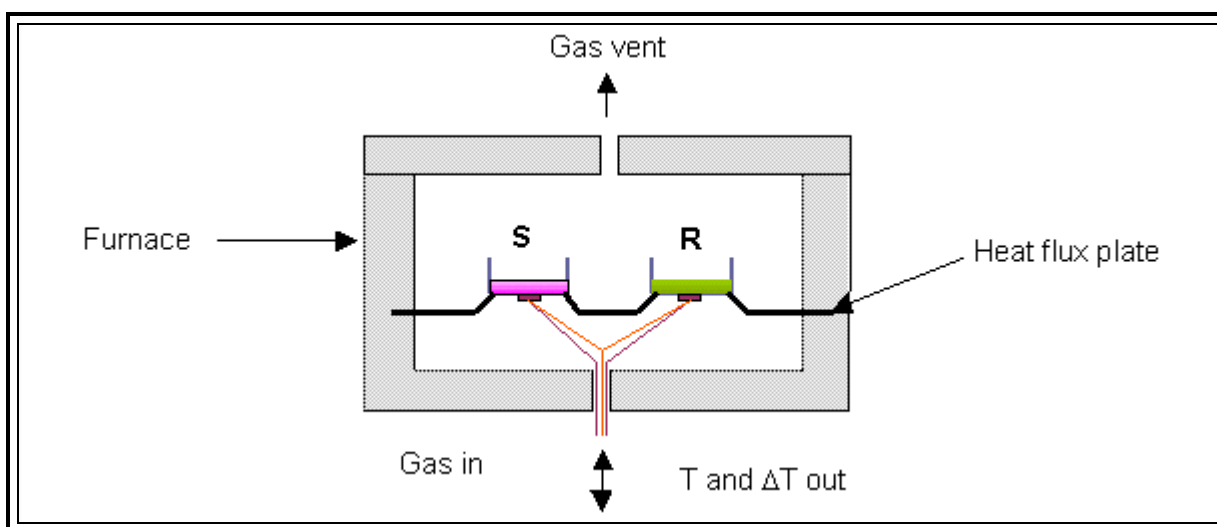


Figure 3.26: Schematic diagram of a heat flux DSC<sup>205</sup>

<sup>204</sup> <http://www.ultrac.com/en/methods/analysis/tga.php> (cited on 15/09/09)

Samples are mounted in a small (0.1 ml) open pinhole, or hermetically-sealed inert pan, made of Al, Pt, quartz, etc. (**Figure 3.27**). The aluminum pinhole pan is much more preferred because it is cheap and is readily available compared to the other pans. The major disadvantage is that they are not reusable.



**Figure 3.27:** DSC sample pans<sup>206</sup>

The main application of DSC is the study of phase transitions, such as melting points as well as endothermic and exothermic decompositions. These transitions involve energy changes or heat capacity changes that can be detected by DSC with great sensitivity. The visual output of a DSC experiment is a curve of heat flux *versus* temperature or *versus* time and is presented as an enthalpy change graph indicating the endothermic or exothermic peaks as illustrated by a positive or negative peak in **Figure 3.28**. The enthalpy changes during the heating process can give a clear indication of the amount of heat energy lost or gained during the phase transition reactions. The heat absorbed or liberated can be used to determine the amount of water lost and the matter burnt or gained during reaction.

---

<sup>205</sup> [www.anasys.co.uk/library/dsc1.htm](http://www.anasys.co.uk/library/dsc1.htm) (cited on 10/09/09)

<sup>206</sup> [www.isithermalanalysis.com/catalog/ps1012.jpg](http://www.isithermalanalysis.com/catalog/ps1012.jpg) (cited on 10/09/09)

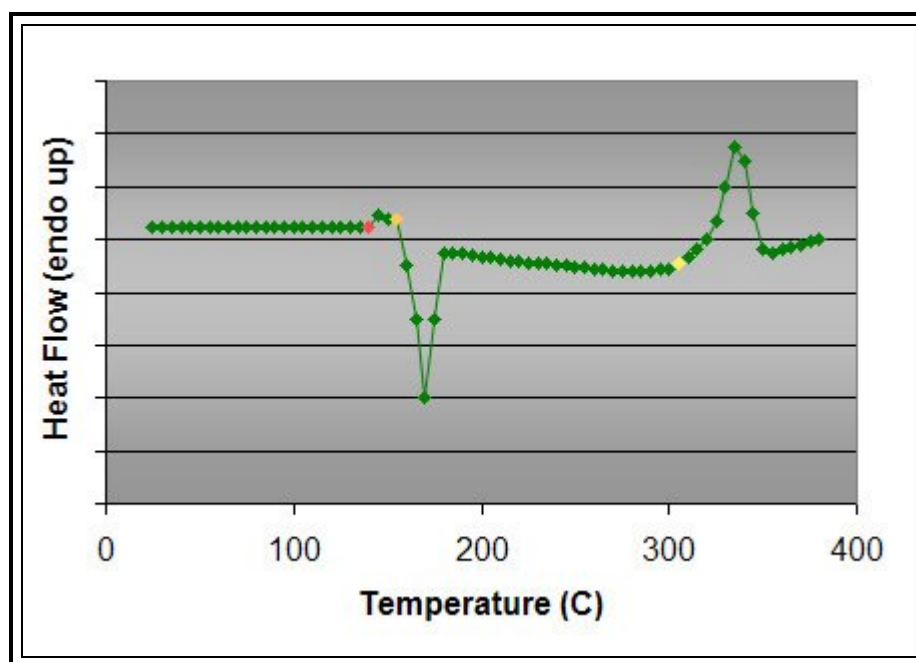


Figure 3.28: DSC graph

The enthalpy of transition can be expressed using **Equation 3.12**;

$$\Delta H = kA \quad \dots 3.12$$

where  $\Delta H$  is the enthalpy of transition,  $k$  is the calorimetric constant and  $A$  is the area under the curve.

### 3.7 Summary

A wide array of methods applicable to ICP-OES, such as the internal standard addition, standard addition and the direct calibration method makes the ICP-OES a versatile technique. For analytical determinations the major legendary attributes of this technique is that it is capable of measuring more than one element at a time and has a wider linear dynamic range ( $10^5$ - $10^6$  orders of magnitude), which enables higher analyte concentrations to be determined. The ICP-OES was shown to be very much dependent on the completeness of the sample dissolution. Microwave digestion turned out to be the best technique for a complete sample digestion under robust conditions such as high pressure and temperatures. Method validation is

essential for the evaluation of the accuracy, precision, traceability, selectivity, uncertainty, ruggedness and robustness of the test method.

# 4 Quantitative determination of rhodium

---

## 4.1 Introduction

Quantitative determinations of rhodium from different inorganic and organometallic samples have been shown to be characterised by low percentage recoveries from the different methods described in **Chapter 1 and 2**. These low recoveries have been widely attributed to either the method of sample preparation or the method of analysis. Modern techniques for both sample preparation and quantification, which have been shown (**Chapter 3**) to be the optimum conditions for optimizing the percentage recovery, will be employed in this study. An investigation to develop an appropriate method for rhodium analysis in this laboratory will be done, using the direct calibration, standard addition and the internal standard addition method to determine the best method for analysis of the CRM. The integrity of the rhodium analyses from the CRM in the different methods used is demonstrated from the determined rhodium recoveries. Validation parameters such as precision, accuracy, robustness and ruggedness will also be determined for the test method.

The main objective of this study was to develop a reliable analytical method to accurately determine and quantify rhodium in different chemical substances. The method was developed using a well known CRM sample to ensure measurement traceability. The selected method was subsequently used to determine the rhodium concentration in rhodium metal, as well as in inorganic and organometallic complexes.

The problems associated with sample preparation and matrix effects that have been hindering rhodium quantification as illustrated in **Chapter 1, Section 1.8** will be fully addressed in this chapter. The solubility of rhodium in different mineral acid(s) will

also be investigated in an effort to determine the appropriate acid for sample dissolution.

## **4.2 General experimental conditions and procedures**

### **4.2.1 Preparation of distilled water**

The distilled water was prepared in the laboratory from an electronic distillatory vessel (Fisons w/FF9/4) which consist of a round bottom flask (20.00 litres) equipped with a heating element, a condenser and an outlet and inlet pipes. Double distilled water was used for all the analytical solution preparations.

### **4.2.2 Weighing**

All the samples were weighed accurately to 0.1 mg at 25 °C using a Scaltec (SBA 33) electronic balance tested under ISO 9001. Analytical samples and reagents used in the study were all weighed by adding a sample in a glass vial that was zeroed on the balance scale.

### **4.2.3 Microwave digestion**

An Anton Paar Perkin-Elmer Multiwave 3000 microwave digestion system equipped with an 8SXF 100 rotor and eight polytetrafluoroethylene (PTFE) reaction vessels were used for the acid dissolution of the CRM and the rhodium metal samples. An internal program for the digestion of the platinum group metals (PGM XF100-8) was selected with conditions as set in **Table 4.1**.

**Table 4.1:** Microwave digestion conditions for the PGM (PGM XF100-8)

Parameter	Condition (Mode PGM XF100-8)
Power	1400 Watts
Ramp	15 min
Hold	15, 45 and 60 min
Fan	1, 1 and 3
Pressure rate	0.5 bar/sec
Infra-red (IR)	240 °C
Pressure	60 bar
Weight	0.5 g
Volume of the acid	10.0 ml
Possible reagents	HNO <sub>3</sub> (65.0 %), HCl (32 %), H <sub>2</sub> SO <sub>4</sub> (99.98 %) and <i>aqua regia</i>

#### 4.2.4 ICP-OES

A Shimadzu ICPS-7510 ICP-OES with a radial-sequential plasma spectrometer was used for the wet chemical analysis of all the samples during the current study. The vertically oriented ICP-OES with the 'radial viewing' plasma was found to be suitable due to its better detection limits, rather than the axial viewing plasma (see **Chapter 3, Section 3.4.4**). The emission intensity measurements were made using the default conditions as indicated in **Table 4.2**.

**Table 4.2:** ICP-OES operating conditions for the rhodium analysis

Parameter	Condition
RF power	1.2 kW
Coolant gas flow rate	14.0 L/min
Plasma gas flow rate	45 L/min
Auxiliary gas flow rate	0.5 L/min
Carrier gas flow rate	0.7 L/min
Sample uptake method	Peristaltic pump
Type of spray chamber	Glass cyclonic
Type of nebulizer	Concentric
Injector tube diameter	3.0 mm

#### 4.2.5 Microscope scanning

The electronic Olympus BX51 microscope was used for the preliminary investigation of the optimum drying temperature of  $\text{RhCl}_3 \cdot x\text{H}_2\text{O}$ . The analyte sample was mounted on a slide and heated from an onset temperature of 35 °C to a maximum temperature of 400 °C. Pictures were taken at different temperature intervals where a change in appearance of the sample was observed indicating a possible dehydration or decomposition.

#### 4.2.6 Thermal gravimetric analysis (TGA)

The TGA was used to determine the percentage water of crystallization in  $\text{RhCl}_3 \cdot x\text{H}_2\text{O}$ . The TGA used in this analysis was the Mettler Toledo TS0801120 model. The sample was first weighed by placing it on a zeroed alumina cup that was suspended on a balance located outside the furnace chamber. The sample was then heated on a specified thermal cycle conditions set in **Table 4.3**. The TGA curve plot of the mass change versus the reference material was recorded.



**Table 4.3:** TGA measurement conditions

Parameter	Condition
Onset temperature ( $T_{\text{onset}}$ )	30 °C
Maximum temperature ( $T_o$ )	550 °C
Rate of heating	10 °C.min <sup>-1</sup>
Gas	Argon
Stabilization time	30 min
Gas pressure	70 ml.min <sup>-1</sup>

#### 4.2.7 Differential Scanning Calorimetry (DSC)

Thermal properties of the  $\text{RhCl}_3 \cdot x\text{H}_2\text{O}$  was determined using the differential scanning calorimetry (DSC 822e, Mettler, Toledo, Switzerland). The sample was first weighed into an aluminium pan. This was then sealed and heated from 30 to 500 °C under nitrogen gas at a heating rate of 5 °C/min. From the DSC scan, the onset temperature ( $T_{\text{onset}}$ ) and the maximum temperature ( $T_{\text{max}}$ ) reached during the decomposition process were recorded.

### 4.3 Reagents and glassware

The ICP rhodium standard solution in  $\text{HNO}_3$  (2 - 3 % conc. range), ICP yttrium standard solution in  $\text{HNO}_3$  (2 - 3 % conc. range),  $\text{RhCl}_3 \cdot x\text{H}_2\text{O}$  (38 - 40 % Rh content), cobalt nitrate ( $\text{Co}(\text{NO}_3)_2 \cdot 6\text{H}_2\text{O}$ ) (99.99 % assay) and the powdered rhodium (99.99 %) were purchased from Sigma-Aldrich and all other chemicals used in this study from Merck Chemicals. All the chemicals and reagents such as ethanol, acetone, acetylacetone (acac), cupferron (cupf) and N,N-dimethylformamide (DMF) were used without further purification, except for triphenylphosphine ( $\text{PPh}_3$ ) which had to be recrystallized in methanol prior to the synthesis of organometallic complexes. The certified powdered rhodium reference material (European Reference Material ERM<sup>®</sup>-504) was bought from Bundesanstalt für Materialforschung und Prüfung (BAM) Company, Berlin in Germany. The beakers used were of the Schott Duran type and the volumetric flasks were of Blau brand, grade (A) type.

## 4.4 CRM preparation and qualitative analysis

The main objective of the CRM was to verify a method that could give analytical results identical (% recovery and RSD) or close to the certified values of the CRM. The method had to satisfy most, or all of the validation parameters as outlined in **Chapter 3, Section 3.3.2 and Table 3.2**. The methods that satisfy all or the majority of the validation parameters were then chosen to determine rhodium in the other samples in line with the objectives of this study.

### 4.4.1 Description of the CRM

The CRM used in this study was the European Reference Material (ERM<sup>®</sup>-504) and was certified by the Bundesanstalt für Materialforschung und Prüfung (BAM) in cooperation with the Committee of Chemists of the GDMB, Gesellschaft für Bergbau, Metallurgie, Rohstoff und Umwelttechnik (see the certificate in **Appendix 7**). The ERM<sup>®</sup>-504 material was obtained as a mixture of used automobile catalysts and was supplied and prepared by a commercial manufacturer. According to the certificate, the material was ignited, ground to a particle size of less than 100 µm and was homogenised thoroughly before bottling. The certified values of platinum, palladium and rhodium of the reference material are given in **Table 4.4**.

**Table 4.4:** Certified concentration values of platinum, palladium and rhodium in 5.0 g mass of the reference material at 95 % confidence interval.

ERM <sup>®</sup> -504 CERTIFIED REFERENCE MATERIAL		
	Certified value (5.00 g)	Uncertainty
Element	Mass fraction in mg.kg <sup>-1</sup>	
Pt	1777	± 15
Pd	279	± 6
Rh	338	± 4

#### **4.4.2 Preparation of the CRM samples**

The powdered ERM<sup>®</sup>-504 (CRM) was dried in an oven at 105 °C for 8 hours before digestion. Eight CRM samples (0.5006 – 0.5041 g) were weighed accurately and transferred quantitatively into a microwave polytetrafluoroethylene (PTFE) vessel. To each PTFE vessel, equal volumes of hydrochloric acid (8 ml) were added and digested under the microwave conditions specified in **Section 4.2.3, Table 4.1**. The resultant mixture was filtered to separate the soluble product from the undigested material. The filtrate was then heated and nitric acid (5 ml; 65.00 %) was added prior to dryness. The addition of nitric acid to the almost dry sample was repeated 3 times to match the acid matrix of the samples with those of the rhodium standards and also to remove the chloride ions as chlorine gas (see **Equation 4.1 in Section 4.6.2.2**) which had the potential of causing interference. The analyte samples that were acidified in nitric acid were then quantitatively transferred to a volumetric flask (50.00 ml), filled up with double distilled water to yield a rhodium concentration of between 3.38 - 3.41 ppm depending on the weighed mass. The analyte solutions were mixed thoroughly to obtain homogenized solutions and were allowed to stand for 5 hours before they were analyzed for rhodium content.

##### **4.4.2.1 Calculations of the theoretical concentration of rhodium in the CRM (0.500 g) sample**

$$\begin{aligned} \text{Mass of rhodium in a 0.5 g sample} &= \frac{338 \text{ mg}}{\text{kg}} \times 0.0005 \text{ kg} \\ &= \mathbf{0.1690 \text{ mg}} \text{ of rhodium in 0.5 g of CRM} \end{aligned}$$

Concentration of rhodium in a 50.0 ml volumetric flask

$$\begin{aligned} &= \frac{0.169 \text{ mg}}{0.05 \text{ dm}^3} \\ &= \mathbf{3.38 \text{ mg.dm}^{-1} \text{ (ppm)}} \text{ (analyte solution)} \end{aligned}$$

#### **4.4.3 Qualitative analysis of the CRM and the selection of the rhodium wavelength**

The presence of the easily ionized elements (EIE) in inorganic samples (see **Chapter 3, Section 3.2.4.3**) poses the potential for difficult line selection criteria, as their interference could cause the rhodium intensity to be altered. A careful selection of the rhodium wavelength that is free from interference was vital for the accuracy of the results.

Qualitative analysis of the CRM was carried out to determine the elements present in the CRM in order to select the most appropriate wavelength with a minimum possible interference for the rhodium analysis. From the qualitative analysis, nineteen different elements were found to be present and these elements include Mg, Al, Ca, Ti, V, Cr, Mn, Fe, Ni, Cu, Zn, Ga, Sr, Rh, Pd, Ba, Pt, Tl and Pb. From this list it is clear that the majority are transition and alkaline metals which all have the potential to cause spectral interference during the rhodium determination. Spectral interference is brought about by the emission of a photon at the same wavelength by both the analyte specie(s) and the interfering element(s) to emit a wrong analyte signal.

The choice of the wavelength in the quantitative analysis of rhodium was made using the ICP-OES “profile” function, or a Win-image.<sup>208</sup> These programmes allow for a rapid semi-quantitative analysis for a multiple wavelength analysis. The working mechanism of these two methods is principally the same and they function by recording the number of scans of an analyte solution and that of the matrix at low concentration. The spectra are then superimposed against each other and the resultant spectrum produced is a combination of all possible interferences and the analyte signal as shown in **Figure 4.1**. Results obtained from this method indicated that rhodium is best analyzed at its most sensitive atomic line emission at 343.489 nm.

---

<sup>208</sup> <http://www.jobinyvon.de/usadivisions/emission/applications/ICP42.pdf> (22/11/09)

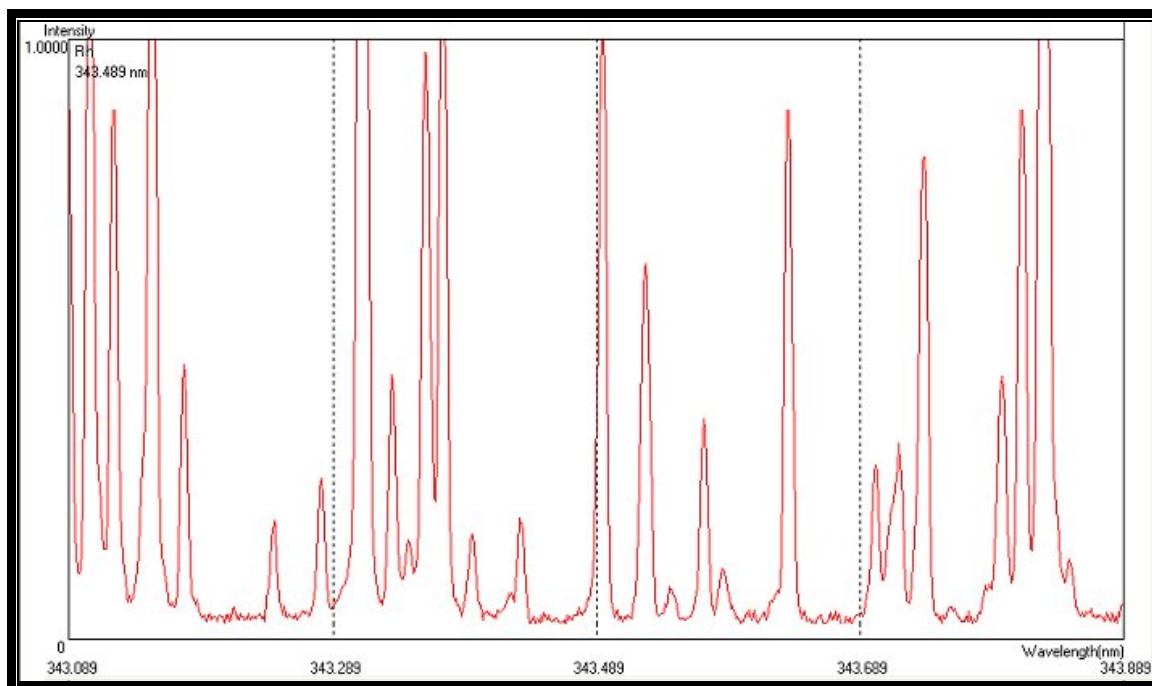


**Figure 4.1:** ICP-OES “profile” function showing the combination of the matrices and the analyte signal in the CRM close to the most sensitive line of rhodium, 343.489 nm

This wavelength was found to be the most suitable line for the rhodium analysis in this study since it was shown to be free from the spectral interference of the elements present in the sample. Elements with emission at the same wavelength were found to be Mo, U, Os, Hf and Tb as shown in **Figure 4.2**, but these elements were not present in this current sample and therefore the wavelength could be used in this study.

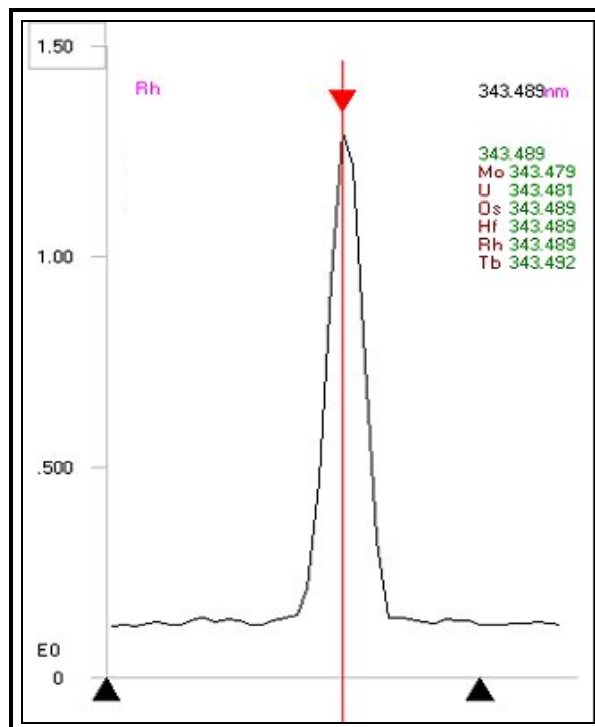


**Figure 4.2:** Rhodium atomic line indicating possible interfering species

## 4.5 Detection limits and quantitative analysis of rhodium in CRM

### 4.5.1 Preparation of calibration curves

Calibration standards were prepared from the original standard solution (1000.0 ppm) to the concentrations of 0.0, 0.1, 0.2, 0.5 and 1.0 ppm into different volumetric flasks using a “Transferpette” micro-pipette. Nitric acid (5.0 ml) was added and the flasks filled up to the mark using double distilled water. The solutions were mixed uniformly to obtain homogenized solutions and were allowed to stand for 5 hours before being used to prepare the calibration curve. The calibration curve of the rhodium standards was plotted against the rhodium concentration as shown in **Figure 4.3**. The sensitivity of the ICP-OES was determined from the gradient of the curve and was found to be 0.7347.

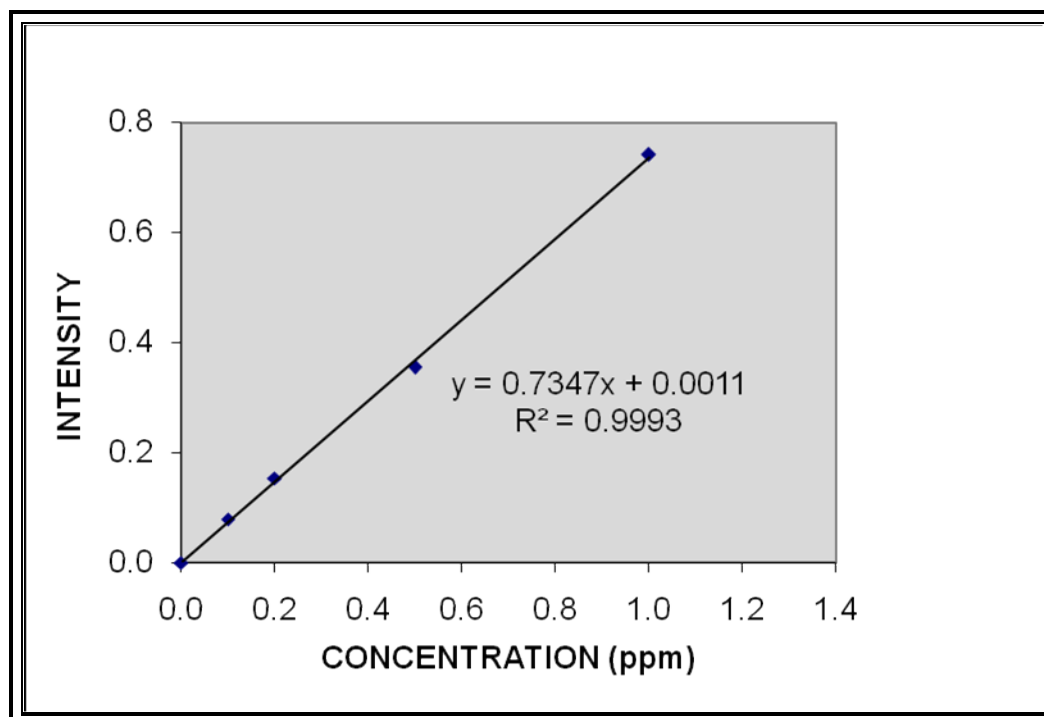


**Figure 4.3:** Calibration curve of rhodium at a wavelength of 343.489 nm

#### 4.5.2 Detection limits of rhodium

The detection limit (LOD) and the limit of quantitation (LOQ) were determined by measuring the intensities of the blank solution 10 times and calculating the standard deviation ( $s$ ) as shown in **Chapter 3, Equation 3.7**. The results of the measurements of the blank intensities are shown in **Table 4.5**.

**Table 4.5:** Determination of the detection limit of rhodium

Measurement number	Intensity of the blank solution
1	0.1323
2	0.1338
3	0.1351
4	0.1327
5	0.1327
6	0.1331
7	0.1327
8	0.1325
9	0.1334
10	0.1314
<b>Average</b>	<b>0.1330</b>
<b>Standard deviation (<math>s</math>)</b>	<b>0.0010</b>

The detection limit (LOD) of the rhodium was calculated as 0.00408 ppm and the limit of quantitation (LOQ) to be 0.04081 ppm from **Chapter 3, Equation 3.9 and 3.10** respectively.

#### **4.5.3 Quantitative determination of rhodium using the direct calibration method for the CRM samples digested in an open beaker**

##### **4.5.3.1 Preparation of the CRM samples**

Eight ERM<sup>®</sup>-504 (CRM) samples (0.4998-0.5043 g) which were dried at 105 °C for 8 hours were accurately weighed and quantitatively transferred into beakers and to each of them, 10.0 ml of a different mineral acid was added {hydrochloric acid (32.00 %), *aqua regia*, nitric acid (65.00 %) and sulphuric acid (99.99 %)} and the mixtures heated for 3 hours. The resultant mixtures were cooled and filtered to separate the soluble product from the undigested material. The filtrates were heated and nitric acid (5 ml; 65.00 %) was added to each prior to dryness. The addition of nitric acid to the almost dry sample was repeated 3 times to match the acid matrix of the analyte samples with those of the rhodium standards. These analyte samples were then quantitatively transferred to volumetric flasks (50.00 ml) and filled with double distilled water to yield a rhodium concentration of between 3.38 - 3.41 ppm depending on the mass weighed. The samples were then left to stand for at least 5 hours before they were analyzed for rhodium content.

##### **4.5.3.2 Preparation of the standard solutions and the quantitative determination of rhodium**

The concentration of the rhodium in the CRM was determined from the calibration curve prepared from the original ICP rhodium standard solution (1000.0 ppm) as described in **Section 4.5.1** but with concentrations of 0.4, 0.8, 2.0, 4.0 and 8.0 ppm. The rhodium concentration was obtained through the extrapolation of the emitted intensity as illustrated in **Chapter 3, Figure 3.6** and the results are shown in **Table 4.6**.



**Table 4.6:** Quantitative results from open beaker digestion of the CRM

Sample	Acid used for digestion	Analysis number	Average intensity	Concentration (ppm)	% Rh recovery	Average Rh recovery
CRM 1	HCl	1	1.6624	2.1138	62.54	62.30
		2	1.6496	2.0976	62.06	
CRM 2	Aqua regia	1	1.2544	1.5972	47.25	46.15
		2	1.1954	1.5225	45.04	
CRM 3	HNO <sub>3</sub>	1	0.8952	1.1424	33.80	33.83
		2	0.8970	1.1443	33.86	
CRM 4	H <sub>2</sub> SO <sub>4</sub>	1	0.6143	0.7866	23.27	23.39
		2	0.6207	0.7948	23.51	
<b>Calibration curve properties</b>					Slope	0.7897
					Intercept	-0.0069
					R <sup>2</sup>	0.9989
<b>Sample measurements and calculations</b>		Weighed mass/ g CRM			0.4998-0.5043 g	
		Theoretical concentration of Rh (ppm)			3.38 - 3.41 ppm	

The results showed an overall low percentage recovery of rhodium from all the CRM samples digested in the acids listed in **Table 4.6**. Although the samples digested in HCl showed a higher rhodium recovery compared to the other samples digested in the other acids, it is anticipated that the low results were as a result of incomplete digestion, centered or due to the choice of the method of determination. The incomplete digestion of the samples as was evident from the digestion step (see **Paragraph 4.5.3.1**) was the main reason for the poor recovery. Another possible factor that could have contributed to the low recovery was that the method of choice which was not suitable or was hampered by factors such as the ones described in **Chapter 3, Section 3.2.4.1** or by matrix effects. All this contributes to the reduction of the percentage rhodium recovered. Characterisation of the CRM before and after digestion (solid remaining after dissolution step) by means of IR spectroscopy are shown in **Figure 4.4**.

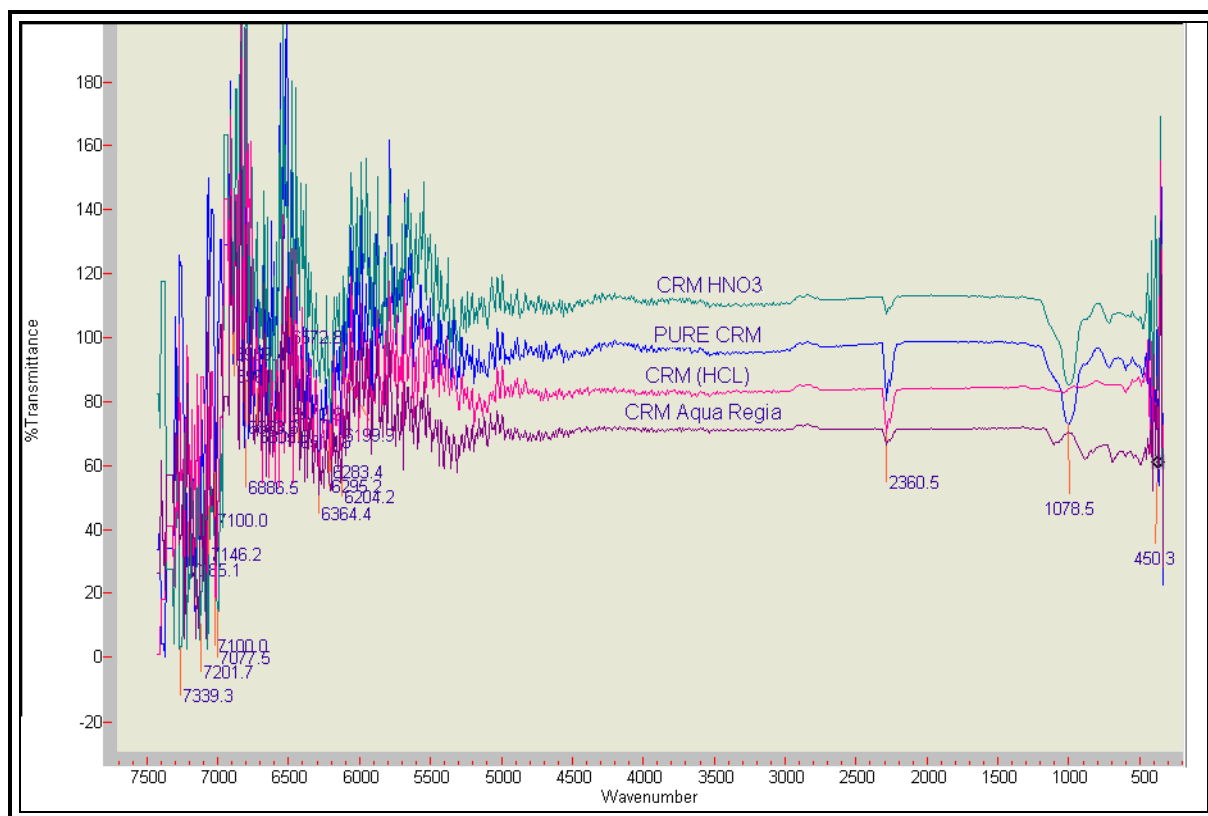


**Figure 4.4:** Comparison of the undigested residue of the CRM in different acids

The IR spectra showed differences in two peaks, 1078 and 2360  $\text{cm}^{-1}$ , which indicate a change in the chemical composition between the original CRM and the resultant solids after digestion. It is clear from the overlapping spectra that there is a decrease of stretching frequency at 2360 and 1078  $\text{cm}^{-1}$  which occurred with an increase in recovery as indicated by the results in **Table 4.6**. The order of the peak strength are CRM > HNO<sub>3</sub> > HCl > *aqua regia* at 2360  $\text{cm}^{-1}$  and CRM > HNO<sub>3</sub> > *aqua regia* > HCl at 1078  $\text{cm}^{-1}$  compared to the recovery order of HCl > *aqua regia* > HNO<sub>3</sub> > H<sub>2</sub>SO<sub>4</sub>. It is clear from these results that the stretching frequencies in the IR spectrum may represent undissolved rhodium containing CRM.

The first step in the investigation of the reasons for the low rhodium recovery was conducted by changing the dissolution process to the microwave digestion method with the conditions set as in **Section 4.2.3, Table 4.1**.

#### **4.5.4 Quantitative determination of rhodium using the direct calibration method from the CRM samples digested in a microwave**

##### **4.5.4.1 Preparation of the CRM samples**

Eight ERM<sup>®</sup>-504 (CRM) samples (0.4996-0.5021 g) which were dried at 105 °C for 8 hours were accurately weighed and quantitatively transferred into microwave polytetrafluoroethylene (PTFE) vessels. To each PTFE vessel, 8 ml of a different mineral acid was added {hydrochloric acid (32.00 %), aqua regia, nitric acid (65.00 %) and sulphuric acid (99.99 %)} and the mixtures were digested under the microwave conditions specified in **Section 4.2.3, Table 4.1**. The resultant mixtures were then filtered to separate the soluble product from the solid precipitate that was formed. The filtrates were then heated for an hour and stopped prior to dryness. Nitric acid (5.00 ml, 65.00 %) was added to each to match the acid matrix of the analyte samples with those of the rhodium standard solutions. The analyte solutions were then quantitatively transferred to volumetric flasks (50.00 ml) and then filled up with double distilled water to yield an approximately 3.38 – 3.40 ppm rhodium concentration. The samples were then left to stand for at least 5 hours before they were analyzed for rhodium content.

##### **4.5.4.2 Preparation of the standard solutions and the quantitative determination of rhodium**

The concentration of the rhodium in the CRM was determined from the calibration curve prepared as described in **Section 4.5.3.2**. The analyte concentration was obtained through the extrapolation of the emitted rhodium intensity. Results obtained from the samples digested in the different acids in a microwave are tabulated in **Table 4.7**.

**Table 4.7:** Quantitative results of rhodium recovery after microwave digestion

Sample	Acid used for digestion	Analysis number	Average intensity	Concentration (ppm)	% Rh recovery	Average Rh recovery
CRM 1	HCl	1	1.1870	1.5118	88.93	89.39
		2	1.3149	1.6172	89.84	
CRM 2	Aqua regia	1	1.0915	1.3909	81.82	80.73
		2	1.1579	1.4335	79.64	
CRM 3	HNO <sub>3</sub>	1	0.5890	0.7545	44.38	44.40
		2	0.6160	0.7996	44.42	
CRM 4	H <sub>2</sub> SO <sub>4</sub>	1	0.4159	0.5353	31.49	31.28
		2	0.4104	0.5591	31.06	
Calibration curve properties			Intercept		-0.0676	
			Slope		0.8549	
			R <sup>2</sup>		0.9991	
Sample measurements and calculations			Weighed mass/g CRM		0.4996-0.5021 g	
			Theoretical concentration of Rh (ppm)		3.38 – 3.40 ppm	

Results obtained from this change in digestion method indicated an increase in rhodium recovery for all the acids but still below the accepted rhodium recovery for method validation purposes. An IR spectrum for the remaining solid after digestion showed a significant reduction in both peaks in the regions, 2360 and 1078 cm<sup>-1</sup> as shown in **Figure 4.5**. This change occurred with increase in percentage recovery for all the CRM samples.

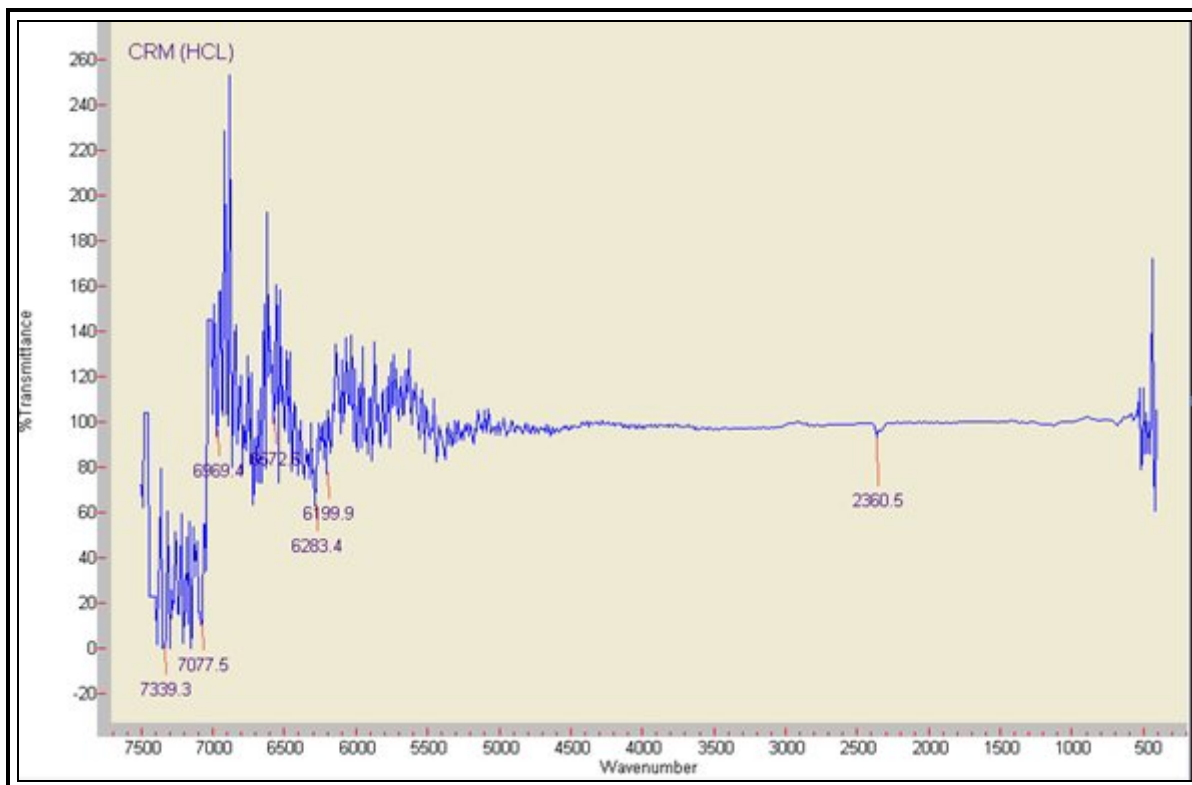


**Figure 4.5:** IR spectrum for the solid remained after CRM digested in microwave conditions in HCl

Both the digestion methods clearly indicated that hydrochloric acid was by far the best digesting medium compared to the other acids and it was thus decided to continue the investigation using HCl as the preferred dissolution medium.

#### 4.5.4.3 Determining the precision of the results after microwave digestion of the CRM samples

The precision of the results was determined after subjecting the five replicates of the CRM (0.4997 - 0.5031 g) using microwave digestion in HCl (32.00 %) and experimental procedure as indicated in the preceding **Section 4.5.4**. The theoretical concentrations for rhodium CRM samples were calculated relative to the certified values of the CRM to be in the range (3.38 – 3.41 ppm) in 50.00 ml volumetric flasks. The results for the analysis are shown in **Table 4.8**.

**Table 4.8:** Determination of precision in % Rh recovery after microwave digestion in HCl

Sample	Acid used for digestion	Average intensity	Concentration (ppm)	% Rh recovery
CRM 1	HCl	2.2875	2.9049	85.94
CRM 2	HCl	2.4187	3.0694	90.81
CRM 3	HCl	2.4049	3.0521	90.30
CRM 4	HCl	2.2756	2.8900	85.50
CRM 5	HCl	2.3226	2.9489	87.25
<b>Average</b>				<b>88.93</b>
<b>RDS (%)</b>				<b>2.73</b>
<b>Calibration curve properties</b>		Slope	0.788	
		Intercept	-0.0298	
		R <sup>2</sup>	0.9992	
<b>Sample measurements and calculations</b>		Weighed mass/ g CRM	0.4997 - 0.5031 g	
		Theoretical concentration of Rh (ppm)	3.38 – 3.41 ppm	

The results obtained revealed a closer similarity to the results previously obtained in **Paragraph 4.5.4.2, Table 4.7**. It is clear from these results that a small relative standard deviation of 2.73 % is obtained and indicates a relatively good precision of these determinations.

#### **4.5.5 Quantitative determination of rhodium from CRM using the standard addition method**

In an attempt to optimize the rhodium percentage recovery and to counteract for any interference caused by the sample matrix, the standard addition method (instead of direct method) was used for the quantification of the rhodium content.

##### **4.5.5.1 Preparation of the CRM analyte samples**

Five replicates of the CRM (0.5002 - 0.5017 g) were prepared as outlined in **Section 4.5.4.1** in HCl. Aliquots (10.00 ml) of the prepared stock solutions were pipetted into a 25.00 ml volumetric flask and diluted as described in the following **Section 4.5.5.2** for the preparation of standard solutions to yield a theoretical

rhodium concentration of 3.39 ppm. The calculations for the resultant concentrations are shown below relative to the certified values of the CRM.

*Example of calculations of the theoretical concentration of rhodium in 0.5 g sample of the CRM*

Rhodium stock solution = **3.40 ppm** (stock solution)

Concentration of rhodium analyte added to the 25.00 ml of the standard solutions

$$= \frac{3.40 \text{ ppm} \times 10.00 \text{ ml}}{25.00 \text{ ml}}$$

$$= \mathbf{1.36 \text{ ppm}} \text{ (rhodium analyte solution)}$$

#### **4.5.5.2 Preparation of the standard solutions and the quantitative determination of rhodium**

Using 25.00 ml a volumetric flasks five rhodium standard solutions of the concentrations, 0.5, 1.0, 2.0, 5.0 and 10.0 ppm were prepared. To each standard solution, equal aliquots of the CRM stock solutions (10.00 ml, 1.36 ppm) were added. To each standard solution, nitric acid (2.25 ml) was added and the flasks filled up to the mark with double distilled water. The solutions were left to stand for 5 hours before analyzed. The intensity of the standard solutions with the analyte solution were measured and plotted against the concentration of the original standard solution to give a linear calibration curve shown in **Figure 4.6**. The experiment was repeated 5 times with a theoretical concentration of approximately 3.39 ppm of the stock solution in a 50.00 ml volumetric flask. The experimental results of the rhodium recovery are shown in **Table 4.9**.

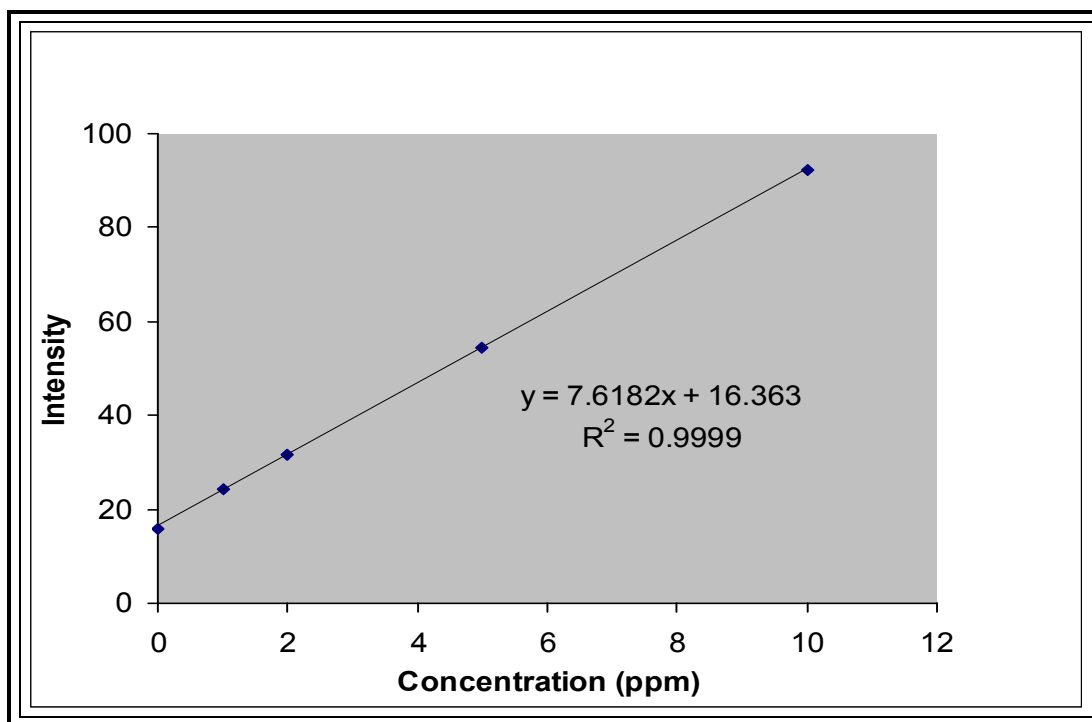


**Figure 4.6:** Quantitative determination of Rh in CRM using the standard addition method

**Table 4.9:** Results of rhodium recovery using the standard addition method

Sample	Acid used for digestion	R <sup>2</sup> value	% Rh recovery
CRM 1	HCl	0.9999	<b>97.94</b>
CRM 2	HCl	0.9999	<b>98.81</b>
CRM 3	HCl	0.9993	<b>97.30</b>
CRM 4	HCl	0.9991	<b>98.50</b>
CRM 5	HCl	0.9997	<b>97.25</b>
<b>Average</b>			<b>97.96</b>
<b>RSD (%)</b>			<b>0.71</b>
<b>Calibration curve properties</b>	Slope		7.6182
	Intercept		16.363
	R <sup>2</sup>		0.9999
<b>Sample measurements and calculations</b>	Weighed mass/ g CRM		0.5002 - 0.5017 g
	Theoretical concentration of Rh (ppm)		3.39 ppm



The results obtained using this method differed only slightly from the certified rhodium value of the CRM. A good linear regression was obtained for the calibration curve (0.9999) and this analyzed method was found to be more suitable for the rhodium analysis than the direct calibration method (c.a. 98.00 % compared to 88.00 %) but still not within the acceptable analyzed recovery range due to matrix and background interference. The possibility of the acid matrix introduced in the sample preparation could not have been ruled out due to the viscosity change that could have occurred between the analyte samples and the standards. The major drawback of this method was the requirement of a larger volume of both the standard and the analyte solutions, which had to be prepared for every successive analysis. The credibility of the sample dissolution was put under the spotlight, questioning whether complete dissolution was achieved in the microwave digestion process or whether the incomplete recovery was simply the failure of the analyzed method. The internal standard addition method was then used to try and eliminate either the solubility problem or the analytical method uncertainty as source for incomplete recovery.

#### **4.5.6 Quantitative determination of rhodium from the CRM using the internal standard addition method**

##### **4.5.6.1 Selection of the internal standard**

One of the critical factors in the analysis of rhodium was the selection of the appropriate internal standard. This was considered critical because the choice of the internal standard would directly affect the results. According to the literature,<sup>209,210</sup> yttrium has been the most preferred and widely used internal standard for the determination of PGM. Elements like tin, magnesium, cobalt, copper, nickel, silver, thallium, molybdenum and lead have been used as internal standards in different spectrometric techniques such as ICP-MS as discussed by Salin *et al.*<sup>211</sup> Among these internal standards, yttrium has been the most recommended internal standard for all the PGM determination.

---

<sup>209</sup> G. A. Zachariadis and P. C. Sarafidou, *Microchim Acta.*, (2009), 166, pp. 77 - 81

<sup>210</sup> J. C. Ivaldi and J. F. Tyson, *Spectrochimica Acta.*, (1996), 51, pp. 1443 - 1450

Cobalt and rhodium are in the same group (VIIIb) and have similar first ionization energies (**Table 4.10**), but quite different from yttrium which has been used as internal standard for PGM analysis. This similarity led us to believe that cobalt can be used as a possible internal standard for rhodium analysis. The element satisfied the properties specified in **Chapter 3, Section 3.2.4.3** which are necessary in choosing the internal standard for an analysis.

**Table 4.10:** Comparison of the 1<sup>st</sup>, 2<sup>nd</sup> and 3<sup>rd</sup> ionization energies of yttrium, rhodium and cobalt

Elements	1 <sup>st</sup> Ionization energy (kJ mol <sup>-1</sup> )
Rhodium	719.68
Yttrium	599.86
Cobalt	760.41
2 <sup>nd</sup> Ionization energy (kJ mol <sup>-1</sup> )	
Rhodium	1744.47
Yttrium	1180.99
Cobalt	1648.27
3 <sup>rd</sup> Ionization energy (kJ mol <sup>-1</sup> )	
Rhodium	2996.86
Yttrium	1979.86
Cobalt	3232.28

The large ionization energy difference between rhodium and yttrium made yttrium less suitable as internal standard for rhodium analysis. Cobalt was therefore included as internal standard on the basis that the element has almost the same thermal behaviour as the rhodium analyte. This was very critical in correcting for the fluctuations in the nebuliser and other matrix effects as the ratio of the ionized or excited analyte species will always be the same as the internal standard. The most preferred line for yttrium and cobalt as internal standards are the most sensitive lines which are 371.030 and 228.616 nm respectively as shown in **Table 4.11**. These lines have less interference compared to other also listed in the table.

---

<sup>211</sup> E. D. Salin, M. Antler and G. Bort, *J. Anal. At. Spectrom.*, 19 (2004), p. 1498

**Table 4.11:** Comparison of the electromagnetic wavelengths, detection limits and interferences for Rh analysis between Y and Co in the ICP-OES analysis<sup>212</sup>

Line	Estimated D.L.*	Order	Type	Interferences
<b>Rhodium</b>				
233.477 nm	0.004 ppm	1	Ion	Ni, Sn, Mo, Nb, Ta
249.077 nm	0.006 ppm	1	Ion	Ta, Co, Fe, W, Cr, Os
343.489 nm	0.004 ppm	1	Atom	Mo, Os, Hf, Th, Ce, Tb
<b>Yttrium</b>				
360.073 nm	0.005 ppm	1	Ion	Ce, Th
<b>371.030 nm</b>	0.004 ppm	1	Ion	Ce
377.433 nm	0.005 ppm	1	Ion	Ta, Th
<b>Cobalt</b>				
238.892 nm	0.01 ppm	1	Ion	Fe, W, Ta
<b>228.616 nm</b>	0.01 ppm	1	Ion	Cr, Ni, Ti
237.862 nm	0.01 ppm	1	Ion	W, Re, Al, Ta
*ICP-OES D.L. are given as radial configuration				

The electromagnetic wavelengths listed for rhodium, yttrium and cobalt are the most commonly used wavelengths and also the most sensitive ones. The selection of the best line is dependent on the presence of the interfering species in the analyte sample. If the interference is low or none for a particular selected line, the same line will be the most preferred line for the analysis. Knowing the detection limit for each particular line is important since it can be used as a guide to where quantifications can start.

<sup>212</sup> <http://www.ivstandards.com/extras/pertable/> (cited on 12/11/09)

#### **4.5.6.2 Determination of rhodium using yttrium and cobalt internal standards**

##### *4.5.6.2.1 Preparation of the CRM samples*

A set of 5 ERM<sup>®</sup>-504 (CRM) samples (0.4999-0.5017 g) which were dried at 105 °C for 8 hours were accurately weighed and quantitatively transferred into separate beakers and 10.0 ml of hydrochloric acid (32.0 %) was added to each, before the mixtures were heated for 3 hours. The resultant mixtures were then cooled and filtered to separate the soluble product from the remaining solid precipitate. The filtrates were then heated for an hour and stopped prior to dryness. Nitric acid (5.00 ml, 65.00 %) was added to each to match the acid matrix of the analyte samples with those of the rhodium standard. The analyte solutions were then quantitatively transferred to a volumetric flasks (50.00 ml) and then filled up with double distilled water to yield an approximately rhodium concentration of 3.38 – 3.39 ppm. The samples were then left to stand for at least 5 hours before analyzed for rhodium.

##### *4.5.6.2.2 Preparation of the the rhodium and yttrium standards*

The standard solutions were prepared by pipetting equal volumes of yttrium (2.00 ml, 50.00 ppm) into each rhodium standard solution (0.5, 1.0, 2.0, 5.0 and 10.0 ppm) in 50.00 ml volumetric flasks. The same volume of yttrium standard solution (2.00 ml; 50.00 ppm) was also pipetted into all the rhodium analyte solutions to match the concentration level of yttrium (2.00 ppm). The prepared standard solutions were left to stand for 5 hours before used. The intensity of the rhodium was then measured from the selected atomic wavelength for rhodium, 343.489 nm and ionic wavelength for yttrium, 371.030 nm.

##### *4.5.6.2.3 Quantitative determination of the percentage recovery of rhodium*

The calibration curve was plotted by comparing the rhodium signal against the yttrium signal ratio as shown in **Chapter 3, Equation 3.2** with the concentration of the rhodium standards. A linear regression analysis was performed to calculate the

regression coefficient ( $r^2$ ) and various other numerical parameters as shown in **Appendix 7**. The results of the analysis are shown in **Table 4.12**.

**Table 4.12:** Experimental results of rhodium determination using yttrium internal standard in HNO<sub>3</sub>

	<b>Sample number</b>	<b>% Rh recovery</b>
	1	140.70
	2	141.06
	3	138.60
	4	139.11
	5	141.85
<b>Average % Rh recovery</b>		<b>140.26</b>
<b>RSD (%)</b>		<b>0.97</b>
<b>Calibration curve properties</b>	Slope	0.0203
	Intercept	0.0026
	R <sup>2</sup>	0.9999
<b>Sample measurements and calculations</b>	Weighed mass/ g CRM	0.4999 - 0.5017 g
	Theoretical concentration of Rh (ppm)	3.38 – 3.39 ppm

The results obtained using yttrium as an internal standard were constantly much higher (>100 %) than the expected value as certified for the CRM. This was attributed to the large difference in ionization energy between yttrium and rhodium. Excitation and emission of the rhodium and yttrium were presumably not of the same level due to the difference in ionization energy.

#### **4.5.6.3 Determination of rhodium using cobalt internal standard**

##### *4.5.6.3.1 Preparation of the CRM samples*

A set of 5 ERM<sup>®</sup>-504 (CRM) samples (0.5000 - 0.5025 g) which were dried at 105 °C for 8 hours were accurately weighed and quantitatively transferred into beakers and 10.0 ml of hydrochloric acid (32.00 %) was added to each, before the mixtures were

heated for 3 hours. The resultant mixtures were then cooled and filtered to separate the soluble product from the remaining precipitate. The filtrates were then heated for an hour and stopped prior to dryness. Nitric acid (5.00 ml, 65.00 %) was added to each to match the acid matrix of the analyte samples with those of the rhodium standard solutions. The acidified (5.00 ml, HNO<sub>3</sub> 65.0 %) analyte solutions were then quantitatively transferred to volumetric flasks (50.00 ml) and then filled up with distilled water to yield an approximately 3.38 – 3.40 ppm of rhodium concentration. The samples were then left to stand for at least 5 hours before analyzed for rhodium.

#### *4.5.6.3.2 Preparation of the rhodium standards and quantitative determination of rhodium*

The standard solutions were prepared by pipetting equal volumes of cobalt (2.00 ml, 50.00 ppm) into each rhodium standard solution (0.5, 1.0, 2.0, 5.0 and 10.0 ppm) in 50.00 ml volumetric flasks. The same volume of cobalt standard solution (2.00 ml; 50.00 ppm) was also pipetted into all the rhodium analyte solutions to match the concentration level of cobalt (2.00 ppm). The prepared standard solutions were left to stand for 5 hours before they were used. The intensity of the rhodium was then measured at the selected atomic wavelength for rhodium, 343.489 nm and ionic wavelength for cobalt, 228.616 nm. The analyte samples were determined for rhodium and the following percentage recoveries were obtained as shown in **Table 4.13**.

**Table 4.13:** Quantitative results of rhodium recovery in the CRM using cobalt internal standard

	<b>Sample number</b>	<b>% Rh recovery</b>
	1	100.16
	2	100.97
	3	99.05
	4	100.23
	5	99.65
<b>Average % Rh recovery</b>		<b>100.01</b>
<b>RSD (%)</b>		<b>0.71</b>
<b>Calibration curve properties</b>	Slope	0.2933
	Intercept	0.0795
	R <sup>2</sup>	0.997
<b>Sample measurements and calculations</b>	Weighed mass/ g CRM	0.5000 - 0.5025 g
	Theoretical concentration of Rh (ppm)	3.38 – 3.40 ppm

The results in **Table 4.13** clearly indicate that the best recovery of rhodium was obtained using cobalt as an internal standard. The success of this method was attributed to the ability of the internal standard to behave in the same manner as the rhodium analyte. Statistical and hypothesis tests were performed at the 95 % confidence interval to determine the rejection and retention of test results using the z-test as discussed in **Chapter 3, Section 3.3.2**. The experimental results were all found to be in the acceptable region of between -1.645 and 1.645 of the z-value at 95 % confidence interval (see the calculations in **Appendix 7**).

The use of cobalt as internal standard was therefore chosen as the preferred method upon which all the subsequent experimental determinations of rhodium in inorganic and organometallic complexes in this study would be based. The cobalt internal standard was chosen on the basis of excellent recovery and its ability to accurately compensate for the matrix-induced signal variations as well as low RSD values. In the case where the unsatisfactory results were obtained, the other two methods would also be used and compared to obtain the best rhodium recovery.

## **4.6 Qualitative and quantitative determination of rhodium in rhodium metal powder (99.99 % purity)**

In order to investigate the applicability of the developed cobalt internal standard addition method, the selected test method was used to determine the percentage recovery of rhodium from the rhodium metal powder. The same microwave digestion conditions were maintained for this sample preparation as well as the ICP-OES conditions as indicated previously. It was also important to test the ruggedness and the accuracy of the method. The results from the qualitative analysis of the rhodium powder indicated the presence of eight elements, K, Na, Mg, Ca, Fe, Pd, Ag and Pt at micro and ultra-micro level. These elements all had the potential of interfering with the analyte emission intensities and therefore causing unreliable results. The rhodium atomic line (343.489 nm) was found to be suitable for this analysis since none of the interfering elements listed in **Section 4.4.3, Figure 4.2** were found to be present in the powdered multi sample. It was also decided to use the direct calibration method in order to compare it with the cobalt internal standard method.

### **4.6.1 Determination of rhodium using direct calibration method**

#### **4.6.1.1 Preparation of the rhodium metal powder samples**

A set of 5 stock rhodium analyte solutions were prepared by weighing samples (0.0043 - 0.0048 g) and quantitatively transferred into a microwave polytetrafluoroethylene (PTFE) vessel. To each PTFE vessel, hydrochloric acid (8 ml; 32.00 %) was added and the samples digested according to the conditions given in **Section 4.2.3, Table 4.2**. The resultant burgundy red solutions, with no precipitate, were then heated to almost dryness and nitric acid (5.0 ml, 65.00 %) was added to each prior to dryness and re-heated. This addition process was repeated 3 times to match the acid matrix of the analyte samples with those of the rhodium standard solutions. The acidified (5 ml, HNO<sub>3</sub>, 65.00 %) analyte solutions were then quantitatively transferred to volumetric flasks (100.00 ml) and then filled to the mark using double distilled water to yield an approximately concentration of 43.00 - 48.00 ppm of the stock solutions. Different aliquots (3.52 – 3.93 ml) of the stock solutions



were pipetted into volumetric flasks (50.00 ml) to yield a theoretical rhodium concentration of 3.38 ppm. The samples were then homogenised and left to stand for at least 5 hours before they were analyzed for rhodium.

#### 4.6.1.2 Preparation of the rhodium standard solutions and the quantitative determination of rhodium

The rhodium standard solutions were prepared in the same way as described in **Section 4.5.1** with the concentrations of 0.5, 1.0, 2.0, 5.0 and 10.0 ppm. The samples were analyzed for rhodium content and the experimental results are shown in **Table 4.14**.

**Table 4.14:** Determination of rhodium recovery from the direct calibration curve

	Sample number	% Rh recovery
	1	65.32
	2	66.01
	3	65.34
	4	66.02
	5	64.82
<b>Average % Rh recovery</b>		<b>65.82</b>
<b>RSD (%)</b>		<b>0.78</b>
<b>Calibration properties</b>	Slope	0.5785
	Intercept	0.154
	R <sup>2</sup>	0.9971
<b>Sample measurements and calculations</b>	Weighed mass/ g rhodium powder (99.99 %)	0.0043 - 0.0048 g
	Theoretical concentration of Rh (ppm)	3.38 ppm

The poor recoveries of rhodium obtained from these results were attributed to the analytical method of choice and also to the matrices affecting the direct calibration method as described in **Chapter 3, Section 3.2.4.1**. Results to date indicate that the direct calibration method is sensitive to interference by other species in solution as revealed by the qualitative analysis indicated in the previous **Section 4.6**.

Differences in analyte composition, such as the concentration of acid and the viscosity of the analyte solutions might also have affected the percentage recovery.

#### **4.6.2 Determination of rhodium using the cobalt internal standard**

##### **4.6.2.1 Preparation of the rhodium metal powder analyte samples**

The rhodium analyte replicates (5) were prepared in the same way as described in **Section 4.6.1.1**. The mass of the 5 replicates of powdered rhodium were in the range of (0.0042 – 0.0047 g) and corresponded to theoretical rhodium concentrations of 42.00 – 47.00 ppm in 100.00 ml volumetric flasks. Different volumes of the aliquots (3.60 - 4.02 ml) were pipetted to 50.00 ml volumetric flasks to yield theoretical rhodium concentrations of 3.38 ppm.

##### **4.6.2.2 Preparation of the standard solution and quantitative determination of rhodium**

The rhodium standard solutions together with the cobalt internal standard solution were prepared identical to that as described **Section 4.5.6.3.2**. The rhodium concentration was obtained by comparing the rhodium (analyte) signal with that of the internal standard as shown in **Chapter 3, Equation 3.2**. The results for the rhodium quantification are shown in **Table 4.15**.

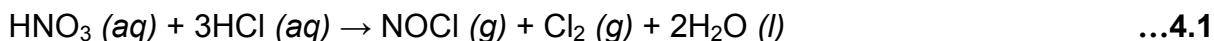
**Table 4.15:** Quantitative determination of rhodium from rhodium powder using cobalt as internal standard

	<b>Sample number</b>	<b>% Rh recovery</b>
	1	100.96
	2	100.37
	3	99.99
	4	97.76
	5	99.39
<b>Average % Rh recovery</b>		<b>99.69</b>
<b>RSD (%)</b>		<b>1.23</b>
<b>Calibration curve properties</b>	Slope	0.2906
	Intercept	0.0261
	R <sup>2</sup>	1.0
<b>Sample measurements and calculations</b>	Weighed mass/ g Rh	0.0042 – 0.0047 g
	Theoretical concentration of Rh (ppm)	3.38 ppm

The quantitative results obtained from the experimental analysis using cobalt as internal standard (**Table 4.15**) revealed excellent rhodium recovery of 99.69 % compared to an average of 65.82 % which was obtained with the direct calibration method.

Good percentage recovery for rhodium (99.0 % +) for all the quantitative runs using the cobalt internal standard indicated complete and efficient microwave dissolution of rhodium powder in HCl, as well as effective and accurate rhodium quantification. The drawback of the sample preparation method was the removal of the HCl through evaporation which was laborious and time consuming. The analyte acid matrix had to be matched with those of the standard solution and a way to obtain this was by adding equal amounts of HNO<sub>3</sub> to the analyte samples. Nitric acid reacts with hydrochloric acid in a volatile reaction to form nitrosyl chloride and chlorine gas according to **Equation 4.1**.<sup>213</sup>

<sup>213</sup> [http://en.wikipedia.org/wiki/Aqua\\_regia](http://en.wikipedia.org/wiki/Aqua_regia) (cited on 12/11/09)



The formation of the nitrosyl chloride and chlorine is observed by the fuming nature of the reaction and the characteristic yellow colour of chlorine gas which is formed during the reaction. Chloride ions are consumed in the reaction and this lowering of  $\text{Cl}^-$  in solution accounts for the better results obtained as the matrices are better matched.

The low percentage recovery in direct calibration are attributed to possible spectral interference and other matrix interference such as those caused by the easily ionized elements (EIE) effects (see **Chapter 3, Section 3.2.4.3**) and the acid matrix effects. The obtained results were validated using the null hypothesis (similar to the CRM) to test for the integrity. The results obtained from these calculations were found to fall within the accepted range (see **Chapter 5**) and therefore were accepted as 100 % recovery at 95 % confidence interval.

## 4.7 Quantitative determination of a rhodium in $\text{RhCl}_3 \cdot x\text{H}_2\text{O}$

Accurate quantitative determination of rhodium in  $\text{RhCl}_3 \cdot x\text{H}_2\text{O}$  required an accurate determination of the sample composition. This was only possible if the number of crystal water molecules in  $\text{RhCl}_3 \cdot x\text{H}_2\text{O}$  was accurately known, which was investigated using DSC and TGA as described in **Section 4.2.7 and 4.2.6** respectively. The literature value of the number of crystal water molecules varies between 2 and 4 and is oftenly predicted as 3 in most of these prepared rhodium salts.<sup>214</sup> This uncertainty of the sample mass due to the unspecified number of crystal waters had the potential of causing a systematic error which ultimately would lead to the loss of accuracy in the rhodium determination.

---

<sup>214</sup> R. Huang and K. H. Shaughnessy, *Chem. Commun.*, (2005), 10, pp. 4484 – 4486

#### 4.7.1 Analysis of $\text{RhCl}_3 \cdot x\text{H}_2\text{O}$ using IR spectroscopy and visual inspection using a microscope

A preliminary investigation of the chemical composition of  $\text{RhCl}_3 \cdot x\text{H}_2\text{O}$  was first carried out using infra-red spectroscopy and the microscope under the operating conditions described in **Section 4.2.5**. This was done to observe any chemical changes which may occur during the drying (heating) process.  $\text{RhCl}_3 \cdot x\text{H}_2\text{O}$  was heated overnight at  $120\text{ }^\circ\text{C}$  to try and remove all the crystal water molecules and to determine whether the temperature was optimum for the drying of  $\text{RhCl}_3 \cdot x\text{H}_2\text{O}$ . The IR scan for the hydrated  $\text{RhCl}_3 \cdot x\text{H}_2\text{O}$  was compared with dried  $\text{RhCl}_3 \cdot x\text{H}_2\text{O}$  as shown in **Figure 4.7**.

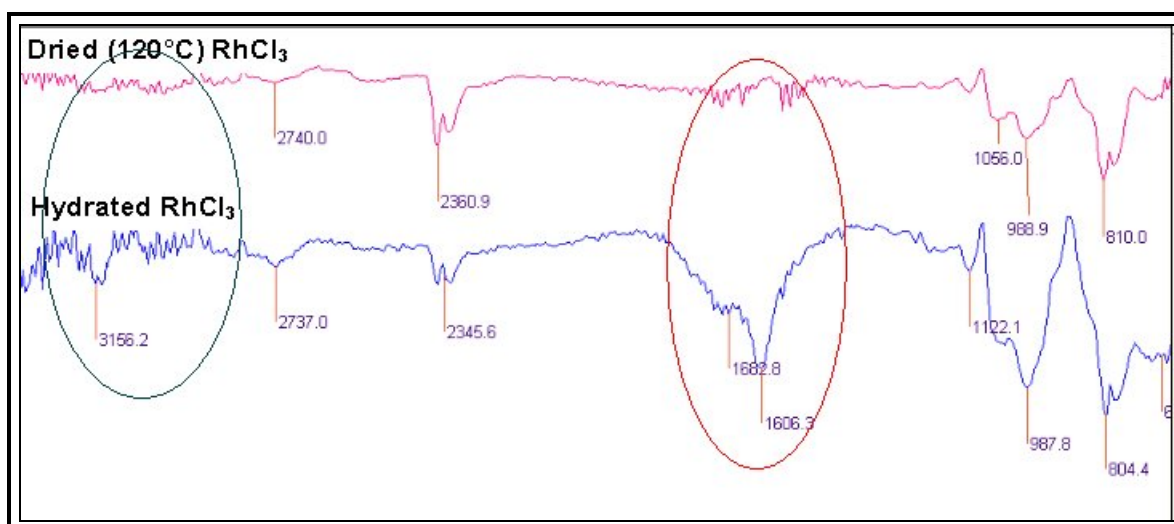


**Figure 4.7:** Comparison of IR scan for dried and hydrated  $\text{RhCl}_3 \cdot x\text{H}_2\text{O}$

The results showed a remarkable difference in the stretching frequencies of the dried  $\text{RhCl}_3$  compared to the hydrated  $\text{RhCl}_3 \cdot x\text{H}_2\text{O}$ . Generally, lattice water absorbs in the region of  $3550 - 3200\text{ cm}^{-1}$  (asymmetric stretching frequency) and  $1630 - 1600\text{ cm}^{-1}$  for bending HOH molecules.<sup>215</sup> The IR spectrum of the hydrated  $\text{RhCl}_3 \cdot x\text{H}_2\text{O}$  clearly have a strong stretching frequency at  $1683$  and  $1606\text{ cm}^{-1}$  and much weaker at  $3156\text{ cm}^{-1}$ , indicating the presence of water in the compound. These stretching frequencies are clearly absent from the dried  $\text{RhCl}_3$ , indicating the removal of the crystal water molecules from the starting material as a result of the drying process.

<sup>215</sup> K. Nakamoto, *Infra-red spectra of Inorganic and Coordination Compounds*, (1970), 2<sup>nd</sup> Ed. p. 166

A further analysis, using a microscope (Olympus BX51) as described in **Section 4.2.5** was carried out to determine whether the temperature was at the optimum for the complete drying of  $\text{RhCl}_3 \cdot x\text{H}_2\text{O}$ . A small amount of  $\text{RhCl}_3 \cdot x\text{H}_2\text{O}$  (0.0082 g) was mounted on a heating pan similar to those used on a DSC analysis (see **Chapter 3, Figure 3.27**) and heated gently from 35 to 400 °C. The changes that occurred at certain temperatures, in this study at 35, 159, 241 and 400 °C were recorded as images shown in **Figure 4.8**

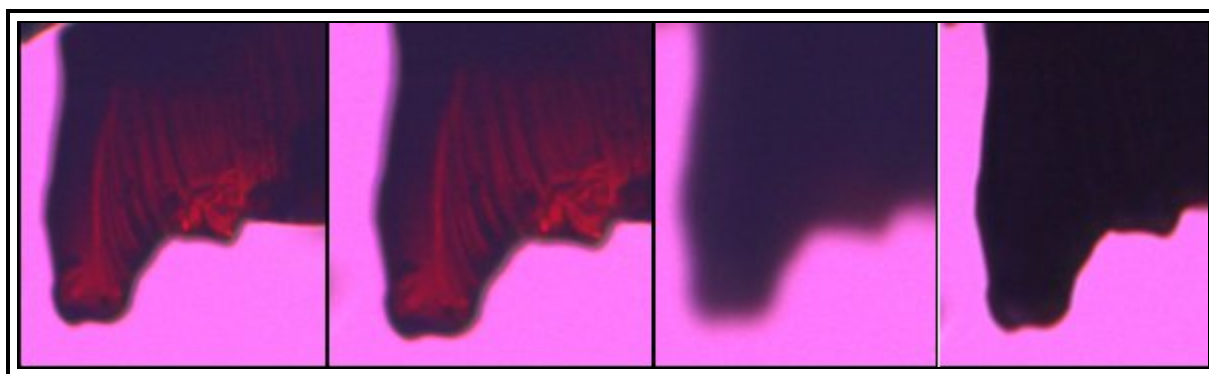


**Figure 4.8:** Changes in  $\text{RhCl}_3 \cdot x\text{H}_2\text{O}$  appearance at 35, 159, 241 and 400 °C respectively (from left to right)

This process revealed a colour change for  $\text{RhCl}_3 \cdot x\text{H}_2\text{O}$  from red to black as the sample was being heated. This change was assumed to be associated with the removal of water as perceived by the IR scan. In an attempt to recover the starting material (400 °C), the dehydrated rhodium sample was cooled and re-exposed to the atmosphere to enable the re-absorption of moisture for 24 hours and then re-analyzed. The results indicated no difference from the decomposed sample, which suggests the formation of the black coloured anhydrous rhodium(III) oxide ( $\text{Rh}_2\text{O}_3$ ) during the heating process (product however not positively identified).<sup>216</sup>

---

<sup>216</sup> E. Wiberg, N. Wiberg and A. F. Holleman, *Inorganic chemistry*, (2001), p. 1493

### 4.7.2 DSC and TGA analysis of $\text{RhCl}_3 \cdot x\text{H}_2\text{O}$

A thermal analysis was also carried out with the aim of determining the number of crystal waters in  $\text{RhCl}_3 \cdot x\text{H}_2\text{O}$  so as to evaluate the success of the rhodium analysis on this sample.

#### 4.7.2.1 Differential scanning calorimetry (DSC)

$\text{RhCl}_3 \cdot x\text{H}_2\text{O}$  (0.00397 g) was mounted on an aluminium sample pan shown in **Chapter 3, Figure 3.27**, injected into the DSC machine and then heated at a rate of  $10\text{ }^\circ\text{C}/\text{min}$  as described in **Section 4.2.7**. **Figure 4.9** shows the heating and the cooling cycles of the sample.

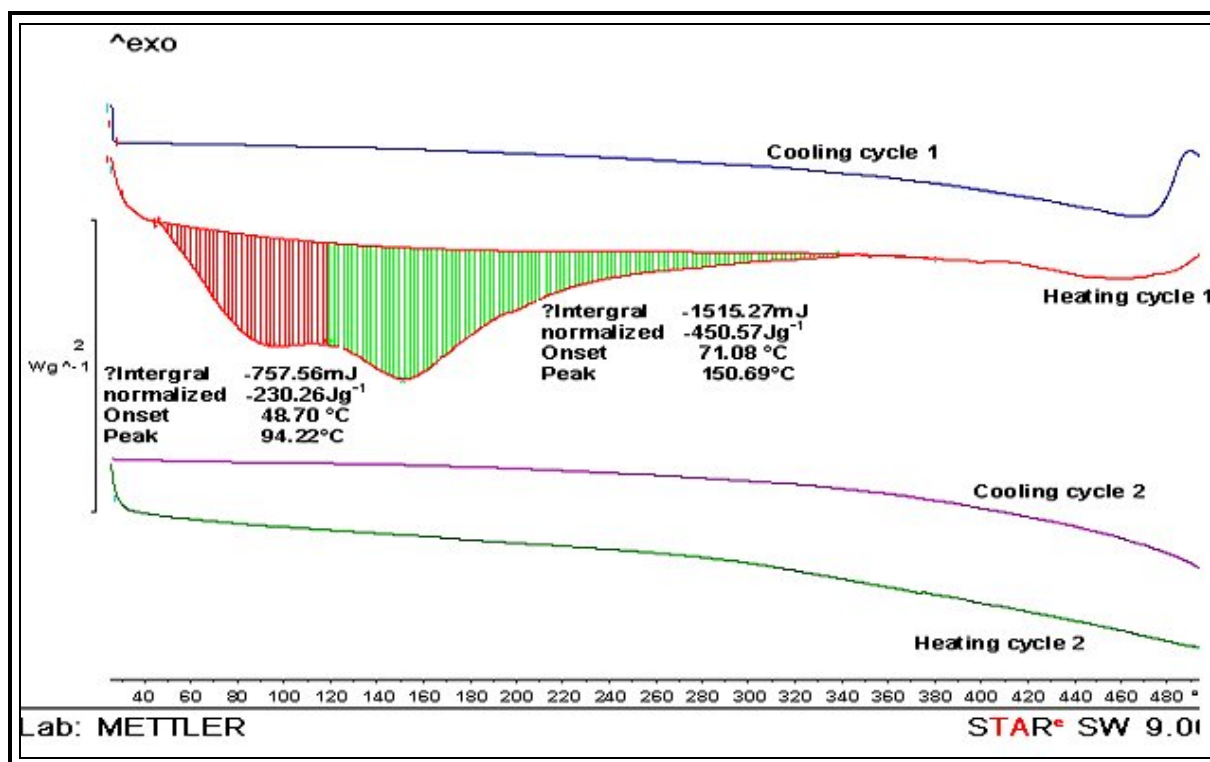


**Figure 4.9:** DSC scan of  $\text{RhCl}_3 \cdot x\text{H}_2\text{O}$

The DSC scan showed 2 heating and cooling cycles. From the heating cycle 1, an endothermic process was observed in which two phases are shown in red and green colours. This endothermic phases represent the weight loss of at least two crystal water molecules from the  $\text{RhCl}_3 \cdot x\text{H}_2\text{O}$  as illustrated by the heat adsorption during the heating process. The area under the curve is estimated to be directly proportional to the amount of energy used for the sample decomposition during the endothermic

process. The total energy required for the first and second endothermic phases was 757.56 and 1515.27 mJ respectively. This total amount of energy indicated the amount of energy used to decompose or dehydrate the  $\text{RhCl}_3 \cdot x\text{H}_2\text{O}$ . The decomposed or dehydrated  $\text{RhCl}_3 \cdot x\text{H}_2\text{O}$  was left to recover in the cooling cycle 1 to determine whether the process was reversible. No phase transitions was observed from cooling cycle 1, 2 and the heating cycle 2, which indicates that the re-adsorption process was not reversible. This result gave a clear indication that once  $\text{RhCl}_3 \cdot x\text{H}_2\text{O}$  is heated beyond an estimated temperature of 340 °C and above,  $\text{RhCl}_3 \cdot x\text{H}_2\text{O}$  is probably not recovered back. This result was also in agreement with the preliminary results of  $\text{RhCl}_3 \cdot x\text{H}_2\text{O}$  observed with the microscope.

From the endothermic phase transition of  $\text{RhCl}_3 \cdot x\text{H}_2\text{O}$  the differences in the energy absorbed by the crystal waters was different due to the possibility of the way they are coordinated in the  $\text{RhCl}_3 \cdot x\text{H}_2\text{O}$  crystal lattice. The second endothermic process required almost double the amount of heat energy to evolve, which gave an indication of the coordination of crystal waters to the rhodium metal. The lower endothermic energy might have indicated a weak coordination whilst the higher energy might have indicated a stronger coordination of the water molecules. The information from the DSC gave the precise amount of the energy required to dry  $\text{RhCl}_3 \cdot x\text{H}_2\text{O}$  as well as indicating the phase transitions during the sample decomposition.

#### **4.7.2.2 Thermal gravimetric analysis (TGA)**

The TGA was also performed in an effort to accurately determine the number of crystal waters by measuring the mass changes in  $\text{RhCl}_3 \cdot x\text{H}_2\text{O}$  as a result of water loss with respect to temperature as illustrated in **Section 4.2.6**. The analyte sample  $\text{RhCl}_3 \cdot x\text{H}_2\text{O}$  (5.52 mg) was placed in an alumina cup and mounted to the furnace chamber that was attached to the balance. The sample cup was heated at a rate of 5 °C/min and changes in mass signals from the balance were plotted against the temperature as shown in **Figure 4.10**.





**Figure 4.10:** Changes in weight (mass) of RhCl<sub>3</sub>·xH<sub>2</sub>O

The TGA graph obtained from the experiments shows three stages of weight loss of RhCl<sub>3</sub>·xH<sub>2</sub>O. The weight loss occurred in stages, starting with 1.43 %, then 5.29 % lastly 8.65 %. A total loss of H<sub>2</sub>O accounting for approximately 15 % of the starting mass of RhCl<sub>3</sub>·H<sub>2</sub>O was observed, implicating that approximately 85 % of the initial RhCl<sub>3</sub>·xH<sub>2</sub>O remained.

Keeping this graph in mind, calculations indicate that a formula mass corresponding to a composition of RhCl<sub>3</sub>·xH<sub>2</sub>O would have accounted for an approximately 7.9 % loss, that of RhCl<sub>3</sub>·2H<sub>2</sub>O for 14.7 % loss and RhCl<sub>3</sub>·3H<sub>2</sub>O for approximately 20 % loss. A value of 15 % therefore is very close to what was calculated for RhCl<sub>3</sub>·2H<sub>2</sub>O. It is important however to stress the fact that for both the TGA and DSC analyses the initial temperatures for the analysis were well above room temperature and that weakly packed crystal waters or adsorbed H<sub>2</sub>O could have been lost before the start of these analyses. Using these techniques, two crystal water molecules can thus at best be regarded as the minimum.

It is also important to note the similarities between the temperatures for this stepwise crystal water loss by these two techniques. The DSC indicated substantial energy absorption at 94 °C which corresponds to 1.5 % mass loss at 89 °C in the TGA. The second major endothermic processes occur at 151 °C in the DSC analysis, compared to the loss of 5 % at 134 °C for the TGA. The last change in mass as observed by the TGA occurred at 196 °C (8.6 %) with no such an energy gain observed with the DSC.

A possible explanation of the difference of the two results is that the second peak in the DSC could have been an average of the 2<sup>nd</sup> and 3<sup>rd</sup> stages in the TGA analysis. This is due to the closeness of their average temperature to the one obtained in DSC analysis. The results from the DSC and the TGA were in agreement, both indicating loss of at least two crystal water molecules.

### **4.7.3 Quantitative analysis of $\text{RhCl}_3 \cdot x\text{H}_2\text{O}$ in $\text{HNO}_3$ (65.0 %) using the cobalt internal standard method**

#### **4.7.3.1 Preparation of the $\text{RhCl}_3 \cdot x\text{H}_2\text{O}$ analyte samples**

$\text{RhCl}_3 \cdot x\text{H}_2\text{O}$  (0.5325 g, 2.545 mmol) was dissolved in a volumetric flask (250.00 ml) and the flask filled to the mark using double distilled water. Aliquots (0.16 ml) of this stock solution were pipetted into volumetric flasks (50.00 ml) to yield an analytical solution of 2.512 - 3.38 ppm (varied depending on the number of water molecules contained, see **Appendix 7**). To each of the analyte samples, aliquots of the cobalt internal standard (2.00 ml; 50.00 ppm) and nitric acid (5.00 ml; 32.00 %) were added. The volumetric flasks were filled up to the mark using distilled water and left to stand for 5 hours before being analyzed.

#### **4.7.3.2 Preparation of the rhodium standard solutions and the quantitative determination of rhodium**

The standard solutions were prepared by pipetting equal volumes of cobalt (2.00 ml, 50.00 ppm) into each rhodium standard solution (0.5, 1.0, 2.0, 5.0 and 10.0 ppm) in 50.00 ml volumetric flasks. Nitric acid (5.00 ml, 65.00 %) was added and the flasks

filled up to the mark with double distilled water. The prepared standard solutions were homogenized and left to stand for 5 hours before used. The quantitative results of the percentage of rhodium recovered from the analysis are shown in **Table 4.16**.

**Table 4.16:** Percentage recovery of rhodium from  $\text{RhCl}_3 \cdot x\text{H}_2\text{O}$

Sample number	1H <sub>2</sub> O	2H <sub>2</sub> O	3H <sub>2</sub> O	4H <sub>2</sub> O
1	84.43	91.14	97.84	104.57
2	83.98	90.65	97.32	104.01
3	84.42	91.13	97.83	104.55
4	84.01	90.69	97.36	104.05
5	84.15	90.83	97.51	104.22
<b>Average % Rh recovery</b>	<b>84.20</b>	<b>90.89</b>	<b>97.57</b>	<b>104.28</b>
<b>RSD (%)</b>	<b>0.26</b>	<b>0.26</b>	<b>0.26</b>	<b>0.26</b>
<b>Calibration curve properties</b>			Slope	0.2851
			Intercept	0.0165
			R <sup>2</sup>	1.000
<b>Sample measurements and calculations</b>	Weighed mass/ g $\text{RhCl}_3 \cdot x\text{H}_2\text{O}$			0.5325 g
	Theoretical concentration of Rh (ppm)			2.51-3.38

It is evident from the quantitative analysis of rhodium in the  $\text{RhCl}_3 \cdot x\text{H}_2\text{O}$  salt that the chemical composition is more likely to be  $\text{RhCl}_3 \cdot 3\text{H}_2\text{O}$  or  $\text{RhCl}_3 \cdot 2\text{H}_2\text{O}$ . The second quantitative determination of rhodium was conducted in samples and standards prepared in hydrochloric acid compared to the current analysis which was performed in nitric acid medium. This investigation was to determine the effects of matching the  $\text{Cl}^-$  ions of the standard solutions to those of the analyte samples towards the rhodium recovery. In both procedures the cobalt internal standard was added in the same concentration. Both the standard solutions and the analyte solutions were matched using HCl and analyzed.

#### **4.7.4 Quantitative analysis of $\text{RhCl}_3 \cdot x\text{H}_2\text{O}$ in HCl (32.0 %) using the cobalt internal standard method**

##### **4.7.4.1 Preparation of the $\text{RhCl}_3 \cdot x\text{H}_2\text{O}$ analyte samples**

The same stock solution of  $\text{RhCl}_3 \cdot x\text{H}_2\text{O}$  (0.5325 g, 2.545 mmol) prepared in **Section 4.7.3.1** was used. Aliquots (0.16 ml) of this stock solution were pipetted into volumetric flasks (50.00 ml) to yield an analytical solution of 2.512 - 3.38 ppm (varied depending on the number of water molecules contained, see **Appendix 7**). To each of the analyte samples, cobalt internal standard (2.00 ppm) and hydrochloric acid (5.00 ml; 32.0 %) were added. The volumetric flasks were filled up to the mark using double distilled water and homogenised before left to stand for 5 hours for analysis.

##### **4.7.4.2 Preparation of the rhodium standards and the quantitative determination of rhodium**

The standard solutions were prepared by pipetting equal volumes of cobalt (5.00 ml, 50.00 ppm) into each rhodium standard solution (0.5, 1.0, 2.0, 5.0 and 10.0 ppm) in 50.00 ml volumetric flasks. Hydrochloric acid (5.00 ml, 32.00 %) was added and the flasks filled up to the mark with double distilled water. The prepared standard solutions were homogenised and left to stand for 5 hours before use.

The numerical calibration equation of the internal standard method was used to calculate the final rhodium concentration in each analytical sample as was the case with the CRM. The quantitative results of the percentage rhodium recovered are shown in **Table 4.17**.

**Table 4.17:** Results of the determination of Rh from  $\text{RhCl}_3 \cdot x\text{H}_2\text{O}$  in HCl

Sample number	1H <sub>2</sub> O	2H <sub>2</sub> O	3H <sub>2</sub> O	4H <sub>2</sub> O
1	86.43	93.29	100.14	106.99
2	86.31	93.17	100.01	106.85
3	85.94	92.76	99.57	106.39
4	85.95	92.78	99.59	106.40
5	86.02	92.85	99.66	106.49
<b>Average % Rh recovery</b>	<b>86.13</b>	<b>92.97</b>	<b>99.79</b>	<b>106.63</b>
<b>RSD (%)</b>	<b>0.26</b>	<b>0.26</b>	<b>0.26</b>	<b>0.26</b>
<b>Calibration curve properties</b>			Slope	0.2174
			Intercept	0.0205
			R <sup>2</sup>	1.000
<b>Sample measurements and calculations</b>	Weighed mass/ g $\text{RhCl}_3 \cdot x\text{H}_2\text{O}$			0.5325 g
	Theoretical concentration of Rh (ppm)			2.51 - 3.38

The recovery of rhodium using HCl as dissolution medium was 100 % if the rhodium salt had a chemical formula of  $\text{RhCl}_3 \cdot 3\text{H}_2\text{O}$ . This result corresponded very well, although not exactly the same, with those obtained for TGA (2.4 crystal waters) and DSC (2 crystal water molecules). A further investigation to determine whether the difference in rhodium recovery was due to the acid matrix interference or due to the increase of the chloride ions (increase in HCl) was conducted. This was done by adding different amounts of the acids (HCl, HBr and  $\text{HNO}_3$ ) to the analyte samples to compare with those of the standard solutions and quantifying the rhodium content.

#### **4.7.5 The effect of unmatched acid matrix (HCl, HBr and $\text{HNO}_3$ ) towards rhodium recovery (ruggedness and /or robustness)**

The sensitivity of rhodium recovery (as indicated by the previous two **Sections 4.7.3 and 4.7.4**) to the use of different acids propelled the investigation of the rhodium recovery using different acids. This investigation was done by adding the different acids to the analyte samples in increments of increasing concentration.

#### 4.7.5.1 Preparation of the $\text{RhCl}_3 \cdot x\text{H}_2\text{O}$ analyte samples

From the  $\text{RhCl}_3 \cdot x\text{H}_2\text{O}$  stock solution prepared in **Section 4.7.3.1**, aliquots (0.16 ml) were pipetted into volumetric flasks (50.00 ml) to yield analytical solutions of between 2.512 - 3.38 ppm (varied depending on the number of water molecules contained, see **Appendix 7**). To 3 sets of the 6 volumetric flasks containing  $\text{RhCl}_3 \cdot x\text{H}_2\text{O}$  analyte solution, different volumes, of HCl, HBr and  $\text{HNO}_3$  corresponding to the number of moles given in **Table 4.18** were added. Cobalt internal standard (2.00 ml; 50.00 ppm) was added and the volumetric flasks were filled up to the mark using distilled water and homogenised before left to stand for 5 hours before analysis.

#### 4.7.5.2 Preparation of the rhodium standards and the quantitative determination of rhodium

The standard solutions were prepared as illustrated in **Section 4.7.3.2** in the same order of concentration. The quantitative results of the percentage rhodium recovered are shown in **Table 4.18**.

**Table 4.18:** Quantitative analysis of rhodium in  $\text{RhCl}_3 \cdot 3\text{H}_2\text{O}$  using unmatched acid matrix

	Sample number	Number of moles of acid	% Rh recovery		
			HCl	HBr	$\text{HNO}_3$
	1	0.00025	97.72	97.85	97.96
	2	0.0005	97.47	93.45	97.47
	3	0.0010	97.11	93.13	96.96
	4	0.1020	96.68	89.90	96.68
	5	0.5100	94.57	86.72	94.57
	6	1.0180	91.90	86.27	91.90
<b>Average % Rh recovery</b>			<b>95.92</b>	<b>91.22</b>	<b>95.91</b>
<b>RSD (%)</b>			<b>2.36</b>	<b>4.88</b>	<b>2.39</b>
<b>Calibration curve properties</b>	Acid matrix		$\text{HNO}_3$ (unmatched)		
	$R^2$		0.9999		
<b>Sample measurements and calculations</b>	Weighed mass/ g $\text{RhCl}_3 \cdot 3\text{H}_2\text{O}$		0.5325 g		
	Theoretical concentration of Rh (ppm)		2.51 - 3.38 ppm		

It is clear from the results in **Table 4.18** that a steady decrease in rhodium recovery was obtained with an increase of all three acids especially for HBr. The preliminary deduction from this investigation of the decrease in rhodium recovery was largely attributed to the differences in viscosity between the rhodium analyte samples and the rhodium standard solutions as well as on the increase of the anion concentration. The complex chemistry of rhodium in aqua/chloro solutions as discussed in **Chapter 1, Section 1.7.1.1** was also considered to be the basis of low rhodium recovery.

The drop in rhodium recovery after a slight change in the acid matrix rendered the robustness of the test method inconsistent. From these results it was clear that the test method was adversely affected by an unmatched acid matrix and results obtained under these conditions were not reproducible (not robust).

The most used analytical grade acids (HCl and HNO<sub>3</sub>) were then chosen to be standardized to ensure precise concentrations in molarity for both solutions (standard and analyte solutions) so as to minimise the variation in acid matrix as seen in **Figure 4.11**. The acids were standardised against a 1.0 M Na<sub>2</sub>CO<sub>3</sub> (99.9 % purity analytical grade) solution. The acids were titrated using a methyl red indicator solution to a first permanent red colour and the concentrations for HCl (32.0 %) was found to be 10.09 M and 14.33 M for HNO<sub>3</sub> (65.0 %).<sup>217</sup>

---

<sup>217</sup> V. Arthur, *Textbook of quantitative inorganic analysis, 4<sup>th</sup> Edition*. (1978), p. 298

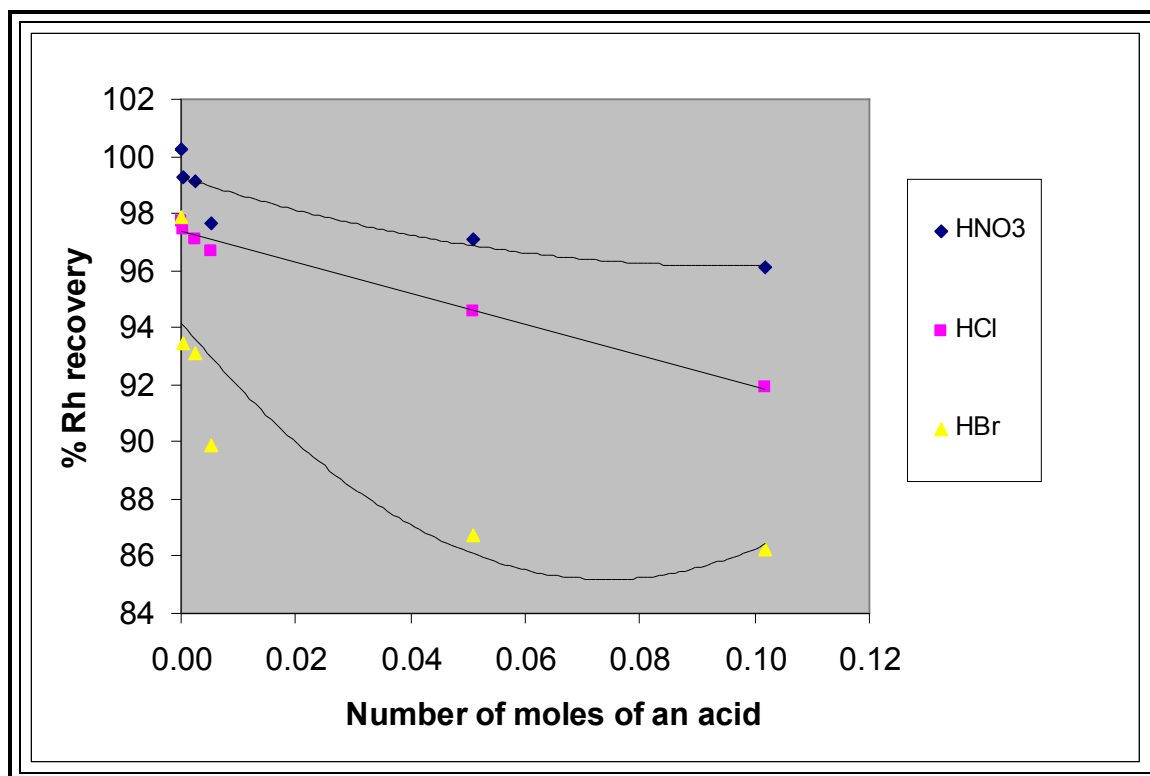


**Figure 4.11:** Effects of the acid matrix towards rhodium recovery

The difference in rhodium recovery was also thought to depend on the ability of the selected acid to carry the analyte sample as an aerosol to the nebuliser (see **Chapter 3, Figure 3.16**) for measurements. This problem was solved when it was realised that such a difference in ICP-OES measurements can be compensated for by ensuring that the acid matrix are matched as shown in **Section 4.7.4** where good results were obtained. The effect of halide ions ( $\text{Cl}^-$  and  $\text{Br}^-$ ) were investigated to determine whether the reduction in rhodium recovery was due to the acid or to the difference in halide concentration. Both the direct calibration method and the internal standard addition were used for this investigation and the results were compared with one another.

#### **4.7.6 Determining the effect of chloride ions ( $\text{Cl}^-$ ) towards rhodium recovery using the direct calibration method**

##### **4.7.6.1 Preparation of the $\text{RhCl}_3 \cdot 3\text{H}_2\text{O}$ analyte samples**

In this part of the study the effect of the chloride ions ( $\text{Cl}^-$ ) towards the rhodium recovery was investigated. Different aliquots of a standard NaCl solution (1.0, 2.0,



3.0, 4.0, 5 ml; 10.0 M) were pipetted into 50.00 ml volumetric flasks containing  $\text{RhCl}_3 \cdot 3\text{H}_2\text{O}$  (0.16 ml; 3.38 ppm). Hydrochloric acid (5.00 ml; 32.0 %) was added to each and the flasks filled up to the mark using double distilled water and homogenised before left for 5 hours to stabilise before analysis.

#### 4.7.6.2 Preparation of the standard solutions and the quantitative determination of rhodium

The standard solutions were prepared as illustrated in **Section 4.5.3.2** with exactly the same working range. The quantitative results of the percentage rhodium recovered are shown in **Table 4.19**.

**Table 4.19:** The effects of chloride ions in rhodium determination

	Sample number	Concentration (NaCl)	% Rh recovery
	1	0.00000	91.45
	2	0.00007	91.55
	3	0.00017	90.46
	4	0.00141	88.38
	5	0.01347	85.89
<b>Average % Rh recovery</b>			<b>89.55</b>
<b>RSD (%)</b>			<b>2.69</b>
<b>Calibration curve properties</b>	Slope		0.6972
	Intercept		0.057
	$R^2$		1.000
<b>Sample measurements and calculations</b>	Weighed mass/ g $\text{RhCl}_3 \cdot x\text{H}_2\text{O}$		0.5325 g
	Theoretical concentration of Rh (ppm)		3.38 ppm

The results showed a significant reduction of the rhodium recovered as the concentrations of both  $\text{Na}^+$  cations and  $\text{Cl}^-$  anions increased. Since  $\text{Na}^+$  is regarded as one of the so-called the easily ionized elements (EIEs) it not surprisingly that the results indicate a suppression of the rhodium intensity during analysis. The trend in decreasing rhodium recovery is shown in **Figure 4.12**.

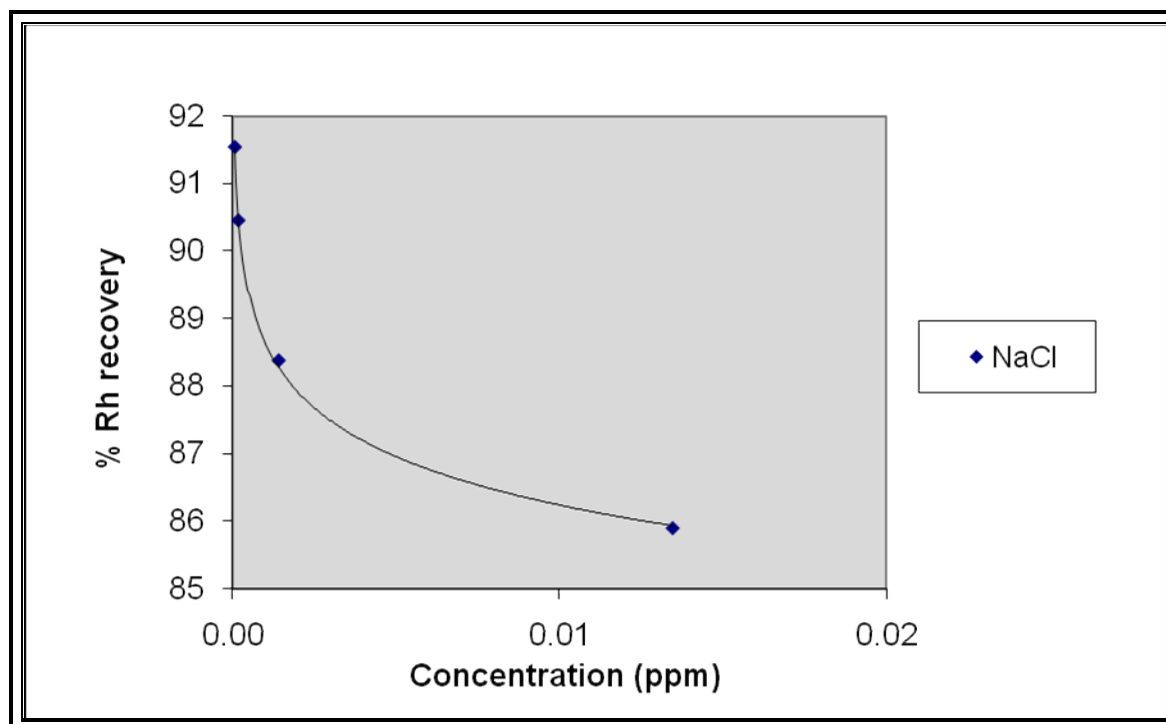


**Figure 4.12:** Decrease in rhodium recovery with increase in concentration of both  $\text{Na}^+$  and  $\text{Cl}^-$  ions.

From this investigation of the effect of the addition of  $\text{Na}^+$  and  $\text{Cl}^-$  ions on rhodium recovery from  $\text{RhCl}_3 \cdot 3\text{H}_2\text{O}$ , it was not clear enough to attribute the reduction in rhodium recovery to  $\text{Cl}^-$  ions only as the  $\text{Na}^+$  ions were also introduced in equal concentration. It was then decided to introduce  $\text{Cl}^-$  ions from different chloride salts to determine the  $\text{Cl}^-$  ion effect on rhodium recovery. Chloride ions were introduced as NaCl, KCl and RbCl to determine whether the  $\text{Cl}^-$  ions or the cations were interfering with the rhodium determination.

#### 4.7.7 Quantitative determination of rhodium in different concentrations of halide salts (NaCl, KCl and RbCl) using the direct calibration method

##### 4.7.7.1 Preparation of the $\text{RhCl}_3 \cdot 3\text{H}_2\text{O}$ and the halide salts solutions

Different aliquots of the prepared solutions of NaCl, KCl and RbCl (1.0, 2.0, 3.0, 4.0, 5.0 ml; 10.0 M) were pipetted into 50.00 ml volumetric flasks containing  $\text{RhCl}_3 \cdot 3\text{H}_2\text{O}$  (0.16 ml; 3.38 ppm) analyte solutions which were prepared in **Section 4.7.3.1**. Nitric acid (5.00 ml) was added to each and the flasks filled up with double distilled water to

yield a theoretical rhodium concentration of 3.38 ppm. The solutions were homogenised and left for 5 hours to stabilise before being analyzed

#### 4.7.7.2 Preparation of the rhodium standard solutions and the quantitative determination of rhodium

The standard solutions used in this experiment were those prepared in **Section 4.5.3.2** for the direct calibration method. The results for the quantitative analysis of this investigation are shown in **Table 4.20** and the relationship between the percentage of rhodium recovered and the increase in cation/chloride ion concentration is shown in **Figure 4.13**.

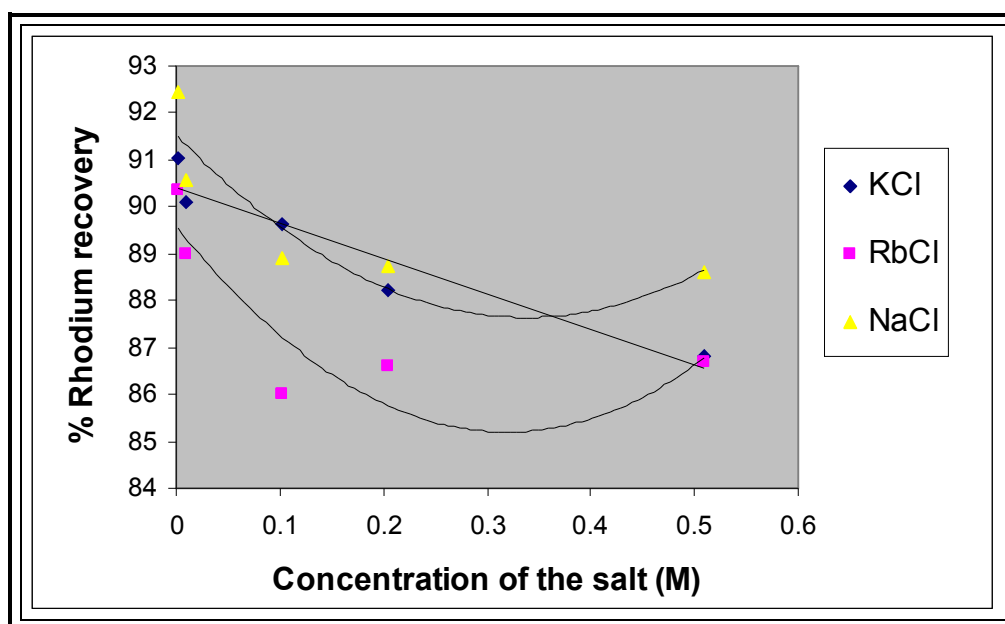


**Figure 4.13:** Effects of halide salts on rhodium recovery

**Table 4.20:** Percentage rhodium recovery from  $\text{RhCl}_3 \cdot 3\text{H}_2\text{O}$  in different chloride salt solutions using direct calibration

	Sample number	Concentration of the salt (M)	% Rh recovery		
			NaCl	KCl	RbCl
	1	0.00102	91.03	90.35	92.45
	2	0.01018	90.12	88.98	90.59
	3	0.10180	89.61	85.99	88.9
	4	0.20360	88.24	86.61	88.73
	5	0.50900	86.81	86.67	88.6
	6	1.01800	84.49	89.81	90.26
<b>Average % Rh recovery</b>			<b>88.38</b>	<b>88.07</b>	<b>89.92</b>
<b>RSD (%)</b>			<b>2.74</b>	<b>2.12</b>	<b>1.66</b>
<b>Calibration curve properties</b>	Acid matrix		HNO <sub>3</sub> (matched)		
	R <sup>2</sup>		0.9999		
<b>Sample measurements and calculations</b>	Weighed mass/ g RhCl <sub>3</sub> ·xH <sub>2</sub> O		0.5325 g		
	Theoretical concentration of Rh (ppm)		2.51 - 3.38 ppm		

It became clear from the above results that if the chloride ions were the only ions responsible for the lower recovery of rhodium, the decreasing trend would have been the same. The different cations which were introduced were also thought to have been responsible for the lower recovery. Further analysis was done in NaCl, KCl and RbCl under the same experimental conditions to determine the effectiveness of the cobalt internal standard in compensating for these halide matrix effects. The results showed a good recovery of the rhodium in the same concentrated salt analyte solutions as shown in **Table 4.21** and the correlation depicted in **Figure 4.14**.

**Table 4.21:** Percentage of rhodium recovered from  $\text{RhCl}_3 \cdot 3\text{H}_2\text{O}$  in different chloride salts using cobalt internal standard

	Sample number	Concentration of the salt (M)	% Rh recovery		
			NaCl	KCl	RbCl
	1	0.01018	99.51	105.67	100.27
	2	0.10180	100.14	104.38	105.82
	3	0.20360	109.53	104.93	105.97
	4	0.50900	101.95	112.46	107.74
	5	1.01800	116.18	112.96	82.31
<b>Average % Rh recovery</b>			<b>105.46</b>	<b>108.08</b>	<b>100.42</b>
<b>RSD (%)</b>			<b>6.83</b>	<b>3.94</b>	<b>10.46</b>
<b>Calibration curve properties</b>	Slope		0.2349		
	Intercept		0.0098		
	R <sup>2</sup>		1.000		
<b>Sample measurements and calculations</b>	Weighed mass/ g $\text{RhCl}_3 \cdot x\text{H}_2\text{O}$		0.5325 g		
	Theoretical concentration of Rh (ppm)		2.51 - 3.38 ppm		

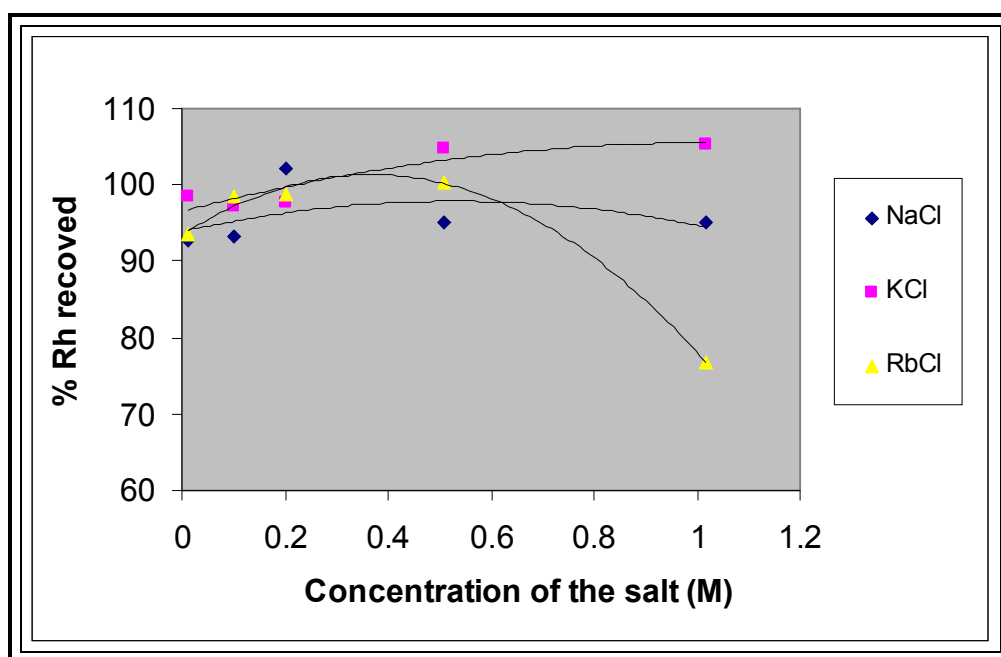


**Figure 4.14:** Matrix correction with cobalt internal standard

The results obtained from this part of the study indicate excellent results in rhodium recovery at lower salt concentrations. A total rhodium recovery at such lower concentrations suggests that the cobalt internal standard was able to compensate for some differences in concentration changes up to a certain limit. This was evidenced by either a sudden drop in rhodium recovery with RbCl or an increase as shown by the NaCl and KCl trend. This observation was also verified by De Klerk *et al.*<sup>218</sup> who investigated the effects of sodium ions in the quantitative determination of PGM.

## 4.8 Synthesis and analysis of organometallic complexes

One of the main objectives of this study was to develop a working method for rhodium determination and to evaluate this method by determining the rhodium content in different organometallic complexes. The organometallic complexes used in this research were all synthesized using  $\text{RhCl}_3 \cdot 3\text{H}_2\text{O}$  as a starting material. Different bidentate ligands such as acetylacetonone (acac) and cupferron (cupf) were added *via* substitution reactions to form the square planar  $[\text{Rh}(\text{L},\text{L}')(\text{CO})_2]$  complex (where  $\text{L},\text{L}' = \text{acetylacetonone or cupferron}$ ) which was then used as the starting material for the subsequent substitution reaction with triphenylphosphine ( $\text{PPh}_3$ ). The last step in these synthetic step reaction scheme involved the oxidative addition of methyl iodide to the square planar rhodium(I) complexes to form a rhodium(III) octahedral complex as shown in the reaction scheme in **Figure 4.15**.

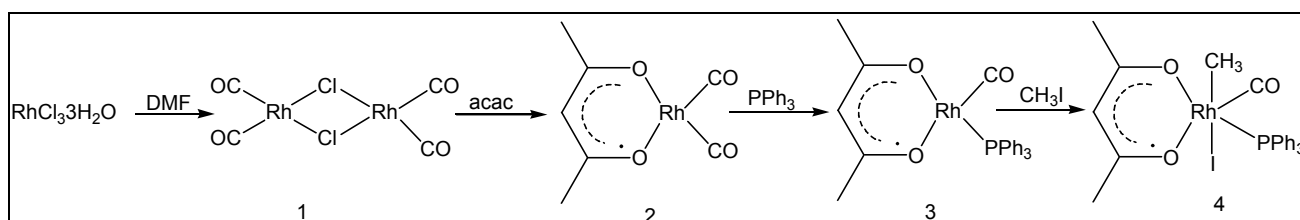


**Figure 4.15:** Synthesis of the different organometallic complexes

The cobalt internal standard addition method which proved to produce excellent results for all the previous quantitative analysis was chosen as the preferred method of analysis. The same experimental conditions for the ICP-OES rhodium determination were applied on the organometallic samples. The open beaker

<sup>218</sup> A. De Klerk and C. J. Rademeyer, *J. Anal. Atomic Spec.* (1997), 12, pp. 1221 - 1223

digestion method using hydrochloric acid was used for sample dissolution for all the organometallic complexes.

#### **4.8.1 Synthesis of different rhodium complexes**

##### **4.8.1.1 Synthesis of $[\text{Rh}(\text{acac})(\text{CO})_2]$ <sup>219</sup>**

A solution of the  $[\text{Rh}_2\text{Cl}_2(\text{CO})_4]$  dimer was prepared by refluxing  $\text{RhCl}_3 \cdot 3\text{H}_2\text{O}$  (0.2023 g; 0.97 mmol) in 10 ml of N,N-dimethylformamide for c.a. 30 min to a light orange colour. Bonati and Wilkinson<sup>220</sup> solved the crystal structure of  $[\text{Rh}_2\text{Cl}_2(\text{CO})_4]$  and confirmed the composition of the complex which yielded the same carbonyl stretching frequencies. An equivalent amount of acetylacetonone (0.12 ml; 0.98 mmol) was added and stirred for 30 min. Addition of 50 ml cold water to the reaction mixture precipitated the burgundy red  $[\text{Rh}(\text{acac})(\text{CO})_2]$  which was removed by centrifugation and purified by recrystallization from acetone. The red product (0.075 g; 0.29 mmol; Mr = 259.06 g/mol, 37.07 % yield) was dried at room temperature and characterized by means of IR spectroscopy as shown by the spectrum with the prominent carbonyl peaks at 2063 and 2000  $\text{cm}^{-1}$  in **Figure 4.16**

---

<sup>219</sup> J. G. Leipoldt, S. S. Basson, L. D. C. Bok and T. I. A. Gerber. *Inorg. Chim. Acta.*, (1978), 26, p. 35

<sup>220</sup> F. Bonati and G. Wilkinson, *J. Chem. Soc.*, (1964), p 3156

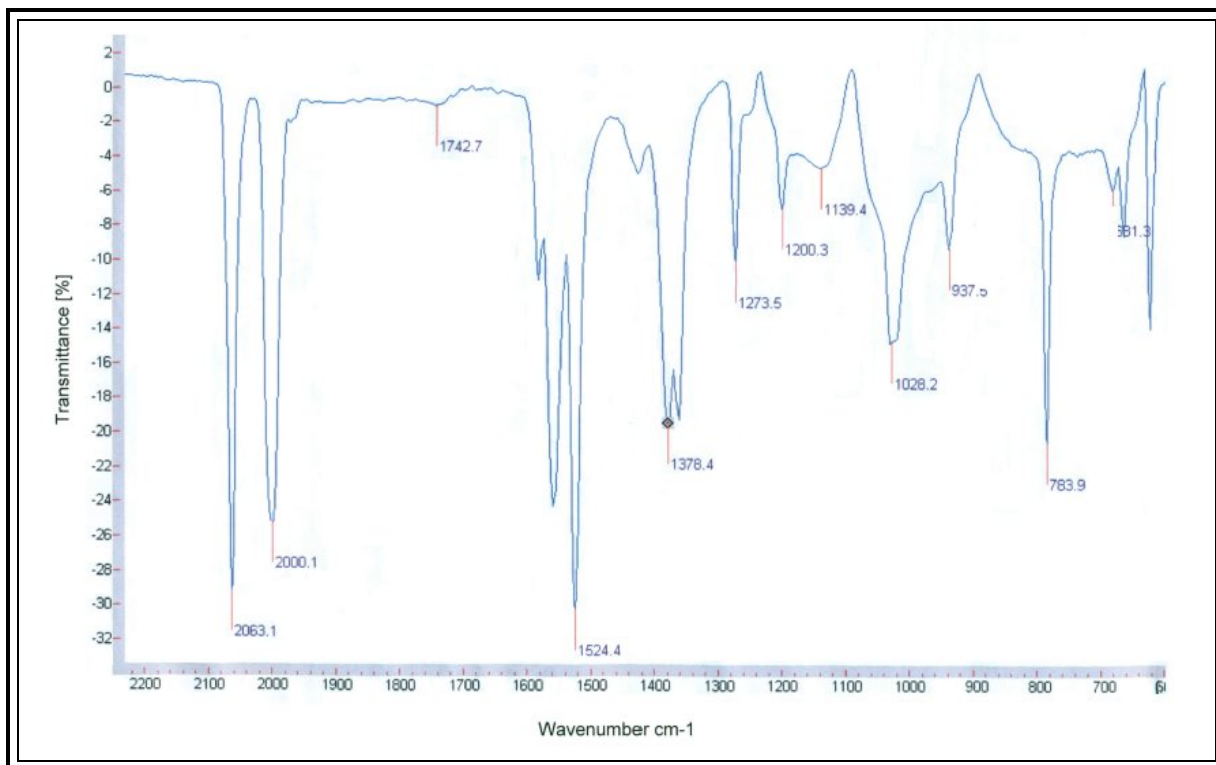


**Figure 4.16:** Infrared spectrum of  $[\text{Rh}(\text{acac})(\text{CO})_2]$

#### 4.8.1.2 Synthesis of $[\text{Rh}(\text{acac})(\text{PPh}_3)(\text{CO})]$ <sup>221</sup>

To a well stirred solution of  $[\text{Rh}(\text{acac})(\text{CO})_2]$  (0.075 g; 0.29 mmol) in 5 ml absolute ethanol, triphenylphosphine,  $\text{PPh}_3$ , (0.0760 g; 0.29 mmol) was added and the solution stirred for 30 min. A yellow precipitate was collected through filtration and washed with ethanol. The product,  $[\text{Rh}(\text{acac})(\text{PPh}_3)(\text{CO})]$ , (0.029 g; 0.046 mmol;  $M_r = 493.34$  g/mol, 20.3 % yield) was characterized by IR spectroscopy as shown in **Figure 4.17**, with the  $\nu_{\text{CO}}$  at  $1977\text{ cm}^{-1}$ . The carbonyl peak was in the same frequency region ( $1980\text{ cm}^{-1}$ ) as that reported by Venter.<sup>222</sup>

<sup>221</sup> A. M. Trzeciak, M. Jon and J. J. Ziolkowski, *React. Kinet. Catal. Lett.*, (1982), 20, p 383

<sup>222</sup> J. A. Venter, *Structural and kinetic study of rhodium complexes of N-aryl-N-nitrosohydroxylamines and related complexes*, PhD study, (2006), p. 105



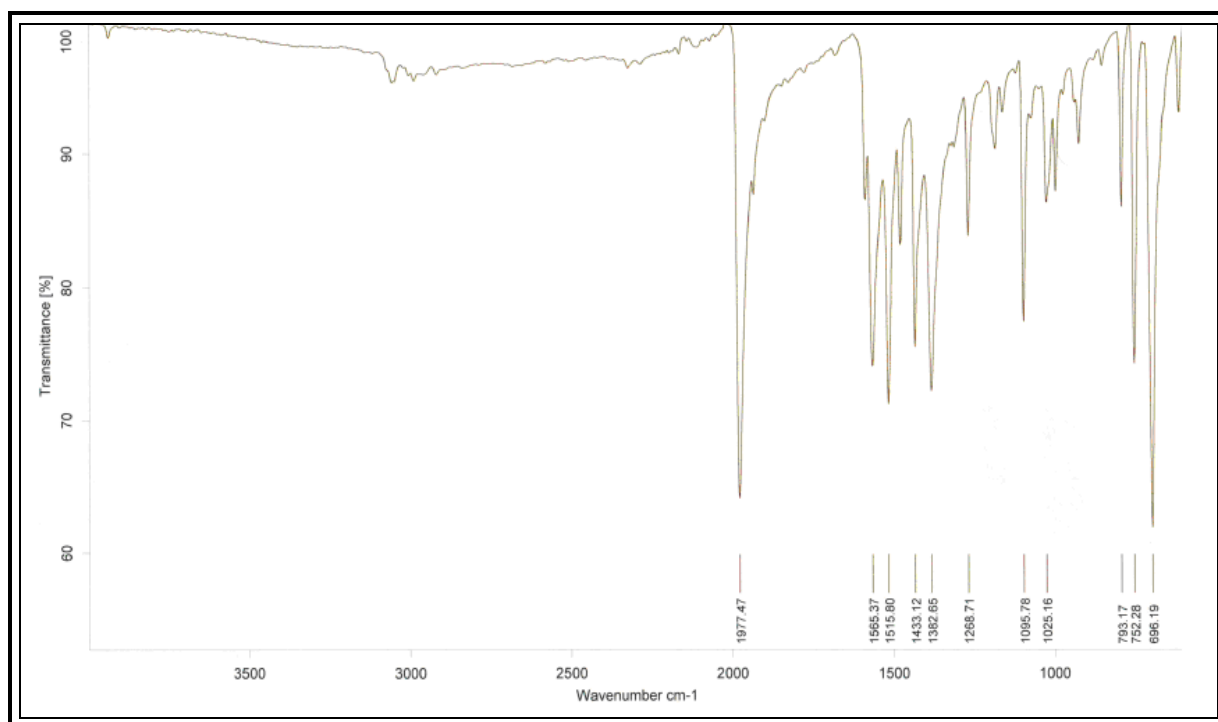


**Figure 4.17:** Infrared spectrum of  $[\text{Rh}(\text{acac})(\text{PPh}_3)(\text{CO})]$

#### 4.8.1.3 Synthesis of $[\text{Rh}(\text{acac})(\text{PPh}_3)(\text{CO})(\text{Me})(\text{I})]$ <sup>223</sup>

The oxidative addition product,  $[\text{Rh}(\text{acac})(\text{CO})\text{PPh}_3(\text{Me})(\text{I})]$ , was prepared by dissolving  $[\text{Rh}(\text{acac})(\text{PPh}_3)(\text{CO})]$  (0.0535 g; 0.11 mmol) in 25 ml acetone and allowed to stir for 15 min before adding  $\text{CH}_3\text{I}$  (0.5 ml; 0.55 mmol (five-fold excess)). The resultant brown-yellow mixture was gently heated ( $<35\text{ }^\circ\text{C}$ ) whilst stirring for 25 min to a clear yellow solution which gradually changed to red. Characterisation of the product (0.0357 g; 0.056 mmol,  $M_r = 635.261\text{ g/mol}$ ; 51.82 % yield) using IR spectroscopy showed the stretching frequency of the carbonyl at  $2043.83\text{ cm}^{-1}$  (**Figure 4.18**). The carbonyl peak was in the same frequency region ( $2060\text{ cm}^{-1}$ ) as that reported by Venter.<sup>224</sup>

<sup>223</sup> S. S. Basson, J. G. Leipoldt, A. Roodt, J. A. Venter and T. J. Van der Walt, *Inorg. Chim. Acta*, (1986), 119, pp. 35 - 38

<sup>224</sup> J. A. Venter, *Structural and kinetic study of rhodium complexes of N-aryl-N-nitrosohydroxylamines and related complexes*, PhD study, (2006), p. 105

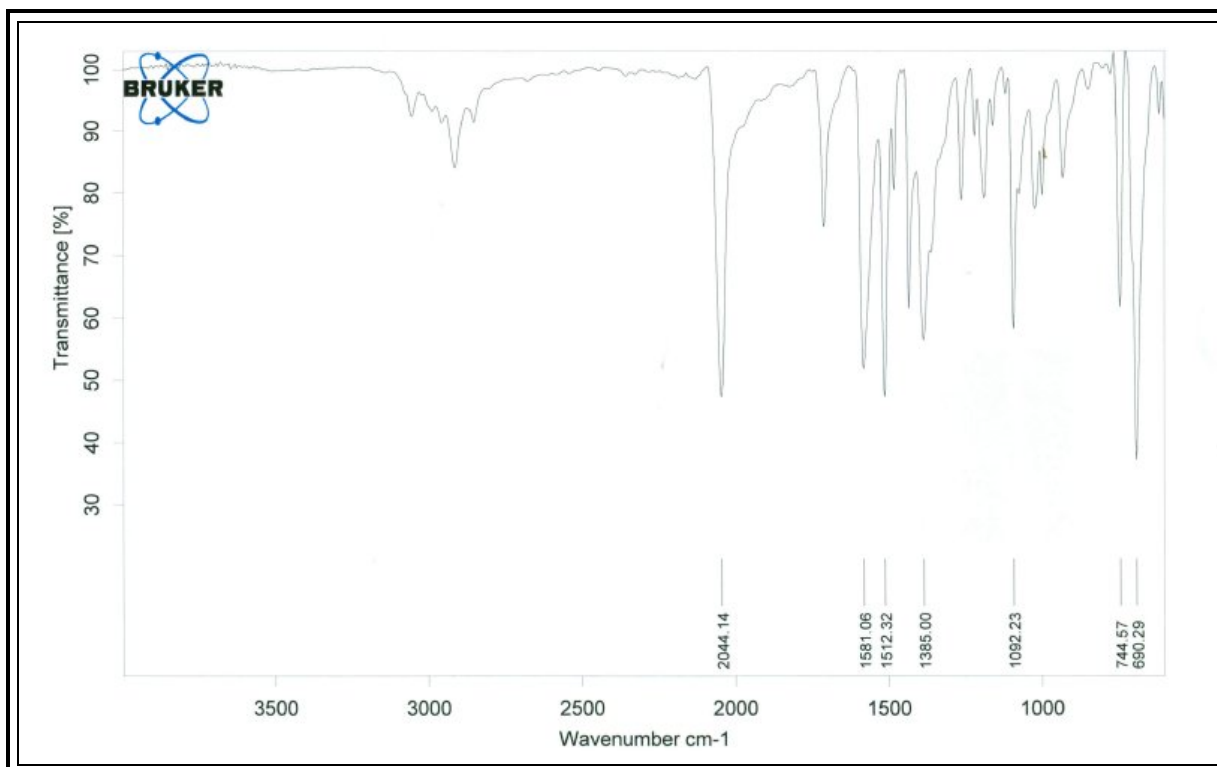


**Figure 4.18:** Infrared spectrum of  $[\text{Rh}(\text{acac})(\text{CO})\text{PPh}_3](\text{Me})(\text{I})$

#### 4.8.1.4 Synthesis of $[\text{Rh}(\text{cupf})(\text{CO})_2]$ <sup>225</sup>

Three drops of double distilled water were added to the deep red crystals of  $\text{RhCl}_3 \cdot 3\text{H}_2\text{O}$  (0.5050 g; 1.92 mmol) and allowed to aggregate. N,N-dimethylformamide, DMF, (15 ml) was added and the solution refluxed gently to a light orange colour. The solution was cooled to room temperature and cupferron (0.3744 g; 2.41 mmol) was added and stirred for 30 min. Cold water (100 ml) was added to the solution and the suspension filtered. The resulting yellow residue was washed with double distilled water (20 ml x 3) and recrystallized using acetone. Characterisation of  $[\text{Rh}(\text{cupf})(\text{CO})_2]$  (0.4213 g; 1.34 mmol;  $M_r = 314.09$  g/mol; yield 69.92 %) was done using IR spectroscopy and the carbonyl stretching frequencies appeared at 2057 and 2011  $\text{cm}^{-1}$  as shown in **Figure 4.19**. The same carbonyl stretching frequencies was obtained by Goswami.<sup>226</sup>

<sup>225</sup> S. S. Basson, J. G. Leipoldt, A. Roodt and J. A. Venter, *Inorg. Chim. Acta*, (1986), 118, pp. 45 - 47

<sup>226</sup> K. Goswami and M. M. Singh, *Transition Met. Chem.*, (1980), 5 p. 83

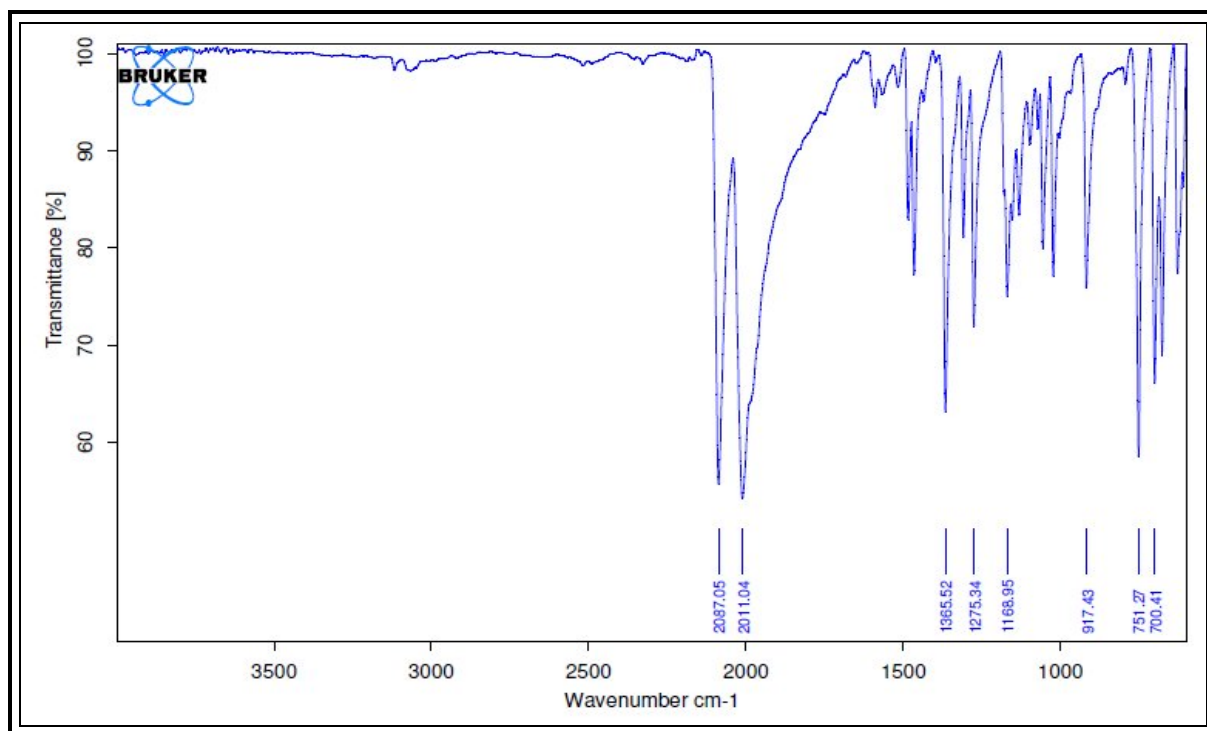


**Figure 4.19:** Infrared spectrum of  $[\text{Rh}(\text{cupf})(\text{CO})_2]$

#### 4.8.1.5 Synthesis of $[\text{Rh}(\text{cupf})(\text{PPh}_3)(\text{CO})]$ <sup>227</sup>

To a well stirred solution of  $[\text{Rh}(\text{cupf})(\text{CO})_2]$  (0.2087 g; 0.67 mmol) in 10 ml of absolute ethanol, an equivalent amount of triphenylphosphine,  $\text{PPh}_3$ , ( 0.1745 g, 0.67 mmol ) was added. The resultant yellow solution was gently stirred for 10 min at room temperature. A yellow precipitate was formed which was filtered and washed with absolute ethanol (5 ml x 3) and left to dry overnight. The product (0.212 g; 0.39 mmol;  $M_r = 548.38$  g/mol; yield 58.18 %) was characterised by IR spectroscopy and the carbonyl stretching frequency appeared at  $1976\text{ cm}^{-1}$ . The carbonyl peak was in the same frequency region of  $1982\text{ cm}^{-1}$  (**Figure 4.20**) as that reported by Venter.<sup>228</sup>

<sup>227</sup> S. S. Basson, J. G. Leipoldt, A. Roodt and J. A. Venter, *Inorg. Chim. Acta*, (1986), 118, pp. 45-47

<sup>228</sup> J. A. Venter, *Structural and kinetic study of rhodium complexes of N-aryl-N-nitrosohydroxylamines and related complexes*, PhD study, University of the Free State, (2006), p. 105

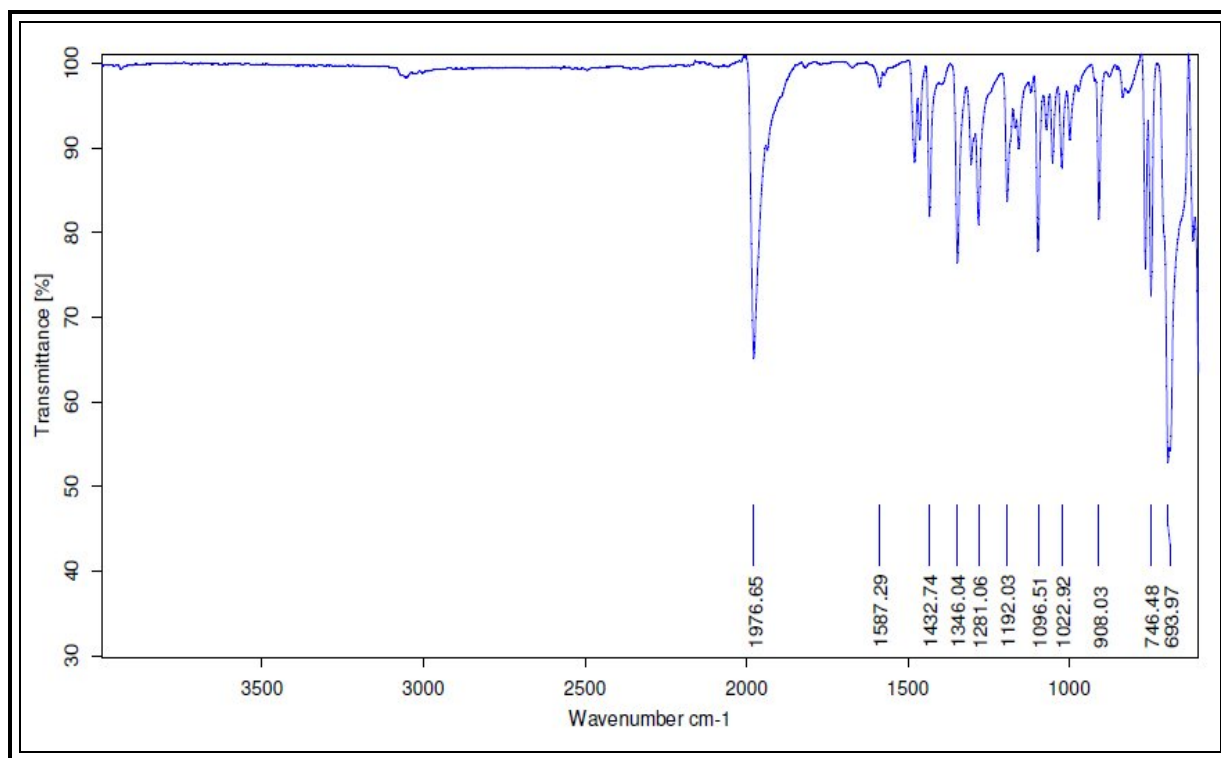


**Figure 4.20:** Infrared spectrum of  $[\text{Rh}(\text{cupf})(\text{PPh}_3)(\text{CO})]$

#### 4.8.1.6 Synthesis of $[\text{Rh}(\text{cupf})(\text{PPh}_3)(\text{CO})(\text{Me})(\text{I})]^{229}$

To a well stirred solution of  $[\text{Rh}(\text{cupf})(\text{PPh}_3)(\text{CO})]$  ( 0.1504 g; 0.22 mmol) in 3 ml acetone,  $\text{CH}_3\text{I}$  (1 ml; 2.20 mmol 10x excess) was added whilst stirring. The resultant yellow solution was left to crystallize slowly at room temperature. A yellow brown needle-like product (0.0772 g; 0.12 mmol; Mr = 690.291 g/mol; 40.78 % yield) was obtained and characterised by IR spectroscopy. The stretching frequency of the rhodium carbonyl was shown to be at  $2045\text{ cm}^{-1}$  as revealed in the spectrum shown in **Figure 4.21**. The carbonyl peak was in the same frequency region ( $2052\text{ cm}^{-1}$ ) as that obtained by Venter.<sup>230</sup>

<sup>229</sup> K. Goswami and M. M Singh, *Transition Met.Chem.*, (1980), 5, p. 83

<sup>230</sup> J. A. Venter, *Structural and kinetic study of rhodium complexes of N-aryl-N-nitrosohydroxylamines and related complexes*, PhD study, University of the Free State, (2006), p. 105

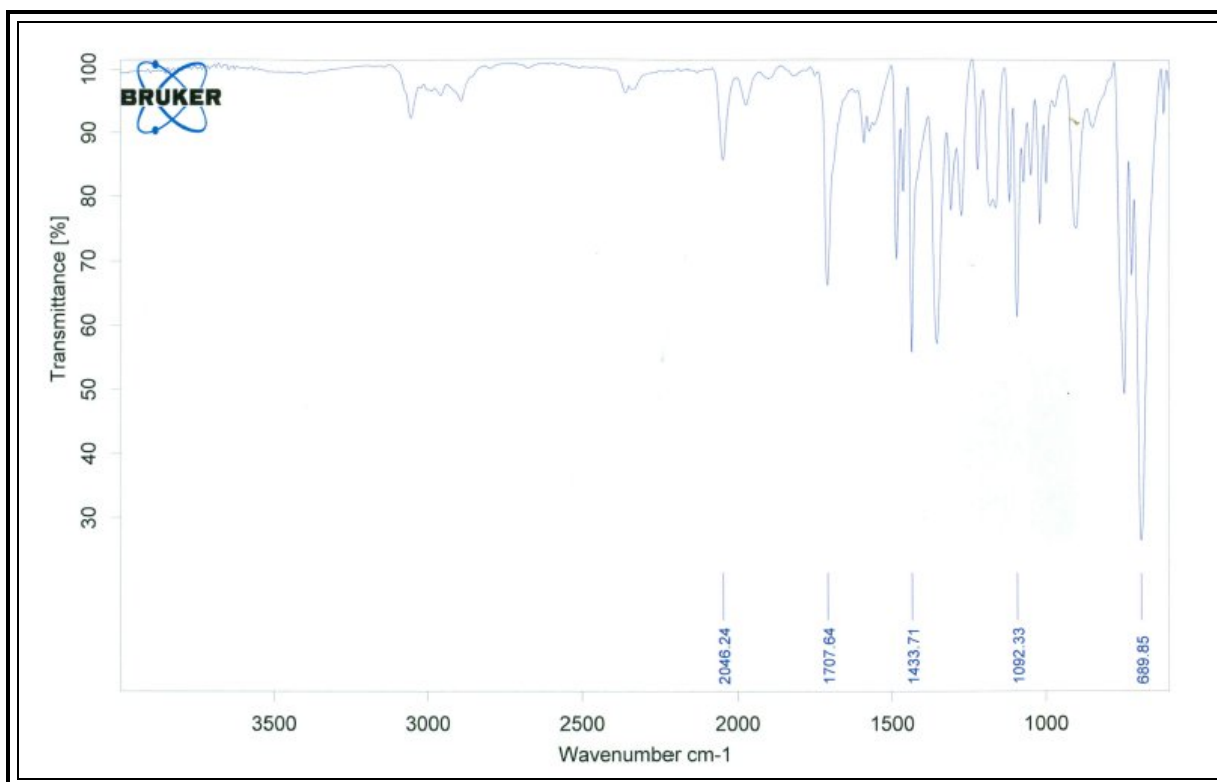


**Figure 4.21:** Infrared spectrum of [Rh(cupf)(PPh<sub>3</sub>)(CO)(CH<sub>3</sub>)(I)]

## 4.8.2 Quantitative determination of rhodium from the newly synthesized organometallic complexes

### 4.8.2.1 Preparation of the organometallic complexes for rhodium determination

Samples of the different organometallic complexes were accurately weighed and their masses recorded as shown in **Tables 4.22 -4.27**. Hydrochloric acid (5 ml; 32.0 %) was added and the samples digested (c.a. 110 °C) in open beakers until the samples were completely dissolved. The dissolved samples were further heated at the same temperature to almost dryness and nitric acid added (5 ml; 65.00 %) prior to dryness and the solution re-heated. The additions of nitric acid to the almost dry samples were repeated 3 times before the samples were quantitatively transferred into 100.00 ml volumetric flasks. Nitric acid (5.00 ml, 65.00 %) was added to the stock solutions and filled up to the mark using double distilled water. Different aliquots of the stock solutions were pipetted in volumetric flasks (50.00 ml) to yield concentrations in the region of 3.38 ppm of rhodium. Cobalt internal standard (2.00 ml; 50.00 ppm) was pipetted into each analyte solution and nitric acid (2.50 ml,

65.00 %) added. The analyte flasks were filled up to the mark using double distilled water before shaken for several minutes to ensure homogeneity and left to stand for 5 hours before being analyzed.

#### 4.8.2.2 Preparation of the standard solutions and the quantitative determination of rhodium

Rhodium standards with the cobalt internal standard were prepared in the same way as described in **Section 4.5.6.3.2**. The experimental results are shown in **Tables 4.22 - 4.27**.

**Table 4.22:** Quantitative determination of rhodium from in  $[\text{Rh}(\text{acac})(\text{CO})_2]$

	Sample number	% Rh recovery
	1	95.62
	2	95.16
	3	95.30
	4	96.77
	5	95.69
<b>Average</b>		<b>95.71</b>
<b>RSD (%)</b>		<b>0.66</b>
<b>Calibration curve properties</b>	Slope	0.2319
	Intercept	0.0136
	$R^2$	1.000
<b>Sample measurements and calculations</b>	Weighed mass/ g $[\text{Rh}(\text{acac})(\text{CO})_2]$	0.042 g
	Theoretical concentration of Rh (ppm)	3.38 ppm

**Table 4.23:** Quantitative determination of rhodium in [Rh(acac)(PPh<sub>3</sub>)(CO)]

	<b>Sample number</b>	<b>% Rh recovery</b>
	1	80.58
	2	81.79
	3	81.65
	4	81.78
	5	81.35
<b>Average</b>		<b>81.43</b>
<b>RSD (%)</b>		<b>0.63</b>
<b>Calibration curve properties</b>	Slope	0.2319
	Intercept	0.0136
	R <sup>2</sup>	1.000
<b>Sample measurements and calculations</b>	Weighed mass/ g [Rh(acac)(PPh <sub>3</sub> )(CO)]	0.0352 g
	Theoretical concentration of Rh (ppm)	3.38 ppm

**Table 4.24:** Quantitative determination of rhodium in [Rh(acac)(PPh<sub>3</sub>)(CO)(CH<sub>3</sub>)(I)]

	<b>Sample number</b>	<b>% Rh recovery</b>
	1	89.84
	2	88.91
	3	89.35
	4	89.47
	5	88.36
<b>Average</b>		<b>89.19</b>
<b>RSD (%)</b>		<b>0.64</b>
<b>Calibration curve properties</b>	Slope	0.2319
	Intercept	0.0136
	R <sup>2</sup>	1.000
<b>Sample measurements and calculations</b>	Weighed mass/ g [Rh(acac)(PPh <sub>3</sub> )(CO)(CH <sub>3</sub> )(I)]	0.025 g
	Theoretical concentration of Rh (ppm)	3.38 ppm

**Table 4.25:** Quantitative determination of rhodium in  $[\text{Rh}(\text{cupf})(\text{CO})_2]$ 

	<b>Sample number</b>	<b>% Rh recovery</b>
	1	103.28
	2	99.13
	3	99.25
	4	98.71
	5	99.50
<b>Average</b>		<b>99.97</b>
<b>RSD (%)</b>		<b>1.87</b>
<b>Calibration curve properties</b>	Slope	0.2319
	Intercept	0.0136
	$R^2$	1.000
<b>Sample measurements and calculations</b>	Weighed mass/ g $[\text{Rh}(\text{cupf})(\text{CO})_2]$	0.0403 g
	Theoretical concentration of Rh (ppm)	3.38 ppm

**Table 4.26:** Quantitative determination of rhodium in  $[\text{Rh}(\text{cupf})(\text{PPh}_3)(\text{CO})]$ 

	<b>Sample number</b>	<b>% Rh recovery</b>
	1	99.53
	2	98.76
	3	99.43
	4	98.80
	5	99.18
<b>Average</b>		<b>99.14</b>
<b>RSD (%)</b>		<b>0.36</b>
<b>Calibration curve properties</b>	Slope	0.2305
	Intercept	0.0093
	$R^2$	1.000
<b>Sample measurements and calculations</b>	Weighed mass/ g $[\text{Rh}(\text{cupf})(\text{PPh}_3)(\text{CO})]$	0.1924 g
	Theoretical concentration of Rh (ppm)	3.38 ppm



**Table 4.27:** Quantitative determination of rhodium in  $[\text{Rh}(\text{cupf})(\text{PPh}_3)(\text{CO})(\text{CH}_3)(\text{I})]$ 

	<b>Sample number</b>	<b>% Rh recovery</b>
	1	98.99
	2	98.25
	3	99.53
	4	98.89
	5	99.72
<b>Average</b>		<b>99.68</b>
<b>RSD (%)</b>		<b>0.35</b>
<b>Calibration curve properties</b>	Slope	0.2319
	Intercept	0.0136
	$R^2$	1.000
<b>Sample measurements and calculations</b>	Weighed mass/ g $[\text{Rh}(\text{cupf})(\text{PPh}_3)(\text{CO})(\text{CH}_3)(\text{I})]$	0.0220 g
	Theoretical concentration of Rh (ppm)	3.38 ppm

Quantitative determination of rhodium from the newly synthesised organometallic complexes revealed an overall good rhodium recovery in all the samples. Excellent results (99.0 % +) were obtained for the rhodium cupferron complexes. The the low recovery of rhodium in  $[\text{Rh}(\text{acac})(\text{CO})(\text{PPh}_3)]$  and  $[\text{Rh}(\text{acac})(\text{CO})(\text{PPh}_3)(\text{Me})(\text{I})]$  can most probably be attributed to impure products, as no recrystallization was performed to purify them. Unreacted starting materials are suspected to be the main cause.

The cobalt internal standard method was shown to be applicable to organometallic complexes and was shown to be an accurate method for rhodium determination. Matrix matching was an important factor in the determination of rhodium. Newly synthesized complexes were treated with  $\text{HNO}_3$  after being digested in  $\text{HCl}$  in order to avoid the acid matrix that was shown to lower the rhodium percentage recovery.

## 4.9 Conclusion

A summary of the rhodium determination in inorganic and organometallic complexes as well as in the certified reference material (CRM) using the cobalt internal standard, is shown in **Table 4.28**.

**Table 4.28:** A summary of the rhodium recovery in CRM, rhodium metal as well as in inorganic and organometallic complexes using the cobalt internal standard addition method

Samples	Average % Rh recovery
<b>CRM</b>	100.10
<b>Rhodium powdered</b>	99.69
<b>Inorganic complex</b> (RhCl <sub>3</sub> ·3H <sub>2</sub> O)	99.79
<b>Organometallic compounds</b> [Rh(acac)(CO) <sub>2</sub> ]	95.71
[Rh(acac)(CO)(PPh <sub>3</sub> )]	81.43
[Rh(acac)(CO)(PPh <sub>3</sub> )(Me)(I)]	89.19
[Rh(cupf)(CO) <sub>2</sub> ]	99.97
[Rh(cupf)(CO)(PPh <sub>3</sub> )]	99.14
[Rh(cupf)(CO)(PPh <sub>3</sub> )(Me)(I)]	99.08
<b>RSD (%)</b>	<b>6.78</b>

Excellent results in rhodium recovery using the cobalt internal standard were obtained from the CRM. The results obtained using the CRM showed to be in total agreement with the certified values of the CRM. The method of determination that yielded the excellent results then formed the basis from which the experimental procedure was derived and also the reference to which rhodium quantification was adopted. The subsequent determinations of rhodium from different samples such as the rhodium metal and inorganic as well as organometallic complexes were conducted using the same procedure. All the results were determined in the same percentage confidence interval (95 %), in line with the certified value of the CRM. A

relatively higher standard deviation of about 7.0 % was obtained and was attributed to the different types of matrices that lowered the rhodium recovery. The method was found to be hampered by an unmatched acid matrix and other matrices such as those caused by the easily ionized elements (EIE). These results were in agreement with those obtained by Garden *et al.*<sup>231</sup> who reported that ICP-OES signals can be suppressed by up to 40 % if the acid matrix is not matched. The acid matrix match was therefore shown to compensate for such drop in rhodium recovery and excellent results (99.79 %) for rhodium from inorganic salts were obtained. Reduced rhodium recoveries for the organometallic complexes with the acetylacetonone ligand were attributed to the impure products containing unreacted starting material. These results for  $[\text{Rh}(\text{acac})(\text{CO})(\text{PPh}_3)]$  and  $[\text{Rh}(\text{acac})(\text{CO})(\text{PPh}_3)(\text{Me})(\text{I})]$  were not in the acceptable range as shown in **Chapter 5**. The precision of this test method was found to be good in all the experimental analyses but accuracy was found to be affected by unmatched acid matrices which rendered the robustness not consistent.

---

<sup>231</sup> L. M. Garden, J. Marshall and D. Littlejohn, *J. Anal. At. Spectrom.*, (1991), 6, pp. 159 - 163

# 5 Validation of results

---

## 5.1 Introduction

Quality assurance forms an important part of analytical chemistry. Good laboratory practice and method validation are two aspects that allow for quality assurance and produce acceptable, accurate results. Good laboratory practices and method validation procedures have been established by international bodies such as the Organisation for Economic Cooperation and Development (OECD) and the International Organisation for Standardization (ISO) of which the ISO 17025 standard is one of the most well known and globally recognized standards for testing and calibration of laboratories.<sup>232</sup> The guidelines for appropriate method validation, especially for regulatory institutions, include selectivity, linearity, precision *etc.* as indicated in **Chapter 3, Section 3.3.2.**

Method validation was used to confirm whether the newly developed analytical procedures employed in this study were suitable for the rhodium determination. The validation results will be used to judge the quality, reliability and consistency of the developed method. The validation process was also conducted to investigate whether the designed method were sensitive to the addition of different acid matrices and to the concentration of the halide salts in the  $\text{RhCl}_3 \cdot x\text{H}_2\text{O}$  analysis. The sensitivity of the method and of the instrument towards rhodium analysis will also be investigated to determine whether the technique was compatible with its intended use.

The main objective of this chapter was to compile all the analytical results and to evaluate it as acceptable for analytical purposes according to ISO 17025 standards.

---

<sup>232</sup> R. P. Gerg, D. Christian, *Analytical Chemistry 6<sup>th</sup> Edition*, John. Wiley and Sons Inc.,(2004), p.126

Validation parameters such as the accuracy, precision, specificity, limit of detection, limit of quantitation, linearity and range, ruggedness and robustness will be evaluated for each rhodium analysis performed in this study using the cobalt internal standard method (**Chapter 4**). Statistical tests will also be used to determine whether the experimental results obtained should be accepted or rejected at 95 % confidence interval using hypothesis testing criteria as described in **Chapter 3, Section 3.3.2**.

## 5.2 Validation of the ICP-OES instrumentation

### 5.2.1 Method description

Validation of the ICP-OES was carried out to ensure that the chosen analytical conditions specified in **Chapter 4, Section 4.2.4, Table 4.1** are acceptable for rhodium determination. Results obtained from measuring the intensities of the blank solution (**Chapter 4, Section 4.5.2**) were checked for precision which was very important in determining the consistency of the measurement. A relative standard deviation (RSD) of 0.75 % was considered to be adequate since it indicated little fluctuations. The other parameters of validations of the ICP-OES were evaluated as described in **Chapter 4, Section 4.5.2** and were recorded in **Table 5.1**.

**Table 5.1:** Validation results of the ICP-OES method

Validation criteria	Parameter	Measurement/ comment
Sensitivity	Gradient (m)	0.7347
Linearity	Regression coefficient ( $r^2$ ) and r	0.9993 and 0.9996
Working range of the standard solutions	Working range	0 - 1 ppm
Precision	RSD	0.7516
LOD	Minimum amount detected	0.004081 ppm
LOD	Minimum amount to be quantified	0.04081 ppm
Selectivity	Element(s) presence Rh	$s_a = 0.01161$
Accuracy of the method	Specificity	$s_b = 0.00493$
Ruggedness	Precision over time	Results reproducible

$s_a$  = standard deviation of the slope

$s_b$  = standard deviation of the intercept

Linearity was calculated from the least squares method described in **Chapter 3, Section 3.3.2, Equation 3.4** and was proved to be the same as the one given by the regression coefficient ( $r^2$ ) of the calibration curve. The measured slope of the graph shows a good correlation between the instrument response and analyte concentrations. The slope gives a clear indication of how sensitive the instrument is towards the rhodium analysis.

### **5.3 Validation of the CRM results**

Accuracy and precision of the method needs to be verified to ensure the proper performance of the method. A certified reference material (CRM) was used to determine the performance of the method during the development process. The CRM was also used to ensure the compatibility of the measurements and to increase the credibility and reliability of the measured experimental results. The CRM (ERM<sup>®</sup>-EB504) was reported to have a mean standard deviation of 2.2 for a mean rhodium concentration of 338 ppm and an uncertainty value of  $\pm 4$ , with  $k = 2$  degrees of freedom (see the certificate in **Appendix 7**) at 95 % confidence interval as defined in the Guide to the Expression of Uncertainty in Measurement (1995) ISO, Geneva.<sup>233</sup>

The results obtained for rhodium determination using cobalt and yttrium internal standards in CRM were validated to determine the credibility and reliability of the test method and the results. All the calculations for the percentage of rhodium recovered from the CRM were performed in accordance with the description of the CRM method of analysis. The acceptance and rejection regions were defined as

---

<sup>233</sup> European Reference Material, Certificate of analysis ERM<sup>®</sup>-504 (2007)

described in **Chapter 3, Section 3.3.2** and the following results in **Table 5.2** were obtained.

The z-statistic test was chosen to determine the rejection region for the CRM because the actual value of the standard deviation was known as it was given on the certificate. Hence, the rejection region for the alternative hypothesis  $H_a: \mu \neq \mu_0$  was defined for all the z values in the region  $z \geq z_{crit}$  or  $z \leq z_{crit}$  as described in **Chapter 3, Figure 3.9**. Experimental results with large positive or negative values exceeding the  $z_{crit}$  of  $\pm 1.64$  will be rejected as shown in **Equation 5.1**.

*Example of the calculation of the hypothesis test for the CRM results in **Table 5.2***

$$z = \frac{3.38 - 3.39}{\left( \frac{0.02}{\sqrt{5}} \right)} = -1.12 \quad \dots 5.1$$

**Table 5.2:** Validation of the CRM results for the cobalt internal standard method

Validation criteria	Parameter/ condition	Measurement	Comment
Sensitivity	Gradient (m)	0.2933	
Linearity	Regression coefficient ( $r^2$ ) and r	0.997 and 0.998	
Working range of the standard solutions	Working range	0.5 - 10.0 ppm	
Precision	RSD	0.71	
Uncertainty of the slope	Intercept (c)	0.0795	
Selectivity of the method	Mg, Al, Ca, Ti, V, Cr, Mn, Fe, Ni, Cu, Zn, Ga, Sr, Rh, Pd, Ba, Pt, Tl and Pb present in sample	$s_a = 0.00936$	Excellent
Accuracy of method	Specificity	$s_b = 0.03338$	Excellent
Robustness	Determination of Rh in different acid matrix	-	-
Ruggedness	Competency of the method at different analysis days, temperature, analyst and assay time	% Rh recovery	Results reproducible
Average % Rh recovery		100.01	
Average concentration (ppm)		3.38	
Standard deviation of the concentration (ppm)		0.02*	
Theoretical average concentration (ppm) $\mu_0$		3.39	
Calculated z value		-1.12	
<b>Decision</b>		Accepted	

- not determined

\* certified value of the standard deviation of the CRM

The calculated z-statistic value is less than the  $z_{crit}$  as determined by the rejection region and the experimental result is therefore accepted at 95 % confidence interval. The same validation criterion was applied to the results obtained using yttrium as internal standard. The results are shown in **Table 5.3** and the z-statistic test was used as it was for the cobalt internal standard.



**Table 5.3:** Validation of the CRM results for the yttrium internal standard method.

Validation criteria	Parameter/ condition	Measurement	Comment
Sensitivity	Gradient (m)	0.0203	
Linearity	Regression coefficient ( $r^2$ ) and r	0.9999 and 0.9999	
Working range of the standard solutions	Working range	0.5 - 10.0 ppm	
Precision	RSD	0.97	
Uncertainty of the slope	Intercept (c)	0.0026	
Selectivity of the method	Mg, Al, Ca, Ti, V, Cr, Mn, Fe, Ni, Cu, Zn, Ga, Sr, Rh, Pd, Ba, Pt, Tl and Pb	$s_a = 0.00009$	
Accuracy of method	Specificity	$s_b = 0.00033$	
Robustness	Determination of Rh in different acid matrix	-	-
Ruggedness	Competency of the method at different different analysis days, temperature, analyst and assay time	% Rh recovery	Results not reproducible
Average % Rh recovery		140.26	
Average concentration (ppm)		4.74	
Standard deviation of the concentration (ppm)		0.02*	
Theoretical average concentration (ppm) $\mu_0$		3.39	
Calculated z value		150.93	
<b>Decision</b>		Rejected	

## 5.4 Validation of the rhodium metal results

The validation process was also extended to the results obtained for the determination of rhodium in the pure rhodium metal sample. The results obtained employing the same experimental conditions used for the CRM were evaluated using the  $t$ -statistic of the hypothesis test. The  $t$ -statistic test was chosen to determine the rejection region since a small number (less than 20) of the experimental

measurements were determined and the estimated standard deviation was not good enough to be approximated as a good estimate of the real standard deviation of the population. Hence, the rejection region for the alternative hypothesis  $H_a: \mu \neq \mu_0$  was chosen for all the  $t$  values in the region  $t \geq t_{crit}$  or  $t \leq -t_{crit}$ . Experimental results with large positive or negative values exceeding the  $t_{crit}$  of  $\pm 2.78$  will be rejected as shown in **Equation 5.2**.

*Example of the calculation of the hypothesis test for the CRM results in **Table 5.4***

$$t = \frac{3.37 - 3.38}{\left( \frac{0.04}{\sqrt{(5-1)}} \right)} = -0.50 \quad \dots 5.2$$

The calculated  $t$ -statistic value is less than the  $t_{crit}$  as determined by the rejection region and the experimental result is therefore accepted at 95 % confidence interval. The results for the validation of the experimental results and other parameters are shown in **Table 5.4**.

**Table 5.4:** Validation of rhodium in rhodium metal at 95 % confidence interval using the cobalt internal standard method

Validation criteria	Parameter/ condition	Measurement	Comment
Sensitivity	Gradient (m)	0.2906	
Linearity	Regression coefficient ( $r^2$ ) and r	1.00 and 1.00	
Working range of the standard solutions	Working range	0.5 - 10.0 ppm	
Precision	RSD	1.23	
Uncertainty of the slope	Intercept (c)	0.0261	
Selectivity of the method	Na, Mg, Ca, Fe, Rh, Pd, Ag and Pt	$s_a = 0.00117$	Excellent
Accuracy of method	Specificity	$s_b = 0.00417$	Excellent
Robustness	Determination of Rh in different acid matrix	-	-
Ruggedness	Competency of the method at different analysis days, temperature, analyst and assay time	% Rh recovery	Results reproducible
Average % Rh recovery		99.69	
Average concentration (ppm)		3.37	
Standard deviation of the concentration (ppm)		0.04	
Theoretical average concentration (ppm) $\mu_0$		3.38	
Calculated $t$ value		-0.50	
<b>Decision</b>		Accepted	

The final results were accepted at 95 % confidence interval under the defined region stated in the previous **Paragraph 5.4**.

## 5.5 Validation of the $\text{RhCl}_3 \cdot 3\text{H}_2\text{O}$ results

Experimental results from the inorganic rhodium salt  $\text{RhCl}_3 \cdot 3\text{H}_2\text{O}$  were validated using the same method as for the CRM. All the validation parameters were evaluated in the same manner as shown in **Table 5.5**.

**Table 5.5:** Validation of rhodium in  $\text{RhCl}_3 \cdot 3\text{H}_2\text{O}$  at 95 % confidence interval using cobalt internal standard method.

Validation criteria	Parameter/ condition	Measurement	Comment
Sensitivity	Gradient (m)	0.2174	
Linearity	Regression coefficient ( $r^2$ ) and r	1.00 and 1.00	
Working range of the standard solutions	Working range	0.5 - 10.0 ppm	
Precision	RSD	0.26	
Uncertainty of the slope	Intercept (c)	0.0205	
Selectivity of the method	Mg and Ca	$s_a = 0.00031$	Excellent
Accuracy of method	Specificity	$s_b = 0.00159$	Excellent
Robustness	Determination of Rh in the presence of HCl, HBr, $\text{HNO}_3$ and different concentration of $\text{Cl}^-$ as well as NaCl, KCl and RbCl	-	Results sensitive to all additions
Ruggedness	Competency of the method at different analysis days, temperature, analyst and assay time	% Rh recovery	Results not reproducible
Average % Rh recovery		99.79	
Average concentration (ppm)		2.68	
Standard deviation of the concentration (ppm)		0.01	
Theoretical average concentration (ppm) $\mu_0$		2.68	
Calculated $t$ value		0.00	
<b>Decision</b>		Accepted	

## 5.6 Validation of the organometallic complexes results

The results for the newly synthesized rhodium complexes were validated to determine whether the developed method was able to accurately determine rhodium under the same conditions as for the CRM. For each complex, listed in **Tables 5.6 - 11**, the validation parameters and the experimental results were evaluated in the same region as for the CRM.

**Table 5.6:** Validation of rhodium in  $[\text{Rh}(\text{acac})(\text{CO})_2]$  at 95 % confidence interval using the cobalt internal standard method

Validation criteria	Parameter/ condition	Measurement	Comment
Sensitivity	Gradient (m)	0.2319	
Linearity	Regression coefficient ( $r^2$ ) and r	1.00 and 1.00	
Working range of the standard solutions	Working range	0.5 - 10.0 ppm	
Precision	RSD	0.66	
Uncertainty of the slope	Intercept (c)	0.0261	
Selectivity of the method	-	$s_a = 0.00051$	Excellent
Accuracy of method	Specificity	$s_b = 0.00183$	Excellent
Robustness	Determination of Rh in different acid matrix	-	-
Ruggedness	Competency of the method at different analysis days, temperature, analyst and assay time	% Rh recovery	Results not reproducible
Average % Rh recovery		95.71	
Average concentration (ppm)		3.23	
Standard deviation of the concentration (ppm)		0.02	
Theoretical average concentration (ppm) $\mu_0$		3.38	
Calculated $t$ value		-13.04	
<b>Decision</b>		Rejected	

**Table 5.7:** Validation of rhodium in [Rh(acac)(CO)(PPh<sub>3</sub>)] at 95 % confidence interval using the cobalt internal standard method

Validation criteria	Parameter/ condition	Measurement	Comment
Sensitivity	Gradient (m)	0.2319	
Linearity	Regression coefficient ( $r^2$ ) and r	1.00 and 1.00	
Working range of the standard solutions	Working range	0.5 - 10.0 ppm	
Precision	RSD	0.63	
Uncertainty of the slope	Intercept (c)	0.0136	
Selectivity of the method	-	$s_a = 0.00051$	Excellent
Accuracy of method	Specificity	$s_b = 0.00183$	Excellent
Robustness	Determination of Rh in different acid matrix	-	-
Ruggedness	Competency of the method at different analysis days, temperature, analyst and assay time	% Rh recovery	Results not reproducible
Average % Rh recovery		81.43	
Average concentration (ppm)		2.75	
Standard deviation of the concentration (ppm)		0.02	
Theoretical average concentration (ppm) $\mu_0$		3.38	
Calculated $t$ value		-63.00	
<b>Decision</b>		Rejected	

**Table 5.8:** Validation of rhodium in [Rh(acac)(PPh<sub>3</sub>)(CO)(Me)(I)] at 95 % confidence interval using the cobalt internal standard method

Validation criteria	Parameter/ condition	Measurement	Comment
Sensitivity	Gradient (m)	0.2906	
Linearity	Regression coefficient ( $r^2$ ) and r	1.00 and 1.00	
Working range of the standard solutions	Working range	0.5 - 10.0 ppm	
Precision	RSD	0.64	
Uncertainty of the slope	Intercept (c)	0.0136	
Selectivity of the method	-	$s_a = 0.00051$	Excellent
Accuracy of method	Specificity	$s_b = 0.00183$	Excellent
Robustness	Determination of Rh in different acid matrix	-	-
Ruggedness	Competency of the method at different analysis days, temperature, analyst and assay time	% Rh recovery	Results not reproducible
Average % Rh recovery		89.19	
Average concentration (ppm)		3.01	
Standard deviation of the concentration (ppm)		0.02	
Theoretical average concentration (ppm) $\mu_0$		3.38	
Calculated $t$ value		-37.00	
<b>Decision</b>		Rejected	

**Table 5.9:** Validation of rhodium in  $[\text{Rh}(\text{cupf})(\text{CO})_2]$  at 95 % confidence interval using the cobalt internal standard method

Validation criteria	Parameter/ condition	Measurement	Comment
Sensitivity	Gradient (m)	0.2319	
Linearity	Regression coefficient ( $r^2$ ) and r	1.00 and 1.00	
Working range of the standard solutions	Working range	0.5 - 10.0 ppm	
Precision	RSD	1.87	
Uncertainty of the slope	Intercept (c)	0.0136	
Selectivity of the method	-	$s_a = 0.00051$	Excellent
Accuracy of method	Specificity	$s_b = 0.00183$	Excellent
Robustness	Determination of Rh in different acid matrix	-	-
Ruggedness	Competency of the method at different analysis days, temperature, analyst and assay time	% Rh recovery	Results reproducible
Average % Rh recovery		99.97	
Average concentration (ppm)		3.38	
Standard deviation of the concentration (ppm)		0.06	
Theoretical average concentration (ppm) $\mu_0$		3.38	
Calculated $t$ value		0.00	
<b>Decision</b>		Accepted	



**Table 5.10:** Validation of rhodium in [Rh(cupf)(PPh<sub>3</sub>)(CO)] at 95 % confidence interval using the cobalt internal standard method

Validation criteria	Parameter/ condition	Measurement	Comment
Sensitivity	Gradient (m)	0.2305	
Linearity	Regression coefficient ( $r^2$ ) and r	1.00 and 1.00	
Working range of the standard solutions	Working range	0.5 - 10.0 ppm	
Precision	RSD	0.36	
Uncertainty of the slope	Intercept (c)	0.0093	
Selectivity of the method	-	$s_a = 0.00029$	Excellent
Accuracy of method	Specificity	$s_b = 0.00102$	Excellent
Robustness	Determination of Rh in different acid matrix	-	-
Ruggedness	Competency of the method at different analysis days, temperature, analyst and assay time	% Rh recovery	Results reproducible
Average % Rh recovery		99.14	
Average concentration (ppm)		3.35	
Standard deviation of the concentration (ppm)		0.01	
Theoretical average concentration (ppm) $\mu_0$		3.38	
Calculated $t$ value		-6.00	
<b>Decision</b>		Rejected	

**Table 5.11:** Validation of rhodium in [Rh(cupf)(PPh<sub>3</sub>)(CO)(Me)(I)] at 95 % confidence interval using the cobalt internal standard method

Validation criteria	Parameter/ condition	Measurement	Comment
Sensitivity	Gradient (m)	0.2319	
Linearity	Regression coefficient ( $r^2$ ) and r	1.00 and 1.00	
Working range of the standard solutions	Working range	0.5 - 10.0 ppm	
Precision	RSD	0.35	
Uncertainty of the slope	Intercept (c)	0.0136	
Selectivity of the method	-	$s_a = 0.00051$	Excellent
Accuracy of method	Specificity	$s_b = 0.00183$	Excellent
Robustness	Determination of Rh in different acid matrix	-	-
Ruggedness	Competency of the method at different analysis days, temperature, analyst and assay time	% Rh recovery	Results not reproducible
Average % Rh recovery		99.08	
Average concentration (ppm)		3.34	
Standard deviation of the concentration (ppm)		0.05	
Theoretical average concentration (ppm) $\mu_0$		3.38	
Calculated $t$ value		-1.60	
<b>Decision</b>		Accepted	

The results indicated an acceptance of the results from the CRM, rhodium metal, RhCl<sub>3</sub>·xH<sub>2</sub>O, [Rh(cupf)(CO)<sub>2</sub>] and [Rh(cupf)(PPh<sub>3</sub>)(CO)(Me)(I)] at the 95 % confidence interval. Excellent recoveries (c.a. 100.0 % +) for the accepted results were obtained, which were all in the defined accepting region of the CRM. The result also showed a good precision (at least 0.01), accuracy (at least 99.0 %) and selectivity/specificity (at least 0.997). Inconsistent results obtained in the validation of the organometallic complexes rendered this method not robust. These poor

recoveries either indicated that this method of analysis was not able to analyze these samples accurately under the chosen conditions or more probably that the samples synthesized were not very pure which led to the low recoveries.

## 5.7 Conclusion

The results for the CRM, rhodium metal and inorganic compounds validated with the use of the cobalt internal standard addition method were in the region of acceptance at 95 % confidence interval. Most of the results validated for the organometallic complexes regarding the method and conditions, revealed a rejection of the results that had low percentages recovery. These results exceeded the limits set by the 95 % confidence interval and were outside the acceptance region defined by the *t*-statistic of the hypothesis test. A summary of the accepted and rejected results using the cobalt internal standard addition are given in **Table 5.12** and a summary of the validation parameters which were investigated during the experimental analysis are given in **Table 5.13**.

**Table 5.12:** A summary of the results accepted or rejected

Material	Accept	Reject
<b>CRM</b>	√	
<b>Rhodium metal</b>	√	
<b>Inorganic</b> (RhCl <sub>3</sub> ·xH <sub>2</sub> O)	√	
<b>Organometallic complexes</b>		
[Rh(acac)(CO) <sub>2</sub> ]		x
[Rh(acac)(CO)(PPh <sub>3</sub> )]		x
[Rh(acac)(CO)(PPh <sub>3</sub> )(Me)(I)]		x
[Rh(cupf)(CO) <sub>2</sub> ]	√	
[Rh(cupf)(CO)(PPh <sub>3</sub> )]		x
[Rh(cupf)(CO)(PPh <sub>3</sub> )(Me)(I)]	√	

**Table 5.13:** A summary of the validated parameters

Method validation procedure	Parameter to be determined	Comment
Confirmation of identity and selectivity/specificity	Linear regression line ( $r^2$ )	Very good, all above 0.997
Limit of detection (LOD)	Minimum amount detected	Very good (0.0040865 ppm)
Limit of quantitation (LOQ)	Minimum amount to be quantified	Very good (0.040865 ppm)
Working and linear ranges	The difference between LOQ and LOL	Wide range (0 to 10 ppm)
Accuracy	Selectivity and specificity ( $r^2$ )	Good
Trueness	Method or reference comparison	99.99 % at 95 % confidence interval
Repeatability	Precision	Good, less than 3 % RSD
Reproducibility of the same results under different matrix	Robustness	Method affected by acid matrix and EIE
Measurement of uncertainty	Accuracy	5 % uncertainty
Sensitivity	The gradient of the calibration	0.7337, good
Ruggedness	Competency of analyst instrument	Results differed with the acid matrix used.

As a final conclusion it can be said that the rhodium analysis using cobalt as internal standard was very successful for the analysis of the rhodium content in different chemical substances and that the results met most of the guidelines within acceptable criterion.

# 6 Evaluation of this study and future research

---

## 6.1 Degree of success with regard to the set objectives

This chapter evaluates the achievements of this study in terms of the objectives set out at the beginning of this study. The main objective as it was outlined in **Chapter 1, Section 1.9**, was to:

- Develop an analytical procedure that can accurately determine and quantify rhodium in the metal and in organometallic and inorganic complexes.
- Establish measurement traceability in analysing a rhodium CRM.
- Statistically validate these methods
- Determine the influence of different acids as well as alkali metal ions on the rhodium recovery.
- Optimize ICP-OES operating conditions for the determination of rhodium at trace levels.

In general, this study has been successful in achieving these objectives as revealed in the previous chapters. The results obtained during this study clearly showed that the developed method using cobalt as internal standard was capable of accurately quantifying rhodium in most of the specified samples in the current study. The efficiency of the method was shown by its ability to recover the rhodium to a level of 100 % as was certified for the reference material (CRM). This ability of the test method to recover the rhodium quantitatively in the CRM revealed that the method was appropriate for rhodium determination. The results obtained using this method were also shown to be reproducible for all the experimental measurements except in the cases where the matrix effects were very complex e.g. in the cases where the concentration of the interfering species (EIE) and acids were high. Accuracy varied depending on the degree of purity of the analyte samples. The metal sample with a

specified degree of purity, yielded excellent results whilst the results for some of the  $\text{RhCl}_3 \cdot x\text{H}_2\text{O}$  and different organometallic samples with unspecified degree of purity yielded varying results. Results obtained using the cobalt internal standard method were compared to those of the direct calibration method and the standard addition method and were found to have better recoveries than the latter techniques.

Validation of the ICP-OES and method showed a remarkable performance of ICP-OES parameters such as accuracy, precision, specificity, limit of detection, limit of quantitation and linearity. The condition chosen also allowed for the determination of the robustness of the  $\text{RhCl}_3 \cdot x\text{H}_2\text{O}$  analysis in presence of different acid and alkali metals. Results indicated that the method was not very robust due to the decrease in rhodium recoveries that was obtained under different matrixes as illustrated in **Chapter 4, Section 4.7.5 and 4.7.7**. Most of the results from the CRM, rhodium metal and  $\text{RhCl}_3 \cdot x\text{H}_2\text{O}$  were found to be in the acceptable range of the hypothesis test at 95 % confidence interval.

## 6.2 Future research

The cobalt internal standard method was shown to be very effective in the determination of rhodium in different samples. Since iridium and rhodium are in the same group of the periodic table, it is possible that in a future study the method can be extended to the determination of iridium in different complexes. The first ionization of iridium is close to those of cobalt and rhodium as shown in **Table 6.1**, which suggest that the cobalt internal standard method is mostly likely to be a suitable method for iridium quantification in different iridium containing samples.

**Table 6.1:** Comparison of the first ionization energies of cobalt, rhodium and iridium

Elements	1 <sup>st</sup> Ionization Energy (kJ mol <sup>-1</sup> )
Cobalt	760.41
Rhodium	719.68
Iridium	865.19

Rhodium determination was shown to be affected by the increase in different acid matrices and easily ionized elements (EIE), the same effects can still further be

investigated for iridium, using the same method of analysis. Losses of accuracy, ruggedness and/or robustness as a result of matrix effects derived from EIE were major problems. Conditions and measures to make corrections for the effects caused by the EIE in both iridium and rhodium can also be investigated and compared in order to determine whether the effects are specific or selective.

The sensitivity/robustness of the rhodium analysis in organometallic samples also needs to be investigated. The low recoveries for some of the rhodium samples need to be investigated in terms of product purity and analyzing method to find the correct answers for these poor results.